

IMPACTS OF CLIMATE CHANGE ON THE TROPHIC FUNCTIONING OF THE
WORLD OCEAN

by

HUBERT DU PONTAVICE

M.Sc., Agrocampus Ouest, 2016

A DISSERTATION SUBMITTED IN PARTIAL FULFILLMENT OF
THE REQUIREMENTS FOR THE DEGREE OF
DOCTOR OF PHILOSOPHY

in

THE FACULTY OF GRADUATE AND POSTDOCTORAL STUDIES
(Zoology)

THE UNIVERSITY OF BRITISH COLUMBIA
(Vancouver)

June 2021

© Hubert du Pontavice, 2021

The following individuals certify that they have read, and recommend to the Faculty of Graduate and Postdoctoral Studies for acceptance, the dissertation entitled:

Impacts of climate change on the trophic functioning of the world ocean

submitted by Hubert du Pontavice in partial fulfillment of the requirements for

the degree of Doctor of Philosophy

in Zoology

Examining Committee:

William Cheung, Professor, Zoology, UBC

Co-supervisor

Didier Gascuel, Professor, UMR ESE, Agrocampus Ouest

Co-supervisor

Daniel Pauly, Professor, Zoology, UBC

Supervisory Committee Member

Yunne Shin, Researcher, UMR Marbec, IRD

External examiner designated by Agrocampus Ouest

Evgeny Pakhomov, Professor, Zoology, UBC

University Examiner for UBC

Laurent Bopp, Professor, LSCE, CNRS

University Examiner for Agrocampus Ouest

Additional Supervisory Committee Members:

Mary O'Connor, Assistant professor, Zoology, UBC

Supervisory Committee Member

THESE DE DOCTORAT DE

L'AGROCAMPUS OUEST

COMUE UNIVERSITE BRETAGNE LOIRE

ECOLE DOCTORALE N° 598

Sciences de la Mer et du littoral

Spécialité: Ecologie Marine

ET

UNIVERSITY OF BRITISH COLUMBIA

THE FACULTY OF GRADUATE AND POSTDOCTORAL STUDIES

Spécialité: Zoology

PAR

HUBERT DU PONTAVICE

Impacts of climate change on the trophic functioning of the world ocean

Thèse présentée et soutenue à Rennes, le

Unité de recherche : UMR ESE (Agrocampus Ouest) et CORU (University of British Columbia)

Thèse N° : H-114_2020-14

Rapporteurs avant soutenance :

Yunne SHIN Directrice de recherche à IRD (France)

Composition du Jury :

Président :

Rapporteurs :

Yunne SHIN Directrice de recherche à IRD (France)

Examineurs:

Daniel PAULY Professeur à UBC (Canada)

Laurent BOPP Directeur de recherche à CNRS (France)

Evgeny PAKHOMOV Professeur à UBC (Canada)

Co-directeurs de thèse :

Didier GASCUEL Professeur à Agrocampus Ouest (France)

William W.L. CHEUNG Professeur à UBC (Canada)

Abstract

Climate change impacts on marine life in the world ocean are expected to increase over the 21st century. In this thesis, I investigated the effects of climate change on biomass flows in marine food webs and their consequences on ecosystem structure and functioning. First, the transfer efficiency and biomass residence time are estimated in the world' shelf seas from 1950 to 2010. Based on the projected ocean warming under two climate scenarios, I highlighted that biomass transfers may be faster and less efficient by 2100 without mitigation of greenhouse gases emissions. Then, using a modelling framework called EcoTroph that is based on a representation of biomass flow, I projected the future of consumer biomass in marine food webs. From the projected changes in temperature and primary production, marine animal biomass is estimated at each trophic level on a $1^\circ \times 1^\circ$ grid of the global ocean from 1950 to 2100. The projections showed that the projected alteration of biomass flows may lead to a global decline in consumer biomass by 2100 under the “no mitigation policy” climate scenario, with more pronounced impacts at higher trophic levels. In the European waters, the EcoTroph model forced by a coupled hydrodynamic-ecosystem model is used to investigate the potential climate change effects on the ecosystem structure and functioning. The results revealed that biomass and catch may decrease by 2100 under the “no mitigation policy” scenario and if fishing mortality remains constant at its current value. Overall, this thesis showed that climate change would alter biomass flows in marine ecosystems, causing a decrease in the future ocean animal biomass and direct repercussions on fisheries.

Résumé

Les effets du changement climatique sur les écosystèmes marins devraient s'accroître au cours du 21^e siècle. Le but de cette thèse était d'étudier ces effets sur les flux de biomasse dans les réseaux trophiques marins et leurs conséquences sur la structure et le fonctionnement des écosystèmes. Tout d'abord, l'efficacité de transfert et le temps de résidence de la biomasse ont été estimés sur les plateaux continentaux de l'océan mondial entre 1950 et 2010. Sur la base des projections du réchauffement de l'océan, nous avons estimé que les transferts de biomasse pourraient devenir plus rapides et moins efficaces d'ici 2100. L'évolution de la biomasse des consommateurs dans les écosystèmes marins a ensuite été modélisée à partir du modèle EcoTroph sur la base des changements projetés de température et de production primaire. Les résultats ont montré qu'une altération des flux de biomasse pourrait entraîner un déclin mondial de la biomasse d'ici 2100, avec des impacts plus prononcés aux niveaux trophiques les plus élevés. Dans les eaux européennes, un modèle EcoTroph forcé par un modèle couplé hydrodynamique-écosystème a été développé pour étudier les effets du changement climatique sur les écosystèmes de la région. Nous avons mis en lumière que la biomasse et les captures pourraient diminuer d'ici 2100 suivant le scénario climatique le plus pessimiste et si la mortalité par pêche reste constante à sa valeur actuelle. Cette thèse a montré que le changement climatique pourrait modifier profondément les flux de biomasse dans les écosystèmes marins, entraînant une diminution de la biomasse animale marine et des répercussions directes sur les pêcheries.

Lay Summary

Climate change impacts on marine life in the world ocean are expected to increase over the 21st century. In this thesis, I investigated the effects of climate change on the structure and functioning of marine ecosystems and the consequences for the future of animals in the ocean and the fisheries production. I found that the effects of fishing and changes in ocean temperature have already substantially altered marine food webs. Without mitigation of greenhouse gas emissions, my research shows that climate change will result in decrease in the biomass and potential fisheries production across the global ocean. Regionally in the waters around Europe, this thesis highlights the potential for reducing climate impacts for marine ecosystems and fisheries through climate-adapted fisheries management. Overall, this thesis provides new scientific knowledge that could help support initiatives that aim to tackle global and regional societal challenges such as the United Nations Sustainable Development Goals.

Preface

I am the primary author of this thesis and the lead author for all chapters. I led the design, implementation, and analyses of all research in this thesis. This thesis was written with the guidance and support of my co-supervisors, Pr. Didier Gascuel and Pr. William W.L. Cheung. Furthermore, coauthors provided insightful thought and contributions to ensure the quality of each chapter for publication.

A version of chapter 2 has been published as:

- du Pontavice, H., Gascuel, D., Reygondeau, G., Maureaud, A. & Cheung, W.W.L. (2019). Climate change undermines the global functioning of marine food webs. *Glob. Change Biol.*, gcb.14944.

DOI: <https://doi.org/10.1111/gcb.14944>

The original draft of the manuscript was researched and written by me. I performed all data analysis presented in this Chapter and primarily collected the data for this manuscript, with help from Gabriel Reygondeau to identify and collect additional data. All authors contributed to writing and revisions for publication.

A version of chapter 3 has been published as:

- du Pontavice, H., Gascuel, D., Reygondeau, G., Stock, C., D., & Cheung, W. W. L. (2021). Climate-induced decrease in biomass flow in marine food webs may severely affect predators and ecosystem production. *Global Change Biology*.

DOI: <https://doi.org/10.1111/gcb.15576>

The original draft of the manuscript was researched and written by me. I performed all data analysis presented in this Chapter and primarily collected the data for this manuscript, with help from Gabriel Reygondeau and Charles Stock to identify and collect additional data. All authors contributed to writing and revisions for publication.

Chapter 4 has been written as a manuscript with co-authors Didier Gascuel and William W.L. Cheung and will be submitted as:

- “Climate-induced changes in ocean productivity and food webs functioning may deeply affect European fisheries catch”

The original draft of the manuscript was researched and written by me. I performed all data analysis presented in this Chapter and collected all the data for this manuscript. All authors contributed to writing and revisions for the preparation.

This dissertation is formatted in accordance with the regulations of Agrocampus Ovest and submitted in partial fulfillment of the requirements for a PhD degree awarded jointly by Agrocampus Ovest and the University of British Columbia. Versions of this dissertation will exist in the institutional repositories of both institutions.

Table of Contents

Abstract	iv
Résumé	v
Lay Summary	vi
Preface	vii
Table of Contents	ix
List of Tables	xiii
List of Figures	xiv
List of Abbreviations	xxiv
Acknowledgements	xxv
Dedication	xxviii
CHAPTER 1: General introduction	2
1.1. An ocean under pressure	2
1.2. The fishing effects on marine life	4
1.2.1. The state of the world's fisheries.....	4
1.2.2. The fishing effects on marine populations.....	5
1.2.3. The fishing effects on marine communities	6
1.2.4. Synergistic effects of fishing and climate.....	7
1.3. The climate change effects on marine ecosystems.....	8
1.3.1. The climate-induced changes in ocean conditions	8
1.3.2. Impacts on primary production	9
1.3.3. Impacts on upper trophic levels	10
1.3.4. The changes in biodiversity and abundance of marine life	12
1.3.5. Trophic amplification of the climate signal	13
1.3.6. Climate-induced alteration of biomass flows	14
1.4. The trophodynamic properties of marine food web.....	16

1.5. Marine ecosystem modelling	18
1.5.1. A large variety of marine ecosystem models	18
1.5.2. Fish-MIP, Fisheries and Marine Ecosystem Model Intercomparison Project	18
1.6. The EcoTroph model	19
1.7. Objectives of the thesis.....	21
CHAPTER 2: Climate change undermines the trophic transfers of marine food webs	24
2.1. Introduction	24
2.2. Materials and Methods.....	26
2.2.1. Study area and catch data	26
2.2.2. Trophic transfer efficiency and biomass residence time calculations	27
2.2.3. Relationships between temperature, trophic transfer efficiency and biomass residence time	31
2.2.4. Past and projected trends in trophic transfer efficiency and biomass residence time	32
2.2.5. Sensitivity analysis	32
2.3. Results.....	33
2.3.1. Relation between sea surface temperature and ecosystem trophodynamics	33
2.3.2. Observed past trends in trophic transfer efficiency and biomass residence time	36
2.3.3. Projections for the end of the century.....	37
2.4. Discussion.....	38
2.4.1. Less efficient and faster transfers in warm waters.....	39
2.4.2. Robustness of the analysis.....	39
2.4.3. Towards faster and less efficient trophic transfers.....	40
2.4.4. Polar ecosystems: the more affected ecosystems?	42
2.5. Conclusion.....	43
CHAPTER 3: Climate-induced decrease in biomass flow in marine food webs may severely affect predators	45
3.1. Introduction	45
3.2. Materials and Methods.....	47
3.2.1. The EcoTroph model	47
3.2.2. Simulating biomass flow from primary production to upper trophic levels.....	50

3.2.3. EcoTroph simulations	54
3.3. Results	55
3.3.1. Changes in ocean conditions and biomass transfers over the 21st century	55
3.3.2. Changes in the trophic structure of marine ecosystems	57
3.3.3. Changes in trophic structure of marine ecosystems	59
3.3.4. Changes in ecosystem production	61
3.4. Discussion	62
3.4.1. Drivers of changes in consumer biomass	63
3.4.2. Trophic amplification induced by less efficient transfer	63
3.4.3. Toward a global decline in fisheries catch?	64
3.4.4. Modelling considerations and sources of uncertainties	65
3.5. Conclusion	67
CHAPTER 4: Climate-induced changes in ocean productivity and food webs functioning may deeply affect European fisheries catch	69
4.1. Introduction	69
4.2. Materials and Methods	71
4.2.1. A regional model for low trophic levels	71
4.2.2. The EcoTroph model	72
4.2.3. Forcing EcoTroph with outputs from the coupled POLCOMS-ERSEM model	75
4.2.4. Study area and fisheries	76
4.2.5. Simulation design	77
4.3. Results	80
4.3.1. The effects of climate change on biomass and catch under a constant fishing mortality scenario	80
4.3.2. Climatic drivers and the changes in catch and biomass	83
4.3.3. Ecosystem impacts under different fishing scenarios	85
4.4. Discussion	86
4.4.1. Heterogeneous responses of European continental shelf ecosystems to climate change	87
4.4.2. Sensitivity analyses and structural uncertainties of the model	88
4.4.3. Contribution of EcoTroph modelling to explore the future of European fisheries	89
4.4.4. Conclusion	90

CHAPTER 5: General discussion and perspectives.....	93
5.1. A contribution to the understanding of biomass flows in marine ecosystems.....	93
5.2. Caveats and limitations.....	95
5.3. A simple and efficient modelling approach to explore the effects of climate change	97
5.3.1. Three processes at play to model the future of marine ecosystems	97
5.3.2. Effect of Iron limitation in a Pacific food web – A complementary study.....	99
5.3.3. EcoTroph in Fish-MIP	100
5.3.4. EcoTroph, a tool to assess the impact of marine heat waves.....	102
5.4. Climate change and fishing in EcoTroph	103
5.4.1. The fishing impacts in EcoTroph	103
5.4.2. From the European case study to the introduction of global fisheries catch in EcoTroph	105
5.5. Concluding remarks.....	107
Bibliography	109
Appendix A – Chapter 2	127
Appendix B – Chapter 3	152
Appendix C – Chapter 4	166
Appendix D – Additional contributions.....	185
Article 1.....	185
Article 2.....	186
Article 3.....	187
Book chapter	188

List of Tables

Table A.2: List of the 72 selected Ecopath models extracted from EcoBase (Colléter <i>et al.</i> 2013) used to calculate the correction parameters of the trophic transfer efficiency and to compare the trophic trophic transfer parameters calculated from biomass and catch.....	130
Table A.4: Description of the eight tested models including a fishing variable and the associated deviance and p-value.....	139
Table A.6: trophic transfer efficiency and biomass residence time estimated by the model in each type of ecosystem.....	145
Table A.8.1: Parameters to estimate trophic transfer efficiency and biomass residence time in each type of ecosystem.....	148
Table A.8.2: total deviance explained by the trophic transfer efficiency and biomass residence time models and deviance explained by each covariate, SST, ecosystem type, SST x ecosystem type.....	148
Table B.1: EcoTroph model: parameters definition and units.....	154
Table B.8: Specific parameters to estimate trophic transfer efficiency of higher trophic levels for each type of ecosystem (equation (9), in the Methods section).....	160

List of Figures

- Figure 1.1: Projected changes in catch potential and the reliance of the human population on fish and their vulnerability of micronutrient malnutrition (Golden *et al.* 2016).** The colour scale on land represents the proportion of fish micronutrient intake relative to the total animal-sourced food for the country's population; the scale on the sea represents the projected changes in maximum catch potential under RCP8.5 by 2100 relative to the 2000s (Figure extracted from IPCC 2019)..... 3
- Figure 1.2: Map of the global fisheries catches between 1950 and 2014** (source: <http://www.seaaroundus.org>, black line refers to the catch officially reported by the FAO)..... 4
- Figure 1.3: global trends in the state of the world's marine fish stocks, 1974–2015 (Figure derived from FAO, 2018)**..... 5
- Figure 1.4: A schematic representation of increased correlation of a marine population (e.g., abundance) to climate forcing under exploitation (Figure extracted from Perry *et al.* 2010)...** 7
- Figure 1.5: Observed and modelled historical changes in the ocean and cryosphere between 1950 and 2100, and projected future changes under low (RCP2.6) and high (RCP8.5) greenhouse gas emissions scenarios (Figure adapted from IPCC 2019)**..... 9
- Figure 1.6: The hotspots of local projected extinction intensity between 2000 and 2050, expressed in proportion to locally extinct species, on average, across three species distribution models under scenario RCP8.5 (Figure extracted from Jones & Cheung 2015)**..... 11
- Figure 1.7: Projected changes in total animal biomass based on outputs from 6 global marine ecosystem models forced with 2 Earth system models and 2 Representative Concentration Pathway (Lotze *et al.* 2019).** The panel (a) is the map of the changes in total animal biomass in 2085–2099 relative to 1986–2005 under RCP8. The panel (b) is the projected changes in global total animal biomass from 1970 to 2099 under RCP2.6 (red) and RCP8.5 (blue). Variability among different ecosystems and Earth system models combinations expressed as the 95% confidence interval (Figure extracted and adapted from Bindoff *et al.* 2019)..... 13
- Figure 1.8: Observed dependence of metabolism on temperature for teleost fishes (Figure derived from Bruno *et al.* 2015)**..... 14
- Figure 1.9: Fish communities identified on bottom trawl stations in 2004 and 2012.** The Atlantic, Arctic and Central communities are represented in red, blue and yellow, respectively. The circles indicate the shallow sub-communities and the triangles indicate the deep sub-communities (Figure extracted from Fossheim *et al.* 2015)..... 16

Figure 1.10: A schematic representation of the trophic functioning of an ecosystem with the theoretical biomass distribution by trophic and trophic transfer processes (Figure extracted and adapted from Gascuel *et al.* 2009)...... 20

Figure 2.1: Map of the coastal areas represented in the dataset and associated to ecosystem types (a). The colours refer to the ecosystem types: polar (in blue), temperate (in orange), tropical (in red) and upwelling (in green). The four graphs (b), (c), (d), and (e) show the past reconstructed trends in sea surface temperature (SST) and the predicted trends under RCP8.5 scenarios (business as usual scenario). Temperature is represented by mean values of SST coming from the three Earth system models used in the study and described in Materials and Methods..... 27

Figure 2.2: Synthetic schematic representation of the method to calculate trophic transfer efficiency and biomass residence time focused on the data that we used and the levels of ecological organization (from species to trophic level to ecosystem). n represents the number of species. 1 ((Froese & Pauly 2000), 2 (Coll  ter *et al.* 2013), 3 (Palomares & Pauly 1998; Gascuel *et al.* 2008), 4 (Pauly and Zeller, 2015)..... 28

Figure 2.3: Schematic representation of biomass flow parameters between two trophic levels. Black arrows represent energy transfers or losses. The prey has a trophic level τ and the predator has a trophic level $(\tau+1)$. The partial transfer efficiency (partial TE) $(P_{\tau+1}/Q_{\tau+1})$ and trophic transfer efficiency $(P_{\tau+1}/P_{\tau})$ are indicated (derived from Gascuel *et al.* 2008; Maureaud *et al.* 2017)..... 30

Figure 2.4: The effect of temperature on the two trophic transfer parameters. The violin plots on the top panels represent the distribution of the mean values of the two trophic transfer parameters: (a) trophic transfer efficiency (TTE) and (b) biomass residence time (BRT) in each ecosystem type over the period 2000–2010. The colours refer to the ecosystem types: polar (in blue), temperate (in orange), tropical (in red) and upwelling (in green). In both panels (c) and (d), solid coloured lines represent the predicted values (i.e., the temperature effect) of TTE and BRT respectively, provided for each ecosystem type by the GLM model. The black dashed lines represent the predicted values of TTE and BRT by an additional GLM model considering only SST as a covariate. The shaded areas refer to the mean predicted value confidence intervals (95%). 5783 grid cells were used to calculate the trends..... 34

Figure 2.5: Trophic transfer efficiencies and biomass residence times in the coastal regions of the global ocean. The panels (a) and (b) represent the observed values over the period 2000–2010 while the other panels exhibit the predicted values from the General Linear Model for: the period 2000–2010 (c) and (d), and projected changes in 2090–2100 relative to 2000–2010 for climate change scenarios for RCP 2.6 (e, f), and RCP 8.5 (g, h)..... 35

Figure 2.6: Past trends of trophic transfer parameters over the period 1950–2010. The dashed lines represent global mean values of the observed trophic transfer efficiency (TTE) (a) and biomass residence time (BRT) (b). Shaded areas refer to bootstrap confidence intervals at 95%. Solid black lines represent theoretical global mean trends of TTE and BRT, computed using the GLM temperature-based model. Light grey lines are trends calculated using three Earth system models (GFDL:

Geophysical Fluid Dynamics Laboratory, MPI: Max Plank Institute, IPSL: Institut Pierre Simon Laplace). 2253 grid cells were used to calculate the trends..... 37

Figure 2.7: The expected changes of trophic transfer at the global scale over the 21st century. Panel (a) shows the projections of trophic transfer efficiency (TTE) and panel (b) shows the projections of biomass residence time (BRT) in the coastal ecosystems between 2000 and 2100 under two climate change scenarios, RCP2.6 and RCP8.5 in green and red, respectively. The dark lines are the mean values of the trophic transfer parameters and the light lines are the values of each general circulation model. Panels (c) and (d) focus on RCP8.5 scenario..... 38

Figure 3.1: Conceptual design of the EcoTroph model and forcing used. The trophic functioning of marine food webs is represented by a biomass flow, with biomass entering the system at trophic level 1 due to net primary production, NPP. Biomass flow reaching each trophic level is then defined by the trophic transfer efficiency at low and high trophic level, TE LTL (derived from the plankton food web model COBALT) and TE HTL (estimated from the sea surface temperature (SST) according to du Pontavice et al. (2019)), respectively. The flow kinetics, which is also forced by SST (Gascuel *et al.* 2008), is a key parameter to derive biomass at each trophic level of the model from the biomass flow (Gascuel & Pauly 2009). One EcoTroph model is implemented each year within each cell of the global ocean, forced by NPP and SST from Earth system models' projections. Credit : adapted from Aurore Maureaud..... 47

Figure 3.2: Projected changes in biomass flow processes between 1950 and 2100 relative to 1986–2005. The changes in net primary production, NPP, (a, b, c), transfer efficiency of low trophic levels, TE LTL, (d, e, f), transfer efficiency of higher trophic levels, TE HTL, (g, h, i) and flow kinetic (j, k, l) are represented on this figure. Panels (a), (d), (g) and (j) represent the changes at global scale for RCP2.6 and RCP8.5. Panels (b), (e), (h) and (k) represent the changes in each ecosystem type under RCP8.5. The shaded areas around the curves in these panels indicate the inter-model variability (i.e., the variability given by the inputs of the 3 different Earth system models) and the color bars outside the box indicate the range of averaged changes of the three Earth system models over 2090–2099. Panels (c), (f), (i) and (l) represent the changes over the period 2090–2099 in each 1°x1° grid cell.. 56

Figure 3.3: Changes in total consumer biomass over the period 1950–2100. (a) Changes in total consumer biomass for RCP2.6 and RCP8.5 relative to the reference period 1986–2005. (b) Mean changes in total consumer biomass for RCP8.5 relative to 1986–2005 in which the contribution of net primary production (NPP), transfer efficiency of lower trophic level (TE LTL), transfer efficiency of higher trophic level (TE HTL) and flow kinetic are isolated. The shaded areas around the curves indicate the inter-model variability and the color bars indicate the ranges of averaged changes of three Earth system models over 2090–2099..... 57

Figure 3.4: Maps of the ensemble mean projections for the three Earth system models of changes in total consumer biomass by 2090–2099 relative to 1986–2005 under (a) RCP2.6 and (b) RCP8.5. Panel (c) represents the changes in consumer biomass by latitude for RCP2.6 and RCP8.5 58

Figure 3.5: Changes in total consumer biomass in each ecosystem type as well as the processes at play for RCP8.5. Panel (a) represents the changes in total consumer biomass for RCP8.5 in each ecosystem type relative to the reference period 1986–2005. Panel (b) represents the mean

contribution of the four processes in each ecosystem type (net primary production (NPP), transfer efficiency of lower trophic level (TE LTL), transfer efficiency of higher trophic level (TE HTL) and flow kinetic). The contribution is framed in red color if biomass projections with one of the three models predicts changes in the opposite direction to those predict with the two other models..... 59

Figure 3.6: Changes in trophic structure under RCP2.6 and 8.5. (a) Biomass trophic spectra for RCP2.6 and RCP8.5 in 2090–2099 and the reference period in 1986–2005, while (b) Changes in biomass for each trophic class of width 0.1 trophic level (TL) between TL = 2 and TL = 5.5 under RCP2.6 and RCP8.5 relative to the reference period 1986–2005. (c) The ratio of biomass trophic spectra in 2090–2099 for RCP8.5 and for the reference period 1986–2005 derived from EcoTroph projections in which each flow parameter is successively isolated (net primary production (NPP), transfer efficiency of lower trophic level (TE LTL), transfer efficiency of higher trophic level (TE HTL) and flow kinetic)..... 60

Figure 3.7: Changes in trophic structure in each ecosystem type for RCP2.6 and 8.5. The two panels show the ratio of the biomass spectrum in 2090–2099 to the reference period 1986–2005 for RCP2.6 (a) and RCP8.5 (b) for each ecosystem type..... 61

Figure 3.8: Changes in production at global scale and in each ecosystem type over the 21st century. Panel (a) represents the changes in total consumer production and biomass and in kinetic under RCP8.5 by 2100 relative to the reference period 1986–2005 while panel (b) represents the changes in total consumer production for RCP8.5 in each ecosystem type. Panel (c) represents the changes in prey (between trophic level (TL) = 2.5 and TL = 3.5) and predator (up to TL = 3.5) under RCP2.6 and RCP8.5..... 62

Figure 4.1: Schematic representation of the EcoTroph model in the European continental shelf sea. The downward green arrows represent the biomass flow from pelagic to benthic-demersal pathways, assumed to be 20% of the flow at each trophic level..... 76

Figure 4.2: Map of the study areas and fisheries catch per unit area (t.km^{-2}) in 2013–2017. The spatial distribution of the annual average catch per area (km^2) between 2013 and 2017 are represented for pelagic species (a) and benthic-demersal (b) species in the 15 ICES divisions. The grey line is the boundary of the POLCOMS-ERSEM model, while codes of each division refer to the numbering used by ICES..... 77

Figure 4.3: Map of the biomass of secondary producers per unit area (ton.km^{-2}) in 2013–2017: (a) for zooplankton, and (b) for benthic secondary producers. On the panel (a), the figures displayed on two divisions (4a and 8c) are the multiplier coefficients to elevate the biomass of pelagic zooplankton so that production support catches at every trophic level..... 78

Figure 4.4: Projected biomass and catch from the European continental shelf trophic systems. EcoTroph projections of biomass (a) and catch (b) trophic spectra (i.e. biomass and catch distribution across trophic levels) for the pelagic and benthic-demersal pathways for the period 2013–2017 (dashed lines) and for the period 2090–2099 (solid lines) under the scenario of constant fishing mortality. The change in total biomass (between TL=2.5 and TL=5.0) (c) and catch (d) between 2020 and 2100 relative to the reference period (2013–2017) are presented under RCP4.5 (green) and

RCP8.5 (red). Panels (e) and (f) show the projected changes in biomass (e) and catch (f) in 2090–2099 relative to 2013–2017 for RCP2.6 (green) and RCP8.5 (red)..... 81

Figure 4.5: Maps of the changes in biomass and catch in 2090–2099 relative to 2013–2017 for the constant fishing mortality scenario. The changes in biomass (a and b) and in catch (c and d) were aggregated between the trophic levels 2.5 and 3.5 (a and c) and between the trophic levels 4 and 5 (b and d)..... 83

Figure 4.6: The drivers of the changes in biomass (a) and catch (b) for the ecosystem. The ratio of catch trophic spectra in 2090–2099 relative to the reference period 2013–2017 derived from the simulations in which each biomass flow parameter is successively isolated (production of secondary producers, transfer efficiency and flow kinetic). The results are presented for RCP8.5 and for the constant fishing mortality scenario..... 84

Figure 4.7: Difference between the two fishing scenarios in the projected changes in biomass and catch in 2090–2099 under RCP8.5. Changes in biomass spectrum (a) and catch spectrum (b) in 2090–2099 relative to the reference period 2013–2017 are represented for the two fishing scenarios under RCP8.5. Additional impact of the constant fishing loss rate scenario (Constant fishing loss rate – constant fishing mortality) in total biomass (c) and catch (d) relative to the reference period are presented under RCP8.5. “morta.” denotes mortality..... 85

Figure 4.8: Differences in fishing mortality and catch in each ICES division between the two fishing scenarios in 2090–2099 under RCP8.5. The panel (a) shows the changes in fishing mortality for the two fishing scenarios in each ICES division. The panel (b) is the map of the ratio of total catch (Constant fishing loss rate/Constant fishing mortality) aggregated between the trophic levels 2.5 and 5..... 86

Figure 5.1: The percent change in total consumer biomass within the Pacific Equatorial Divergence province for the control (solid line) and the lowered phytoplankton iron uptake experiment (dashed line) within the EcoTroph (black) and APECOSM (red). The multi-model mean \pm the standard deviation from the Fish-MIP exercise for the same region forced by IPSL-CM5a output is shown in a thin black solid and dashed line. All changes are relative to 1986–2005. The effect of lowered phytoplankton iron uptake for each model is shown with a red (APECOSM) or black (EcoTroph) arrow..... 99

Figure 5.2: Comparison of the EcoTroph projections with the Fish-MIP projections. Changes in total consumer biomass between 1970 and 2100 relative to the reference period 1986–2005 for 5 ecosystem models and for EcoTroph, for RCP8.5 and with the earth system model IPSL..... 101

Figure 5.3: Map of the predicted fraction of NPP that reaches the seabed (Derived from van Denderen et al. 2018; Supplementary materials).....107

Figure A.3: (a) Correction factor for each trophic level and for each ecosystem type calculated using the Ecopath models from Ecobase. (b) Predicted mean values of TTE including the correction terms in solid line and removing the correction terms in dashed line. The colors refer to the ecosystem types: polar in blue, temperate in orange, tropical in red and in upwelling in green..... 137

Figure A.4.1: Predicted values of TTE (a) and BRT (b) from the models including only SST. The orange curve represents the model without fishing variables and the blue curves represent the predicted values from the model including the 3 categories of catch volume from low amount of catch (in light color) to high amount of catch (in dark color).....	140
Figure A.4.2: Predicted values of TTE (a) and BRT (b) in polar (in blue), temperate (in orange), tropical (in red) and in upwelling (in green) ecosystems for each categories of catch volume from low amount of catch (in light color) to high amount of catch (in dark color).....	140
Figure A.5: (a.) Distribution and mean values of TTE in each ecosystem type and (b.) distribution and mean values of BRT in each ecosystem type (b.). The red dots and the associated values are the mean values of TTE and BRT for each ecosystem type. Comparison between TTE (c.) and BRT (d.) calculated from biomass data and from catch data in a selection of 72 Ecopath models. Colors represent the models ecosystem types (tropical in red, temperate in yellow, polar in blue and upwelling in green). The black line is the identity line($x=y$) and the dashed grey line is the linear relation between indicators calculated from biomass and catch data.....	142
Figure A.6: Predicted values of trophic transfer efficiency and biomass residence time in polar (in blue), temperate (in orange), tropical (in red) and in upwelling (in green) ecosystems between TL=2 and TL=4 (in solid lines) and between TL=2.5 and TL=4 (in dashed lines).....	144
Figure A.7.1: Map of the selection of 153 non-adjacent grid cells far away from at least 1000km.....	146
Figure A.7.2: One of the residual variograms for the trophic transfer efficiency and the biomass residence time, respectively, of the full models developed in the study (black dots) and the model based on the subsample of 153 non-adjacent grid cells (red dots). The red line indicates the minimum distance between the grid cells (1000km).....	146
Figure A.7.3: Predicted values of trophic transfer efficiency (a) and biomass residence time (b) in polar (in blue), temperate (in orange), tropical (in red) and in upwelling (in green) ecosystems for the full models developed in the study (solid lines) and for the mean of the 100 models using the 100 subsamples (dashed lines).....	147
Figure A.8.1: Standardized residuals for the trophic transfer efficiency model. Panel (a) represents the standardized residuals versus the fitted values. Panels (b) and (c) refer to the standardized residuals versus SST and ecosystem type categories, respectively. The global distribution of the standardized residuals is represented on (d) and their distribution for each ecosystem type on (e). Panel (f) is the residuals normal Q-Q plot with the Q-Q line (dashed line). The colors refer to the ecosystem types: polar (in blue), temperate (in orange), tropical (in red) and upwelling (in green).....	149
Figure A.8.2: Standardized residuals for the biomass residence time model. Panel (a) represents the standardized residuals versus the fitted values. Panels (b) and (c) refer to the standardized residuals versus SST and ecosystem type categories, respectively. The global distribution of the standardized residuals is represented on (d) and their distribution for each ecosystem type on (e). Panel (f) is the residuals normal Q-Q plot with the Q-Q line (dashed line). The	

colors refer to the ecosystem types: polar (in blue), temperate (in orange), tropical (in red) and upwelling (in green)..... 150

Figure A.9: Mean values of the observed past trend in trophic transfer efficiency and biomass residence time in each ecosystem type. The colors refer to the ecosystem types: polar (in blue), temperate (in orange), tropical (in red) and upwelling (in green). Shaded areas refer to bootstrap confidence intervals at 95%..... 151

Figure B.1.1: Schematic representation of biomass flow parameters between two trophic levels (TLs). Black arrows represent energy transfers. The prey has a TL τ and the predator has a TL $(\tau + 1)$ (derived from du Pontavice, 2019; Gascuel et al., 2008; Maureaud et al., 2017) 153

Figure B.1.2: Illustration of the transition from a discrete to continuous representation of biomass flow in an ecosystem. Grey broken lines refer to the trajectories of single particles along trophic levels, while the continuous line refers to the mean trajectory of biomass flow from low to upper trophic levels. (From Gascuel et al. 2008) 154

Figure B.2: Map of the areas represented in the dataset and the associated ecosystem types. The colors refer to the ecosystem types: Arctic (in light blue), Antarctic (in dark blue), temperate (in orange), tropical (in red) and upwelling (in green)..... 156

Figure B.3.1: Change in TE LTL (transfer efficiency for low trophic levels; black line and axis) and SST (sea surface temperature; blue line and axis) for GFDL and under RCP8.5 between 1950 and 2100 relative to the reference period 1986-2005..... 157

Figure B.3.2: Difference between delta SST (SST in [2090-2099] - SST in [1986-2005]) for RCP8.5 and RCP2.6 (black points). The two lines represent the two linear selected after and before 2031 158

Figure B.3.3: Mean transfer efficiency of the planktonic food web for the period 1986-2005. It is estimated from the planktonic food web COBALT model developed by Stock et al. (2014a, b) (see Methods in the main text)..... 158

Figure B.3.4: Distribution of TE LTL in each ecosystem type for the period 1986-2005. The vertical lines represent the median TE LTL for each ecosystem type 159

Figure B.5: Inter-model variability of the changes in total consumer biomass under RCP 8.5 in 2090-2099 relative to 1986-2005. Panel (a) represents the variability of the projected changes of biomass among the models (Coefficient of variation in %). Panel (b) shows the grid cells where the three models do not predict the same direction of changes. The color in each grid cell refers to the model that predicts changes in biomass in the opposite direction to those predict by the two others models..... 161

Figure B.6: Comparison of the EcoTroph projections with the Fish-MIP projections. Changes in total consumer biomass between 1970 and 2100 relative to the reference period 1986-2005 for 5 ecosystem models and for EcoTroph, for RCP8.5 and with the earth system model IPSL..... 162

Figure B.7: Projected changes in sea surface temperature (SST) between 1950 and 2100 relative to 1986-2005. Panel (a) represents the changes in SST at global scale for RCP2.6 and RCP8.5. Panel (b) represents the change in each ecosystem type under RCP8.5. The shaded areas around the

curves in (b) indicate the inter-model variability and the colour bars outside the box indicate the range of averaged changes of the three Earth system models over 2090–2099. Panel (c) represents the change over the period 2090–2099 in each 1°x1° grid cell. Panels (d) and (f), show the relationships between SST and, flow kinetic (Gascuel et al., 2008) and TE HTL (transfer efficiency of higher trophic levels; du Pontavice et al., 2020), respectively. Panels (e) and (g), represent the warming effects (from 0 to 10°C increase) on flow kinetic and TE HTL, respectively. In panel (d), the different curves represent the temperature effect on flow kinetic for five trophic levels since flow kinetic depends on temperature and trophic level. Supplementary material B.8: Contribution of each biomass flow parameters to the changes in total biomass consumer for the three Earth system models..... 163

Figure C.1.1: Global projected changes in biomass and catch at each trophic level in 2090-2099 relative to 2013-2017 for four top down configurations ($\alpha=0.4$ and $\gamma=0.5$; $\alpha=0$ and $\gamma=0.5$; $\alpha=0.8$ and $\gamma=0.5$; $\alpha=0.4$ and $\gamma=1$). The change in biomass (a) and catch (b) are presented the simulation where fishing mortality is constant and equal to its value in 2013-2017 for RCP8.5..... 167

Figure C.1.2: Maps of the changes in biomass in 2090-2099 relative to 2013-2017 for four top down configurations: ($\alpha=0.4$ and $\gamma=0.5$; $\alpha=0$ and $\gamma=0.5$; $\alpha=0.8$ and $\gamma=0.5$; $\alpha=0.4$ and $\gamma=1$). The changes are aggregated between the trophic level 3 and 3.9 (a, c, e, g) and between the trophic level 4 and 5 (b, d, f, h). The changes were calculated with a constant fishing mortality equal to its value in 2013-2017 for RCP8.5. The displayed percentages for biomass (b, d, f, h) represent the percentage of amplification between the changes in biomass at the lower and the upper trophic levels..... 168

Figure C.1.3: Maps of the changes in catch in 2090-2099 relative to 2013-2017 for four top down configurations: ($\alpha=0.4$ and $\gamma=0.5$; $\alpha=0$ and $\gamma=0.5$; $\alpha=0.8$ and $\gamma=0.5$; $\alpha=0.4$ and $\gamma=1$). The changes are aggregated between the trophic levels 2.5 and 3.5 (a, c, e, g) and between the trophic level 4 and 5 (b, d, f, h). The changes were calculated with a constant fishing mortality equal to its value in 2013-2017 for RCP8.5. The displayed percentages (b, d, f, h) represent the percentage of amplification between the changes in catch at the lower and the upper trophic levels..... 169

Figure C.2.1: Global projected changes in biomass and catch at each trophic level in 2090-2099 relative to 2013-2017 for a coupling parameter à 20% (coupling parameter of the study) and at 40% (coupling parameter for the sensitivity analysis). The change in biomass (a) and catch (b) are presented the simulation where fishing mortality is constant and equal to its value in 2013-2017 for RCP8.5..... 170

Figure C.2.2: Maps of the changes in biomass in 2090-2099 relative to 2013-2017 for a coupling parameter à 20% (coupling parameter of the study) and at 40% (coupling parameter for the sensitivity analysis). The changes are aggregated between the trophic level 2.5 and 3.5 (a, c) and between the trophic level 4 and 5 (b, d). The changes were calculated with a constant fishing mortality equal to its value in 2013-2017 for RCP8.5. The displayed percentages for biomass (b, d) represent the percentage of amplification between the changes in biomass at the lower and the upper trophic levels..... 171

Figure C.2.3: Maps of the changes in catch in 2090-2099 relative to 2013-2017 for a coupling parameter à 20% (coupling parameter of the study) and at 40% (coupling parameter for the sensitivity analysis). The changes are aggregated between the trophic level 2.5 and 3.5 (a, c) and

between the trophic level 4 and 5 (b, d). The changes were calculated with a constant fishing mortality equal to its value in 2013-2017 for RCP8.5. The displayed percentages for biomass (b, d) represent the percentage of amplification between the changes in catch at the lower and the upper trophic levels..... 172

Figure C.3.1: Projected changes in production of secondary producers (left column) and sea surface temperature (SST; right column) between 2020 and 2100 relative to the reference period 2013-2017 for the ICES divisions 4a, 4b, 4c, 6a. The production is divided into the pelagic zooplankton group (in green) and the benthic fauna group (in brown) and the changes are presented for two scenarios RCP4.5 (dotted lines) and RCP8.5 (solid lines). The changes in SST are presented for the two scenarios RCP4.5 (green) and RCP8.5 (red)..... 173

Figure C.3.2: Projected changes in production of secondary producers (left column) and sea surface temperature (SST; right column) between 2020 and 2100 relative to the reference period 2013-2017 for the ICES divisions 7a, 7b, 7d, 7e, 7f, 7g and 7h. The production is divided into the pelagic zooplankton group (in green) and the benthic fauna group (in brown) and the changes are presented for the two scenarios RCP4.5 (dotted lines) and RCP8.5 (solid lines). The changes in SST are presented for the two scenarios RCP4.5 (green) and RCP8.5 (red)..... 174

Figure C.3.3: Projected changes in production of secondary producers (left column) and sea surface temperature (SST; right column) between 2020 and 2100 relative to the reference period 2013-2017 for the ICES divisions 8a, 8b, 8c, 9a. The production is divided into the pelagic zooplankton group (in green) and the benthic fauna group (in brown) and the changes are presented for the two scenarios RCP4.5 (dotted lines) and RCP8.5 (solid lines). The changes in SST are presented for the two scenarios RCP4.5 (green) and RCP8.5 (red)..... 175

Figure C.4: Map of the ratio between the theoretical unexploited ecosystem and the exploited ecosystem in 2017-2017 for production (a and b) and for biomass (c and d) as well as for lower trophic levels (between TL=2.5 and TL=3.5) (a and c) and for upper trophic levels (between TL=4 and TL=5) (b and d)..... 176

Figure C.5.1: The drivers of the changes in biomass in four ICES divisions (4a, 4b, 4c, 6a) for total biomass, benthic biomass and pelagic biomass. The ratio of biomass trophic spectra in 2090-2099 to the reference period 2013-2017 are derived from the simulations in which each flow parameter is successively isolated (Production of secondary producers, transfer efficiency and Kinetic). The results are presented for RCP8.5 and for the constant fishing mortality simulation.. 178

Figure C.5.2: The drivers of the changes in biomass in seven ICES divisions (7a, 7b, 7d, 7e, 7f, 7g, 7h) for total biomass, benthic biomass and pelagic biomass. The ratio of biomass trophic spectra in 2090-2099 to the reference period 2013-2017 are derived from the simulations in which each flow parameter is successively isolated (Production of secondary producers, transfer efficiency and Kinetic). The results are presented for RCP8.5 and for the constant fishing mortality simulation..... 179

Figure C.5.3: The drivers of the changes in biomass in seven ICES divisions (8a, 8b, 8c, 9a) for total biomass, benthic biomass and pelagic biomass. The ratio of biomass trophic spectra in 2090-2099 to the reference period 2013-2017 are derived from the simulations in which each flow

parameter is successively isolated (Production of secondary producers, transfer efficiency and Kinetic). The results are presented for RCP8.5 and for the constant fishing mortality simulation.. 180

Figure C.6.1: The drivers of the changes in catch in four ICES divisions (4a, 4b, 4c, 6a) for total catch, benthic catch and pelagic catch. The ratio of catch trophic spectra in 2090-2099 to the reference period 2013-2017 are derived from the simulations in which each flow parameter is successively isolated (Production of secondary producers (in green), transfer efficiency (in blue) and Kinetic (in red)). The results are presented for RCP8.5 and for the constant fishing mortality simulation..... 181

Figure C.6.2: The drivers of the changes in catch in seven ICES divisions (7a, 7b, 7d, 7e, 7f, 7g, 7h) for total catch, benthic catch and pelagic catch. The ratio of catch trophic spectra in 2090-2099 to the reference period 2013-2017 are derived from the simulations in which each flow parameter is successively isolated (Production of secondary producers (in green), transfer efficiency (in blue) and Kinetic (in red)). The results are presented for RCP8.5 and for the constant fishing mortality simulation..... 182

Figure C.6.3: The drivers of the changes in catch in seven ICES divisions (8a, 8b, 8c, 9a) for total catch, benthic catch and pelagic catch. The ratio of catch trophic spectra in 2090-2099 to the reference period 2013-2017 are derived from the simulations in which each flow parameter is successively isolated (Production of secondary producers (in green), transfer efficiency (in blue) and Kinetic (in red)). The results are presented for RCP8.5 and for the constant fishing mortality simulation..... 183

Figure C.7: The changes in biomass of secondary producers against the changes in sea surface temperature in each division for the constant fishing mortality (a and b) and for the constant fishing loss rate (c and d) simulations. The changes in total biomass and catch are presented as colour gradients red and orange, respectively..... 184

List of Abbreviations

APECOSM	Apex Predators ECOSystem Model
BOATS	BiOeconomic mArine Trophic Size-spectrum
BRT	Biomass Residence Time
COBALT	Carbon, Ocean Biogeochemistry, and Lower Trophics
DBEM	Dynamic Bioclimate Envelope Model
DPBM	Dynamic Pelagic Benthic
ERSEM	European Regional Seas Ecosystem Model
FAO	Food and Agriculture Organization
Fish-MIP	Fisheries and Marine Ecosystem Model Intercomparison Project
GFDL	Geophysical Fluid Dynamics Laboratory
IPCC	Intergovernmental Panel on Climate Change
IPSL	Institut Pierre Simon Laplace
ICES	International Council for the Exploration of the Sea
MPI	Max Plank Institute
NPP	Net Primary Production
POLCOMS	Proudman Oceanographic Laboratory Coastal Ocean Modelling System
RCP	Representative Concentration Pathways
SST	Sea Surface Temperature
TL	Trophic Level
TTE	Trophic Transfer Efficiency
TTE HTL	Trophic Transfer Efficiency of High Trophic Levels
TTE LTL	Trophic Transfer Efficiency of Low Trophic Levels

Acknowledgements

First and foremost, I would like to thank my two supervisors Didier Gascuel and William Cheung for giving me the opportunity to pursue my PhD. I have had the privilege of learning how to be a scientist from two very fine examples. As supervisors, you have given me the best support and have had trust in my abilities, which were a great motivator for me. You offered me the possibility to travel between UBC and Agrocampus Ouest, what has been a fantastic experience.

Didier merci tout d'abord d'avoir conçu ce projet de recherche ambitieux et de m'avoir offert la possibilité de le défendre au concours de l'Ecole Doctorale VAS. Je retiens en particulier ton optimisme sans faille et ta bonne humeur communicative qui ont très largement contribué au plaisir que j'ai eu à réaliser cette thèse sous ton encadrement. Je suis particulièrement reconnaissant du soutien que tu m'as toujours apporté et de tes encouragements dans les moments plus délicats. Quoi de mieux quand je n'avais pas face à des problèmes récalcitrants, que de passer dans ton bureau. Je ressortais toujours gonflé à bloc avec plein de pistes à explorer!

William, first, I thank you for your great patience and perseverance to help me to establish the Joint PhD Agreement! It was a great pleasure for me to work with you in CORU. Your guidance and insights have had invaluable for my Ph.D. You have always encouraged me to explore new promising ways and to improve the scientific rigour of my research.

I would also like to thank the Nippon Foundation - Nereus Program for funding one year of my Ph.D. and offering me the great privilege and opportunity to be a Nereus fellow. A special thanks to Yoshi and William for leading this outstanding program and to Andres and Vicky for their incredible work as program managers. Discussing and collaborating with all the fellows, PIs and collaborators of Nereus coming from different institutes and research fields was particularly thrilling.

I thank my Ph.D. committee members from both UBC and Agrocampus Ouest: Daniel Pauly, Mary O'Connor, Olivier le Pape, Olivier Maury, Morgane Travers-Trolet and Matthieu Colléter. They guided me over the course of my degree, and gave me precious comments and suggestions.

I would also like to thank all the researchers who advised me and with whom I collaborated for my Ph.D. project. In particular, I thank Charles Stock for providing global plankton data and many insights regarding our modelling approach, Susan Kay for providing regional biogeochemical and plankton data and Daniel Pauly for his valuable feedback and advice.

Je tiens également à exprimer mon infinie reconnaissance à Jérôme qui m’a appris à me servir d’un ordinateur ! Tu as été extrêmement patient et bienveillant avec moi ! Tout le temps et l’énergie que tu m’as accordés m’ont permis d’acquérir des compétences primordiales pour ma thèse. Je voudrais également remercier Gabriel pour son accompagnement au quotidien pendant mes périodes à UBC. Je pense qu’on peut s’accorder sur le fait que tu as été mon co-encadrant officiel. Ton implication dans mes travaux de recherche et tes conseils ont grandement contribué à l’aboutissement de cette thèse. Je retiens notamment nos échanges sur des questions de biogéographie et de plancton, deux mondes que j’ai découvert à travers nos discussions. Je remercie également Aurore qui m’a prodigué de précieux conseils concernant les indicateurs de transfert trophique qu’elle a développés au cours de son stage de Master.

During my thesis, I had the opportunity to work on several side projects more or less linked to my PhD regarding the metapopulation of common soles in Eastern English Channel, the survival of salmon in North Atlantic, the future of French fisheries, the consequences of the uncertainties in the biological iron cycle and the trophic transfer efficiency within marine ecosystems. Therefore, I would like to thank all the researchers with whom I collaborated on these projects and, in particular, Marine Randon, Maxime Olmos, Alessandro Tagliabue, Tyler Eddy, Martin Doray, Olivier le Pape and Etienne Rivot.

I offer my enduring gratitude to the faculty, staff and students at UBC who welcomed me at the Institute for the Oceans and Fisheries and in CORU: Juliano, Tayler, Virginie, Colette, Oai Li, Ravi, Vicky, Muhammed, William, Andres, Patricia, JJ, Tomoka, Travis, Melanie, Deng... I owe particular thanks to Ursula and Rick for welcoming in Vancouver and for their kindness. I would also like to thank warmly Gabriel and Claire for their kindness and the great moments spent together in Vancouver.

Ces remerciements s’adressent également à toute l’équipe de Rennes qui a très largement contribué au plaisir que j’ai eu à réaliser cette thèse. Tant de bon moments passés à vos côtés entre les apéros du vendredi soir, les sessions de course du midi, les sorties en mer... Mais plus généralement, je retiens votre bonne humeur et votre gentillesse au quotidien. Dans le désordre et au risque d’oublier certaines personnes, un grand merci à Olivier, Didier, Hervé, Etienne, Jérôme, Thomas, Marie, Kat’, Cath’, Maxime, PY, Erwan, Louise, JB, Julie, Auriane, Lucille, Elodie, Amélie, Ilan, Maud, Shani, Morgane, Jennifer, Sophie, Mathilde, Vianney, Pierre, Jean-Eude... Quelques remerciements spéciaux s’imposent également. Merci à tous les coureurs de l’équipe et particulier à Jérôme, Olivier, Thomas, PY, Marine et bien sûr Etienne (célèbre pour sa Rivotite) qui, grâce à votre motivation sans faille, m’avez permis de garder un corps d’athlète (ou presque) tout au long de ma thèse! Merci aussi à Olivier, Max, Erwan, Marine et

Thomas pour les sessions de chasse sous-marine à la recherche de coquilles, d'huitres (pour certaine), d'araignées...

Je remercie également mes copains et amis pour tous les bons moments passés ensemble et sans lesquels la vie n'aurait pas la même saveur. Je tiens particulièrement à remercier PY avec qui j'ai commencé et avec qui je termine cette thèse, je te remercie pour ton soutien, ton écoute et tous les bons moments qu'on a passé tout au long de ces 3-4 années.

Je remercie évidemment ma famille pour m'avoir toujours encouragé et apporté leur soutien indéfectible et leur affection. Enfin, et surtout, je tiens à adresser le plus grand des mercis à Anne et Anatole. Merci Anne de me supporter depuis toutes ces années, d'avoir toujours cru en moi et d'être à mes côtés dans les bons comme dans les moments les plus délicats. Je te suis particulièrement reconnaissant d'avoir mis ta vie professionnelle entre parenthèse en me suivant à Rennes et à Vancouver pour que je puisse réaliser cette thèse. Anatole, si tu lis un jour cette thèse (ou juste les remerciements), je te remercie pour le bonheur que tu me procures au quotidien. Ta joie de vivre, tes éclats de rire et ta simple présence me rappellent tous les jours ce qui est essentiel dans la vie.

To Anne and Anatole,

CHAPTER 1

General introduction

CHAPTER 1: General introduction

"What is a scientist after all? It is a curious man looking through a keyhole, the keyhole of nature, trying to know what's going on."

Jacques-Yves Cousteau

This opening chapter aims to state the challenges face by the oceans and introduce the conceptual and methodological approach developed in the thesis. After highlighting the importance of the oceans and the threats and pressures affecting marine ecosystems, we present the status of the world fisheries and their main consequences on marine life. In the third part, we detail the already observed and projected effects of climate-induced changes in ocean conditions on the structure and functioning of marine ecosystems. Then, we focus on the trophodynamics properties of aquatic food webs which determine the features of biomass flows in marine food webs. A special attention is paid to the EcoTroph modelling approach which is the conceptual and methodological framework of the thesis, after presenting the diversity of marine ecosystems modelling and their importance to understand the future of marine ecosystems. Finally, we detail the objectives, the hypothesis and the structure of the thesis.

1.1. An ocean under pressure

The ocean covers 363 million km², a surface equivalent to 71% of the earth's surface and contains about 97% of the Earth's water. Nearly 2.4 billion people - 40% of the world's populations - live within 100 km (Small & Cohen 2004) of the sea and over 3 billion people depend directly or indirectly on marine and coastal biodiversity for their livelihoods (CBD 2010). Fish is one of the most important sources of animal protein, rich in essential micronutrients and fatty acids and constitutes the primary sources of protein for a billion people worldwide (Golden *et al.* 2016). In 2015, worldwide fish provide about 17%, and 7% of all proteins, of animal protein consumed by the global population (FAO 2018).

Besides their role of food supply, marine and coastal ecosystems provide several other services to people including ecosystem support, water supply, renewable energy, benefits for health and well-being, tourism and trade. The ocean also plays a fundamental role in the regulation and control within the climate system by storing and distributing large amounts of heat around the globe

via ocean currents. Particularly, it absorbed 93% of the excess heat and between 20 and 30% of the carbon dioxide from human-induced greenhouse gas emissions to the atmosphere (Gattuso *et al.* 2015; IPCC 2019a).

As the world population is experiencing unprecedentedly rapid demographic change, human uses of the ocean are expanding and causing various and cumulative anthropogenic pressures. The different sources of pressures, including climate change, overfishing, habitat degradation, pollution, invasion of non-indigenous species and marine litter, are impacting directly or indirectly the structure and the functioning of marine ecosystems (Coll *et al.* 2008; Halpern *et al.* 2015; IPCC 2019b). A study published in 2015 highlighted that 97.7% of the world ocean is affected by multiple stressors with 66% of the ocean that experienced increases in cumulative impacts between 2008 and 2013 (Halpern *et al.* 2015). All these pressures threaten the ecosystem services provided by the ocean on which human well-being depends. For instance, Golden *et al.* (2016) showed that more than 10% of the world population could face micronutrient and fatty-acid deficiencies due to the decline fisheries catch potential by 2050 under a “no mitigation policy” scenario for climate change, especially in low-latitude regions such as in the Pacific Islands and West Africa (Figure 1.1; Golden *et al.* 2016; Bindoff *et al.* 2019).

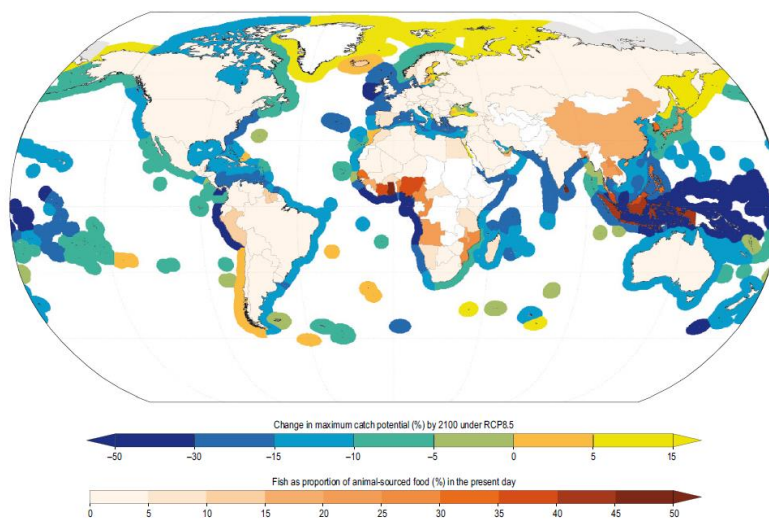


Figure 1.1: Projected changes in catch potential and the reliance of the human population on fish and their vulnerability of micronutrient malnutrition (Golden *et al.*, 2016). The colour scale on land represents the proportion of fish micronutrient intake relative to the total animal-sourced food for the country’s population; the scale on the sea represents the projected changes in maximum catch potential under RCP8.5 by 2100 relative to the 2000s (Figure extracted from IPCC 2019).

In this thesis, I will focus on two of the biggest anthropic pressures which deeply affect marine ecosystems at global scale: the exploitation of fish resources and the climate change.

1.2. The fishing effects on marine life

1.2.1. The state of the world's fisheries

The development of fisheries has led to major changes in marine ecosystems worldwide. Global fisheries catch continuously increased since the 1950s and reached a peak in 1996 with about 130 million tons of catch (Pauly & Zeller 2016). Since the 2000s, global catches have been decreasing (Figure 1.2; Pauly & Zeller 2016). In parallel, global fishing effort has been increasing since the 1950s with a doubling of the global fishing fleet between 1950 and 2015 driven by the substantial expansion of the motorized vessels (Rousseau *et al.* 2019). The development of global marine fishing fleets results mainly from the expansion of European fisheries after World War II, and later by the rapidly growing Asian fisheries since the 1980s (Anticamara *et al.* 2011; Worm & Branch 2012).

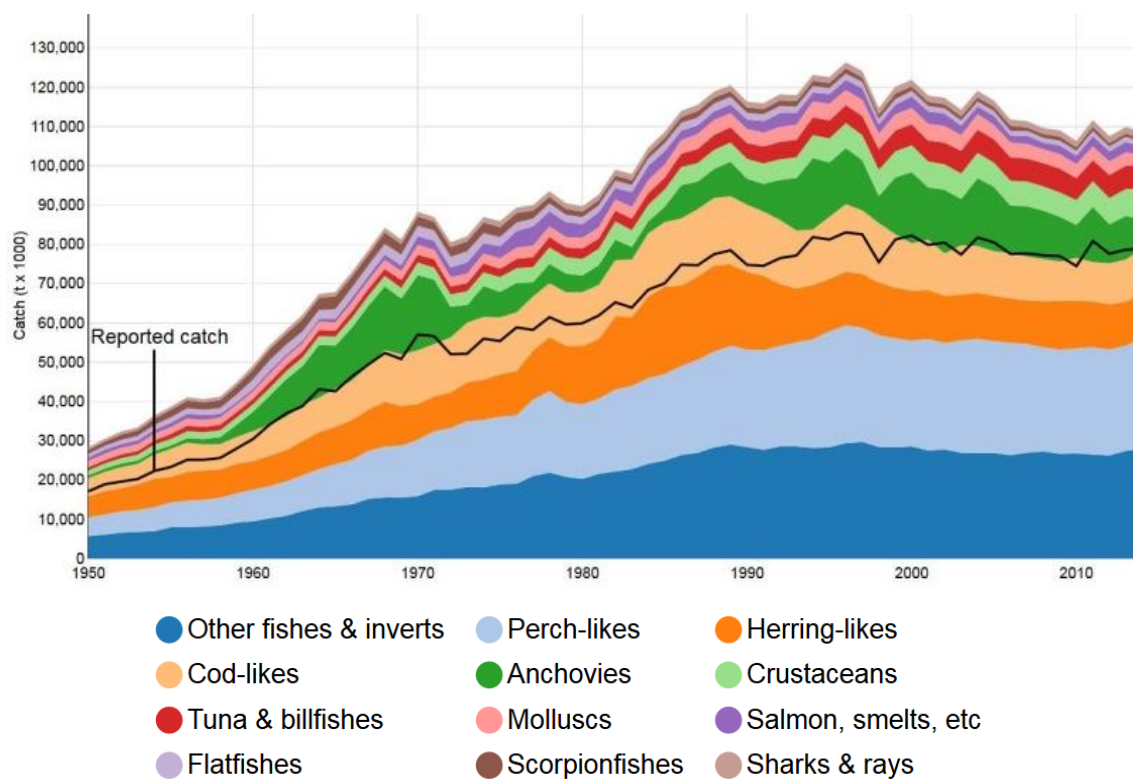


Figure 1.2: Map of the global fisheries catches between 1950 and 2014 (source: <http://www.seaaroundus.org>, black line refers to the catch officially reported by the FAO).

The development of the world fisheries raised major concerns regarding the state of the exploited stocks. According to the United Nations' Food and Agriculture Organization (FAO), the proportion of assessed fish stocks within biological sustainable levels is decreasing since the 1970s from 90% in 1974 to 67% in 2015 (Figure 1.3; FAO 2018). At the same time, the proportion of overfished stocks is increasing from 10% to 28–33% of the world's assessed fish stocks (Branch *et al.* 2011; FAO 2018) and it appears that 7–14% of these stocks are collapsed (Worm *et al.* 2009; Branch *et al.* 2011). Also, the over-exploitation of fish stocks could be underestimated because many fish stocks are not monitored or/and not assessed (Worm *et al.* 2009). In recent years, while more effective fisheries management in developed countries reduced the proportion of overexploited stock (Hilborn *et al.* 2020), over-exploitation continued in many developing countries (Ye & Gutierrez 2017; FAO 2018).

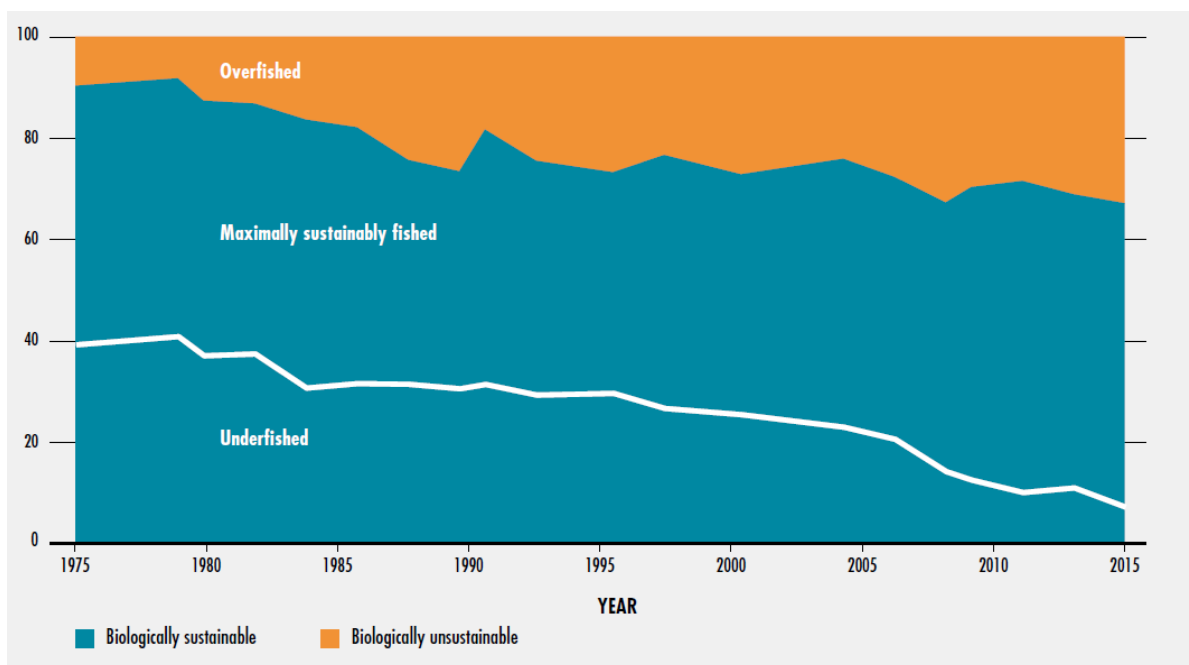


Figure 1.3: global trends in the state of the world's marine fish stocks, 1974–2015 (Figure derived from FAO 2018).

1.2.2. The fishing effects on marine populations

Fishing has led to decreases in abundance of exploited species with many overexploited fish stocks at the global scale (Costello *et al.* 2016; FAO 2018) and is recognized as the main cause of impact on marine biodiversity by IPBES (IPBES 2019). Marine predatory fish have been affected in

the last 50 years with major declines in fish stock abundance in many ecosystems and at global scale (Myers & Worm 2003; Ward & Myers 2005; Tremblay-Boyer *et al.* 2011; Christensen *et al.* 2014; McCauley *et al.* 2015; IPBES 2019) including biologically vulnerable fish stocks in the deep ocean (Devine *et al.* 2006). The size-selective harvesting of marine populations by commercial fisheries can alter their demographic structure by decreasing the average body size and age (Ricker 1981; Law 2000; Hutchings 2005; Anderson *et al.* 2008). Such changes can result in an increasingly unstable population dynamic due to changes in demographic parameters and a higher sensitivity of the population to recruitment and ultimately to environmental variability (Anderson *et al.* 2008; Hidalgo *et al.* 2011). Substantial changes in growth rates and size and age at maturation has also been widely observed as a response to the selective removal of larger and older individuals by fisheries (Law 2000; Conover & Munch 2002; Olsen *et al.* 2004; Edeline *et al.* 2007; Jørgensen *et al.* 2009; Enberg *et al.* 2012).

1.2.3. The fishing effects on marine communities

These effects at organism and population level have been propagated at community level by modifying species assemblages and thus species interactions (Bianchi 2000; Ward & Myers 2005; Heithaus *et al.* 2008). Removal of one part of the ecosystem can result in cascading effects through the trophic levels below and reorganizations of the entire food web. An example of trophic cascade was observed in the Northwest Atlantic ecosystem where the collapse of the cod in the 1980s led to the restructuring of the entire ecosystem from cod preys to phytoplankton (Frank 2005). Furthermore, overfishing of predators led to a decrease in the mean trophic level of the catch since the 1950s, a phenomenon termed “fishing down the marine food web” (Pauly 1998). That means that the depletion of high trophic level species caused by overfishing has altered the structure of the food web leading to a shift in communities towards lower trophic level and a replacement of high trophic level species in the fisheries with lower trophic level species. However, when it is only observed in catch data, this decrease in the mean trophic level can also be due to a “fishing through the food web” effect (Essington *et al.* 2006), i.e., the introduction of low trophic level species in the fisheries which can be due to a change in the fishing strategies induced by economical or technological changes, without any decrease of predators abundance. “Fishing down” versus “fishing through” have been the subject of scientific controversies, while several studies concluded both processes often simultaneously occurred (e.g., Gascuel *et al.* 2016 in European waters).

Overfishing of forage fish may affect the upper trophic levels as well (Pikitch *et al.* 2014). By transferring production from zooplankton to top predators, forage fish play a pivotal role in marine

food web. They constitute a substantial food source for many predators including piscivorous fish, seabirds, marine mammals, large pelagic and can exert bottom up control on the upper part of the food web (Cury *et al.* 2011; Smith *et al.* 2011; Kaplan *et al.* 2013; Pikitch *et al.* 2014). However, the forage fish removal by fisheries does not systematically lead to a decrease in top predator and remains contentious among fisheries scientists (Pikitch *et al.* 2014; Hilborn *et al.* 2017). The high sensitivity of forage fish populations to climate-driven changes in marine ecosystems and the diet flexibility of many predators might reduce the strength of the connection between the abundances of top predators and forage fish (Engelhard *et al.* 2014a; Hilborn *et al.* 2017).

1.2.4. Synergistic effects of fishing and climate

The fishing-induced alteration of the structure of populations and ecosystems can reduce the level of ecosystems resilience and stability, compromising the recovery of fish stocks and the capacity of fisheries to buffer the long-term climate changes and climate variability (Figure 1.4; Perry *et al.*, 2010; Planque *et al.*, 2010). The increase in sensitivity to climate variability is especially due to the removal of large-old individuals, spatial contraction and alteration of life history traits. The changes of metapopulation structure can also alter the capacity of populations to withstand climate variability and change. Overall, the reduction of the diversity (genetic, specific and functional) and the complexity of marine ecosystems tend to reduce their resilience to perturbations.

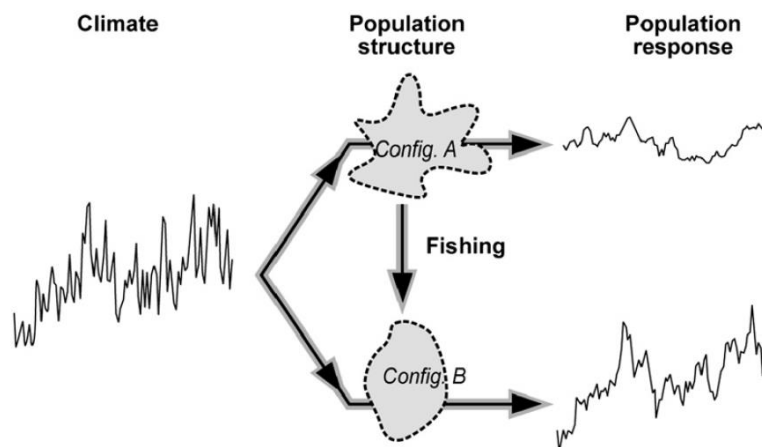


Figure 1.4: A schematic representation of increased correlation of a marine population (e.g., abundance) to climate forcing under exploitation (Figure extracted from Perry *et al.* 2010).

In the European seas, this situation was revealed in the North Sea where climate and fishing acted synergistically by deeply modifying the ecosystem structure from zooplankton community to

the Atlantic cod population (Kirby *et al.* 2009; Engelhard *et al.* 2014b). Similarly, over the 20th century, in the Western English Channel, the long-term investigation of demersal fish assemblages showed a reshaping of the demersal community through size-dependent responses of species to climate change and fishing (Genner *et al.* 2010). The authors of this study suggested that the changes in abundance of smaller species were closely linked to changing thermal conditions while the decline in abundance and body size of larger species was primarily induced by size-selective overharvesting (Genner *et al.* 2010)

1.3. The climate change effects on marine ecosystems

1.3.1. The climate-induced changes in ocean conditions

Human activities have perturbed the natural carbon cycle by releasing massive quantity of greenhouse gas in the atmosphere since the mid 1800 (IPCC 2014, 2019b), consequently affecting the earth climate and ocean systems (Bindoff *et al.* 2019). As a result, the ocean is becoming warmer, acidifying and its oxygen content is decreasing relative to pre-industrial level (IPCC 2014, 2019b; Gattuso *et al.* 2015; Hoegh-Guldberg *et al.* 2018; Bindoff *et al.* 2019). The ocean has substantially warmed from the surface to the deeper layer (700-2000m) and even likely the deep ocean below 2000m (IPCC 2019b). The sea surface temperature has increased by 0.83°C in the 2010s relative to 1870–1899 according to the outputs of 10 Earth system models (Bopp *et al.* 2013; Gattuso *et al.* 2015). In parallel, the surface water pH has declined by 0.11 over the same period (Bopp *et al.* 2013; Gattuso *et al.* 2015). According to IPCC (2019), a decrease of the oxygen content was also observed in the open ocean with a likely loss of oxygen of 0.5–3.3% over the period 1970–2010 and an expansion of the oxygen minimum zones by a range of 3–8%, especially in the tropical regions.

Unmitigated climate change is expected to lead to continuous ocean warming, acidification and decline in oxygen content (Figure 1.5; IPCC 2019). To analyze the future global climate dynamics, Earth system models are developed to project the future changes in climate and ocean properties under different scenarios of greenhouse gas emissions. The Intergovernmental on Climate Change (IPCC) uses a set of four scenarios called Representative Concentration Pathways (RCPs, http://sedac.ipcc-data.org/ddc/ar5_scenario_process/RCPs.html). They are based on the possible range of radiative forcing values by the end of the 21st century (2.6, 4.5, 6.0 and 8.5W.m⁻²). For example, the low emission “strong mitigation” scenario (RCP2.6) is projected to keep global mean atmosphere temperature 2°C while under the “no mitigation policy” scenario (RCP8.5), greenhouse gas concentration will continue to rise throughout the 21st century. Under RCP8.5, the Earth system

models has projected the sea surface warming of 2.73°C, the decline of the surface pH of 0.33 and the decrease in oxygen content of the surface waters by 3.48% in 2090–2099 relative to the period 1990–1999.

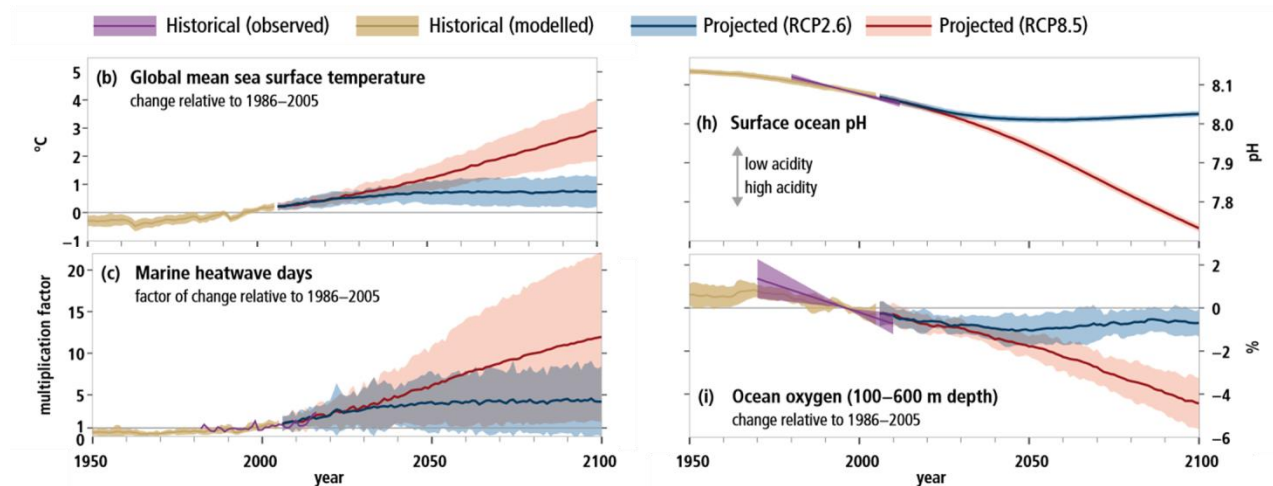


Figure 1.5: Observed and modelled historical changes in the ocean and cryosphere between 1950 and 2100, and projected future changes under low (RCP2.6) and high (RCP8.5) greenhouse gas emissions scenarios (Figure adapted from IPCC 2019).

The profound changes in the physical and chemical properties of the ocean result in serious implications for marine life induced by multiple processes acting at all the ecological scales from organisms to ecosystem levels (Poloczanska *et al.* 2016; Pecl *et al.* 2017; Cheung 2018; Bindoff *et al.* 2019; Lotze *et al.* 2019).

1.3.2. Impacts on primary production

Phytoplankton, which provides 90% of the oceanic primary production, plays an essential role in marine food webs in channelling energy and biomass up marine food webs. Phytoplankton biomass is predominately driven by nutrient availability, light limitation and temperature (Steinacher *et al.* 2010). Although long-term trends in global ocean primary production have not emerged out of their natural variations, several studies have shown local, regional and seasonal changes in ocean chlorophyll or primary production (Boyce *et al.* 2014; Gregg & Rousseaux 2014). Simulation of primary production using Earth system models projected global decrease over the course of the 21st century (Bopp *et al.* 2013; Cabré *et al.* 2015; Laufkötter *et al.* 2015)

However, the large uncertainties of projections under the contrasting RCPs are exacerbated by model uncertainty and internal climate variability (Frölicher *et al.* 2016). The projected evolution

of ocean primary productivity shows a tendency for decreasing the net primary production (NPP) in the low-latitude regions and an increasing NPP at high latitudes. The declines in NPP in tropical and subtropical regions are predominantly a consequence of climate-driven changes in nutrient supply (largely due to increasing stratification) and in metabolic processes notably linked to ocean warming. In contrast, the projected increase in NPP at high latitudes is mainly due to the increase in light availability and iron supply (Bopp *et al.* 2013; Cabré *et al.* 2015; Laufkötter *et al.* 2015).

1.3.3. Impacts on upper trophic levels

Ocean warming affects marine organisms through species thermal preference and tolerance (Pörtner & Peck 2010; Kroeker *et al.* 2013; Deutsch *et al.* 2015; Nagelkerken & Connell 2015). Specifically, for marine ectotherms (whose regulation of body temperature depends on external heat), their physiological functions are directly impacted by the increases in temperature with direct effects on metabolism leading to changes in body function, growth rate, maximum body size and reproductive rates (Pörtner & Peck 2010; Kroeker *et al.* 2013; Deutsch *et al.* 2015; Poloczanska *et al.* 2016; Pauly & Cheung 2017). Besides, other climatic stressors such as oxygen reduction or ocean acidification may exacerbate the sensitivity of marine species to temperature, although the range of tolerance to the multiple environmental stressors is highly variable among taxonomic groups and life stages - the early stages generally being more sensitive (Kroeker *et al.* 2013; Poloczanska *et al.* 2013; Nagelkerken & Connell 2015; Cripps *et al.* 2016; Pauly & Cheung 2017; Pörtner *et al.* 2017).

Marine population's distribution can also shift in response to changing conditions by decreasing their ability to survive in their current realized niche or by increasing their ability to live in a new area. The capacity of organisms to track a suitable habitat as a response to changes in ocean conditions may be regulated by multiple factors such as the rate of reproduction, the generation times, dispersal ability, abundance, and geographical range (Bates *et al.* 2014; Poloczanska *et al.* 2016; Pinsky *et al.* 2020). They are associated generally with either an expansion of populations at the northern boundary of its species range or a contraction of populations at the southern boundary of its species range or the combination of the two latter processes (Poloczanska *et al.* 2016). While general observations and expectations are poleward distribution shifts (Poloczanska *et al.* 2013, 2016) and could reach, at global scale, 25km per decade for the high carbon emission scenario over the middle of the 21st century (Figure 1.6; Jones & Cheung 2015), patterns in distribution shifts show substantial differences in rates and directions. That includes east-west and depth distribution shifts in response to complex local/regional changes in ocean condition and geographical barriers (Burrows *et al.* 2011, 2014; Pinsky *et al.* 2013; Poloczanska *et al.* 2016). For example, in the North Sea, the whole

demersal fish assemblage was deepened by 3.6 m per decade since the 1980s (Dulvy *et al.* 2008) and in the Gulf of Mexico where the coastlines prevent poleward shifts, the demersal fish and invertebrate assemblages shift deeper too (Pinsky *et al.* 2013).

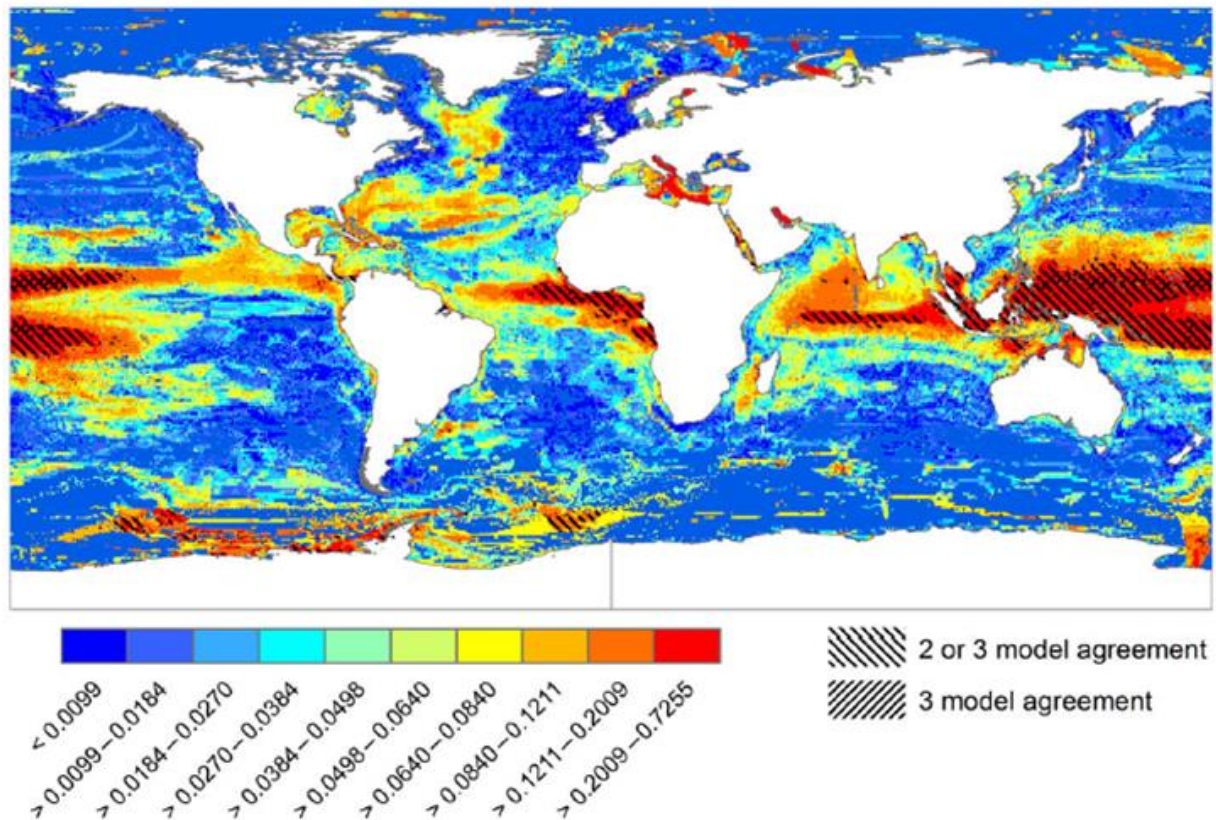


Figure 1.6: The hotspots of local projected extinction intensity between 2000 and 2050, expressed in proportion to locally extinct species, on average, across three species distribution models under scenario RCP8.5 (Figure extracted from Jones & Cheung 2015).

In parallel, marine populations have changed the timing of their biological events to earlier in the year to adapt their phenological behaviour to changing conditions (Poloczanska *et al.* 2016). The observed and expected changes in timing and production of plankton communities (Edwards & Richardson 2004; Schlüter *et al.* 2010) can cause potentially decoupling of production peaks leading to mismatches between plankton preys and their predators (Asch *et al.* 2019; Ferreira *et al.* 2020). Shifts in larval phenology have already been observed in several fish populations. For instance, a study focused on 43 species between 1951 and 2008 revealed that 35% seasonal peaks of larval abundance occurred early and that the phenological shift was correlated with changes in sea surface temperature and mesozooplankton volume (Asch 2015). Moreover, phenology of migratory behaviour can be

affected by climate shifts to warmer conditions as shown by Dufour *et al.* (2010) for Albacore, *Thunnus alalunga*, and Bluefin, *Thunnus thynnus*, tunas which arrive earlier to productive zones in the Bay of Biscay. As for geographic distribution, uniform responses are not expected due to the heterogeneous changes in ocean conditions and seasonal shifts across the globe (Burrows *et al.* 2011)

The differential responses to climate change across marine species and populations result in a reorganization of species assemblages with changes in community structure and trophic interaction (Pinsky *et al.* 2020). Shifts in distributions and concomitant effects on community structure of fish stocks have been shown for benthic and demersal communities (Perry 2005; Poulard & Blanchard 2005; Dulvy *et al.* 2008; Simpson *et al.* 2011) and for pelagic communities (Hughes *et al.* 2014; Montero-Serra *et al.* 2015).

1.3.4. The changes in biodiversity and abundance of marine life

The global changes in marine ecosystems tend to alter the biodiversity and the abundance of marine life. The changes of the structure of ecosystems are expected to induce a reorganization of marine biodiversity whose magnitude would depend on the intensity of the changes in ocean conditions (Tittensor *et al.* 2010; Beaugrand *et al.* 2015; Jones & Cheung 2015). The direction and the intensity of the changes in biodiversity would be highly variable over space. In tropical ecosystems, the changing of ocean conditions and especially ocean warming combined with the expansion of stratified waters would lead to local extinctions and loss of diversity (Figure 1.5). In polar and temperate ecosystems, the changes in biodiversity would be associated with local species invasions (Cheung *et al.* 2009; Michel *et al.* 2012; Beaugrand *et al.* 2015; Frainer *et al.* 2017).

The global decline of the abundance of marine species may be another consequence of the climate-induced alterations of structure and functioning of marine ecosystems. An ensemble of six global marine ecosystem models forced with two Earth system models under various emissions scenarios has projected a decline in global animal biomass of $4.3 \pm 2.0\%$ under RCP2.6 and $15.0 \pm 5.9\%$ under RCP8.5 by 2085–2099 relative to 1986–2005 (Figure 1.6; Lotze *et al.* 2019). These projections reflect mainly the responses of marine ecosystems to the changes in NPP and temperature without fishing inducing strong biomass increases at high latitudes and decreases at middle to low latitudes (Lotze *et al.* 2019).

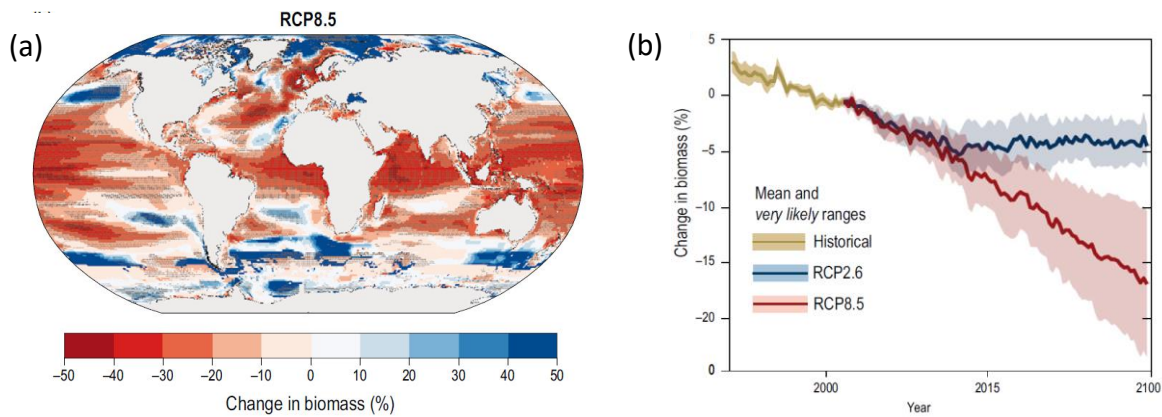


Figure 1.7: Projected changes in total animal biomass based on outputs from 6 global marine ecosystem models forced with 2 Earth system models and 2 Representative Concentration Pathway (Lotze *et al.* 2019). The panel (a) is the map of the changes in total animal biomass in 2085–2099 relative to 1986–2005 under RCP8. The panel (b) is the projected changes in global total animal biomass from 1970 to 2099 under RCP2.6 (red) and RCP8.5 (blue). Variability among different ecosystems and Earth system model combinations expressed as the 95% confidence interval (Figure extracted and adapted from Bindoff *et al.* 2019).

1.3.5. Trophic amplification of the climate signal

Changes at low trophic levels may affect higher trophic levels through trophic amplifications. This process describes the propagation of the climate signal up from primary producers to upper trophic levels through the decline (or increase) of biomass along the food web. The trophic amplification of primary production changes has been previously shown for phytoplankton and zooplankton using different planktonic food web models and different Earth system models (Chust *et al.* 2014; Stock *et al.* 2014a; Kwiatkowski *et al.* 2019). For example, negative trophic amplification between phytoplankton and zooplankton driven by tropical and subtropical regions are predicted by various modelling work (Chust *et al.* 2014; Stock *et al.* 2014a; Kwiatkowski *et al.* 2019). The exacerbation of projected biomass decline of phytoplankton may be explained by a decline in growth efficiency of mesozooplankton, an increase in mesozooplankton trophic level, and a decrease of coupling between phytoplankton and zooplankton (Stock *et al.* 2014a). Besides, trophic amplifications might be enhanced by the changes in phytoplankton stoichiometry. The reductions in nitrogen and phosphorous phytoplankton contents might result in a decline in zooplankton growth efficiency (Kwiatkowski *et al.* 2019). However, trophic attenuation in temperate regions and positive trophic amplification in polar oceans are also expected (Chust *et al.* 2014). The effects of climate change on marine trophic amplification for the higher trophic levels have been few explored, with

previous works focused on the past local changes (e.g., Kirby & Beaugrand 2009; Lindley *et al.* 2010) or general observations (Lotze *et al.* 2019).

1.3.6. Climate-induced alteration of biomass flows

Another major consequence of the climate-induced changes in marine ecosystems is related to the alterations of the transfers of biomass and energy in food webs. The observed and projected changes in marine ocean conditions are expected to affect biomass flows through multiple processes acting at different ecological scales.

At the individual organism scale, metabolic theory predicts that increasing temperature results in the increase in the rate of most biological processes including individual growth and respiration (See Figure 1.8; Gillooly *et al.* 2001; Brown *et al.* 2004; Bruno *et al.* 2015).

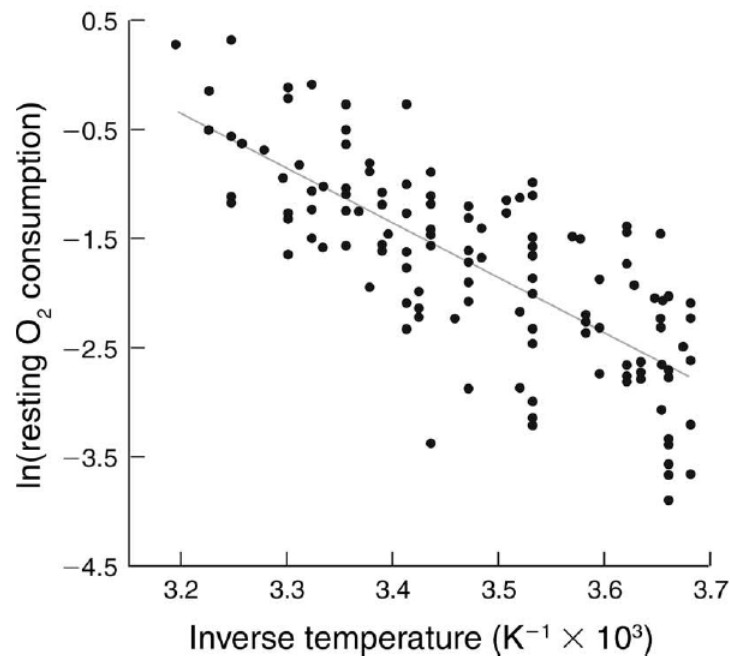


Figure 1.8: Observed dependence of metabolism on temperature for teleost fishes (Figure derived from Bruno *et al.* 2015).

The projected changes in biogeochemistry such as acidification may also induce direct and indirect effects on biomass flow (Nagelkerken & Connell 2015; Cripps *et al.* 2016). For example, Cripps *et al.*, 2016 showed that acidification has affected the calanoid copepod, *Acartia tonsa*, though species-specific biochemical changes of its phytoplankton preys and gender-specific respiratory responses impacting its metabolic rate. These changes at the individual level are expected to propagate at the

population scale especially through changes in survival and reproduction. In marine populations, the survival rate of the early life stages, which determine the amount biomass transferred to the adult population, is generally highly variable and sensitive to ocean conditions (Cushing 1969, 1990; Pörtner & Peck 2010). Climate-induced shifts in plankton seasonality are expected to produce mismatches between larval stages (linked to the spawning period) and their preys (see chapter 1, section 1.3.3.). The juvenile stages of marine populations may also be vulnerable to change in ocean conditions through the direct effects of warming or indirect effects (e.g., food availability, predation, or migration timing) (Siddon *et al.* 2013; Olmos *et al.* 2020).

At the community scale, climate change influences biomass flow through many processes acting together at different scales. The reorganization of marine food web induced by climate-induced shifts in species distributions is one of the main processes affecting the biomass transfer (Bindoff *et al.* 2019; Pinsky *et al.* 2020). Maureaud *et al.* (2017) showed that the differences in species assemblages across biomes are linked to differences in transfer efficiency and flow kinetic (see the following section 1.4). While, polar ecosystems are characterized by high transfer efficiency and slow flow kinetic, in tropical ecosystems biomass are lower and faster. In parallel, at large spatial scale, temperature is correlated with trait composition of marine communities inducing a “fast-slow continuum” of fish life-histories (Beukhof *et al.* 2019). In the Northern hemisphere, marine food webs are changing toward an increasing dominance and geographical expansion of fast-growing, early-maturing and short-lived species (Beukhof *et al.* 2019). Hence, ocean warming may induce a reshaping of species assemblages with increases of warm-favouring species and decreases in cold-favouring species. Regionally, such patterns have been observed with borealization regions (see Figure 1.9; Fossheim *et al.* 2015) and tropicalization and subtropicalization of temperate ecosystems of temperate regions (Horta e Costa *et al.* 2014; Verges *et al.* 2014; Montero-Serra *et al.* 2015).

These observed and projected macroscale changes in structure and functions of marine ecosystems suggest that climate change will tend to deeply affect change in biomass flow.

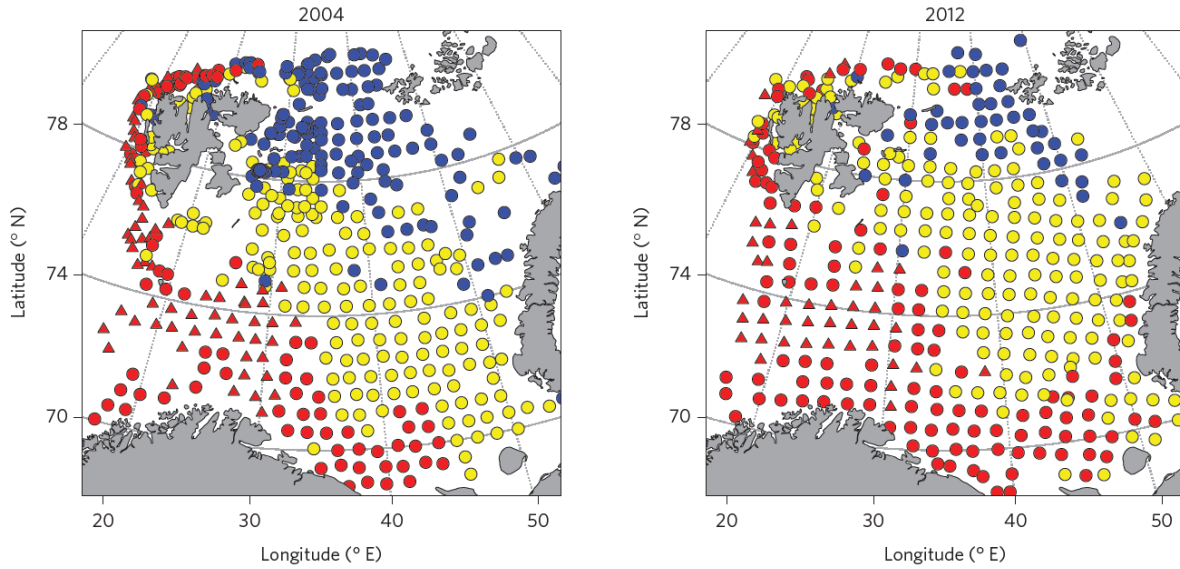


Figure 1.9: Fish communities identified on bottom trawl stations in 2004 and 2012. The Atlantic, Arctic and Central communities are represented in red, blue and yellow, respectively. The circles indicate the shallow sub-communities and the triangles indicate the deep sub-communities (Figure extracted from Fossheim *et al.* 2015).

1.4. The trophodynamic properties of marine food web

Lindeman (1942) defines the ecosystem as “the system composed of physical-chemical-biological processes within a space-time unit of any magnitude, i.e., the biotic community plus its abiotic environment”. A key aspect of the research on marine ecosystem functioning has been the study of trophic dynamics to answer two questions: How does the food web work? And how do the anthropogenic stressors modify it? The representation of aquatic or marine ecosystems is classically based on the trophic level concept and the Eltonian pyramid (Elton 1927; Lindeman 1942). Each species can be positioned at fractional trophic levels (Odum & Heald 1975; Adams *et al.* 1983) resulting from the proportion of each prey in the diet of each species.

One of the goals of trophodynamics approach is to identify the properties of the system emerging from the food web structure and functioning. Transfer efficiency, flow kinetic and food-chain length are noteworthy, as they are directly linked to trophic structure and functioning. Food-chain length is defined as the number of transfers of energy or organic matter from the base to the top of a food web (Ryther 1969; Post 2002) is closely related to the structure of the food web while transfer efficiency and flow kinetic are related to its functioning. The latter two properties determine the

biomass flow between trophic levels. While transfer efficiency quantify “how much” of the biomass is transferred from one trophic level to the next, flow kinetic specify “how fast” biomass is transferred within the food web.

Transfer efficiency also called trophic transfer efficiency is the ratio of biomass production of a given trophic level to that of the previous level (called “progressive efficiency” in Lindeman, 1942). Transfer efficiency is a critical emergent property of marine ecosystems as subtle variations can lead to large differences in production and biomass (Lindeman 1942; Ryther 1969; Chassot *et al.* 2010; Stock *et al.* 2017a). This food web property has been widely studied (e.g., Jennings *et al.* 2002; Coll *et al.* 2008; Libralato *et al.* 2008; Calbet *et al.* 2014; Irigoien *et al.* 2014; Stock *et al.* 2017). It is also a required parameter in many applications in marine ecology such as the estimation of biomass flow in production models (e.g., Jennings *et al.* 2008; Gascuel *et al.* 2011; Tremblay-Boyer *et al.* 2011; Carozza *et al.* 2016) and calculate the proportion of primary production required to sustain fisheries (e.g., Pauly & Christensen 1995; Chassot *et al.* 2010).

The variability in fisheries production resulting from different values of transfer efficiency (e.g., Chassot *et al.* 2010; Stock *et al.* 2017; Link & Watson 2019) and the fishing-induced alteration of the structure of marine food webs (see Chapter 1, Section 1.2.3) suggests that fishing exploitation is one of the main drivers of variations in trophic transfer efficiency. Maureaud *et al.* (2017) supports this assumption by highlighting that the fishing-induced changes in species assemblages are responsible for the past increase in transfer efficiency in several heavily exploited ecosystems. Also, the differences in transfer efficiency across biomes (high toward the polar and low at the low latitudes; (Rosenberg 2014; Maureaud *et al.* 2017) and the climate-induced alteration of biomass flow (see details in Chapter 1, section 1.3.6) indicates strong sensitivity of transfer efficiency to climate change.

Flow kinetic measures of the velocity of transfers within the food web and is the inverse of the biomass residence time is the average time a unit of biomass spends at a given trophic level before going up in the food web through predation (Gascuel *et al.* 2008; Schramski *et al.* 2015). These properties are directly related to the biomass present at each trophic level of the food web (higher residence time results in more biomass at each trophic level) (Gascuel *et al.* 2008).

Fishing is expected to be a prominent driver of the changes in flow kinetic. The obvious decrease of the life expectancy of individuals in exploited stocks and the fishing-induced dominance of small, fast-growing organisms in the overexploited ecosystems (see Chapter 1, Section 1.2.2) lead to the decline of the residence time of biomass in food webs (Maureaud *et al.* 2017). Furthermore, the

alterations of the climate-induced changes in ocean conditions - especially through ocean warming - are expected to accelerate biomass transfer in marine food webs (see Chapter 1, Section 1.3.6).

1.5. Marine ecosystem modelling

1.5.1. A large variety of marine ecosystem models

Over the last few decades, a wide range of ecosystem models have been developed to improve our understanding of marine ecosystem functioning. These models have been developed to answer a broad variety of fundamental and applied questions mainly related to the effects of fishing and climate change. Examples of these models include Ecopath with Ecosystem (EwE; Christensen & Pauly 1992), Atlantis (Fulton *et al.* 2004, 2011), Object-oriented simulator of marine ecosystem exploitation (Osmose; Shin & Cury 2001, 2004), Dynamic Bioclimate Envelope Model (DBEM; Cheung *et al.* 2011), Apex Predators ECOSystem Model (APECOSM; Maury 2010) and Dynamic Pelagic Benthic Model (DPBM; Blanchard *et al.* 2012)

Each ecosystem model is characterized by its own assumptions to represent biota, its interactions with the environment as well as its level of complexity. For example, while Atlantis and EwE define predator-prey interactions by a diet preference matrix (Christensen & Pauly 1992; Fulton *et al.* 2004), in Osmose, predation is assumed to be opportunistic and based on the size of preys relative to that of its predator (Shin & Cury 2004). Alternatively, food web can be modelled as a flow of energy/transfer from the primary producer to the top consumer (top predators like tunas or certain shark species). For example, size spectrum models assume that body size is a central trait to describe individuals (Trebilco *et al.* 2013; Blanchard *et al.* 2017) and the flow of energy across size classes within a biological community (Andersen *et al.* 2016). These models have been used widely to assess the responses of ecosystems to fishing activities (Benoît & Rochet 2004; Blanchard *et al.* 2014) and climate change (Blanchard *et al.* 2012; Barange *et al.* 2014), and to improve our understanding of the food web functioning (Jennings *et al.* 2008; Jennings & Collingridge 2015).

1.5.2. Fish-MIP, Fisheries and Marine Ecosystem Model Intercomparison Project

Fish-MIP was created to bring various models and modelling groups together to produce ensemble projections to assess the impacts of fisheries and climate change on marine ecosystems (www.isimip.org/about/marine-ecosystems-fisheries/; Tittensor *et al.* 2018). The strength of Fish-

MIP lies in the combination of multiple ecosystem models based on different modelling approach ranging from population-based to functional traits- and size-based structure.

In the first part of the project, an ensemble of global-scale marine ecosystem models undertook simulation experiments to project future changes in marine animal biomass under various emission scenarios (Bryndum-Buchholz *et al.* 2019; Lotze *et al.* 2019). The main findings of Fish-MIP are detailed previously in the section 1.3.3. Overall, the first standardized ensemble projections revealed that global ocean animal biomass consistently declines under all emission scenarios, driven by increasing temperature and decreasing primary production with an amplification of the impacts at higher trophic levels (Lotze *et al.* 2019). The next step of the project will be to identify the underlying processes inducing variability across the different ecosystem models to better understand why they respond differently to climate change.

1.6. The EcoTroph model

A class of model that represents trophodynamics by biomass flow across trophic levels is called EcoTroph, originally developed by Gascuel *et al.* (2005, 2009 and 2011). Specifically, EcoTroph represents an ecosystem by the continuous distribution of the biomass along trophic levels (TL) (Figure 1.10). This distribution is called the biomass trophic spectrum (Gascuel *et al.* 2005). The biomass enters the food web at TL=1, as generated by primary producers, and recycling by the microbial loop. Between TL=1 and TL=2, the biomass is composed of mixotrophs, i.e., of organisms that are simultaneously primary producers and first-order consumers, such as giant clams. Their biomass is usually low, and is conventionally split between biomass at TL=1 and 2. Then, at TLs higher than 2, the biomass is composed of heterotrophic organisms with mixed diet and fractional TLs resulting in a continuous distribution of biomass along TLs. In EcoTroph, trophic functioning can be described by a biomass flow moving from lower to higher TL. Each organic particle moves up the food web according to continuous processes (ontogenetic changes in TLs) and abrupt jumps due to predation. All particles jointly constitute a biomass flow (Gascuel *et al.* 2008).

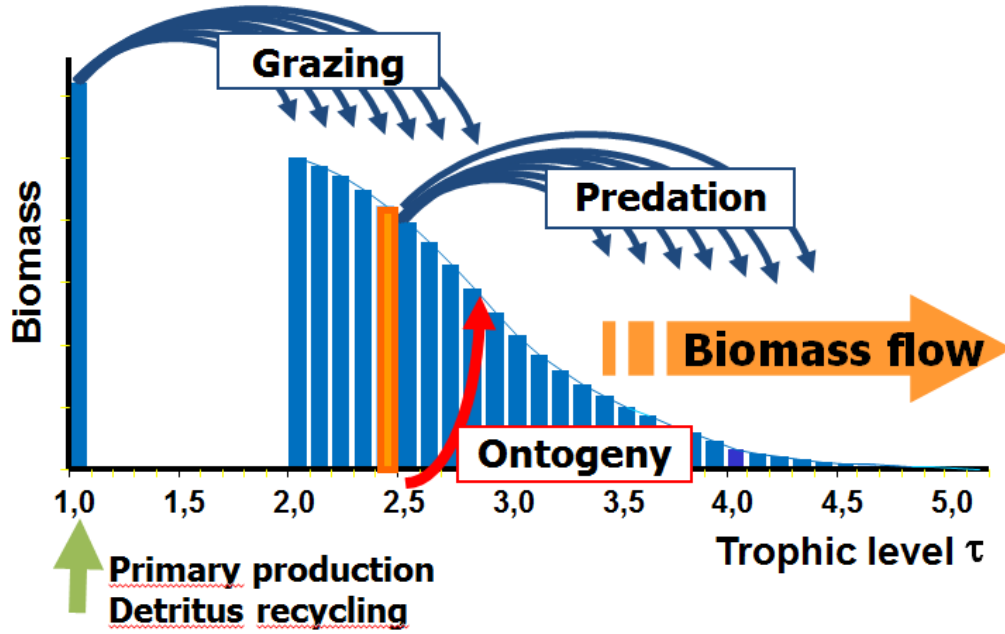


Figure 1.10: A schematic representation of the trophic functioning of an ecosystem with the theoretical biomass distribution by trophic and trophic transfer processes (Figure extracted and adapted from Gascuel *et al.* 2009).

Based on the usual equations of fluid dynamics, the biomass at TL τ (i.e., in the trophic class $[\tau, \tau+\Delta\tau]$) under steady-state conditions is given by:

$$B_{\tau} = \frac{\Phi_{\tau}}{K_{\tau}} \times \Delta\tau$$

where Φ_{τ} is the biomass flow, i.e. the amount of biomass that moves up the food web through the trophic class $[\tau, \tau+\Delta\tau[$ (expressed in t.yr^{-1}), and K_{τ} the flow kinetic, which quantifies the speed of the biomass flow. EcoTroph defines the biomass flow Φ_{τ} as a density of production at $\text{TL}=\tau$. Therefore, the production of a trophic class $[\tau, \tau+\Delta\tau[$ is:

$$P_{\tau} = \int_{\tau}^{\tau+\Delta\tau} \Phi(\tau) \times d\tau = \Phi_{\tau} \times \Delta\tau$$

Production is commonly expressed in t yr^{-1} . In fact, it implicitly refers to the conversion of biomass eaten at $\text{TL}=\tau-1$, into predator tissues whose mean TL is τ . Therefore, in a TL-based approach

such as EcoTroph, production has to be expressed in $\text{t.TL}^{-1}.\text{yr}^{-1}$, i.e. tons moving up the food web by 1 TL on average during 1 year. As natural losses occur during trophic transfers (through non-predation mortality, respiration, and excretion), the biomass flow $\Phi\tau$ is a decreasing function of TL calculated as:

$$\Phi(\tau + \Delta\tau) = \Phi(\tau)e^{-\mu\tau\Delta\tau}$$

where $\mu\tau$ (expressed in TL^{-1}) is the mean rate of natural loss over a $[\tau, \tau+\Delta\tau[$ interval. It implies that the biomass flow at a given TL depends on the flow from lower TLs. It also defines the trophic transfer efficiency between continuous TLs as $\exp(-\mu\tau)$. The speed of the biomass flow $K\tau$ (flow kinetic) depends on the turnover of the biomass, and is defined using mean values per trophic class (Gascuel *et al.* 2008).

Such an approach provides a simplified but effective representation of the food web functioning to evaluate the effects of fishing and climate change. EcoTroph has been used to estimate the living biomass of the ocean and the fishing impact at global scale (Tremblay-Boyer *et al.* 2011) and at regional and local scale (Coll  ter *et al.* 2012; Gasche *et al.* 2012; Valls *et al.* 2012; Gasche & Gascuel 2013; Halouani *et al.* 2015; Moullec *et al.* 2017) and to validate estimates of the mesopelagic fish biomass in the open ocean (Irigoin *et al.* 2014).

1.7. Objectives of the thesis

Climate change has been affecting a wide range of biological and ecological processes, and will continue in the coming decades and ultimately the transfer of energy and biomass within marine food webs. The expected changes in biomass flow are a major issue for the future of fisheries and other goods and services provided by marine ecosystems. The goal of my research is to understand the impacts of climate-induced perturbations of biomass flow on the structure and functioning of marine food webs.

The proposed thesis aims to answer the following specific questions:

- How does temperature affect the biomass transfer in marine ecosystem?
- What will be the consequences of ocean warming on the biomass flow over the 21st century?
- How will the changes in biomass transfer and ocean conditions affect the productivity and the stability of marine ecosystems?

- What will be the consequences for the future catches and fisheries?

Specifically, based on these questions, I developed three overarching hypotheses for this study:

H1. Biomass transfer within marine food webs can be studied through the trophic transfer efficiency and the residence time. I hypothesize that the trophic transfer efficiency and residence time of coastal and shelf sea ecosystems in the world are linked to ocean temperature and will respond to ocean warming.

H2. Ocean warming will impact the biomass transfer and the biomass residence time across global ocean ecosystems, and together with the projected changes in net primary production, consumer biomass in the ocean will be affected with regional differences in the 21st century.

H3. In the exploited marine ecosystems, fishing activities and climate change are required to be considered together to understand the future productivity and stability of marine ecosystems.

This PhD thesis is mainly based on the EcoTroph modelling approach to test these hypotheses in three chapters. As a first step, **Chapter 2** examines the influence of temperature on global biomass transfers from marine secondary production to fish stocks. By combining fisheries catches in all coastal and shelf sea areas and life history traits of exploited marine species, two emerging food web properties, the trophic transfer efficiency (TTE) and the biomass residence time (BRT), are estimated in all the marine coastal ecosystems. Then, the temperature-induced changes in TTE and BRT are projected under two RCPs by the end of the century. In **chapter 3**, the EcoTroph model is used to explore the future of marine consumer biomass which is determined by three key climate-related factors: primary production entering the food web, trophic transfer efficiency, and flow kinetic. Using climate projections of three Earth system models, the changes in biomass are estimated by 2100 in every 1°x1° grid cell in the global ocean under two RCPs. Furthermore, we examine the processes at play and the spatial patterns of the changes. **Chapter 4** focuses on the European continental shelf ecosystems and investigates the effects of climate change on the trophic structure of biomass and catch by the 2100. Based on the projected changes in biomass of pelagic and benthic secondary producers and the current reported fisheries catch (period 2013–2017), we modelled the future changes in biomass and catch at each trophic level for two fishing strategies. Finally, **chapter 5** summarizes and discusses the finding of the thesis. Some recommendations for future research and model refinements are presented to further explore the future of marine ecosystems and services they provide.

CHAPTER 2

Climate change undermines the trophic transfers of marine food webs

CHAPTER 2: Climate change undermines the trophic transfers of marine food webs

2.1. Introduction

In marine ecosystems, temperature is one of the main factors affecting species physiology (Pörtner & Farrell 2008; Cheung *et al.* 2013b), biogeography (Tittensor *et al.* 2010), trophic dynamics (Pörtner *et al.* 2014; Boyce *et al.* 2015) and ecosystem services such as food provision. A growing number of studies have shown that modifications of the natural fluctuation of ocean temperature have caused shifts in the geographic distribution of marine species and phenology from plankton to top predators (Perry 2005; Dulvy *et al.* 2008; Cheung *et al.* 2009; Beaugrand *et al.* 2010; Pinsky *et al.* 2013; Poloczanska *et al.* 2013). These biogeographical shifts have resulted in a reorganization of marine species assemblages in various ecosystems across the global ocean (Beaugrand *et al.* 2014; Kortsch *et al.* 2015, 2018) and influenced the composition of fisheries catches (Cheung *et al.* 2013b; Stuart-Smith *et al.* 2015).

At the individual scale, warmer temperature results in faster exothermic biogeochemical reactions and higher metabolic rates (Brown *et al.* 2004; Bruno *et al.* 2015). Consequently, warmer temperature conditions may induce an increase in the speed of biomass transfer in the food web and a reduction of the biomass residence time. In addition, higher organism metabolic rates imply larger losses by respiration, and may cause a decrease in the efficiency of biomass transfers by affecting growth (Palomares & Pauly 1998; Heilmayer *et al.* 2004; Pörtner *et al.* 2012; Barneche & Allen 2018). These changes at the individual level are expected to propagate at the population and hence community levels (Brown *et al.* 2004; Bruno *et al.* 2015; Schramski *et al.* 2015; Barneche & Allen 2018; Pinsky *et al.* 2020).

In particular, changes in species composition induced by warmer waters may result in the selection of species characterized by a shorter lifespan and higher respiration rates at every level of the food web, therefore leading to faster and less efficient biomass transfers, respectively. Several studies suggest profound reshuffles of marine communities due to anthropogenic changes in ocean conditions (Cheung *et al.* 2009; Pereira *et al.* 2010; Pörtner *et al.* 2014; Rutterford *et al.* 2015; Bindoff *et al.* 2019). However, the consequences of ocean warming on properties of biomass flow remain unexplored and unquantified.

Here, we used a trophodynamic approach, initially developed by Lindeman (1942), to analyze the impact of sea water temperature on biomass flowing in ecosystems, from primary consumers to top predators. Two parameters summarize these biomass transfers through the food web and are expected to change in a warming ocean: the trophic transfer efficiency and the biomass residence time. Trophic transfer efficiency (TTE) is the fraction of energy transferred from one trophic level (TL) to the next and summarizes all the losses in the food web at each TL (Lindeman 1942; Strayer 1991; Pauly & Christensen 1995; Jennings *et al.* 2002; Libralato *et al.* 2008; Niquil *et al.* 2014; Schramski *et al.* 2015; Stock *et al.* 2017a). TTE is measured as the ratio between the production rate of two adjacent TLs (Lindeman 1942; Baumann 1995; Pauly & Christensen 1995; Ricklefs & Miller 2000; Libralato *et al.* 2008). This property of the food web has been widely studied (Jennings *et al.* 2008; Andersen *et al.* 2009; Chassot *et al.* 2010; Irigoien *et al.* 2014; Stock *et al.* 2017a) and some studies suggest that it spatially varies among biomes or ecosystem types (Libralato *et al.* 2008; Chassot *et al.* 2010; Schramski *et al.* 2015; Stock *et al.* 2017a).

Biomass residence time (BRT) is the average amount of time a unit of biomass spends at a given TL before trophic transfer to higher TLs in the food web through predation (Gascuel *et al.* 2008; Schramski *et al.* 2015). BRT (expressed in years) is inversely proportional to the speed of biomass transfer across TLs. It directly affects the biomass present at each TL of the food web (longer residence time results in greater biomass at each TL).

The aim of this study is to analyze how the temperature-induced spatial patterns in species composition affect biomass transfers in marine food webs, and how these transfers are expected to change over the 21st century. We focus on community-level biological responses driven by changes in species assemblages. The study and analysis are performed for the coastal regions of the global ocean which currently support the bulk of fisheries production, and where catch data are used as insights on the features of the marine community structure.

First, we measure TTE and BRT based on fisheries catch species composition over the period 2000–2010 and determine how these two parameters vary along the temperature gradient in the global coastal marine ecosystems. Second, to detect the past changes in biomass transfers and determine if ocean warming has already affected them, we analyze the trends in TTE and BRT between 1950 and 2010 and we compare the observed and modelled trends using sea water temperature. Finally, we project TTE and BRT by 2100 using simulated changes in sea water temperature based on three Earth system models under two contrasting greenhouse gas emissions scenarios.

2.2. Materials and Methods

2.2.1. Study area and catch data

Since the composition of species assemblages is unknown in many coastal marine ecosystems that we studied, we estimated trophic transfer parameters based on catch data, assuming they can be considered as a proxy of the true features of the food web. This assumption will be further discussed and sensitivity analyses were conducted.

Annual reconstructed catch data made available by the SeaAroundUs project from 1950 to 2010 (Pauly and Zeller, 2015) were used. This set of data is spatially disaggregated by taxon on a 1°x1° spatial grid of the world ocean. The reconstruction is based on the official records of the Food and Agriculture Organization (FAO), with the addition of undeclared artisanal and subsistence fisheries, recreational catches, discarded bycatch and illegal and unreported catch (Pauly and Zeller, 2015). We removed catch of rare taxa representing less than 0.05% of the total catches for each year and catches from unidentified species. Biogeography of coastal and shelf areas were delimited using the distribution of coastal biomes identified by Reygondeau *et al.* (2013) and adapted from Longhurst (2007). To ensure that parameters issued from the catch composition in each grid cell is representative of the food web, we removed grid cells where unidentified species represented more than 50% of the total catch, and cells where one single species represented more than 75% of the catch. Finally, we kept only grid cells where there were more than 10 species excluding rare taxa.

After passing the dataset through the above filters, the final dataset consists of 5,783 (75% of the cells) 1° latitude x 1° longitude grid cells and 1760 taxa in coastal and shelf seas. Each cell was classified as one of the 3 biomes: tropical, temperate and polar biomes. Upwelling ecosystems were added using the biogeographical provinces described by Reygondeau *et al.* (2013) (Figure 2.1).

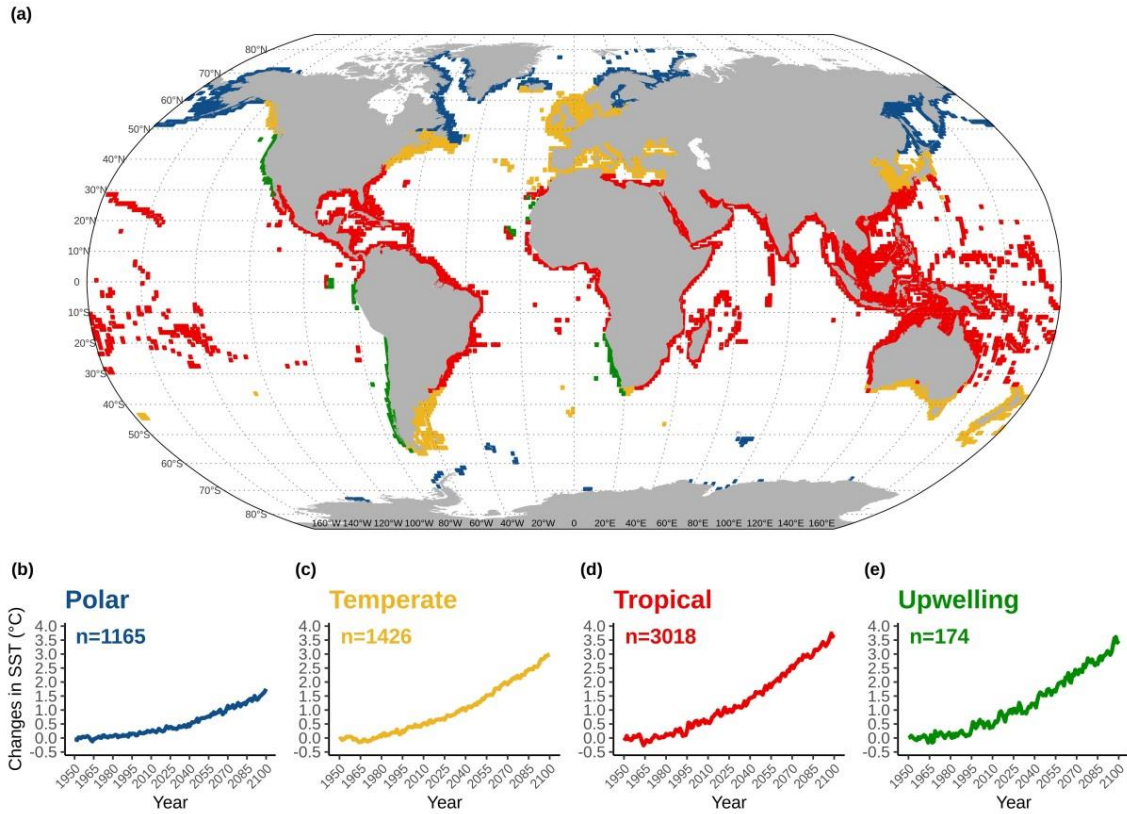


Figure 2.1: Map of the coastal areas represented in the dataset and associated to ecosystem types (a). The colours refer to the ecosystem types: polar (in blue), temperate (in orange), tropical (in red) and upwelling (in green). The four graphs (b), (c), (d), and (e) show the past reconstructed trends in sea surface temperature (SST) and the predicted trends under RCP8.5 scenarios (business as usual scenario). Temperature is represented by mean values of SST coming from the three Earth system models used in the study and described in Materials and Methods.

2.2.2. Trophic transfer efficiency and biomass residence time calculations

Trophic transfer efficiency (TTE) and biomass residence time (BRT) were estimated within each grid cell using a trophodynamic approach based on two indicators: the efficiency cumulated indicator (ECI) and the time cumulated indicator (TCI). The method to calculate TTE and BRT is summarized in Figure 2.2.

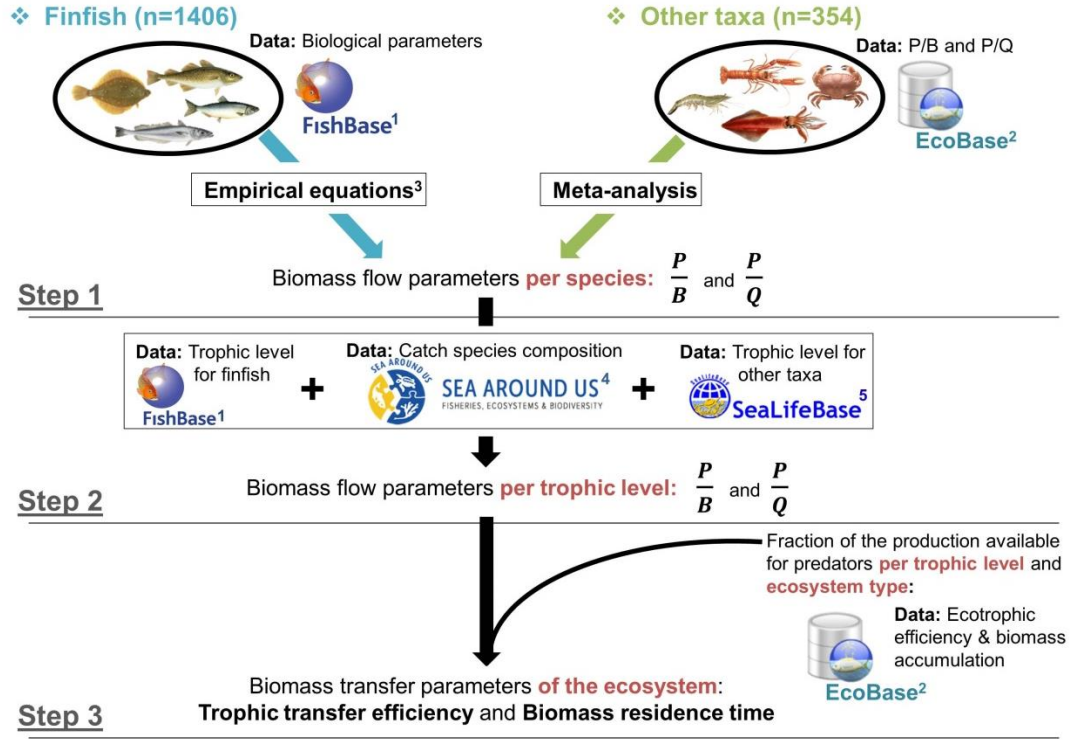


Figure 2.2: Synthetic schematic representation of the method to calculate trophic transfer efficiency and biomass residence time focused on the data that we used and the levels of ecological organization (from species to trophic level to ecosystem). n represents the number of species. 1 ((Froese & Pauly 2000), 2 (Colléter *et al.* 2013), 3 (Palomares & Pauly 1998; Gascuel *et al.* 2008), 4 (Pauly and Zeller, 2015).

Trophic transfer efficiency (TTE)

The efficiency cumulated indicator (ECI) developed by Maureaud *et al.* (2017) quantifies the fraction of secondary production transferred from TL=2 to TL=4, considering only metabolism losses due to respiration and excretion (see partial transfer efficiency (partial TE) in Figure 2.3). It was calculated for each grid cell i and each year y , as an aggregation from TL=2 to TL=4 of the production to consumption ratio $(P/Q)_{\tau,i,y}$ which can be defined as the “gross food conversion efficiency” (Christensen & Pauly 1993) at $TL=\tau$, with the following equations:

$$ECI_{i,y} = \prod_{\tau=2.0}^{4.0} \left(\left(\frac{P}{Q} \right)_{\tau,i,y} \right) \quad \text{Eq. 1}$$

P/Q is firstly calculated for each species or taxon j , as the ratio of P/B (Production to Biomass) to Q/B (Consumption to Biomass). For finfish, these taxon-specific ratios are calculated according to the empirical equations of Gascuel *et al.* (2008) and (Palomares & Pauly 1998) and based on life history traits and thermal habitat (see Appendix A - Supplementary material A.1). The required data (asymptotic weight, Von Bertalanffy growth coefficient, diet type and aspect ratio) were taken from FishBase (<http://www.fishbase.org>, Froese & Pauly 2000). For the other species (e.g., cephalopods, crustaceans), the taxon-specific P/B and P/Q ratios were extracted from EcoBase (Coll  ter *et al.* 2013) (see Appendix A - Supplementary material A.1).

Then, taxon-specific P/Q ratios were transformed into a P/Q trophic spectra (Gascuel *et al.* 2005). To consider the within-taxon variability of trophic levels, catches of every taxon were distributed over a range of trophic classes (following a lognormal distribution and using classes with a width of 0.1 TL). Trophic spectra were obtained by averaging the taxon-specific P/Q ratios weighted by the resulting catch per taxon and trophic class.

Since the ECI calculation does not account for losses in trophic transfers related to non-predation natural mortality and biomass accumulation, ECI is measuring a partial transfer efficiency, and is likely to overestimate the true trophic transfer efficiency (TTE). To account for such overestimation, partial transfer efficiency was converted into TTE by introducing a correction term based on Ecotrophic Efficiency (EE, Christensen & Pauly 1992) and Bacc (biomass accumulation rate within each species or taxon). Thus (EE - Bacc) measures the fraction of the production of a given taxon not transferred to detritus and not accumulated by the taxon, and thus available for trophic transfers through consumption by predators (see theoretical graph on Figure 2.3). EE and Bacc were extracted from coastal Ecopath models (see Appendix A - Supplementary material A.2) included in the EcoBase database (Coll  ter *et al.* 2013). The extracted data were then used to calculate a correction factor for each trophic level τ and for each ecosystem type i (see Appendix A - Supplementary material A.3). Finally, the two components of TTE—the fraction of loss due metabolism (P/Q) and the non-predation natural mortality and biomass accumulation (EE-Bacc)—are combined. Thus, the trophic transfer efficiency between TL=2 and TL=4, can be estimated as a product of all trophic classes; the estimate, which represents TTE across two trophic levels, is transformed into TTE expressed per trophic level by taking a square root of the term (Eq.2):

$$TTE_{i,y} = \left[\prod_{\tau=2.0}^{4.0} \left(\left(\frac{P}{Q} \right)_{\tau,i,y} \cdot (EE - B_{acc})_{\tau,\beta} \right) \right]^{\frac{1}{2}} \quad \text{Eq. 2}$$

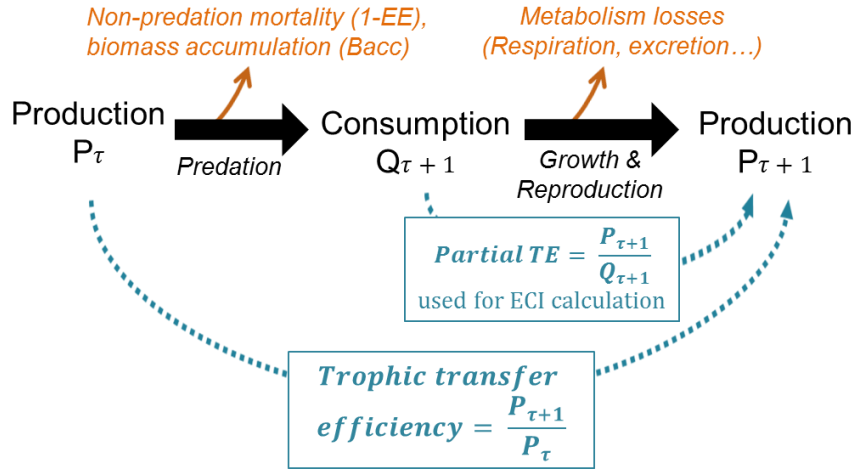


Figure 2.3: Schematic representation of biomass flow parameters between two trophic levels. Black arrows represent energy transfers or losses. The prey has a trophic level τ and the predator has a trophic level $(\tau+1)$. The partial transfer efficiency (partial TE) ($P_{\tau+1}/Q_{\tau+1}$) and trophic transfer efficiency ($P_{\tau+1}/P_\tau$) are indicated (derived from Gascuel *et al.*, 2008; Maureaud *et al.*, 2017).

Biomass residence time (BRT)

The BRT, which is called the time cumulated indicator (TCI) by Maureaud *et al.* (2017), was calculated by aggregating the time spent by each unit of biomass within small trophic level classes of $\Delta\tau = 0.1$ TL, when moving into the food web from TL=2 to TL=4. Gascuel *et al.* (2008) showed that the mean speed of the biomass flow passing through a given trophic level can be measured as the production to biomass ratio (P/B). Therefore, as a speed is defined by a distance divided by time, the time a unit of biomass needs on average to cross a trophic class from TL= τ to TL= $\tau + \Delta\tau$ is equal to $\Delta\tau/(P/B)$. Thus, the BRT between TL=2 and TL=4, can be estimated as a sum for all trophic classes, according to:

$$BRT_{i,y} = \sum_{\tau=2.0}^{4.0} \frac{\Delta\tau}{\left(\frac{P}{B}\right)_{\tau,i,y}} \quad \text{Eq. 3}$$

BRT is the biomass residence time in the food web, between TL=2 and TL=4, for cell i and year y . P/B ratio was first calculated by species or taxon (see Appendix A - Supplementary material A.2), and converted into P/B trophic spectra using the above described method, thus providing an estimate for every trophic class.

Data used for the calculations

TTE and BRT were calculated for each year between 1950 and 2010 in each grid cells. This computation is using the annual catch species composition from the SeaAroundUs database. Trophic levels for each species or taxon were obtained from Fishbase and SeaLifeBase (<http://www.sealifebase.org>, Palomares & Pauly 2018). We used sea surface temperature (SST) to estimate the thermal habitat of fish required to calculate the taxon-specific ratios (see Appendix A - Supplementary material A.1) for every year between 1982 and 2010 from NOAA, using the Optimum Interpolation (OI) V2 dataset derived from in situ and satellite SSTs (<https://www.esrl.noaa.gov/psd/data/gridded/data.noaa.oisst.v2.html>).

2.2.3. Relationships between temperature, trophic transfer efficiency and biomass residence time

In order to understand how the two trophic transfer parameters vary spatially and to determine their relationship to temperature in the recent past, the average values over the period 2000–2010 of TTE and BRT were estimated in each cell. Then, two generalized linear models (GLM), with TTE and BRT per grid cell as the dependent variables and sea water temperature as independent variable, were developed. The models consider an ecosystem type effect (tropical, temperate, polar or upwelling), in order to highlight potential non-temperature-related differences in ecosystem structure. The interaction between sea water temperature and ecosystem type is also integrated in the models to take into account the differences in temperature effects among the four ecosystem types.

All statistical analyses were performed with the free software environment R (v.3.4.4, <http://cran.r-project.org>). The best-fitted family distribution and link function were selected among gamma distribution (with identity, logarithmic and inverse link function), inverse Gaussian distribution (with identity, logarithmic and inverse link function), and Gaussian distribution (with identity and inverse link function) with log-transformed dependent variable or not. We finally chose to select models based on a Gaussian distribution on log-transformed trophic transfer parameters:

$$\log(X) = \text{Intercept} + SST + \text{ecosystem type} + SST \cdot \text{ecosystem type} + \varepsilon \quad \text{with } \varepsilon = N(0, \sigma^2).$$

X is TTE or BRT and ε is the normally distributed error with mean of 0 and variance of σ^2 .

Adequacy of the GLMs was evaluated by checking the distribution of model residuals for homoscedasticity, normality, the fraction of deviance explained by the model, and by each variable.

The significance of the parameters was assessed using Wald chi-square tests. Laurent's correction was applied to the models to obtain unbiased estimations from log-transformed data (Laurent 1963).

2.2.4. Past and projected trends in trophic transfer efficiency and biomass residence time

In order to contrast projections over the 21st century against the past variability and trends, TTE and BRT were estimated from 1950 to 2010, based on the fisheries catch species compositions. These observed past trends were compared to temperature-based estimates using the GLM statistical model. Then, we projected TTE and BRT by 2100 in the four ecosystem types, using yearly values of SST predictions from three Earth system models, respectively developed by the Geophysical Fluid Dynamics Laboratory (GFDL-ESM2M, Dunne *et al.* 2012), the Max Plank Institute (MPI-ESM-MR, Giorgetta *et al.* 2013) and the Institut Pierre Simon Laplace (IPSL-CM5A-MR, Dufresne *et al.* 2013). Spatial distribution of ecosystem types was assumed unchanged by 2100. Final projections of TTE and BRT were built by averaging results from the three general circulation models, under two contrasted Representative Concentration Pathways (RCPs, i.e., climate change scenarios from IPCC; http://sedac.ipcc-data.org/ddc/ar5_scenario_process/RCPs.html): RCP2.6 where radiative forcing level reaches 3.1 W/m² by mid-century and returns to 2.6 W/m² by 2100 (strong mitigation scenario), and RCP8.5 where rising radiative forcing pathway reaches 8.5 W/m² in 2100 (no effective mitigation scenario).

2.2.5. Sensitivity analysis

TTE and BRT time are studied here using post-filtered catch data (see Study area and catch data in Materials and Methods), assuming that the features of the biomass flow of the exploited fraction of marine food webs reflect the features of the biomass flow of the entire marine food web. We recognize that the use of catch data to describe marine ecosystem functioning and structure may lead to biased estimators, due to selective fisheries and changes in the fishing strategies over time and space (Branch *et al.* 2010; Pauly *et al.* 2013). To evaluate the potential effects of these biases, two sensitivity analyses were conducted (Appendix A - Supplementary material A.4 and A.5). First, we tested the robustness of our models by adding the effects of the catch per surface area (as an indicator of the fishing intensity) and the mean trophic level of catch (MTL, as an indicator of the fishing strategy at the ecosystem level). Second, we used a selection of Ecopath ecosystem models to compare the estimates of the trophic transfer parameters based on species assemblages in the ecosystems or in the catch.

Since we estimated the two trophic transfer parameters from TL=2 to TL=4 based on catch data, a large fraction of the biomass at lower levels is made up of species such as zooplankton, benthic invertebrates, or larvae not targeted by fishing. Thus, in our catch dataset, species less than or equal to TL of 2.5 represent only between 4 and 8% of the annual global catch. As a consequence, the catch composition between TL=2 and TL=2.5 is unable to reflect the species composition in the ecosystem, what may also lead to bias in our estimates. This potential bias was tested by modelling the temperature effect on the two trophic transfer parameters using only catches between TL=2.5 and TL=4 (Appendix A - Supplementary material A.6).

Our data, TTE and BRT are spatially autocorrelated. This autocorrelation is supposed to be captured by the models. Nevertheless, if a spatial autocorrelation remains in the residuals of the GLMs, the key assumption that residuals are independent and identically distributed is violated, and parameter estimates may be biased. Consequently, we tested the potential spatial autocorrelation bias on our models by comparing the developed models and models based on 100 subsamples with no or a weak spatial autocorrelation (Appendix A - Supplementary material A.7).

Finally, the natural non-predation mortality was taken into account in our analysis by adding a correction which reduces the TTE values. The correction is calculated on the average of ecotrophic efficiency and biomass accumulation by aggregating 72 Ecopath models per ecosystem type. Since these parameters may be modelling dependent and inaccurate in some models, we tested the introduction of this supplementary loss in the model by comparing the sea temperature effect including or not this correction (Appendix A - Supplementary material A.3).

2.3. Results

2.3.1. Relation between sea surface temperature and ecosystem trophodynamics

Trophic transfer efficiency (TTE) and biomass residence time (BRT) over the recent period 2000–2010 differ significantly among ecosystem types (p-value <0.001). Polar ecosystems exhibit the most efficient but the slowest biomass transfers with TTE of $10.4\% \pm 2.7$ and BRT of $4.4 \text{ years} \pm 1.3$ between TL=2 and TL=4 (Figure 2.4a, b). In contrast, trophic transfers in upwelling and tropical ecosystems appear faster with $2.8 \text{ years} \pm 2.2$ and $1.9 \text{ years} \pm 1.9$ respectively but less efficient with $5.9\% \pm 0.7$ and $6.5\% \pm 0.6$. Intermediate values are estimated in temperate ecosystems with $2.8 \text{ years} \pm 0.9$ and $8.1\% \pm 2.4$.

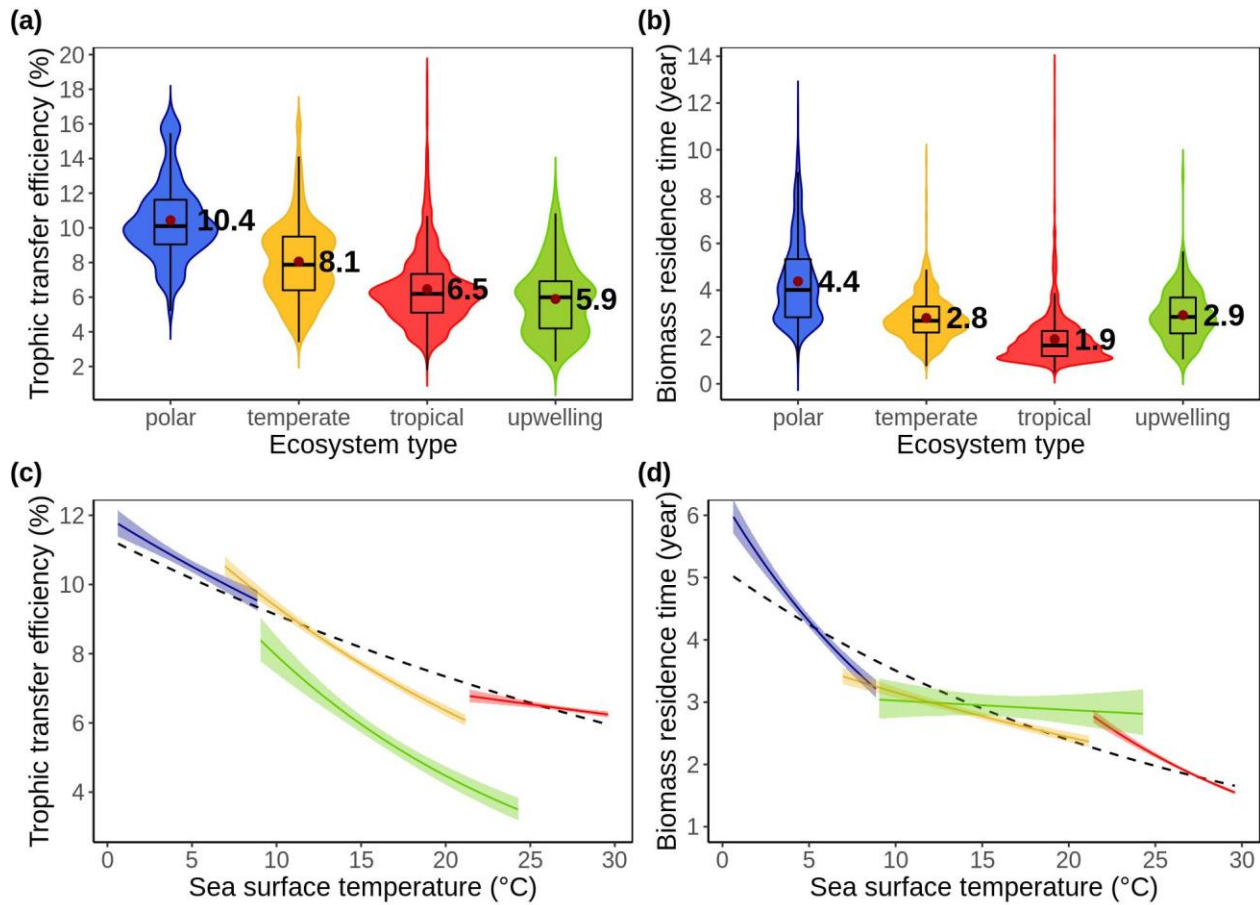


Figure 2.4: The effect of temperature on the two trophic transfer parameters. The violin plots on the top panels represent the distribution of the mean values of the two trophic transfer parameters: (a) trophic transfer efficiency (TTE) and (b) biomass residence time (BRT) in each ecosystem type over the period 2000–2010. The colours refer to the ecosystem types: polar (in blue), temperate (in orange), tropical (in red) and upwelling (in green). In both panels (c) and (d), solid coloured lines represent the predicted values (i.e., the temperature effect) of TTE and BRT respectively, provided for each ecosystem type by the GLM model. The black dashed lines represent the predicted values of TTE and BRT by an additional GLM model considering only SST as a covariate. The shaded areas refer to the mean predicted value confidence intervals (95%). 5783 grid cells were used to calculate the trends.

The same spatial patterns emerged for the two trophic transfer parameters (see related maps on Figure 2.5a, b). In the colder coastal waters, for example in the Bering Sea and in the Antarctica Coast, TTE and BRT exhibit high values, while in the warmer waters for example along the African coast and in the continental shelf of Southeast Asia, biomass is transferred faster and less efficiently. Some exceptions exist, such as in the Gulf of Mexico, which exhibits high TTE values, and in the Indian Ocean between Seychelles and Mauritius showing a high BRT.

Our models indicate that SST and ecosystem type have both a statistically significant effect on the studied biomass flow parameters. Furthermore, SST explained 34.7% and 48.7% of the total deviance for TTE and BRT respectively, while the interaction between SST and the ecosystem type explained an additional 5.4% and 2.3% for these two parameters (see Appendix A - Supplementary material A.8).

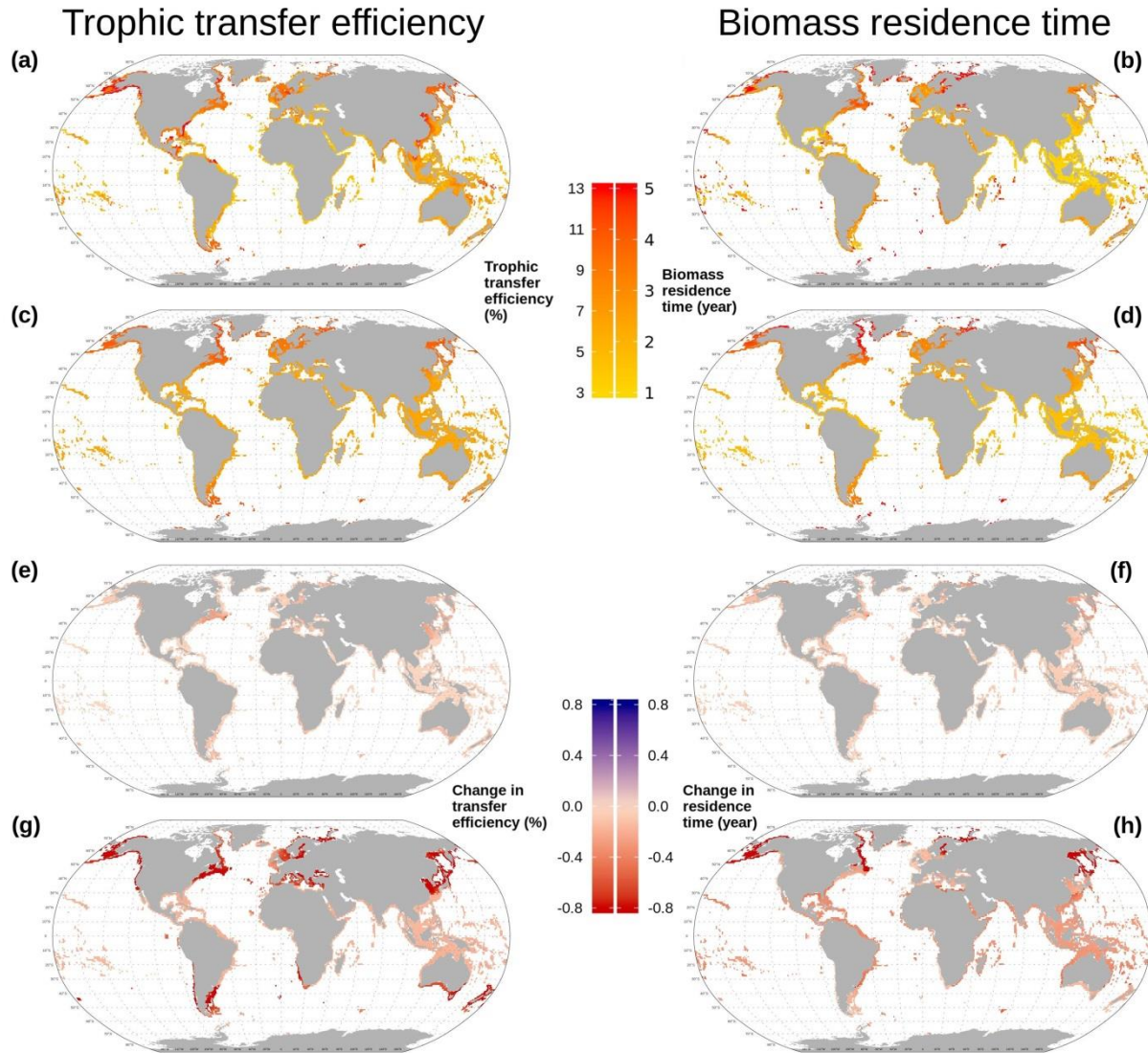


Figure 2.5: Trophic transfer efficiencies and biomass residence times in the coastal regions of the global ocean. The panels (a) and (b) represent the observed values over the period 2000–2010 while the other panels exhibit the predicted values from the General Linear Model for: the period 2000–2010 (c) and (d), and projected changes in 2090–2100 relative to 2000–2010 for climate change scenarios for RCP2.6 (e, f), and RCP8.5 (g, h).

The decreasing relationship between sea temperature and TTE or BRT is consistent across ecosystem types, although the variations in temperature sensitivity of these food web parameters between the ecosystem types were not expected (Figure 2.4c, d). Temperature sensitivity for TTE is higher in temperate and upwelling zones, followed by polar and tropical ecosystems. In contrast, BRT is more sensitive to temperature in polar and tropical ecosystems followed by temperate and upwelling ecosystems.

2.3.2. Observed past trends in trophic transfer efficiency and biomass residence time

Over the period 1950–2010, the observed global mean of TTE, computed from the catch composition, significantly increased from 7.1% to 7.6% (Figure 2.6a, p-value linear model <0.001), while BRT decreased from 2.5 to 2.2 years (Figure 2.6b, p-value linear model <0.001). The changes in TTE and BRT occurred mainly before the mid-1990s, then TTE stopped its increase and BRT decreased at a slower pace. These increasing TTE and decreasing BRT are observed in every ecosystem type (see Appendix A - Supplementary material A.9) except for TTE in polar ecosystems where the estimates increased from 1950 to 1978 before a steep decrease at the beginning of the 1980s and then an increase until 2010. The outputs of the temperature-based model show that BRT should have decreased at a slower rate than observed, while the TTE should have decreased slightly in place of increasing. Thus, changes in the species composition of the catch have affected the observed parameters which cannot be explained only by the temperature effect. This suggests that faster and more efficient trophic transfers have resulted from direct fishing-induced impacts on species assemblages.

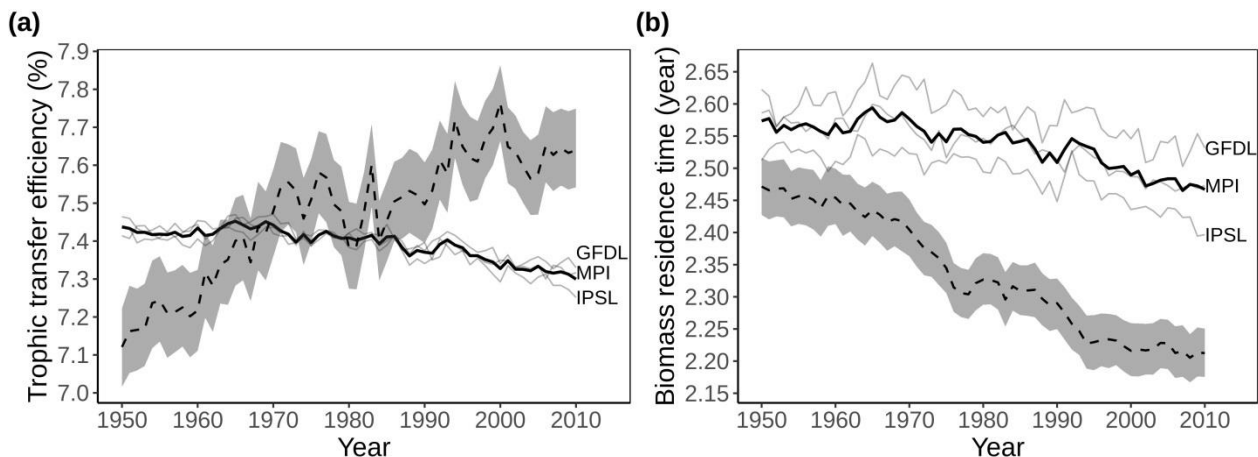


Figure 2.6: Past trends of trophic transfer parameters over the period 1950–2010. The dashed lines represent global mean values of the observed trophic transfer efficiency (TTE) (a) and biomass residence time (BRT) (b). Shaded areas refer to bootstrap confidence intervals at 95%. Solid black lines represent theoretical global mean trends of TTE and BRT, computed using the GLM temperature-based model. Light grey lines are trends calculated using three Earth system models (GFDL: Geophysical Fluid Dynamics Laboratory, MPI: Max Plank Institute, IPSL: Institut Pierre Simon Laplace). 2253 grid cells were used to calculate the trends.

2.3.3. Projections for the end of the century

TTE and BRT should decrease until 2040, regardless of the climate scenario or the Earth system model considered (Figure 2.7a, b). From 2000 to 2040, global averages are projected to decrease slightly by 0.09% for TTE and by 0.09 years for BRT. After 2040, TTE and BRT remain stable in the scenario RCP2.6, while the decrease accelerates for both indicators in scenario RCP8.5. Overall, under RCP8.5, we projected a 0.5% loss of TTE (from 7.7 to 7.2%) and a 0.4 year decrease in BRT (from 2.7 to 2.3 years) over the period 2000–2100.

The geographical distributions of the projected changes in TTE and BRT under RCP8.5 scenario show that the two trophic transfer parameters should decrease everywhere by the end of the 21st century (2100), with the largest changes expected at high latitudes (Figure 2.4g, h). In polar, upwelling and temperate ecosystems, the projected losses in TTE are around 0.8% by 2100, while they are much lower around 0.2% in tropical ecosystems (Figure 2.7c). The BRT will be more affected by ocean warming in polar ecosystems than in others, with more than a 1.0 year decrease by 2100, compared to 0.4 years (~5 months) in tropical ecosystems, 0.2 years (~2 months) in temperate ecosystems, and almost no effect in upwelling ecosystems, on average (Figure 2.7d).

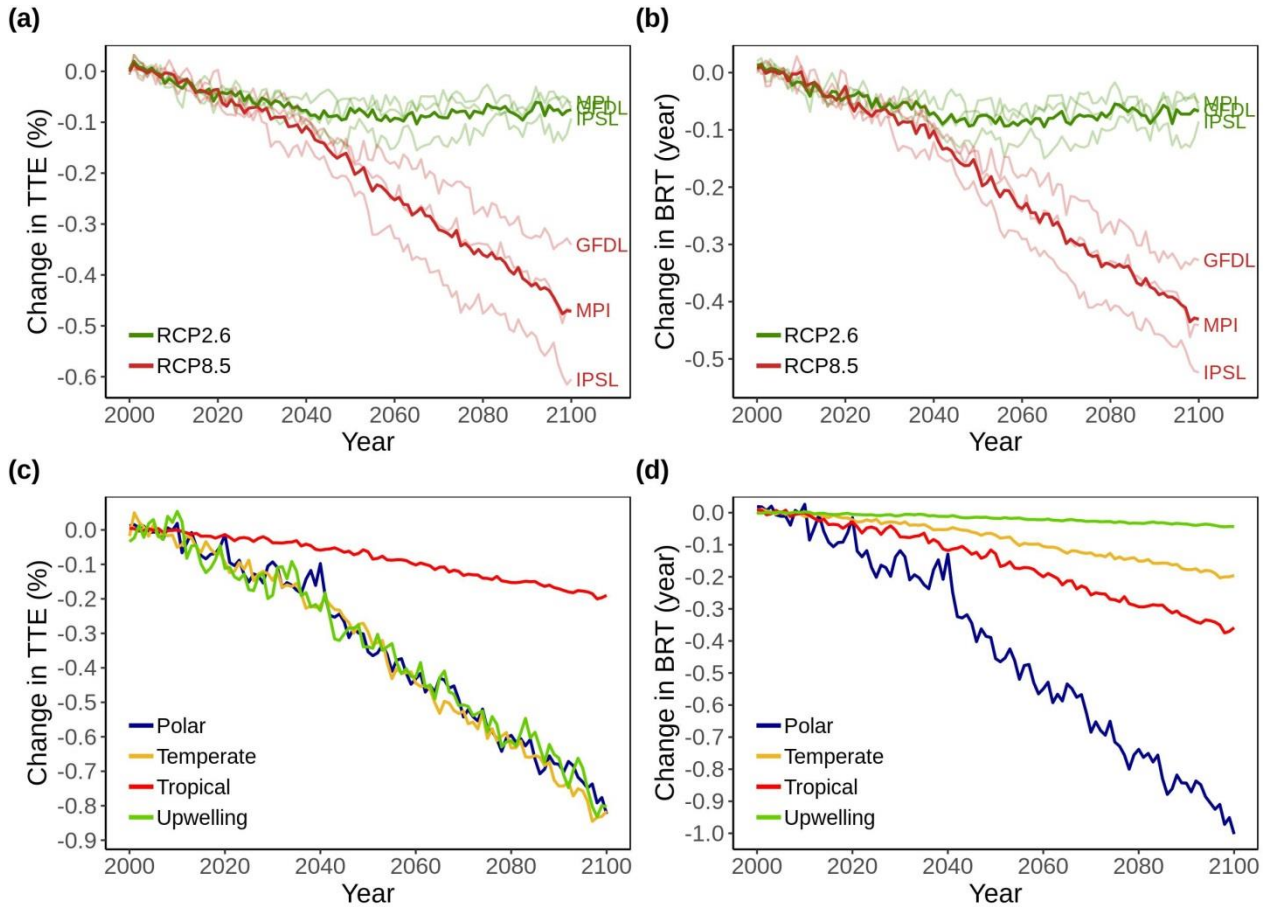


Figure 2.7: The expected changes of trophic transfer at the global scale over the 21st century. Panel (a) shows the projections of trophic transfer efficiency (TTE) and panel (b) shows the projections of biomass residence time (BRT) in the coastal ecosystems between 2000 and 2100 under two climate change scenarios, RCP2.6 and RCP8.5 in green and red, respectively. The dark lines are the mean values of the trophic transfer parameters and the light lines are the values of each general circulation model. Panels (c) and (d) focus on RCP8.5 scenario.

2.4. Discussion

Our results provide estimates of average TTE and BRT in coastal marine food webs, at the global scale and per ecosystem type. We show that human-induced changes in species assemblages may already have affected the functioning of coastal marine food webs and are expected to have greater impacts over the 21st century. Specifically, the trophodynamics of coastal marine ecosystems have already changed and are expected to amplify their rate of change in the coming decades.

2.4.1. Less efficient and faster transfers in warm waters

Our study shows that sea water temperature significantly influences biomass transfers through the food web in global coastal marine ecosystems. The warmest coastal ecosystems are characterized by low-efficient and fast biomass transfers through the food web. These characteristics indicate that species assemblages are dominated, at each TL, by species with low TTE because of large energy losses due to their metabolism processes that scale with temperature (Brown *et al.* 2004; Schramski *et al.* 2015). Also, the BRT is shorter in tropical coastal ecosystems so the biomass transfer between a prey and its predator is faster at each TL. These trophic functioning properties may be explained by species assemblages where communities may be dominated by short-living and fast-growing species. In contrast, in polar and temperate ecosystems, biomass is transferred more efficiently and slowly, where a unit of biomass spends more time in the food web. Such trophodynamic properties may be explained by species assemblages dominated by long-living and slow-growing species in colder waters as suggested by several authors in polar ecosystems (e.g., Pörtner *et al.* 2005; Murphy *et al.* 2016; Peck 2016). As the biomass transfer indicators are calculated using trophic spectra, the observed contrasts between warm and cold waters do not result from the distribution of long- or short-living species among food webs (more predators and less preys in cold waters), but from differences occurring at every TL (longer living preys and predators in cold waters in contrast to warm waters).

The natural non-predation mortality is an additional factor reducing TTE by introducing supplementary losses, although it appeared to have little effect on the differences in TTE between the ecosystem types (Appendix A - Supplementary material A.3). Finally, the low TTE in upwelling is consistent with the literature (Coll *et al.* 2008; Libralato *et al.* 2008) and may be due to the highly variable productivity of upwelling ecosystems. This lack of stability, which characterizes immature or disturbed ecosystems (*sensus* Odum 1969), is likely to result in a weakly structured food web with fast and inefficient biomass transfers.

2.4.2. Robustness of the analysis

As we use catch data to study TTE and BRT, fishing effort, in addition to temperature, might affect trophic flow in marine ecosystems. The assessment of the potential effects of the confounding factors from fishing shows that the temperature sensitivity of these indicators remains supported (Appendix A - Supplementary material A.4 and A.5). First, we found that the fishing intensity (catch per km²) and the fishing strategies (MTL) have only a small effect on TTE estimates while BRT estimates are more sensitive to fishing intensity (Appendix A - Supplementary material A.4). However,

the effects of sea water temperature and ecosystem type on BRT remained highly significant and qualitatively unchanged even after accounting for the effects of fishing. Secondly, based on data from the selected Ecopath models, the absolute values of BRT and TTE are overestimated and underestimated, respectively, when using catch data instead of biomass data (Appendix A - Supplementary material A.5). However, here too, qualitative results regarding the temperature effect and the variability among ecosystem types remained consistent.

Furthermore, it appeared that the exclusion of the lowest TLs affects mainly cold waters and upwelling ecosystems, decreasing the estimated TTE and increasing BRT (Appendix A - Supplementary material A.6). However, the variations due to the lower TLs of the food web do not modify the order of magnitude and the trends regarding sea water temperature and ecosystem type effects.

The potential bias due to the spatial autocorrelation is low for TTE with a slight effect in tropical ecosystems (Appendix A - Supplementary material A.7). Regarding BRT, the effect is a bit stronger, suggesting that we underestimated BRT in temperate and tropical ecosystems (greater values without the spatial autocorrelation) and we underestimated the temperature effects in polar and tropical ecosystems (greater slopes without the spatial autocorrelation).

The introduction of the natural non-predation mortality as an additional loss in TTE estimates by adding a correction factor (Appendix A - Supplementary material A.3) has a rather low effect on the GLMs outputs. It induces an overall decrease in TTE but that does not change substantially either the temperature effect or the differences between the ecosystem types. Even if it is imperfect especially because we use potentially biased modelled parameters, we consider that the inclusion of the correction is better than ignoring the additional losses.

More generally, the observed temperature effects and predicted changes in trophic transfer are likely to be underestimated because our study is taking into account only the effect of community structure on the ecosystem functioning. Additional ocean warming effects at individual and population levels are also expected to change the trophic transfer within marine food webs.

2.4.3. Towards faster and less efficient trophic transfers

The global decrease in BRT and increase in TTE over the period 1950–2010 is likely partly driven by the global increase in fishing pressure as previously shown by Maureaud *et al.* (2017), who focused on quantifying the fishing effects on trophodynamics over the Large Marine Ecosystem. Majorities of fishing activities tend to select the targeted large and long-living species causing a decrease in their abundance compared to small species with fast life histories (Jennings *et al.* 1999;

Cheung *et al.* 2007; Planque *et al.* 2010; Shephard *et al.* 2012). Our results suggest that the same fishing effects occur within each trophic class leading to shorter biomass residence time and less efficient energy transfer in marine food webs. Such a trend may be considered as an adaptive reaction to the fishing pressure (Maureaud *et al.* 2017), leading to more efficient, but simplified and potentially less resilient food web.

The global decreasing trend of TTE estimated using the modelled temperature-based GLM (Figure 2.6a) is not consistent with the observed TTE over the period 1950–2010. The opposition between observed and modelled trends can be derived from the dominant fishing pressure. The decrease in the modelled TTE is driven by ocean warming, while the increase in the observed TTE between 1950 and the mid-1990s can likely be attributed to the growing amount of fishing pressure (Pauly & Zeller 2016; Maureaud *et al.* 2017). Following Pauly & Zeller (2016), global fishing catch reached its maximal value in 1996 and stabilized until now. Therefore, the stabilization of the TTE trend from the mid-1990s can be assumed to be caused by the effects of constant fishing catch over already exploited system and the growing effect of ocean warming (Beaugrand *et al.* 2019). In parallel, the decreasing trend in BRT between 1950 and the mid-1990s is consistent with the observed BRT (Figure 2.6b). However, the decrease in observed BRT is steeper between 1950 and the mid-1990s. That can also be attributed to the increasing fishing pressure. As for TTE, the trend in observed BRT stabilized between 2000 and 2010 probably due to the decreasing fishing effects and the growing effect of ocean warming.

In the coming decades, as ocean warming is expected to intensify and by hypothesizing that global fishing pressure will stabilize, the trend in TTE may reverse and decrease (Figure 2.7a, c) while BRT may globally continue to decrease (Figure 2.7b, d). Consequently, the greater losses of production between every TL due to the decrease in TTE and BRT in the food web may lead to a decrease in biomass and production at each TL.

Our projections of changes in trophic transfer functioning only result from the expected modifications in species assemblages induced by warming. At the species level, responses to warming may differ from one species to the other, depending on their thermal tolerance and life histories (Perry *et al.* 2010; Pörtner & Peck 2010), and leading to changes in their own productivity and/or biogeographical shifts of their spatial distribution. In addition, indirect effects due to changes in species interactions can enhance the changes in marine community structure and functioning (Bruno *et al.* 2015).

2.4.4. Polar ecosystems: the more affected ecosystems?

Ocean warming effects on the trophic transfer parameters exhibit substantial differences between ecosystem types. TTE and BRT in polar ecosystems are projected to strongly decrease by 2100 due to its high sensitivity to temperature (Figure 2.4). Such a high thermal sensitivity of TTE and BRT in polar ecosystems is likely due to the narrow thermal window of the polar species that inhabit stable ecosystems (Peck *et al.* 2004; Sunday *et al.* 2011; Pörtner *et al.* 2014). The changes in biomass transfer may also be exacerbated by the reshuffling of polar ecosystems structure induced by the observed and projected poleward shifts in species distribution and the expansion of subpolar/boreal communities with faster and less efficient biomass flow properties (Cheung *et al.* 2009; Kortsch *et al.* 2015; García Molinos *et al.* 2016; Frainer *et al.* 2017). In addition, although the complexity and the diversity of the planktonic food web in polar ecosystems are equivalent to temperate ecosystems (Smetacek & Nicol 2005; Michel *et al.* 2012), the relatively low coastal marine biodiversity of high TL species (Tittensor *et al.* 2010; Worm & Lotze 2016) may accelerate the rate of decline of polar species. Such declines of endemic and sea ice dependent species are already observed at some locations (e.g., krills in the Southern Ocean, (Atkinson *et al.* 2004). Besides, the effects of temperature may also be abrupt in polar ecosystems due to more frequent and extreme marine heatwaves (Frölicher *et al.* 2018).

Species inhabiting in tropical ecosystems has also a relatively narrow thermal window that could explain the high thermal sensitivity of BRT (Poloczanska *et al.* 2016). However, TTE in tropical ecosystems exhibits a low thermal sensitivity and thus a moderate projected decrease by 2100. The higher biodiversity in tropical ecosystems may help buffer the warming effects on biomass transfer at lower latitudes. Therefore, in tropical ecosystems the BRT is expected to largely decrease but the losses in production between each TL may be weakly impacted. However, as our projections are based on current temperatures, we likely underestimate the effects of ocean warming on tropical ecosystems since these ecosystems will experience unprecedentedly observed temperature levels associated with more frequent and extreme marine heatwaves (Frölicher *et al.* 2018).

BRT in temperate ecosystems exhibits a low thermal sensitivity to ocean warming probably due to the wide thermal window of the marine species living in temperate regions, as the result of the high seasonal variability (Sunday *et al.* 2011). However, TTE is highly sensitive to temperature leading to a high projected decrease in TTE while BRT is projected to decrease moderately.

2.5. Conclusion

In summary, our results show that biomass transfers in marine food webs have globally become more efficient and faster over the period 1950–2010, which may be explained, at least partially, by the past increase in global fishing pressure. Such changes may have compensating effects on the whole ecosystem biomass, as faster transfers imply less biomass per TL, while more efficient transfers are reducing the losses. We also found that temperature plays a key role to determine the properties of the biomass flow in marine coastal ecosystems. While warm coastal ecosystems are characterized by less efficient and fast biomass transfers, in colder coastal ecosystems, biomass transfers are slower and more efficient. Our model projections suggest that the increase in sea temperature is expected to shift the global ocean towards faster and less efficient biomass transfers by 2100 with especially drastic changes in polar ecosystems. These changes in trophic functioning have cumulative effects and will likely lead to a decrease in biomass through increasing losses of production at each TL, and decreasing BRT in the food web. Ultimately, they may severely affect the catch potential of fisheries across the globe by the end of the century.

CHAPTER 3

**Climate-induced decrease in
biomass flow in marine food
webs may severely affect
predators**

CHAPTER 3: Climate-induced decrease in biomass flow in marine food webs may severely affect predators

3.1. Introduction

Human-induced climate change is already impacting ocean ecosystems by driving major changes in their physical and chemical properties and the impacts are expected to intensify over the 21st century particularly under insufficient carbon mitigation (IPCC 2014; Bindoff *et al.* 2019). One of the marine ecosystem components that are impacted by changes in ocean properties is net primary production (NPP) that plays an essential role in fueling energy and biomass up marine food webs. Total NPP of the ocean is projected to decrease over the course of the 21st century (Bopp *et al.* 2013; Cabré *et al.* 2015; Laufkötter *et al.* 2015). Regionally, NPP is projected to decrease in the low-latitude regions and to increase at high latitude, mainly due to the stratification-induced exacerbation of nutrient limitation at low latitude and to an alleviation of light limitation as a result of loss of sea ice at high latitude (Bopp *et al.* 2013; Cabré *et al.* 2015; Laufkötter *et al.* 2015).

These projected changes in NPP as well as the changing ocean conditions are impacting the physiology and biogeography of marine organisms with cascading effects on ecosystem structure and functions (Bindoff *et al.* 2019). Ocean warming, deoxygenation and ocean acidification alter the physiology and fitness of marine organisms (Pörtner & Farrell 2008; Pörtner & Peck 2010; Pörtner *et al.* 2017), causing shifts in species distribution (Pinsky *et al.* 2013; Poloczanska *et al.* 2013; Jones & Cheung 2015), phenology (Burrows *et al.* 2014; Asch *et al.* 2019) and changes in biomass transfers (Maureaud *et al.* 2017; du Pontavice *et al.* 2019; Eddy *et al.* 2021). Differences in the rate of responses to climate change within marine communities and between regions disrupt existing ecosystem structure and functioning such as biomass flow in marine food webs (Dulvy *et al.* 2008; Verges *et al.* 2014; Montero-Serra *et al.* 2015; Barton *et al.* 2016; Kortsch *et al.* 2018).

Recent global projections based on several ecosystem models show that climate change is expected to induce a mean global biomass decrease in marine ecosystems (Lotze *et al.* 2019) mainly due to a decrease in production fueling marine food webs (NPP) amplified on animal biomass further up the food web by warming-induced changes in metabolic rates (Stock *et al.* 2014a, 2017b;

Kwiatkowski *et al.* 2019; Lotze *et al.* 2019). Different hypotheses are proposed to explain the climate-induced amplification of biomass decline including phyto- and zooplankton size composition, lengthening of food chains, reduced zooplankton growth efficiency and changes in metabolic rates (Stock *et al.* 2014a; Kwiatkowski *et al.* 2019; Lotze *et al.* 2019).

Only a few studies (e.g., Petrik *et al.*, 2020) have explored both ecosystem biomass and production. For each ecosystem compartment, the latter is issued from animal growth and reproduction, implicitly referring to a gross production of living biomass (Gascuel *et al.*, 2008, 2011; Appendix B – Figure B.1.1), which can be used in the system to feed the food web, detritus compartment, and fisheries if any, or to constitute a net production changing the current biomass of the considered compartment. The ecosystem production defines the capability of the ecosystem to replenish, e.g., following human impacts, and is therefore a key factor to study the future of fisheries whose sustainability is not directly related to biomass, but more to the exploited part of the gross production.

Analysis combining global fisheries catch data and information on fish life history traits showed that marine ecosystem trophodynamics, as indicated by the trophic transfer efficiency of energy through the food web and the residence time of biomass within each trophic level (TL), are sensitive to changes in ocean temperature (du Pontavice *et al.* 2019). However, the roles of these trophodynamic processes that govern the flow of energy through marine ecosystems in determining the relationship between NPP and upper TL production under climate change have not been explicitly explored.

Here, we aim to understand how future changes in ocean conditions would affect key ecosystem functions such as biomass transfers, consumer biomass and production (defined here for $TLs \geq 2$), and ecosystem trophic structure. We use a trophodynamic ecosystem model – EcoTroph (Gascuel 2005; Gascuel & Pauly 2009; Gascuel *et al.* 2011) – to examine biomass flows within marine ecosystems and project future changes in biomass and production in the global ocean in the 21st century. The EcoTroph projections are forced with the outputs of three Earth system models (ESMs) under two emission scenarios (Representative Concentration Pathways, RCPs), RCP26 (strong mitigation scenario) and RCP8.5 (“no mitigation policy” scenario). Fishing exploitation and temporal dynamics were not explicitly considered in the model and, thus we projected climate change impacts on a theoretical unexploited ocean ecosystem under the steady state assumption. Based on the results from the simulation modeling, we examine the impacts of climate change on biomass flows and the resulting ecosystem biomass and production and discuss their implication for the sustainability of fisheries.

3.2. Materials and Methods

3.2.1. The EcoTroph model

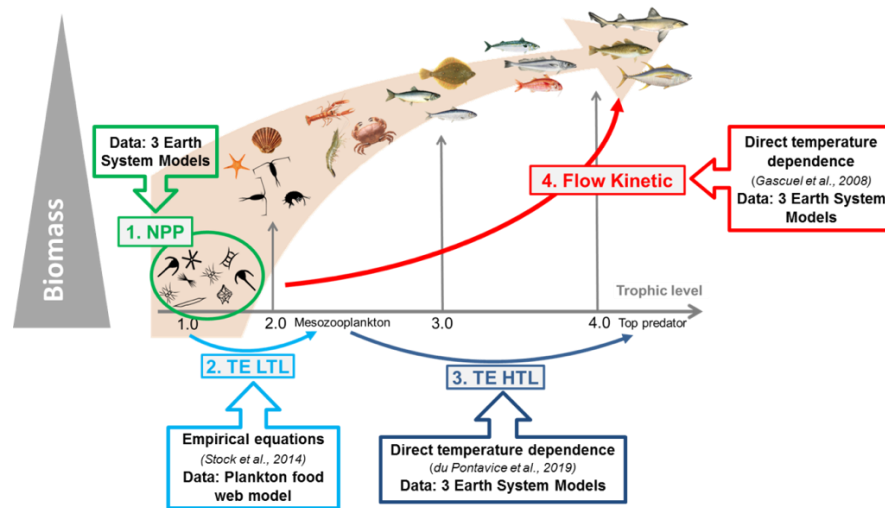


Figure 3.1: Conceptual design of the EcoTroph model and forcing used. The trophic functioning of marine food webs is represented by a biomass flow, with biomass entering the system at trophic level 1 due to net primary production, NPP. Biomass flow reaching each trophic level is then defined by the trophic transfer efficiency at low and high trophic level, TE LTL (derived from the plankton food web model COBALT) and TE HTL (estimated from the sea surface temperature (SST) according to du Pontavice et al. (2019)), respectively. The flow kinetics, which is also forced by SST (Gascuel *et al.* 2008), is a key parameter to derive biomass at each trophic level of the model from the biomass flow (Gascuel & Pauly 2009). One EcoTroph model is implemented each year within each cell of the global ocean, forced by NPP and SST from Earth system models' projections. Credit : adapted from Aurore Maureaud.

EcoTroph is an ecosystem modeling approach through which the ecosystem trophic functioning is modeled as a continuous flow of biomass surging up the food web, from lower to higher TLs, through predation and ontogenic processes (Figure 3.1, Gascuel et al., 2005, 2011). EcoTroph is founded on the principle that an ecosystem can be represented by a continuous distribution of the biomass along TLs, i.e., a biomass trophic spectrum (Gascuel *et al.* 2005). Biomass enters the food web at TL = 1, as generated by the photosynthetic activity of primary producers and recycling of nutrients by the microbial loop. Only mixotrophs, i.e., organisms that are simultaneously primary producers and first-order consumers, would be at TLs between TL = 1 and TL = 2. Their biomass is usually low, and is conventionally split between biomasses at TL = 1 and TL = 2. Biomass at TLs higher than 2 is

composed of heterotrophic organisms with mixed diet and fractional TLs resulting in a continuous distribution of biomass along TLs (considered here as consumers).

To facilitate the computation of EcoTroph, biomass spectrum is aggregated by small TL classes that include all organisms within the lower and upper TLs of each class. Thus, EcoTroph does not represent individual species explicitly; instead, species are combined into classes based only on their TLs. As a convention (and based on previous studies; Gasche et al., 2012; Gascuel et al., 2005) we considered trophic classes of width $\Delta\tau = 0.1$ TL to be an appropriate resolution and a range starting at TL = 2 (corresponding to the first-order consumers), up to TL = 5.5, an appropriate range to cover all top predators in marine systems (Cortes, 1999; Pauly, 1998).

Another key principle behind EcoTroph is that trophic functioning of aquatic ecosystems may be viewed as a continuous biomass flow moving from lower to higher TLs. Each organic particle moves up the food web by continuous processes (representing an organism's ontogenetic changes in TLs as it grows) and abrupt jumps due to predation events. By combining the flows of all particles in a food web, the aggregated biomass flows can be represented by a continuous function (see Appendix B – Figure B.1.2). Thus, the continuous function of biomass flow in EcoTroph represents the mean flow of biomass of individual organisms and is not an approximation of a discrete process (Gascuel *et al.* 2008).

The flow of biomass in a biomass spectrum in EcoTroph is represented by the traditional equations of fluid dynamics. Specifically, the continuous biomass flow, $\Phi(t, \tau)$, is described by (details on equations and notations in Appendix B - Supplementary material B.1):

$$\Phi(t, \tau) = B(t, \tau)K(t, \tau) \quad \text{Eq. 1}$$

where $\Phi(t, \tau)$, the quantity of biomass moving up through TL τ , at every moment, t , due to predation, is expressed in $t \text{ year}^{-1}$, $B(t, \tau)$ the density of biomass at TL = τ expressed in $t \text{ TL}^{-1}$, and $K(t, \tau)$ the flow kinetic expressed in TL year^{-1} . The flow kinetic measures the speed of the biomass flow in the food web, from low to high TLs, and is inversely proportional to biomass residence time, i.e., the time each organism stays at a given level of the food web depending of its life expectancy.

Under steady-state conditions, the Equation 1 becomes:

$$B(\tau) = \frac{\Phi(\tau)}{K(\tau)} \quad \text{Eq. 2}$$

The biomass flow $\Phi(\tau)$ is not conservative with a loss rate $\psi(\tau)$ at TL = τ , such as:

$$\frac{d\Phi(\tau)}{d\tau} = -\psi(\tau) \Phi(\tau) \quad \text{Eq. 3}$$

Furthermore, the biomass flow $\Phi(\tau)$ can be expressed as a decreasing function of TL (see details in Appendix B - Supplementary material B.1):

$$\Phi(\tau + \Delta\tau) = \Phi(\tau)e^{-\mu_\tau\Delta\tau} \quad \text{Eq. 4}$$

Where $\Phi(\tau)$ is the biomass flow at TL τ (i.e., at the start of the trophic class $[\tau, \tau + \Delta\tau[$), μ_τ (expressed

in TL⁻¹) represents the mean natural losses within the trophic class through non-predation mortality, excretion, and respiration. It defines the transfer efficiency, TE, within the trophic class $[\tau, \tau + \Delta\tau[$ such as:

$$TE = e^{-\mu_\tau} \quad \text{Eq. 5}$$

A discrete approximation of the continuous distribution $B(\tau)$ is used for mathematical simplification (details on equations in Appendix B - Supplementary material B.1). Hence, the model state variable becomes B_τ , the biomass (in metric tons) present at every moment under steady-state conditions within the TL class $[\tau, \tau + \Delta\tau[$ and Equation 2 becomes:

$$B_\tau = \frac{1}{K_\tau} \Phi_\tau \Delta\tau \quad \text{Eq. 6}$$

where Φ_τ and K_τ are the mean biomass flow (in t year⁻¹) and the mean flow kinetic (in TL year⁻¹) within the trophic class $[\tau, \tau + \Delta\tau[$, respectively. The mean flow kinetic K_τ varies per trophic class

and is directly defined using mean values per trophic class based on an empirical model previously developed by Gascuel et al. (2008) (see below).

Finally, EcoTroph defines the biomass flow $\Phi(\tau)$ as the density of production at $TL = \tau$. Therefore, the production P_τ of the trophic class $[\tau, \tau+\Delta\tau]$ is:

$$P_\tau = \int_{\tau}^{\tau+\Delta\tau} \Phi(\tau) d\tau = \Phi_\tau \Delta\tau \quad \text{Eq. 7}$$

Production is commonly expressed in $t \text{ year}^{-1}$ that implicitly refers to the conversion of biomass eaten at $TL \tau-1$, into predator tissues whose mean TL is τ . Therefore, in a TL -based approach such as EcoTroph (wherein the width of trophic classes may differ from 1 TL), production has to be expressed in $t \text{ TL year}^{-1}$, i.e., tons moving up the food web by 1 TL on average during 1 year. Hence, EcoTroph highlights that biomass stems from the ratio of the production to the flow kinetic.

3.2.2. Simulating biomass flow from primary production to upper trophic levels

In EcoTroph, biomass flow and the resulting biomass from primary production to upper trophic levels are modeled using three distinct properties of marine food web potentially affected by climate change: (i) primary production fueling the food web (Eq. 7 at $\tau=1$), (ii) trophic transfer efficiency quantifying biomass which is transferred at each trophic level (Eq. 5), and (iii) flow kinetic measuring the speed of this biomass transfer (Eq. 2 and 6).

Trophic transfer efficiency of low trophic levels

In this study, we modeled the trophodynamics of the planktonic food web separately from those of the upper part of the food web. Projections of annual average vertically integrated net primary production (NPP) from 1950 to 2100 were obtained from the outputs of global coupled atmosphere-ocean-biogeochemistry Earth system models (ESMs, described in the section below). EcoTroph considers NPP as biomass production at $TL = 1$ i.e., $P_1 = \text{NPP}$ (Eq. 7). The flows of detritus biomass are not considered in this study and we discussed the implications of this assumption on the results and conclusions of this study.

While transfers of energy through the plankton food web can be complex (Friedland *et al.* 2012), a robust pattern revealed in numerous previous analyses is a tendency for more efficient energy transfers to fish in more productive regions (Armengol, Calbet, Franchy, Rodríguez-Santos, & Hernández-León, 2019; Ryther, 1969; Stock, Dunne, & John, 2014). This pattern arises because a) the dominance of picophytoplankton in low productivity regions (Agawin *et al.* 2000; Irwin *et al.* 2006; Morán *et al.* 2010; Heneghan *et al.* 2016; Armengol *et al.* 2019) creates long food chains between primary producers and fish, and b) the limited surplus energy above basal metabolic costs of small zooplankton in subtropics reduces the planktonic transfer efficiency (Stock & Dunne, 2010; Stock, Dunne, & John, 2014).

To estimate variations in the plankton food web transfer efficiency across ocean biomes, we used simulations from the Carbon, Ocean Biogeochemistry, and Lower Trophics (COBALT) global ecosystem model, which has been shown to capture observed variations in the flow of energy across ocean biomes (Stock *et al.* 2014b, a). Based on the outputs of COBALT, we estimated the transfer efficiency between the primary production and the mesozooplankton production, TE LTL, as:

$$TE\ LTL_{y,i} = \left(\frac{MEZOO\ PROD_{y,i}}{NPP_{y,i}} \right)^{1/(MEZOO\ TL_{y,i} - 1)} \quad Eq. 8$$

Where $NPP_{y,i}$ is the net primary production in the grid cell, i , for the year y , and $MEZOO\ PROD_{y,i}$ and $MEZOO\ TL_{y,i}$ are the mesozooplankton production and trophic level in the grid cell i for the year y . Transfer efficiency of low TLs (TE LTL) was calculated each year y , between 1950 and 2100 for RCP8.5 in every cell, i , of a two-dimensional horizontal $1^\circ \times 1^\circ$ grid covering the global ocean (Appendix B – Figure B.2). $NPP_{y,i}$ and $MEZOO\ PROD_{y,i}$ were directly extracted from COBALT while $MEZOO\ TL_{y,i}$ was calculated using biomass flows between mesozooplankton and its preys in COBALT.

Transfer efficiency of low TLs is used to quantify the transfer efficiency between $TL = 1$ and $TL = 2$. Between $TL = 2$ and $TL = 3$, we assume a linear change from TE LTL (Eq. 8) at $TL = 2$ and TE HTL (described in the following section) at $TL = 3$. For $TL > 3$, we apply TE HTL to estimate the transfer efficiency. The spatial pattern and the distribution of transfer efficiency of low TLs for each ecosystem over the reference period 1986–2005 are available in the Figures S3.3 and S3.4.

To apply EcoTroph, the projected values of transfer efficiency at low TLs under the low and high greenhouse gas emissions scenarios are required. For the high greenhouse gas emissions scenario, we calculated the transfer efficiency of low TLs using the COBALT outputs projected for RCP8.5 as described above. For the low emissions scenario, since the COBALT model was not available

for RCP2.6, we assumed that transfer efficiency follows the same global trend from 1950 to 2030 under RCP2.6 and RCP8.5. We made such assumption because the projected changes in SST, a key determinant of the transfer efficiency of low TLs, followed a similar pathway under RCP2.6 and RCP8.5 for this time period (see trends in SST and transfer efficiency of low TLs in the Appendix B – Figure B.3.1). We defined the year 2031 as a breaking point from which the global trends in SST under RCP8.5 and RCP2.6 diverge (see Appendix B – Figure B.3.2). Thus, for the time period from 2031 onwards, we assumed that the transfer efficiency of low TLs under RCP2.6 was the average of transfer efficiency of low TLs under RCP8.5 over the decade 2026–2036 (5 years before and after 2031) (detailed method in Appendix B - Supplementary material B.3).

Trophic transfer efficiency of higher trophic levels

In EcoTroph, the trophic transfer efficiency of the higher TLs (TL ≥ 2) takes into account the losses at each trophic class and is used to estimate the fraction of biomass which is transferred from one TL to the next (Eq. 5). In this analysis, we use the temperature-dependent high TLs transfer efficiency (TE HTL) estimates derived from du Pontavice et al., (2019):

$$\text{TE HTL} = e^{(-2.162 + \text{SST}(-0.025 + a) + b)} \times 1.038 \quad \text{Eq. 9}$$

where a and b are specific parameters for each ecosystem type (polar, temperate, tropical and upwelling; Table S4 and Appendix B – Figure B.2) and SST is the sea surface temperature. This relationship between SST and transfer efficiency of higher TLs was obtained by combining global fisheries catch data and information on fish life history traits (du Pontavice *et al.* 2019). Thus, the warming-induced variations in transfer efficiency of higher TLs reflect the changes in species assemblages induced by ocean warming. These estimates of transfer efficiency of higher TLs were calculated between TL = 2 and TL = 4 in all the coastal ecosystems and highlighted that biomass transfers are characterized by “efficient-inefficient continuum” along a temperature gradient (see the relationship between temperature and transfer efficiency of higher TLs in Appendix B – Figure B.7f). Biomass flows tend to be efficient in cold waters but less efficient in warmer waters. The temperature dependent transfer efficiency of higher TLs estimates are negatively linked to SST with a strong sensitivity to temperature in polar ecosystems and a lower sensitivity in tropical ecosystems (du Pontavice *et al.* 2019). Besides, upwelling ecosystems stands out as an exception with low transfer efficiency of higher TLs but a strong sensitivity to the changes in temperature (see the warming effect on the transfer efficiency of higher TLs in Appendix B – Figure B.7g).

Flow kinetic

Flow kinetic measures the velocity of biomass transfers from lower to upper TLs and depends on the biomass turnover. To estimate flow kinetic at TL = τ , we used an empirical equation (Gascuel *et al.* 2008) as a function of SST and TL (τ):

$$K_{\tau} = 20.19\tau^{-3.26}e^{0.0.41SST} \quad \text{Eq. 10}$$

The relationship between flow kinetic, and TL and SST derived from a statistical model based on 1,718 groups from 55 published Ecopath models (Gascuel *et al.* 2008). This study showed that P/B can be considered as a measure of the trophic flow kinetic since P/B is a rate of regeneration of the biomass over a unit of time (see detail in Gascuel *et al.*, 2008). In contrast to the empirical equation used for the transfer efficiency of higher TLs which is fitted for marine consumers (TLs ≥ 2 ; du Pontavice *et al.*, 2020), the flow kinetic equation was fitted through all marine groups from primary producers to top predators (Gascuel *et al.* 2008) and includes the changes in kinetic along the food web. Thus, flow kinetic depends on the position in the food web. While, at low TLs, biomass transfers are faster due to species assemblages dominated by short-living species, biomass transfers are slower at upper TLs mainly composed of long-living species (Gascuel *et al.* 2008). Furthermore, the flow kinetic is negatively linked to SST since the species assemblages in warm waters are characterized by shorter life expectancy than in colder waters (see the temperature effect on flow kinetic in Appendix B – Figure B.7c, d; Gascuel *et al.*, 2008).

Hence, consumer production is determined by NPP, mainly driven by nutrient availability, light limitation and temperature (Steinacher *et al.* 2010), and by the trophic transfer efficiencies, here defined for low or high TLs, respectively, as emergent properties of food web dynamics and species assemblages across the food web. Then, at each TL, consumer biomass is calculated as the product of consumer production and the inverse of the flow kinetic. In this implementation of EcoTroph, all climate effects are bottom-up and potential top-down effects are not included. The implications on our projections will be further discussed. Figure 3.1 illustrates a conceptual schema of our approach with the four variables at play to estimate ecosystem biomass and production. Each of them, detailed above, is affected by climate change.

3.2.3. EcoTroph simulations

EcoTroph model is applied separately to 41,135 grid cells in a two-dimensional horizontal 1° latitude x 1° longitude grid covering the global ocean (Appendix B – Figure B.2). Biogeography of grid cells were delimited using the distribution of biomes identified by Reygondeau et al., (2013) and adapted from Longhurst (2007). Each cell was classified as one of the 3 biomes: tropical, temperate and polar biomes. Polar biome was divided into the Arctic and Antarctic ecosystem types to consider the specificity of each of the areas, especially in terms of projected changes in primary production. Upwelling ecosystems were added using the biogeographical provinces described by Reygondeau et al., (2013) (Appendix B – Figure B.2). Biomass and production were calculated for TLs between 2 and 5.5 at intervals of $\Delta\tau = 0.1$, for every year between 1950 and 2100, using projected NPP and SST in each grid cell as inputs. The data comes from three Earth system models (ESMs) developed by three institutes: Geophysical Fluid Dynamics Laboratory (GFDL-ESM2M; Dunne et al., 2012), Max Plank Institute (MPI-ESM-MR; Giorgetta et al., 2013) and Institut Pierre Simon Laplace (IPSL-CM5A-MR; Dufresne et al., 2013). Moreover, we considered two contrasting scenarios: RCP2.6, radiative forcing level reaches 3.1 W m^{-2} by mid-century, and returns to 2.6 W m^{-2} by 2100 (strong mitigation scenario) and RCP8.5, rising radiative forcing pathway leading to 8.5 W m^{-2} in 2100 (“no mitigation policy” scenario). All the changes in parameters, production and biomass were calculated relatively to the IPCC’s AR5 (in which the three above described ESMs were used; IPCC, 2014) reference period 1986–2005.

To quantify the uncertainty induced by the three ESMs, the inter-model variability was estimated by calculating the standard deviation of the changes coming from the three ESMs in 2090–2099 relative to 1986–2005. Then, we mapped the grid cells where the three models do not predict the same direction of the changes (e.g., one predicts an increase while the two others predict a decrease) (see Appendix B – Figure B.5a, b).

A set of additional simulations was designed to estimate the contribution of each process determining the biomass flow on the total consumer biomass and trophic structure. We examined the response of consumer biomass to the four following biomass flow processes: (1) NPP, (2) transfer efficiency of higher TLs, (3) transfer efficiency of low TLs and (4) flow kinetic. In order to understand how biomass of marine ecosystems responds to changes in ocean conditions, we isolated successively the response of each of the four processes. For this analysis, we ran four sets of simulations for each of the three ESMs using RCP8.5. Each of the simulations isolates one biomass flow parameter, which varies over the period 1950–2100 while the others remain constant and equal to their mean values during the reference period 1986–2005. For example, to isolate the effects of NPP, we set kinetic,

transfer efficiencies of higher TLs and low TLs at their mean values during the reference period, while NPP vary over 1950–2100.

3.3. Results

3.3.1. Changes in ocean conditions and biomass transfers over the 21st century

This study projects that the flows of biomass in marine ecosystems will change substantially by 2100 under scenarios of climate change. First, the global NPP exhibits a mean projected decrease of 7.2% and 1.0% for RCP8.5 and RCP2.6, respectively, in 2090–2099 relative to 1986–2005 with large differences among ESMs under RCP8.5 (Figure 3.2a). Specifically, at global scale and under RCP8.5, NPP is projected to decrease by 13.4% and 8.1% for MPI and IPSL, respectively, but no change in NPP is projected by GFDL in 2090–2099 relative to 1986–2005. Large decreases in NPP are projected in low-latitude tropical ecosystems (12.3% by 2090–2099 relative to 1986–2005), largely driven by warming-induced stratification (Cabr  *et al.* 2015; Laufk tter *et al.* 2015) (Figure 3.2b). In contrast, in high-latitude polar ecosystems, NPP is projected to increase with large variations between ESMs (Figure 3.2c).

The global average low TL transfer efficiency is projected to decline by 3.5% and 1.0% under RCP8.5 and RCP2.6, respectively (Figure 3.2d). While the projected changes in transfer efficiency are small in Antarctic, temperate and upwelling ecosystems, the transfer efficiency is projected to decrease largely in tropical ecosystems (-8.8%) and increase in Arctic ecosystems (Figure 3.2e).

The changes in transfer efficiency of higher TLs are projected to decrease, on average, by 4.6% and 1.1% under RCP8.5 and RCP2.6, respectively by the end of the 21st century relative to 1986–2005 (Figure 3.2g). However, since the sensitivity of temperature varies among ecosystem types (du Pontavice *et al.* 2019) and the sea surface warming is projected to vary spatially (Appendix B – Figure B.7g), the higher TLs transfer efficiency is projected to decrease substantially in upwelling and temperate ecosystems (-14.7% and -8.5%, respectively, in 2090–2099 relative to 1986–2005) while in the other ecosystem types, the mean projected decline is relatively low (Figure 3.2h).

Finally, the mean flow kinetic within marine food web (between TL = 2 and TL = 5.5) is projected to increase, on average, by 11.8% and 2.6% for RCP8.5 and RCP2.6, respectively by 2090–2099 relative to 1986–2005 (Figure 3.2j). The changes in mean flow kinetic follow closely the changes in sea surface temperature. The projected ocean warming thus result in increases in flow kinetic in

almost all ecosystems except in Antarctic ecosystem (Figure 3.2k) where the projected changes in SST by 2100 is small (Appendix B – Figure B.7b).

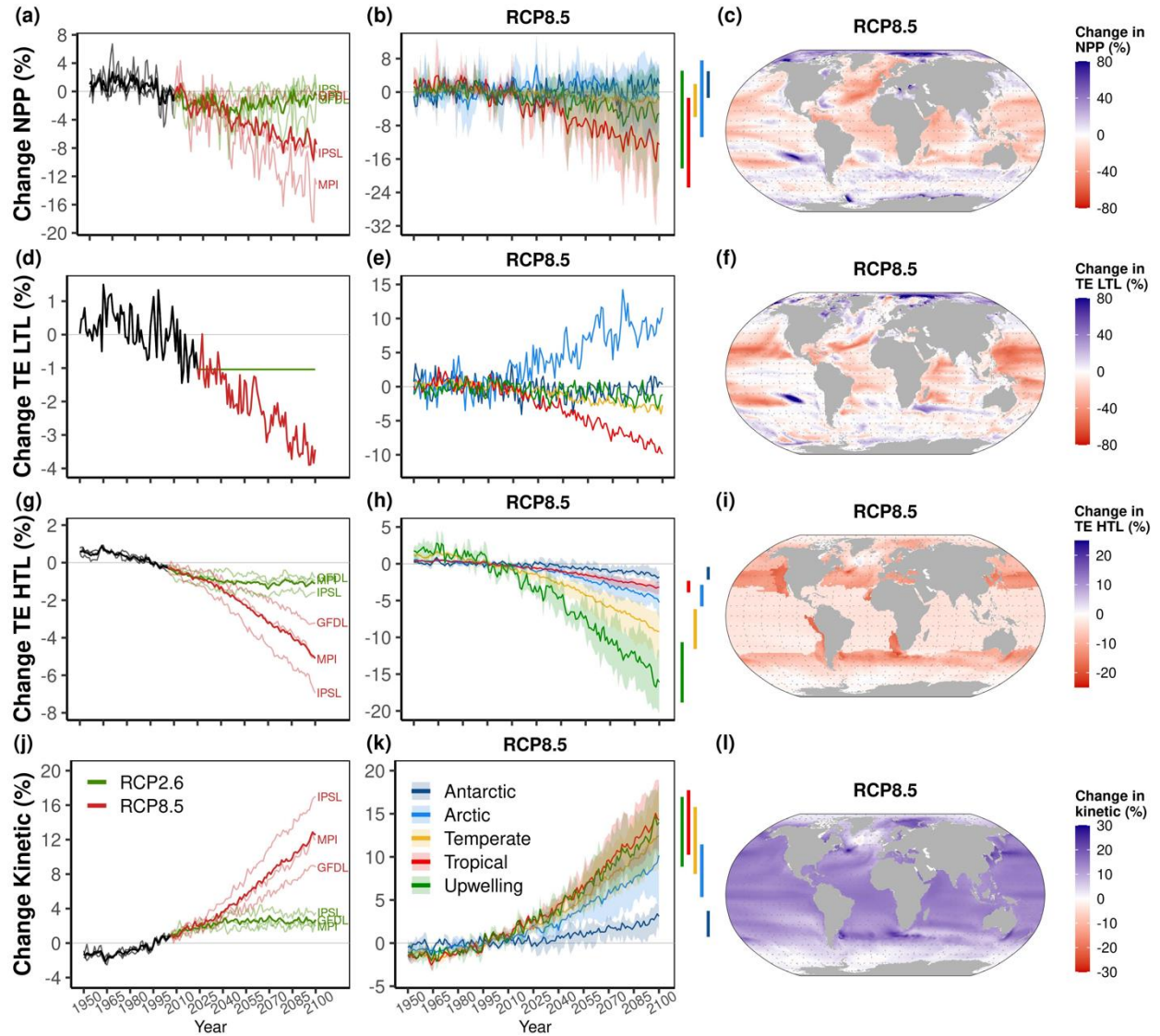


Figure 3.2: Projected changes in biomass flow processes between 1950 and 2100 relative to 1986–2005. The changes in net primary production, NPP, (a, b, c), transfer efficiency of low trophic levels, TE LTL, (d, e, f), transfer efficiency of higher trophic levels, TE HTL, (g, h, i) and flow kinetic (j, k, l) are represented on this figure. Panels (a), (d), (g) and (j) represent the changes at global scale for RCP2.6 and RCP8.5. Panels (b), (e), (h) and (k) represent the changes in each ecosystem type under RCP8.5. The shaded areas around the curves in these panels indicate the inter-model variability (i.e., the variability given by the inputs of the 3 different Earth system models) and the color bars outside the box indicate the range of averaged changes of the three Earth system models over 2090–2099. Panels (c), (f), (i) and (l) represent the changes over the period 2090–2099 in each 1°x1° grid cell.

3.3.2. Changes in the trophic structure of marine ecosystems

The model projects a global mean decrease in total consumer biomass (i.e., total animal biomass with $TLs \geq 2$) in the ocean by 18.5% (from 12% with GFDL to 22.9% with IPSL) with RCP8.5 and 4.5% with RCP2.6 by 2090–2099 relative to 1986–2005 (Figure 3.3a).

We found that the projected increase in flow kinetic contributes the most to the global projected decrease in total consumer biomass relative to the contributions from changes in NPP and trophic efficiencies (Figure 3.3b). The intermodel variations in global biomass projections are largely a result of the differences in NPP projections between the three ESMs (Figure 3.3b).

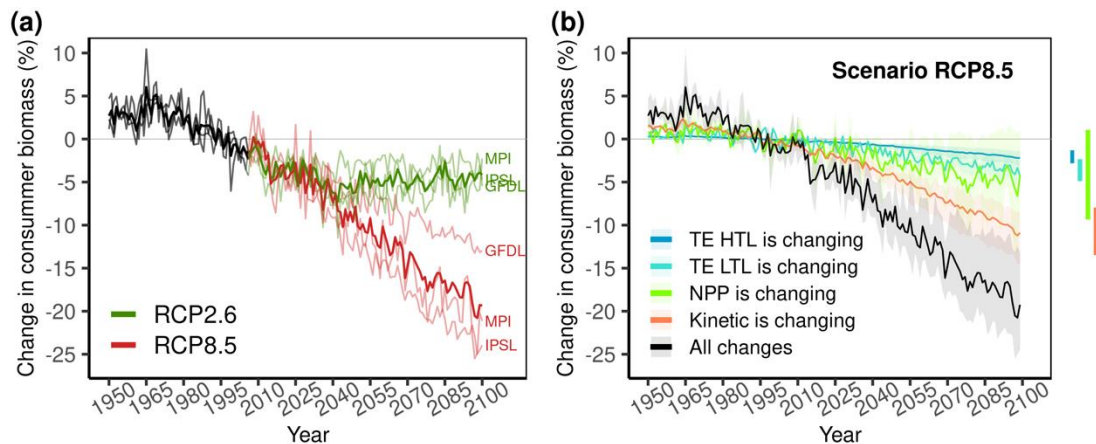


Figure 3.3: Changes in total consumer biomass over the period 1950–2100. (a) Changes in total consumer biomass for RCP2.6 and RCP8.5 relative to the reference period 1986–2005. (b) Mean changes in total consumer biomass for RCP8.5 relative to 1986–2005 in which the contribution of net primary production (NPP), transfer efficiency of lower trophic level (TE LTL), transfer efficiency of higher trophic level (TE HTL) and flow kinetic are isolated. The shaded areas around the curves indicate the inter-model variability and the color bars indicate the ranges of averaged changes of three Earth system models over 2090–2099.

Climate-induced changes in total consumer biomass are projected to vary widely between different parts of the global ocean (Figure 3.4a, b). Specifically, major gains in biomass are projected in the Arctic Ocean, along the coast of Antarctica and in the south-eastern Pacific Ocean. The ensemble mean total consumer biomass is projected to decline strongly between 40° S and 50° N latitude (Figure 3.4c). Notably, under RCP8.5, total consumer biomass is projected to decrease in 2090–2099 relative to 1986–2005, on average, by 28%, 18%, 16% and 10% in tropical, upwelling, temperate and

Arctic ecosystems, respectively (Figure 3.5a). Overall, the spatial patterns of changes in total consumer biomass are similar between RCP8.5 and RCP2.6 but the magnitude of changes is larger under RCP8.5. The areas wherein the projected decrease in biomass exceeds 25% represent 43% of the total ocean surface area for RCP8.5 in 2090–2099 and only 2.5% for RCP2.6.

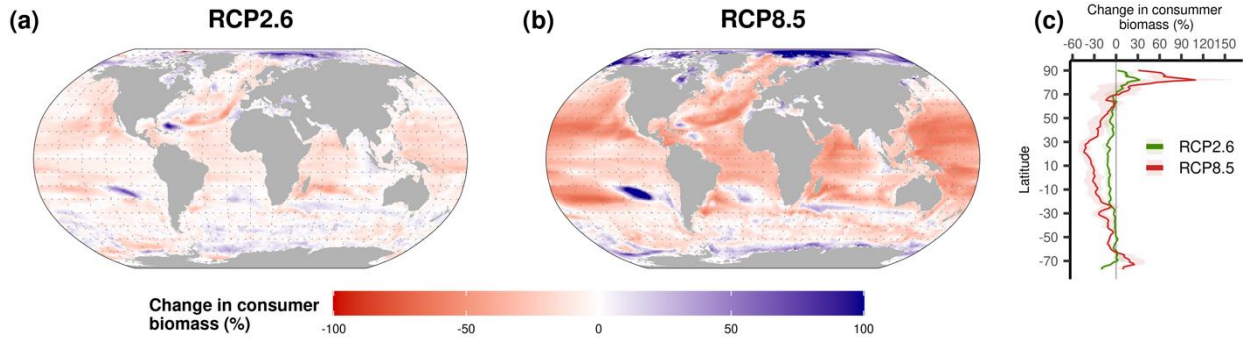


Figure 3.4: Maps of the ensemble mean projections for the three Earth system models of changes in total consumer biomass by 2090–2099 relative to 1986–2005 under (a) RCP2.6 and (b) RCP8.5. Panel (c) represents the changes in consumer biomass by latitude for RCP2.6 and RCP8.5.

In all the ecosystems, warming-induced increases in flow kinetic negatively affect total consumer biomass while the effects of climate change on transfer efficiencies and NPP vary between ecosystem types. In Arctic ecosystem, total consumer biomass is negatively affected by the increases in flow kinetic and transfer efficiency of higher TLs. Simultaneously, the projected decrease in transfer efficiency of low TLs positively affects total consumer biomass. In Antarctic ecosystems, the projected increase in NPP compensates the warming-induced increase in flow kinetic. In temperate ecosystems, flow kinetics and transfer efficiencies (at low and higher TLs) are projected to be the main drivers of the changes in total consumer biomass, while in upwelling ecosystem the decrease in biomass is mainly driven by the decrease in flow kinetics, NPP and transfer efficiency of higher TLs. In tropical ecosystems, the sharp projected decline in total consumer biomass is explained by the climate-induced changes in flow kinetics, NPP and transfer efficiency of low TLs.

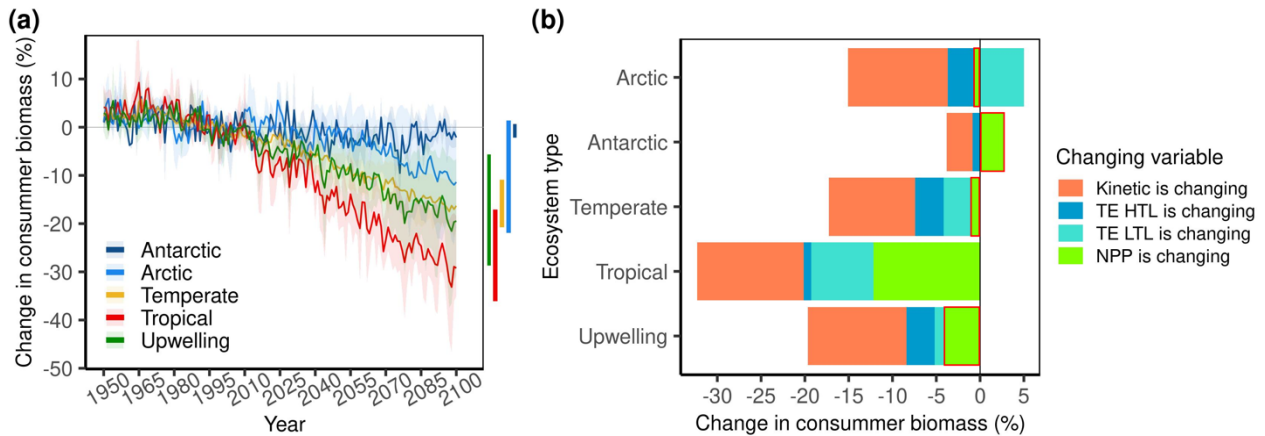


Figure 3.5: Changes in total consumer biomass in each ecosystem type as well as the processes at play for RCP8.5. Panel (a) represents the changes in total consumer biomass for RCP8.5 in each ecosystem type relative to the reference period 1986–2005. Panel (b) represents the mean contribution of the four processes in each ecosystem type (net primary production (NPP), transfer efficiency of lower trophic level (TE LTL), transfer efficiency of higher trophic level (TE HTL) and flow kinetic). The contribution is framed in red color if biomass projections with one of the three models predicts changes in the opposite direction to those predict with the two other models.

3.3.3. Changes in trophic structure of marine ecosystems

Our results also highlight the effects of climate change on biomass at each TL from primary consumers to the top predators since the EcoTroph model represents the food web as a biomass distribution per TL (Figure 3.6). We show that the projected distribution of biomass across different TLs for RCP2.6 remains close to those of the contemporary ocean (1986–2005, Figure 3.6a and Figure 3.7a) while the distribution of the biomass for RCP8.5 is modified, with the largest impacts on high TL species (Figures 3.6b and 3.7b). For RCP8.5, the model projects, on average, a 21.3% decline in predator biomass in 2090–2099 relative to 1986–2005 for TLs between 3.5 and 5.5 which mainly refer to predatory fishes (e.g., cods, tunas, groupers). In contrast an 18.8% decrease in biomass is projected for TLs between 2.5 and 3.5 which usually refers to forage fishes (e.g., herring, capelin) and invertebrates (e.g., shrimps, crabs). Under the strong mitigation scenarios (RCP2.6), the declines in biomass at higher TLs are less pronounced (Figure 3.6b and black line in Figure 3.7b).

Faster biomass flow (i.e., larger flow kinetic) projected under climate change produces a nearly uniform ~10% reduction in biomass across TLs by the end of the 21st century relative to 1986–2005 (Figure 3.6c). However, the decrease in transfer efficiency at higher TLs causes a more pronounced decline in biomass at higher TLs. Since the higher TLs represent only a small fraction of total biomass, the changes in biomass at higher TLs have relatively small effect on total consumer

biomass (Figure. 3.6a). However, species at higher TLs include some of the most valuable species, thus the impacts for global fisheries may be exacerbated where the transfer efficiency at higher TLs is the most affected by ocean warming.

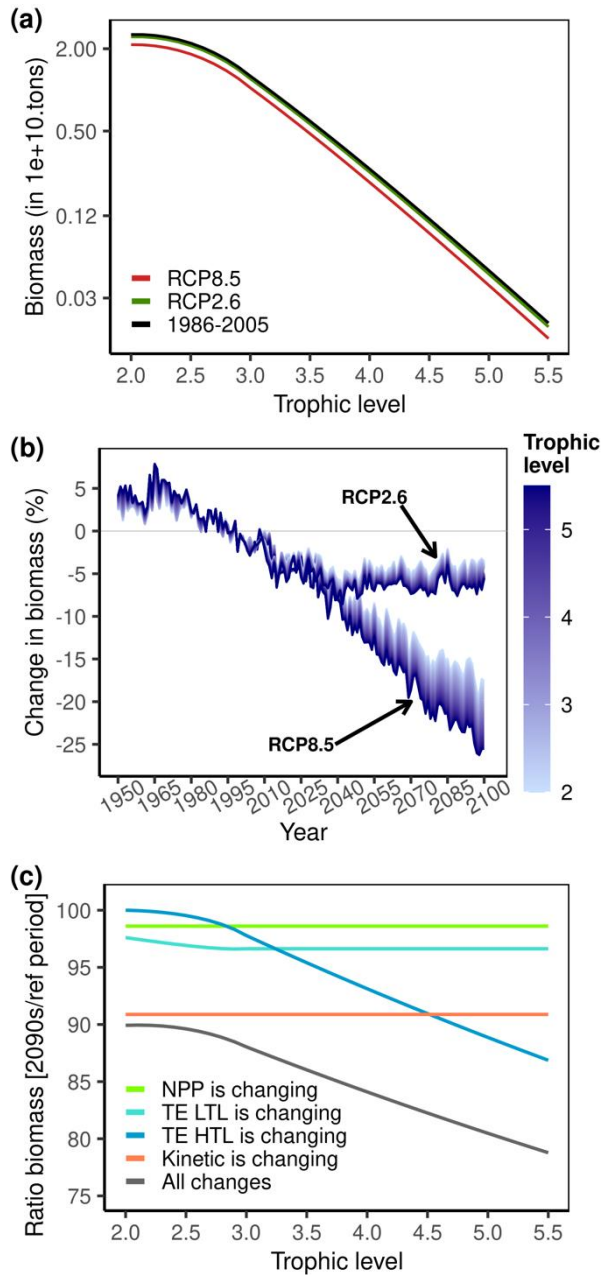


Figure 3.6: Changes in trophic structure under RCP2.6 and 8.5. (a) Biomass trophic spectra for RCP2.6 and RCP8.5 in 2090–2099 and the reference period in 1986–2005, while (b) Changes in biomass for each trophic class of width 0.1 trophic level (TL) between TL = 2 and TL = 5.5 under RCP2.6 and RCP8.5 relative to the reference period 1986–2005. (c) The ratio of biomass trophic spectra in 2090–2099 for RCP8.5 and for the reference period 1986–2005 derived from EcoTroph projections in which each flow parameter is successively isolated (net primary production (NPP), transfer efficiency of lower trophic level (TE LTL), transfer efficiency of higher trophic level (TE HTL) and flow kinetic).

The changes in trophic structure differ from one ecosystem type to the other, for both RCPs (Figure 3.7a and b). The differences in biomass decline between low and high TLs are particularly important in upwelling, temperate and Arctic ecosystems (Figure 3.7a and b) where the warming-induced changes in transfer efficiency of higher TLs are the highest (see Figure 3.2h).

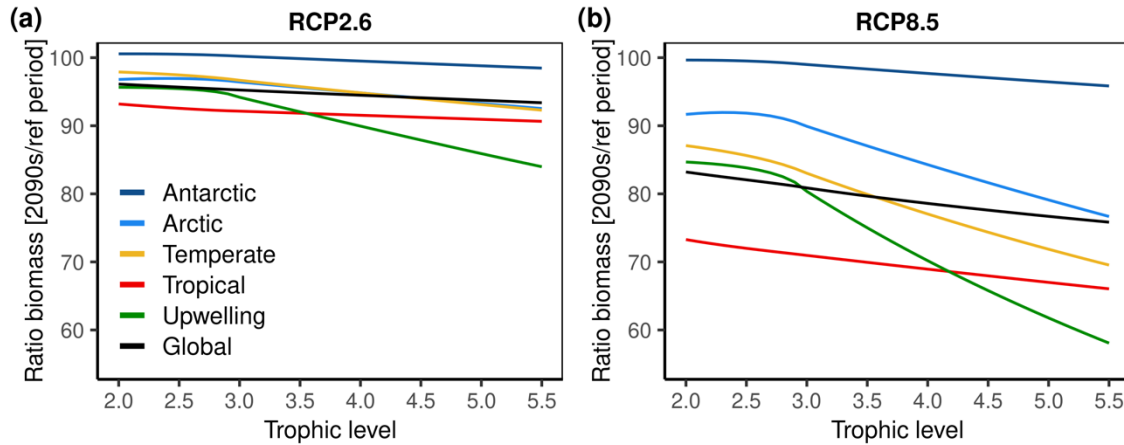


Figure 3.7: Changes in trophic structure in each ecosystem type for RCP2.6 and 8.5. The two panels show the ratio of the biomass spectrum in 2090-2090 to the reference period 1986–2005 for RCP2.6 (a) and RCP8.5 (b) for each ecosystem type.

3.3.4. Changes in ecosystem production

While our projections indicate a decline in total consumer biomass by, on average, 18.4%, total consumer production is projected to decrease by 12.0% “only”, by 2090–2099 relative to 1986–2005 under RCP8.5 (Figure 3.8a). The lower decrease in production is mechanistically due to the warming-induced increase in flow kinetic (+11.8% under RCP8.5) since production is the product of biomass and flow kinetic. Hence, we projected that total consumer production may increase in the Arctic and Antarctic ecosystems by, on average, 1.7% and 1.8%, respectively, by 2090–2099 despite the great inter-ESM uncertainty (blue bars in Figure 3.8b). In the other ecosystem types (Figure 3.8b), the declines in total consumer production are projected to be attenuated compared to those in biomass with differences in change of about 10% (e.g., in tropical ecosystem, the projected decrease in the ensemble mean total consumer biomass reaches 28.3% while total consumer production is projected to decrease by 18.4%). Similar to the trend in biomass, production of higher TLs is projected to be more affected than lower TLs (Figure 3.8c). Specifically, EcoTroph projects, on average, a 16.3% decline in predator production (TLs between 3.5 and 5.5) while prey production (TLs between 2.5 and 3.5) is projected to decrease by 13.1% (Figure 3.8c).

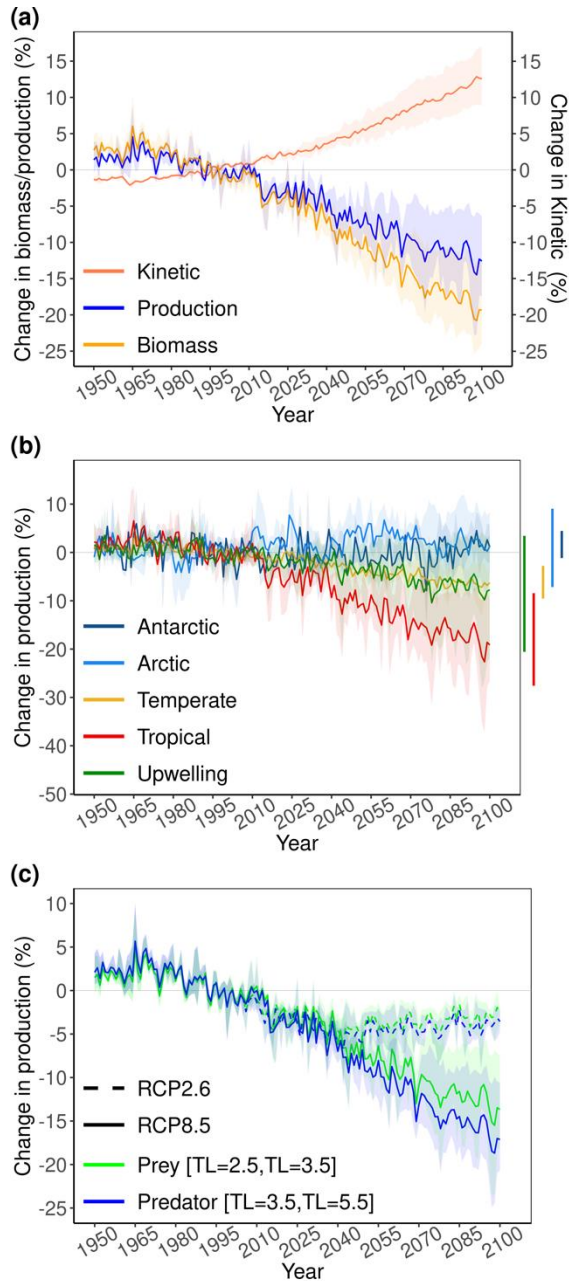


Figure 3.8: Changes in production at global scale and in each ecosystem type over the 21st century. Panel (a) represents the changes in total consumer production and biomass and in kinetic under RCP8.5 by 2100 relative to the reference period 1986–2005 while panel (b) represents the changes in total consumer production for RCP8.5 in each ecosystem type. Panel (c) represents the changes in prey (between trophic level (TL) = 2.5 and TL = 3.5) and predator (up to TL = 3.5) under RCP2.6 and RCP8.5.

3.4. Discussion

Through modeling marine ecosystems as trophic spectrum, we project a drastic decline in consumer biomass and production throughout the 21st century under the “no mitigation policy” scenario (RCP 8.5) driven by a change in the biomass flow in marine food webs. The projected changes in biomass also vary widely spatially because of regional differences in changes in ocean biogeochemical and physical conditions and the characteristics of the ecosystems. In addition, we

found an amplification of climate-induced changes in biomass and production at higher TLs relative to lower TLs in various ecosystems (temperate, upwelling and Arctic), potentially leading to pronounced declines of highly commercially valuable large fish species.

3.4.1. Drivers of changes in consumer biomass

This study shows that changes in net primary production, flow kinetics and transfer efficiencies drive changes in global ocean biomass and production. Specifically, we highlighted that the changes in total consumer biomass and production are largely driven by the balance between the effects of trophodynamic constraints (imposed by net primary production) and the temperature-dependent flow kinetic and transfer efficiencies (at higher TLs). At global scale, the main driver of the changes of total consumer biomass is the flow kinetic which is directly affected by global ocean warming. In other words, in a warming ocean which favors short-living species, each unit of biomass spends less time at a given TL and subsequently at all TLs, which leads the total biomass to decrease (Gascuel *et al.* 2008). In parallel, the warming-induced decrease in transfer efficiency of higher TLs affects both consumer production and biomass due to larger energy losses between each TL (du Pontavice *et al.* 2019). The increase in sea water temperature affects both the quantify of matter and energy which is transferred through the food (decrease in trophic transfer efficiency) and the speed at which biomass transfer occurs (increase in flow kinetic). Thus, temperature-induced changes in flow kinetic and trophic transfer efficiency may contribute independently and cumulatively to the decline in consumer biomass.

Previous studies suggest that changes in these trophodynamic processes are caused by changes in species assemblages induced by the increase in sea water temperature (Gascuel *et al.* 2008; Maureaud *et al.* 2017; du Pontavice *et al.* 2019). Hence biomass transfers tend to be faster but less efficient at each TL in warmer waters (Gascuel *et al.* 2008; du Pontavice *et al.* 2019) due to species assemblages more and more dominated by fast-growing, short-living, early-maturing species as suggested by Beukhof *et al.* (2019).

3.4.2. Trophic amplification induced by less efficient transfer

Our findings suggest an amplification of the changes in biomass from low to high TL components of the ecosystem, with a more pronounced decrease in high TLs. This process describes the propagation of the climate signal from low to upper TLs through the decline (or increase) of biomass along the food web. Trophic amplification has been previously shown for phytoplankton and zooplankton using different planktonic food web models and different Earth system models (Chust *et*

al. 2014; Stock *et al.* 2014a; Kwiatkowski *et al.* 2019). At the upper trophic levels, Petrik *et al.* (2020), based on a spatially explicit mechanistic model of three functional types of fish, showed the amplification of the projected changes in productivity by grouping functional types by trophic level. In a complementary way and using a trophic-level-based model, our projections highlighted a continuous and progressive amplification of changes in biomass and production when moving up the food web. This process arises from the cumulative effect all along the food web of the warming-induced decline in transfer efficiency at each trophic level. The alteration of the trophic structure of marine ecosystems supports the concerns regarding the consequences of trophic downgrading (Estes *et al.* 2011) which can be characterized by trophic cascades due to the decrease in predator biomass. Indeed, several studies showed the impacts of top predators depletion on marine ecosystem functioning (Heithaus *et al.* 2008; Baum & Worm 2009; Ferretti *et al.* 2010; Estes *et al.* 2016) and stability (Britten *et al.* 2014; Rasher *et al.* 2020). Despite their low biomass (compared to the lower TLs), predators at TL higher than 3.5 currently support more than 35% of the world fisheries (Branch *et al.* 2010). Therefore, our results suggest that changes in transfer efficiencies induced by climate change may be a key player in the expected decrease of the world potential fisheries catch (FAO 2018; Bindoff *et al.* 2019).

In a recent compilation of marine ecosystems models (the FISH-MIP model intercomparison project; Lotze *et al.*, 2019), a trophic amplification process was highlighted with combined biomass of higher trophic levels declining more strongly than lower trophic levels. While this amplification was consistent across the majority of FISH-MIP models, differences in fundamental structures and ecological processes lead to large differences in the projected shifts in total consumer biomass, with global declines by 2100 ranging from ~12% to ~20% in RCP8.5. The trophodynamic constraints due to changes in ocean conditions filtered through EcoTroph support the high end of this response (Appendix B – Supplementary materials B.6).

3.4.3. Toward a global decline in fisheries catch?

While FISH-MIP results focused on biomass (Lotze *et al.* 2019), our results also highlighted the significant impact of climate change on the gross natural production of marine ecosystems. This result is a key issue for fisheries whose sustainability is not directly related to biomass, but more to production and to the exploited part of production. The EcoTroph approach reveals that production may be impacted by lower NPP, and less efficient trophic transfers along the food web. However, the expected faster energy flow may not have any effect on production, but a large impact on the biomass. In other words, using projections changes in biomass to infer the coming effect of climate change on

catch potential may lead to an overestimation of this effect. The loss in biomass will be partially counterbalanced by faster turnover which makes each unit of biomass more productive. Considering predator at TLs higher than 3.5, the projected change in potential catch (by 2100 under RCP8.5) would be closer to 16.3%, based on production, than to 21.3% as expected from biomass. Trophic amplification in production (and not in biomass) is consistent with the projections based on a mechanistic model resolving trophic interactions and basic life cycle processes (Petrik *et al.* 2020). Interestingly, while we projected a decrease of 12.0% in total fish production, Petrik *et al.* (2020) projected total fisheries yield declines by 11.8% using a simple representation of fishing (constant over space, time and TL). However, they projected larger differences in fisheries yield between the low and the high TLs.

Our projections imply potential repercussions on the global catch potential and on its distribution, with different consequences in the different ecosystem types. Tropical ecosystems would be the most impacted (-28.3% and -18.4% in biomass and production, respectively) but with a low amplification due to low changes in transfer efficiency. Thus, large decreases in fisheries yield would be experienced at all TLs from forage fish to predator species in these regions where many nations show a high socioeconomically dependency on fisheries (Golden *et al.* 2016; Bindoff *et al.* 2019). Conversely, in temperate and polar ecosystems, the decline in fisheries yield may be lower especially if we consider the projected decline in production (instead of biomass). However, in these ecosystems we projected large changes in food web structure (through trophic amplification processes) which may result in major changes in catch structure. While fisheries targeting low and mid TLs species may be moderately affected by climate change, fisheries targeting upper TLs species may be much more impacted. To mitigate socioeconomically impacts of these changes, fisheries management should adapt its methods to address declines in total catch but also changes in catch structure.

3.4.4. Modelling considerations and sources of uncertainties

Our modelling approach is the first application of EcoTroph linking the trophic ecology and the projected changes in ocean conditions. Within the TL-based models (e.g., Ecopath with Ecosim), EcoTroph may be viewed as a synthetic approach in the use of the TL concept for ecosystem modelling in which individual species are combined into classes. Therefore, EcoTroph does not explicitly resolve the climate-induced impacts on individual species and population. Instead, the model assumes that the shifts in environmental conditions will lead to the emergence of new biomass transfer features in theoretical steady state ecosystems.

So far, in our implementation of EcoTroph, the model accounts for steady states (see equations 2 and 4). Hence, one of the challenges in future studies will be to develop a new generation of the model, integrating time dynamic processes in order to analyze the propagation of impacts and their aggregation on a larger scale. Such a dynamic EcoTroph model may, for instance, allow at exploring the expected effects of widespread increases in marine heat waves frequency and intensity which is a major source of concern for the future productivity and stability of marine ecosystems. A recent modeling work focusing on the northeast Pacific has showed that by 2050 marine heat waves could more than double the magnitude of the impacts on fish stocks biomass and spatial distribution due to long-term climate change (Cheung & Frölicher 2020).

Although EcoTroph can include top-down effects induced by fishing pressure (e.g., Gasche et al., 2012; Halouani et al., 2015), in the present implementation of the model the effects of trophic cascades are not included, thus the model is only driven by bottom-up processes. Since we projected that the largest species are the ones most affected, the release of top-down predation pressure may induce an increase in production of the smaller prey species. Hence, the introduction of top-down effects should exacerbate the projected changes in trophic structure.

The major source of uncertainty in our projections of production and biomass is due to a large inter-model variability in NPP projections (Appendix B – Supplementary material B.5; Bopp et al., 2013; Laufkötter et al., 2015). As in EcoTroph, ocean primary production (or the related phytoplankton biomass) is a pivotal component of several marine ecosystem models by sustaining and limiting the biomass of higher TLs (e.g., Blanchard et al., 2012; Carozza et al., 2016; Cheung et al., 2011; Jennings & Collingridge, 2015). Hence, identifying the sources of the current uncertainty associated with future NPP and constraining estimates is one of the major challenges in understanding the responses of marine food web to climate change (Vancoppenolle *et al.* 2013; Kwiatkowski *et al.* 2017). These variations in NPP projections are particularly large in Arctic ecosystems with substantial differences in the direction of changes among the ESMs (see Appendix S5). In contrast to NPP, the projections in flow kinetic and transfer efficiency of the higher TLs, which are functions of temperature, appear relatively consistent across the three ESMs.

In our study, we considered variations in planktonic food web structure through the estimates of transfer efficiency of low TLs. Accounting for these variations is essential to understand biomass and production dynamics in marine ecosystems, since transfer efficiency of low TLs constraints the fraction of energy available for the upper TLs (Friedland *et al.* 2012; Petrik *et al.* 2019). The introduction of transfer efficiency of low TLs is expected to provide more realistic estimates of climate change effects, though we recognize that it does not capture the full diversity of pathways connecting

phytoplankton and fish. While this study considered variations in the pelagic plankton food web transfer efficiency across trophic gradients, future efforts could consider more complete pelagic, benthic and mesopelagic pathways (Friedland *et al.* 2012; Stock *et al.* 2017b; Petrik *et al.* 2019).

Moreover, the flows of detritus biomass are not considered in this study. In open ocean, the bulk of the transfer of energy occurs between phytoplankton and zooplankton but, in continental shelf ecosystems, NPP also fuels benthic pathway through downward coupling (Woodland & Secor 2013; Duffill Telsnig *et al.* 2018; Cresson *et al.* 2020). Hence, by considering only the pelagic energy transfer in plankton food web, we have likely underestimated the fraction of energy which fuel the food web.

The projected changes in transfer efficiency of higher TLs and flow kinetic can be a result of changes in species assemblages under ocean warming (Gascuel *et al.* 2008; du Pontavice *et al.* 2019), but other negative climate-induced biological responses at individual (e.g., decrease in body size; Cheung *et al.*, 2012) and population levels (e.g., change in phenology; Thackeray *et al.*, 2016) that may amplify the overall climate change impacts on flow kinetic and trophic transfer efficiency, are not represented. Thus, our approach can be considered conservative and the decline in the global marine biomass and production we projected is likely to be underestimated.

3.5. Conclusion

Overall, our modelling approach signal the significant impact of climate change on marine animal biomass but also on production over the 21st century. The latter, which is a key issue for fisheries, is projected to decline but to a lesser extent than biomass due to a compensation effect induced by faster trophic transfer under ocean warming. Hence, we emphasize the importance of considering production to provide insights regarding the future catch potential. Furthermore, the projected changes in trophic structure through a trophic amplification process show that marine predator (TL \geq 3.5) may be particularly affected by climate change.

CHAPTER 4

**Climate-induced changes in
ocean productivity and food
webs functioning may
deeply affect European
fisheries catch**

CHAPTER 4: Climate-induced changes in ocean productivity and food webs functioning may deeply affect European fisheries catch

4.1. Introduction

Climate change is altering ocean conditions with consequences on the structure and functioning of marine ecosystems (Bindoff *et al.* 2019). In the Northeast Atlantic Ocean, climate-induced shifts in distributions and the concomitant effects on community structure of fish stocks have already been shown for benthic and demersal communities (Perry 2005; Poulard & Blanchard 2005; Dulvy *et al.* 2008; Baudron *et al.* 2020) as well as for pelagic communities (Hughes *et al.* 2014; Montero-Serra *et al.* 2015). These changes are generally associated with an expansion of populations located at the northern boundary of their species' range, while populations located at the southern boundary tend to contract (Poloczanska *et al.* 2016). Changes in species distribution under ocean warming reshape community structure, with increases in dominance of warm-water species and decreases in cold-water species (ter Hofstede *et al.* 2010; Simpson *et al.* 2011; Montero-Serra *et al.* 2015).

The continued reshaping of the structure of marine ecosystems under climate change in the 21st century may induce profound negative consequences on the future fisheries production of European seas. Previous work integrating ecophysiology and phytoplankton dynamics projected a decrease in maximum fisheries catch potential of exploited fish and invertebrates stocks in the Northeast Atlantic under climate change by 2050 (Cheung *et al.* 2011). However, such projections do not account for the cascading effects of changes in fish stocks on ecosystem structure and function (Cheung *et al.* 2016). Moreover, changes in fishing levels will also add to, and potentially interact with (Perry *et al.*, 2010; Planque *et al.*, 2010), climate-related changes in fish stocks and ecosystems (Blanchard *et al.* 2011; Cheung *et al.* 2011, 2018). To generate scenarios that are more representative of the reality of European fisheries, it is important to consider the current fishing exploitation patterns and plausible fishing scenarios for the futures.

In a recent work, the EcoTroph modelling framework was used to explore the future of marine consumer biomass and trophic structure at the global scale (see Chapter 3; du Pontavice *et al.* under

review - Chapter 3). In EcoTroph, the trophic functioning of aquatic ecosystems is modelled as a continuous flow of biomass surging up the food web, from lower to upper trophic levels (TLs), through predation and ontogenic processes (Gascuel 2005; Gascuel & Pauly 2009; Gascuel *et al.* 2011). du Pontavice *et al.* (under review - Chapter 3) projected that the alterations of the trophic functioning of marine ecosystems would lead to a global decline in consumer biomass as well as in the abundance of predators. These projections, however, did not consider the effects of fishing exploitation. Moreover, the global-scale simulations do not adequately resolve the physical, biogeochemical and ecological dynamics of marine ecosystems at the scale of European waters, such as the dynamics of coastal waters in Earth system models (Asch *et al.* 2016) and pelagic-benthic linkages in the global EcoTroph modelling (du Pontavice *et al.* under review - Chapter 3). The pelagic-benthic linkages are particularly important for food webs of continental shelf ecosystems such as the European Sea (Blanchard *et al.* 2011; Woodland & Secor 2013; Kopp *et al.* 2015).

Here, we adapt the EcoTroph approach to project the climate—and fishing—induced changes in biomass and fisheries catch in European waters in the 21st century under two contrasting greenhouse gases emissions scenarios. Our study focuses on 15 ICES (International Council for the Exploration of the Sea) divisions of the European continental shelf that range from the Portuguese waters to the North Sea. In each of the divisions, we apply the EcoTroph approach to model the ecosystems and calculate its biomass and production for each TL. We account for the pelagic-benthic linkages by subdividing the biomass flows into the pelagic and the benthic-demersal pathways, and accounting for the flows from the pelagic to the latter pathways. Furthermore, the EcoTroph simulations are driven by ocean conditions projections from a regional, high resolution, coupled hydrodynamic-ecosystem model called European Regional Seas Ecosystem Model (ERSEM; Butenschön *et al.*, 2016) under greenhouse gas emissions scenarios. In addition, we explore the effects of the inclusion of two fishing scenarios on the projected biomass and catches European marine ecosystems.

As a first step, the model is applied for the period 2013–2017 to establish a reference state of the 15 ICES divisions. Then, based on two Representative Concentration Pathways (RCPs), we explore the potential changes in biomass, fisheries catch and trophic structure in the 15 ICES division between 2020 and 2100. In order to explore the fisheries ability to react and adapt, two exploitation scenarios were considered. Finally, we identify the drivers of the future changes in biomass and catch by successively isolating each of them.

4.2. Materials and Methods

In order to consider the effects of climate change on both the secondary production entering the ecosystem and the functioning of the food web of higher TLs, a one way coupled ERSEM/EcoTroph approach was developed, where EcoTroph was used to model the biomass flows for intermediate and high TLs, from the biomass of secondary producers (zooplankton and benthic secondary producers) projected by a regional, high resolution, hydrodynamic-ecosystem model for low TLs.

4.2.1. A regional model for low trophic levels

We projected changes in zooplankton and benthic secondary producer biomass and their production based on the outputs from the ERSEM model v15.06 (Butenschön *et al.* 2016; Copernicus Climate Change Service 2020). ERSEM is an ecosystem model with a focus on marine biogeochemistry, pelagic plankton, and benthic secondary producers. It simulates the cycles of carbon and the major nutrient elements (nitrogen, phosphorous and silicon) within the marine environment. ERSEM has a grid resolution of 0.1° latitude \times 0.1° longitude and is coupled to a regional ocean circulation model, POLCOMS (the Proudman Oceanographic Laboratory Coastal Ocean Modelling System; Copernicus Climate Change Service 2020). The coupled hydrodynamic biogeochemical model is driven at the open ocean boundaries by an Earth System Model developed at the Max Planck Institute (MPI-ESM-LR; Giorgetta *et al.* 2013) in combination with downscaled atmospheric forcing data generated using the Swedish Meteorological and Hydrological Institute Rossby Centre Regional Atmospheric Model.

We used two sets of outputs ERSEM: the mean annual carbon biomass of zooplankton and benthic secondary producers from 2006 to 2099. In the model, zooplankton was subdivided into three size classes of zooplankton categorized as heterotrophic flagellates, microzooplankton, and mesozooplankton while benthic secondary producers included three types of benthic fauna: suspension feeders, deposit feeders and meiobenthos (Butenschön *et al.* 2016).

The variables were available in a two-dimensional horizontal grid of $0.1^\circ \times 0.1^\circ$ covering the Northwest European shelf (see the spatial extent of the model in Figure 1). The outputs of ERSEM were available for the period from 2006 to 2099 for two RCPs: RCP4.5 representing a scenario under which global radiative forcing level would be at 4.5 W/m^2 in the year 2100 (“moderate mitigation” scenario) and RCP8.5 representing rising radiative forcing pathway leading to 8.5 W/m^2 in 2100 (“no mitigation policy” scenario).

4.2.2. The EcoTroph model

General EcoTroph modelling framework

In EcoTroph, the ecosystem trophic functioning is modelled as a continuous flow of biomass surging up the food web, from lower to higher TLs, through predation and ontogenic processes. The detail of the EcoTroph equations and the mathematical development are fully detailed in du Pontavice et al. (2021) and in the Chapter 3.

Ecosystem is represented by the continuous distribution of the biomass along TLs. The biomass enters the food web at TL = 1, as generated by the photosynthetic activity of is called the biomass trophic spectrum primary producers, and recycling by the microbial loop. Then, at TLs higher than 2, the biomass is composed of heterotrophic organisms with mixed diet and fractional TLs resulting in a continuous distribution of biomass along TLs. This distribution is represented using small trophic classes aggregating all organisms of the related TL. As a convention (and based on previous studies; Gascuel et al. 2005; Gasche et al. 2012; Pontavice et al. 2021) we considered trophic classes of width $\Delta\tau = 0.1$ TL to be an appropriate resolution and a range starting at TL = 2 (corresponding to the first-order consumers), up to TL = 5.5, an appropriate range to cover all top predators in marine systems (Cortes, 1999; Pauly, 1998).

The continuous biomass flow (i.e., the quantity of biomass moving up through TL, τ , at every moment, t) is:

$$\Phi(t, \tau) = B(t, \tau)K(t, \tau) \quad \text{Eq. 1}$$

where $\Phi(t, \tau)$ is expressed in $t \cdot \text{year}^{-1}$, $B(t, \tau)$ the density of biomass at TL = τ expressed in $t \cdot \text{TL}^{-1}$, and $K(t, \tau)$ the flow kinetic expressed in $\text{TL} \cdot \text{year}^{-1}$.

Under steady-state conditions, the Equation 1 becomes:

$$B(\tau) = \frac{\Phi(\tau)}{K(\tau)} \quad \text{Eq. 2}$$

A discrete approximation of the continuous distribution $B(\tau)$ is used for mathematical simplification. Hence, the model state variable becomes $B\tau$, the biomass (in tons) under steady-state conditions within the trophic class $[\tau, \tau + \Delta\tau[$ and the Equation 2 becomes:

$$B_{\tau} = \frac{1}{K_{\tau}} \Phi_{\tau} \Delta\tau \quad \text{Eq. 3}$$

where Φ_{τ} and K_{τ} are the mean biomass flow (in t.year⁻¹) and the mean flow kinetic (in TL.year⁻¹) within the trophic class $[\tau, \tau + \Delta\tau[$, respectively.

The biomass flow $\Phi(\tau)$ is not conservative and can be expressed as a decreasing function of TL (see details in du Pontavice et al., 2021):

$$\Phi(\tau + \Delta\tau) = \Phi(\tau) e^{-(\mu_{\tau} + \varphi_{\tau})\Delta\tau} \quad \text{Eq. 4}$$

where μ_{τ} (expressed in TL⁻¹) represents the mean natural losses within the trophic class $[\tau, \tau + \Delta\tau[$ and φ_{τ} (expressed in TL⁻¹) is the fishing loss rate. μ_{τ} defines the transfer efficiency, TE, within the trophic class $[\tau, \tau + \Delta\tau[$ such as:

$$TE = e^{-\mu_{\tau}} \quad \text{Eq. 5}$$

while φ_{τ} is a rate that determines the amount of biomass flow lost during trophic transfers in the food web to the fishery and can be estimated from the amount of catch Y_{τ} that is taken from the production P_{τ} :

$$1 - \frac{Y_{\tau}}{P_{\tau}} = e^{-\varphi_{\tau}} \quad \text{Eq. 6}$$

Finally, EcoTroph defines the biomass flow $\Phi(\tau)$ as a density of production at TL = τ . Therefore, the production P_{τ} of the trophic class $[\tau, \tau + \Delta\tau[$ is:

$$P_{\tau} = \int_{\tau}^{\tau + \Delta\tau} \Phi(\tau) d\tau = \Phi_{\tau} \Delta\tau = B_{\tau} K_{\tau} \quad \text{Eq. 7}$$

Production is commonly expressed in t.yr⁻¹ that implicitly refers to the conversion of biomass eaten at TL $\tau-1$, into predator tissues whose mean TL is τ . Therefore, in a TL-based approach such as

EcoTroph (wherein the width of trophic classes may different from 1 TL), production has to be expressed in t.TL.yr⁻¹, i.e., tons moving up the food web by 1 TL on average during 1 year.

Flow kinetic and trophic transfer efficiency

Flow kinetic measures the velocity of biomass transfers from lower to upper TLs and depends on the biomass turnover. To estimate flow kinetic at TL = τ , we used an empirical equation (Gascuel et al., 2008) as a function of SST and TL (τ):

$$K_{\tau} = 20.19 \times \tau^{-3.26} \times e^{(0.041 \cdot SST)} \quad \text{Eq. 8}$$

The trophic transfer efficiency (TE) takes into account the losses at each trophic class and is used to estimate the fraction of biomass which is transferred from one TL to the next (Eq. 5). In this study, we used the SST-dependent transfer efficiency between TL=2.5 and TL=4 and for temperate ecosystems (du Pontavice *et al.* 2019):

$$TE = e^{(-2.224 + SST(-0.023 - 0.011) + 0.105)} \times 1.078641 \quad \text{Eq. 9}$$

Integration of fishing effects in EcoTroph

Firstly, biomass flow is affected by fishing through fishing loss rate (φ) (see Equations 4 and 6).

Secondly, the model takes into account the effect of fishing mortality on the life expectancy of organisms and on their flow kinetics, K_{τ} . It is calculated for the exploited state following the methodology developed by Gascuel *et al.* (2008, 2011) and is defined as:

$$K_{exploited,\tau} = K_{\tau} \left[1 + \alpha \frac{B_{exploited,pred}^Y - B_{unexploited,pred}^Y}{B_{unexploited,pred}^Y} \right] + F_{\tau} \quad \text{Eq. 10}$$

Fishing reduces the life expectancy of individuals and reduces the time they spend in a trophic class; flow kinetic is, thus, faster with higher fishing mortality rate, $F_{\tau} = Y_{\tau}/B_{\tau}$. Additionally, the kinetic depends partly on the changes in abundance of predators ($B_{unexploited,pred}^Y$ and $B_{exploited,pred}^Y$) that can be altered by fishing. More predators increase the predation mortality rate of their preys and such

top-down control is introduced into the model by Eq. 3. The coefficient α defines the intensity of the top-down control and may vary between 0 (no top-down control) and 1 (all natural mortality depends on predator abundance). The coefficient γ is varying between 0 and 1 and defines the functional relationship between prey and predators. In this study, we used conventional values $\alpha=0.4$ which is assumed an intermediate top-down intensity (Gascuel *et al.* 2011) and $\gamma=0.5$ which is non-linear functional relationship between prey and predator. A sensitivity analysis in Appendix C (Supplementary material C.1) explored different top-down control with $\alpha=0$ (no top-down control), $\alpha=0.8$ (top-down driven ecosystem) and $\gamma=1$ (linear effects of the abundance of predators).

4.2.3. Forcing EcoTroph with outputs from the coupled POLCOMS-ERSEM model

Previous studies incorporated projected changes in net primary production as a driver for simulating ecosystem dynamics using the EcoTroph model (du Pontavice *et al.* under review - Chapter 3; Tremblay-Boyer *et al.* 2011). Here, we instead used the biomass of secondary producers (zooplankton and benthos) projected by the ERSEM model as a lower TL forcing. To represent the trophic structure of marine food webs on the continental shelf more accurately, the biomass flow in EcoTroph was divided into two trophic pathways: a pelagic pathway that was driven by zooplankton and a benthic-demersal pathway fuelled at its base by benthic fauna (figure 4.1). In the pelagic pathway, species were assumed to feed exclusively on pelagic preys. In contrast, species belonging to the benthic-demersal pathway feed on benthic and pelagic preys. In this study, we included the energy flow from the pelagic to the benthic-demersal pathway in EcoTroph (Woodland & Secor 2013; Kopp *et al.* 2015; Giraldo *et al.* 2017; Day *et al.* 2019), assuming that, at each EcoTroph trophic class, a fraction of the biomass flow in the pelagic pathway is transferred to the flow in the benthic-demersal pathway. The intensity of the benthic-pelagic coupling was set to 20% for all the TLs, and the sensitivity of the model outputs to the intensity of the coupling was tested (Appendix C - Supplementary material C.2). Specifically, we increased the pelagic to benthic-demersal biomass flow from 20% to 40%. In addition, we used sea surface temperature (SST) projections from POLCOMS-ERSEM to estimate the flow kinetics (Eq. 8) and the trophic efficiencies (Eq. 9) per TL. The trend in secondary producers and SST are presented in Appendix C (Supplementary material C.3)

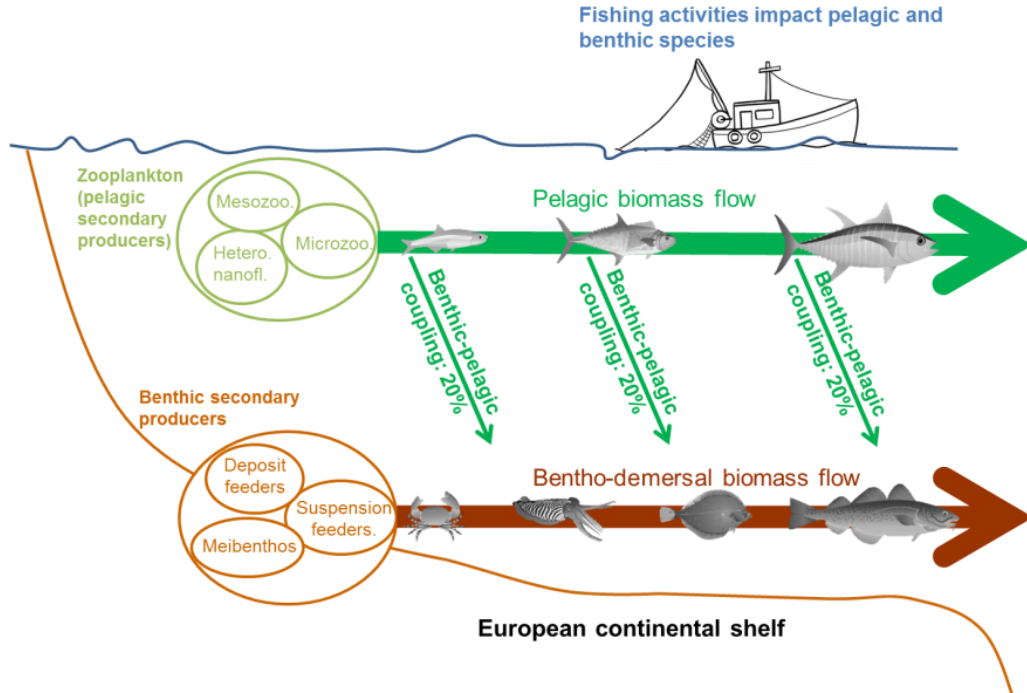


Figure 4.1: Schematic representation of the EcoTroph model in the European continental shelf sea. The downward green arrows represent the biomass flow from pelagic to benthic pathways, assumed to be 20% of the flow at each trophic level.

4.2.4. Study area and fisheries

Our study focused on 15 ICES divisions of the European continental shelf from the North Sea to the Strait of Gibraltar (Figure 4.2). The area included the North Sea, Western Scotland, Irish Sea, Western Ireland, Celtic Sea, English Channel, Bay of Biscay and Portuguese Waters.

Catch data from 2013 to 2017 were obtained from the ICES data collection (ICES 2020). The fisheries catch statistics were reported annually by the national offices and, then, prepared and published by ICES in the official catch statistics dataset for the Northeast Atlantic. The catch statistics included catch of fish, crustaceans, molluscs and other aquatic organisms, at the spatial resolution of ICES divisions. A low proportion of catch was reported for a pool of two or three ICES divisions. These catches were distributed among divisions proportionally to the mean allocated catch of the period. 722 species were reported to have been exploited by the fisheries in the study area in FishBase (<http://www.fishbase.org>, Froese & Pauly 2020) and SeaLifeBase (<http://www.sealifebase.org>, Palomares & Pauly 2020). For each species, we assigned a trophic pathway (pelagic or benthic-demersal) based on their feeding affinity reported in FishBase. If information on feeding affinity is not available, we used information on their associated habitat to categorize their trophic pathway

(Figure 4.1). Furthermore, trophic level of each species was also obtained based on estimates from FishBase and SeaLifebase.

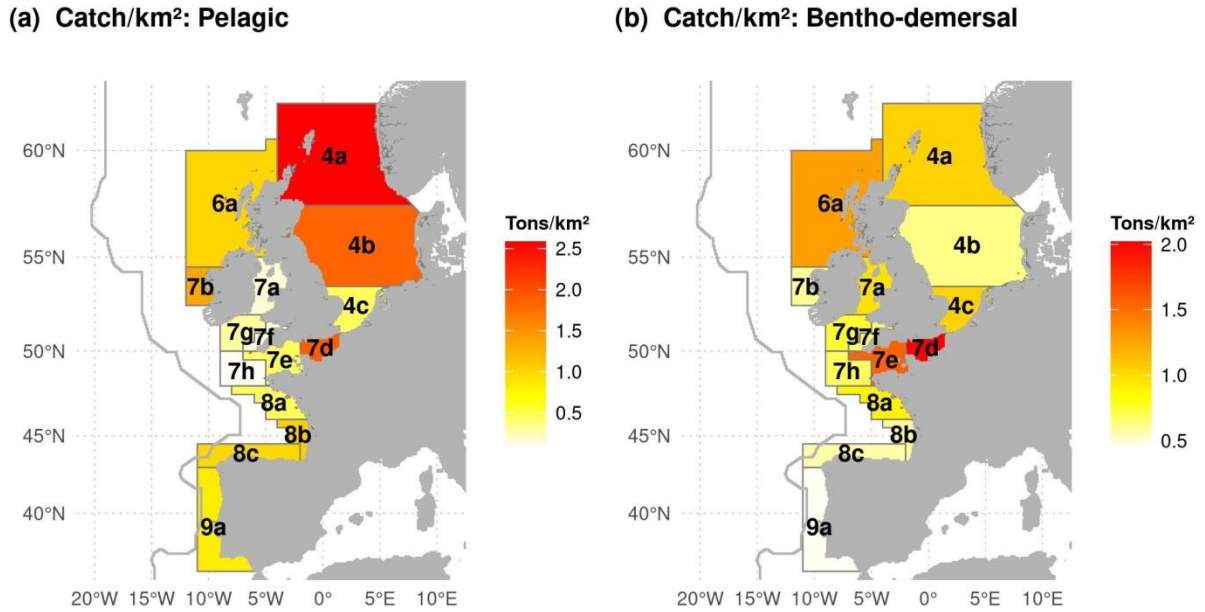


Figure 4.2: Map of the study areas and fisheries catch per unit area (t.km⁻²) in 2013–2017. The spatial distribution of the annual average catch per area (km²) between 2013 and 2017 are represented for pelagic species (a) and benthic-demersal (b) species in the 15 ICES divisions. The grey line is the boundary of the POLCOMS-ERSEM model, while codes of each division refer to the numbering used by ICES.

4.2.5. Simulation design

EcoTroph model for the reference period 2013–2017

We defined the reference state of the ecosystems in the 15 ICES divisions by modelling the trophic structure in 2013–2017 using EcoTroph. In each ICES division, fishing activities were represented by the annual average total catch per TL over the period. Estimated annual average biomass of secondary producers entering the food web from each division was obtained from the ERSEM outputs (Figure 4.3). Secondary producers included zooplankton and benthic secondary producers that were assumed to constitute the bulk of the biomass in trophic classes between TL=2 and TL=2.4. The estimated biomass was converted into production based flow kinetic according to equation 7.

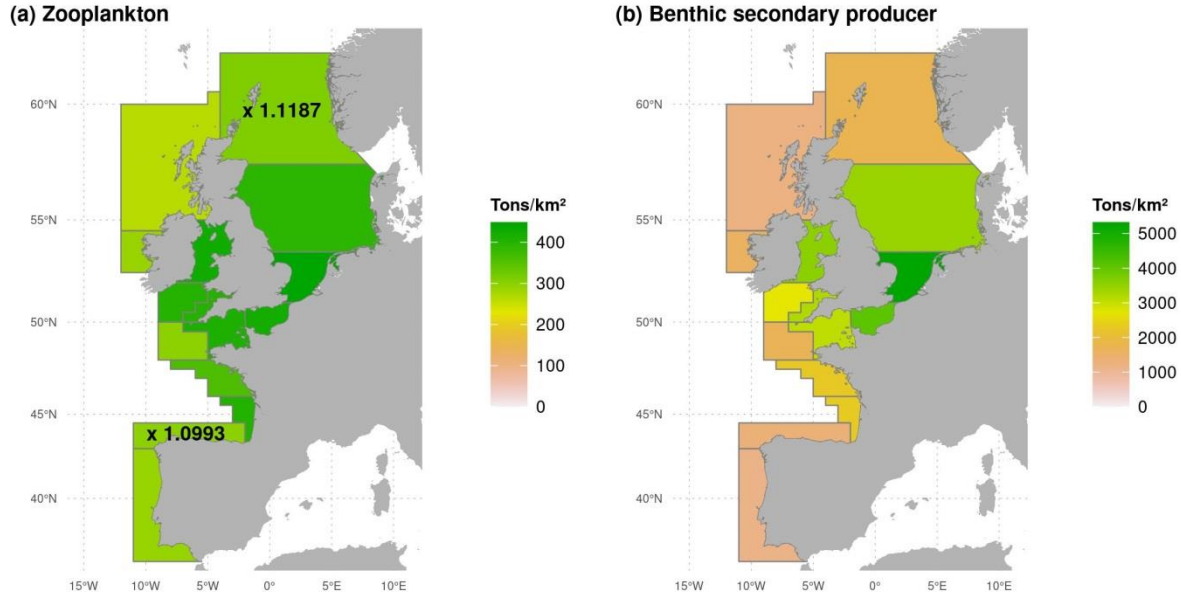


Figure 4.3: Map of the biomass of secondary producers per unit area (ton.km⁻²) in 2013–2017: (a) for zooplankton, and (b) for benthic secondary producers. On the panel (a), the figures displayed on two divisions (4a and 8c) are the multiplier coefficients to elevate the biomass of pelagic zooplankton so that production support catches at every trophic level.

Preliminary analysis revealed that, in ICES divisions 4a (north of the North Sea) and 8c (south of the Bay of Biscay), the biomass of zooplankton from ERSEM was not sufficient to sustain pelagic catch, thus validate the constraint of conservation of energy in EcoTroph. This issue could be due to two main reasons: (i) the biomass of zooplankton was underestimated; (ii) pelagic species could move and feed outside the boundary of the ICES divisions. To resolve this issue, we multiplied the zooplankton biomass from ERSEM by a coefficient to obtain the minimum zooplankton biomass required to support the catch at every TL (1.12 and 1.10 in divisions 4a and 8c, respectively).

Biomass, production, fishing mortality, fishing loss rate were simulated in each ICES division for the period 2013–2017 and were used as the reference state to calculate the changes by the end of the century (Appendix C - Supplementary material C.4).

Projecting biomass and catches

We projected changes in biomass and catches in the 15 ICES division between 2020 and 2099, under RCP4.5 and RCP8.5 scenarios and two fishing scenarios using EcoTroph. The first fishing scenario was a constant fishing mortality (F) scenario in which fisheries in 2090–2099 catch the same proportion of the biomass at each TL than 2013–2017. In this scenario, the mean projected catch in 2090–2099, $Y_{2099, \tau}$, at TL τ was estimated from:

$$Y_{2099,\tau} = F_{\tau} \times B_{2099,\tau} \text{ where } F_{\tau} = \frac{Y_{current,\tau}}{B_{current,\tau}}$$

F_{τ} , $Y_{current,\tau}$ and $B_{current,\tau}$ are the fishing mortality, the catch and the biomass, respectively, at TL τ , for the current period (2013–2017). $B_{2099,\tau}$ is the biomass at TL τ in 2090–2099.

In the second scenario, fisheries in 2090–2099 were assumed to catch the same proportion of the production at each TL than 2013–2017. Therefore, we considered the ratio Y/P as a constant and in this scenario, $Y_{2099,\tau}$ was estimated from:

$$Y_{2099,\tau} = (1 - e^{-\varphi_{\tau}}) \times P_{2099,\tau} \text{ where } (1 - e^{-\varphi_{\tau}}) = \frac{Y_{current,\tau}}{P_{current,\tau}}$$

$P_{current,\tau}$ and $P_{2099,\tau}$ are the production, at TL τ , for the current period (2013–2017) and in 2090–2099, respectively. Therefore, in the constant fishing mortality scenario, fishing level is adjusted according to the available biomass. In contrast, in the constant fishing loss rate scenario, fishing level is adjusted according to the ecosystem production.

Changes in SST and the biomass of secondary producers were projected by ERSEM. The multiplier coefficients for secondary producers in EcoTroph calculated in divisions 4a and 8c for the period 2013–2017 were applied to the projections between 2020 and 2099.

For each RCP-fishing scenario combination, we projected the changes in biomass, production and catch by 2099 relative to the reference period (2013–2017). We then aggregated the projection by three trophic classes: consumers between TL=2.5 and TL=5 (excluding the secondary producers as they are inputs) or for low (between TL=2.5 and 3.5) and high TLs (between TL= 4 and TL=5).

Simulations to identify the drivers of the biomass and catch changes

A last set of simulations was designed to identify the drivers of the changes in total consumer biomass and trophic structure. Hence, the three biomass flow parameters were investigated: (1) the production entering the food (production of secondary producers), (2) the trophic transfer efficiency and (3) the flow kinetic.

In order to understand how biomass and catch responded to climate-induced changes in the three parameters, we ran 3 sets of simulations. In each simulation, we isolated one biomass flow parameter, which varies over the period 2020–2099 while the others remain constant and equal to their mean values during the reference period 2013–2017. The sensitivity to biomass flow parameters was studied by using the scenario RCP8.5 and the constant fishing mortality scenario.

All analyses and simulations were performed in the R environment (R Core Team 2020).

4.3. Results

4.3.1. The effects of climate change on biomass and catch under a constant fishing mortality scenario

Aggregating across the 15 ICES divisions on the European continental shelf, the projected biomass in the 21st century from EcoTroph under constant fishing mortality scenario was dominated by the benthic-demersal pathway at all TLs (Figure 4.4a). On average, 88.6% and 87.7% of the total biomass were from the benthic-demersal components of the trophic system in 2013–2017 and 2090–2099, respectively. Conversely, catches were mainly from the lower TLs pelagic component (between TL=2.8 and TL=3.8) (77.4% and 78.9% in 2013–2017 and 2090–2099, respectively) and the higher TLs benthic-demersal component (up to TL=4.2) of the trophic systems (Figure 4.4b).

Changes in temperature and secondary production were projected to affect biomass at all TLs (Figure 4.4a). Total biomass from TL=2.5 to TL=5 of the systems was projected to decrease by 14% under RCP8.5 and 10% under RCP4.5 by 2090–2099 relative to the period 2013–2017 (Figure 4.4c). Notably, under RCP8.5, biomass was projected to decrease abruptly between 2040 and 2060, increase briefly in 2070–2080 but then continue to decrease afterward. Total catches followed a similar trend and were projected to decline by 11.0% under RCP8.5 and 8.8% under RCP4.5 by 2090–2099 relative to 2013–2017 (Figure 4.4b).

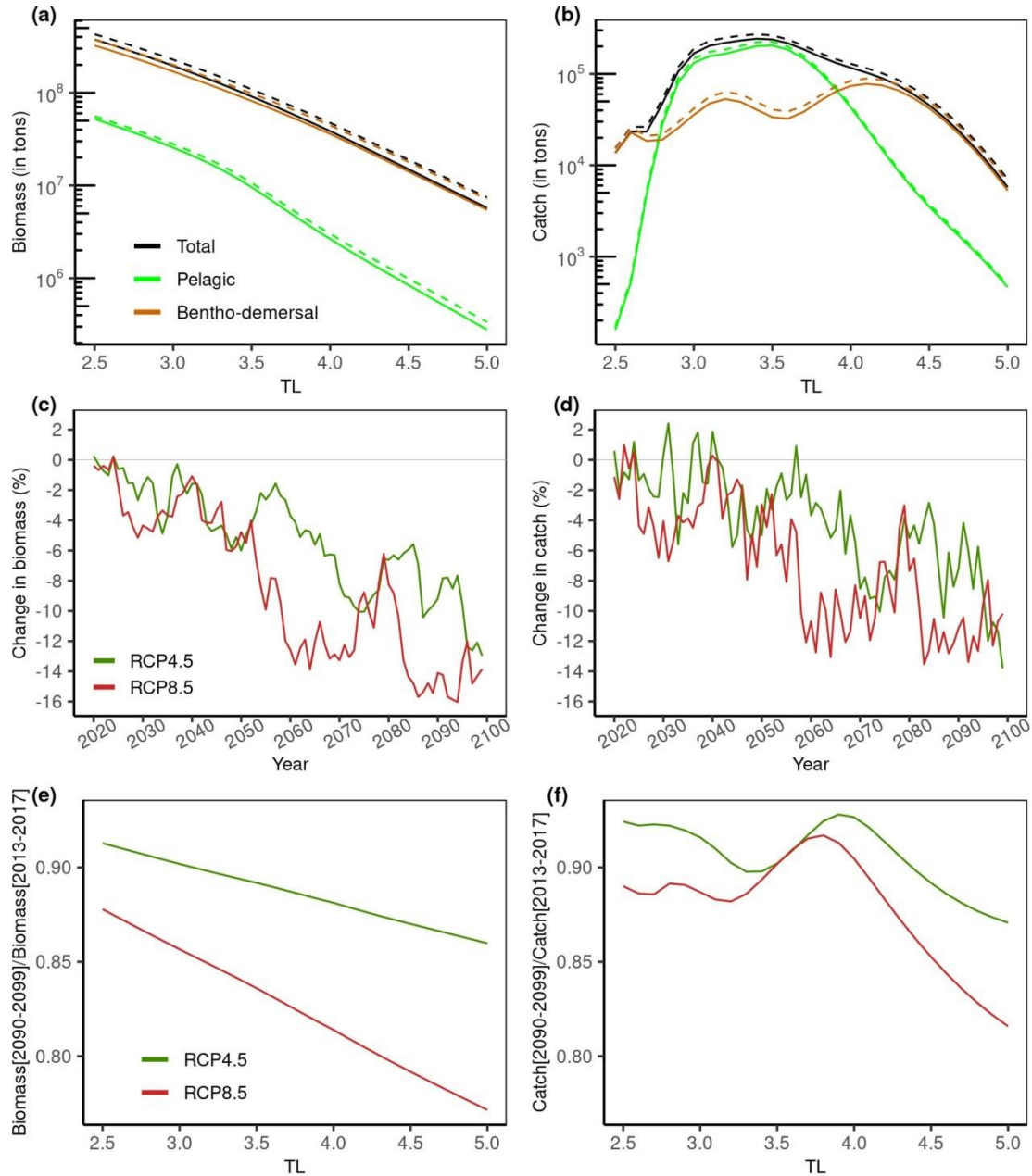


Figure 4.4: Projected biomass and catch from the European continental shelf trophic systems. EcoTroph projections of biomass (a) and catch (b) trophic spectra (i.e. biomass and catch distribution across trophic levels) for the pelagic and benthic-demersal pathways for the period 2013–2017 (dashed lines) and for the period 2090–2099 (solid lines) under the scenario of constant fishing mortality. The change in total biomass (between TL=2.5 and TL=5.0) (c) and catch (d) between 2020 and 2100 relative to the reference period (2013–2017) are presented under RCP4.5 (green) and RCP8.5 (red). Panels (e) and (f) show the projected changes in biomass (e) and catch (f) in 2090–2099 relative to 2013–2017 for RCP2.6 (green) and RCP8.5 (red).

The projected changes in biomass and catch from the upper part of the food webs across the simulation timeframe were larger than the changes from the lower TLs components (Figure 4.4e, f). The magnitude of the projected decreases in biomass was significantly (p -value linear model $>2e-16$

for both RCPs) and negatively (slope= -0.04TL^{-1} and -0.02TL^{-1} for RCP8.5 and RCP2.6, respectively) related to TLs (from -12% at TL=2.5 to -23% at TL=5 under RCP8.5) (Figure 4.4e). The relationship between the magnitude of projected catch decreases and TL was overall non-linear, with, however, a large linear and significant catch decreases (linear model fitted between TL=4 and TL=5: p-value = $1.83\text{e-}10$ and slope = -0.09 TL^{-1} for RCP8.5) when TL is higher than 4.0 (Figure 4.4f). The decrease in catch was projected to be -18% at the highest TLs (TL=5) under RCP8.5.

The projected changes in biomass and catches varied between the ICES divisions in the European continental shelf sea, with the Celtic Sea (7h, 7g, 7j), the middle of the North Sea (4b), and the Southern Bay of Biscay having the largest projected changes (8b) (Figure 4.5a, b). In these six divisions, the total decrease in biomass was, on average, of $19.8 \pm 1.6\%$ by 2090–2099 relative to 2013–2017 under RCP8.5, and as much as $26.8 \pm 1.6\%$ at TL=5.

The biggest projected changes in catch were located in the Celtic Sea (especially in division 7h with a 24% decrease) and in the Bay of Biscay (4b with a 21% decrease). The catches at higher TLs decreased more than those lower in the trophic system in every ICES division (except in the Western Scotland division) (Figure 4.5c, d).

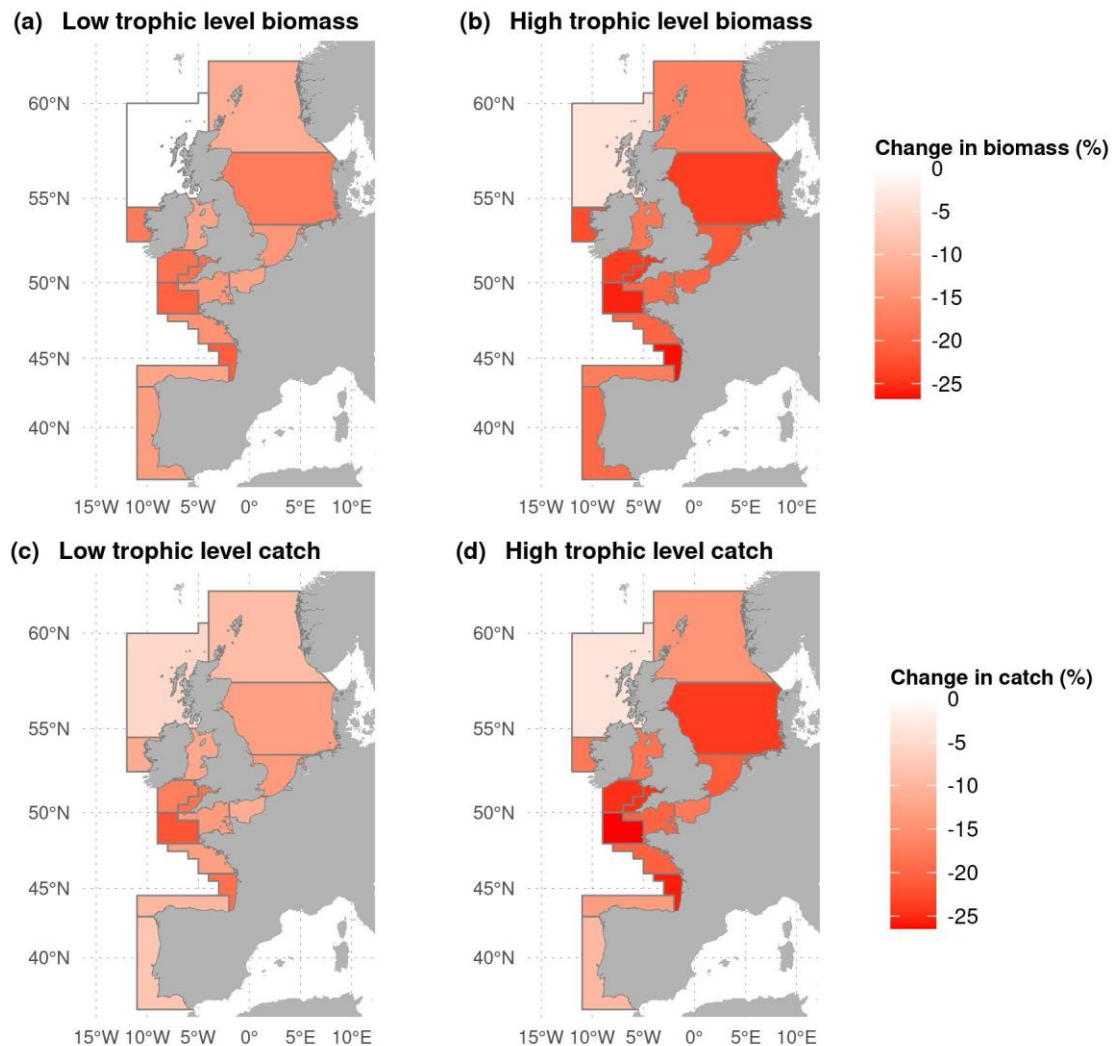


Figure 4.5: Maps of the changes in biomass and catch in 2090–2099 relative to 2013–2017 for the constant fishing mortality scenario. The changes in biomass (a and b) and in catch (c and d) were aggregated between the trophic levels 2.5 and 3.5 (a and c) and between the trophic levels 4 and 5 (b and d).

4.3.2. Climatic drivers and the changes in catch and biomass

Different climate-related drivers (changes in temperature and secondary production), and the transfer efficiency and flow kinetics affected the projected changes in biomass and catches differently.

The temperature-induced decrease in transfer efficiency caused the projected decline in total catch and biomass; the decreases in catch and biomass were more pronounced at higher TLs (blue lines, Figure 4.6a, b). Besides, the temperature-induced increase in flow kinetic was negatively related to the total catch and biomass (red lines, Figure 4.6a, b), except for catches between TL=3 and TL=3.8

at which catches increased and then decreased again with higher TL (Figure 4.6b). Pelagic catches dominated the total catches from TL=3 to TL=3.8 (Figure 4.4b) at which predation mortalities were projected to decrease in some divisions that contributed to the increases in catches (such as in the division 4a; see Appendix C - Supplementary material C.6 - Figure C.6.1). Total biomass was projected to decrease as a result of the decreases in secondary production, especially for the benthic-demersal pathway (green line, Figure 4.6a).

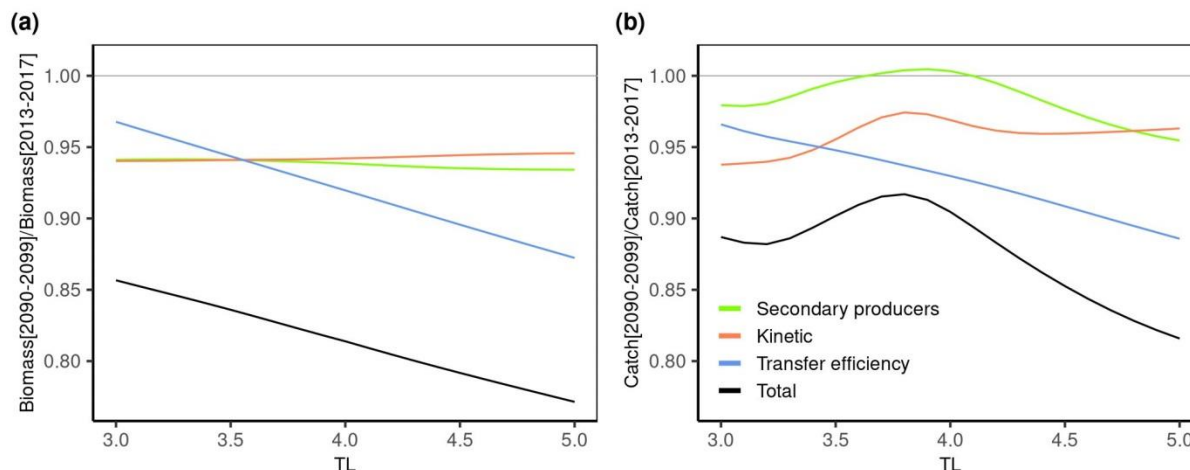


Figure 4.6: The drivers of the changes in biomass (a) and catch (b) for the ecosystem. The ratio of catch trophic spectra in 2090–2099 relative to the reference period 2013–2017 derived from the simulations in which each biomass flow parameter is successively isolated (production of secondary producers, transfer efficiency and flow kinetic). The results are presented for RCP8.5 and for the constant fishing mortality scenario.

The relationship between biomass, catches and secondary production varied between the different ecosystems across the ICES region because of the differences in relative importance of transfer efficiency and flow kinetic in affecting biomass flows. For example, in the Southwestern Celtic Sea division (7h), wherein the decline in catch is projected to be maximal, secondary production and temperature (affecting both the transfer efficiency and the flow kinetic) strongly affected the pelagic and benthic-demersal catches (Appendix C - Supplementary material C.3 and C6 - Figure C.3.2 and Figure C.6.2). Conversely, in the Eastern English Channel (7d), the projected increase in zooplankton production was countered by the warming-induced decrease in transfer efficiency and enhancement of flow kinetics that subsequently led to an overall decrease in total catches (Appendix C - Supplementary material C6 - Figure C.6.2).

4.3.3. Ecosystem impacts under different fishing scenarios

The projected total biomass under the “constant fishing mortality strategy” scenario was slightly lower than those under the “constant fishing loss rate strategy” scenario (-0.007% between 2013–2017 and 2090–2099) while projected catches were higher under the “constant fishing mortality strategy” scenario (+4.438% between 2090 and 2099; Figure 4.7c, d). As warmer sea temperature implies faster trophic transfers, and thus higher flow kinetics K , the constant fishing loss rate scenario led to an increase in the fishing mortalities $F = \varphi \times K$ over the century. Such an increase in the fishing pressure induced a slightly larger impact of climate change on the biomass, especially for the highest trophic levels (Figure 4.7a), while partially compensating the effect of climate change on catch, leading to a lower decrease especially at intermediate or low trophic levels (Figure 7b).

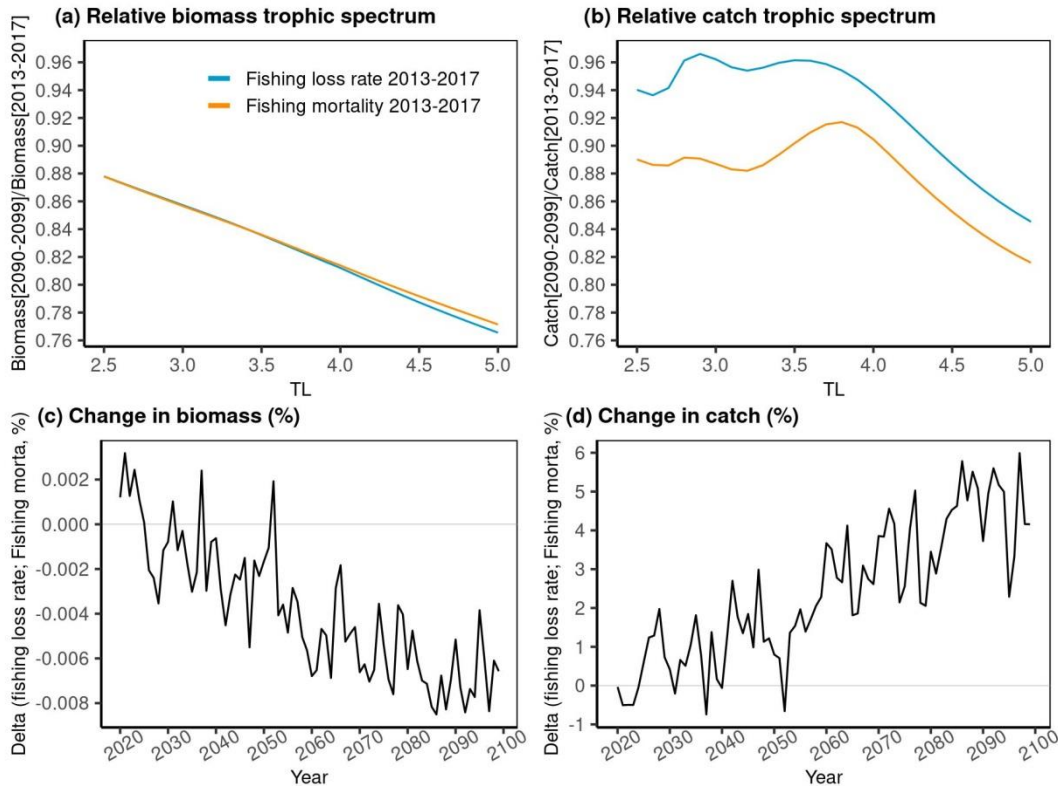


Figure 4.7: Difference between the two fishing scenarios in the projected changes in biomass and catch in 2090–2099 under RCP8.5. Changes in biomass spectrum (a) and catch spectrum (b) in 2090–2099 relative to the reference period 2013–2017 are represented for the two fishing scenarios under RCP8.5. Additional impact of the constant fishing loss rate scenario (constant fishing loss rate – constant fishing mortality) in total biomass (c) and catch (d) relative to the reference period are presented under RCP8.5. “morta.” denotes mortality.

At the division scale, under a constant fishing loss rate, fishing mortality was projected to increase by 5 to 8% over the 21st century (Figure 4.8a, b). Accordingly, the projected total catches were larger for this constant fishing loss rate scenario in every ICES division (Figure 4.8b). In three ICES divisions, the middle and the south of North Sea (4b and c) and the Eastern English Channel (7d), the catches were 8.5% higher for the constant fishing loss rate scenario. Interestingly, the ICES divisions which experience the larger differences between the two fishing scenarios were those where the largest changes in sea surface temperature were projected (Appendix C - Supplementary material C.7).

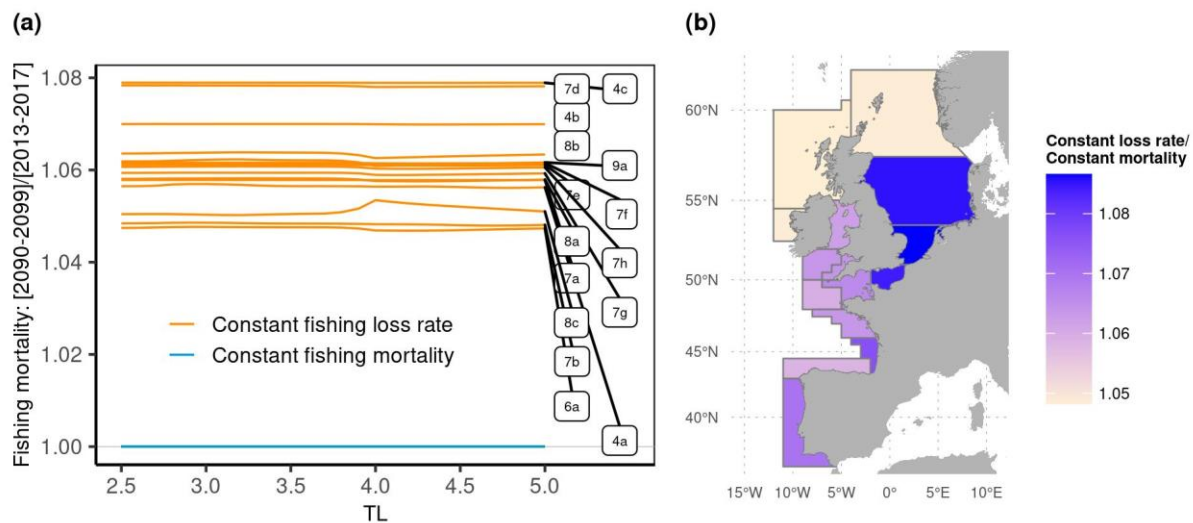


Figure 4.8: Differences in fishing mortality and catch in each ICES division between the two fishing scenarios in 2090–2099 under RCP8.5. The panel (a) shows the changes in fishing mortality for the two fishing scenarios in each ICES division. The panel (b) is the map of the ratio of total catch (Constant fishing loss rate/Constant fishing mortality) aggregated between the trophic levels 2.5 and 5.

4.4. Discussion

Our results show that biomass and catch in European continental shelf ecosystems would be affected by climate through alteration of biomass flow. More aggressive mitigation of greenhouse gas emissions can reduce such impacts, while fisheries management is key for adaptation.

4.4.1. Heterogeneous responses of European continental shelf ecosystems to climate change

The interacting effects of the projected changes in secondary production and ocean temperature under climate change largely would alter the functioning of marine ecosystems in the Northeast Atlantic. Across all the studied ecosystems, net primary production (NPP) in the 21st century is projected to decrease by 8% under RCP4.5 and RCP8.5 scenarios according to POLCOMS-ERSEM (Copernicus Climate Change Service 2020), consequently leading to a decrease in secondary biomass production and biomass flows for both the pelagic and benthic-demersal pathways. Simultaneously, ocean warming projected in the region is expected to perturb the flow kinetic and trophic transfer efficiencies (Gascuel *et al.*, 2008; du Pontavice *et al.*, 2019). The underlying process is that warmer water temperatures are expected to favour short-lived species with faster metabolic rates across the food webs (Beukhof *et al.*, 2019; du Pontavice *et al.*, 2019 - Chapter 2, du Pontavice *et al.*, under review - Chapter 3). The increase in dominance of short-lived species is already evidenced in the observed shifts in species distribution with increasing dominance of warm-water (shorter-lived) species and decreases in cold-water (longer-lived) species in the Northeast Atlantic ecosystems (ter Hofstede *et al.* 2010; Simpson *et al.* 2011; Montero-Serra *et al.* 2015). Hence, on the one hand, warmer temperature accelerates and reduces the efficiency of the biomass transfer. On the other hand, the overall climate-induced decrease in secondary production induces an overall decrease of the biomass fuelling the food web.

The variabilities of the changes in SST and secondary producers explain the spatial variations in the response of projected changes in biomass and catch in the European waters. In some ICES division, such as in Western Scotland, the projected increases in secondary production partly were partly compensated the warming-induced impacts of trophic transfer toward higher TL, leading to almost constant total biomass and catches. In contrast, in the middle of the North Sea, the Celtic Sea and the south of the Bay of Biscay, where changes projected warming and decrease in secondary production by ERSEM are the highest, biomass and catches were projected to be amongst the biggest compared to other regions.

Our findings also suggest an amplification of the changes in biomass and catch from low to high TL components of the ecosystems. This process describes the propagation of the climate signal up from low TLs to upper TLs through the decline (or increase) of biomass along the food web. The stronger decline in biomass and catch of higher TLs arises from reduced transfer efficiencies associated with increasing temperature. This is consistent with the trophic amplification induced by warming for the higher TLs revealed at global scale (Lotze *et al.*, 2019; du Pontavice *et al.*, under

review - Chapter 3) and locally in the North Sea (Kirby & Beaugrand 2009; Lindley *et al.* 2010). Here, the amplification of the changes in the catch is reinforced because pelagic species mainly composed of low TLs species are less affected than benthic species mainly composed of high TLs.

4.4.2. Sensitivity analyses and structural uncertainties of the model

In this study, we attempted to improve the representation of the trophodynamic pathways by subdividing the ecosystems into pelagic and benthic-demersal components. However, our study may have underestimated the degree of the coupling in the shallowest ICES divisions (e.g., the Eastern English Channel), assuming that the production which is transferred from the pelagic to the benthic pathway is constant over TLs and areas (ICES division). In contrast, several recent studies showed that the degree of benthic-pelagic coupling vary widely over depth with stronger coupling in shallow coastal areas in Europeans continental shelf (Kopp *et al.* 2015; Giraldo *et al.* 2017; Cresson *et al.* 2020). Cresson *et al.*, (2020) highlighted major differences in benthic-pelagic coupling between the Bay of Biscay (division 8b) and the Eastern English Channel (7d in our study). Thus, quantitative estimates regarding the spatial variability of the benthic-pelagic coupling may improve the spatial patterns of our projections.

To test the consequences of the potential underestimation of the benthic-pelagic coupling on the projections, we doubled the production transferred from pelagic to benthic pathways in every division (Appendix C - Supplementary material C.1). The sensitivity analysis showed that with a stronger pelagic-benthic coupling, biomass and catch would be slightly less impacted by climate change (with differences of about 0.2% and 0.15% for the catch and biomass, respectively) (Appendix C - Supplementary material C.1). Therefore, the projected changes in biomass and catches are not sensitive to the intensity of the overall benthic-pelagic coupling.

In the study, we considered that each ICES division is an independent ecosystem without exchange between these ecosystems. In each division, we assumed that secondary production (zooplankton and benthos) fuel the entire ecosystem without seasonal migration (e.g., species that feeds in a division and which is caught in another). This is a reasonable assumption for benthic and demersal species which are highly dependent on their habitats. This assumption, however, is more questionable for pelagic species since some studies highlighted that several pelagic fish stocks in the Northeast Atlantic undertake extensive seasonal migrations (Macer 1977; Uriarte *et al.* 2001; Hátún *et al.* 2009; Trenkel *et al.* 2014). In the future, the model can be further developed by incorporating quantitative knowledge regarding the seasonal migrations between the considered ICES divisions.

While the projected changes in transfer efficiency and flow kinetic can be a result of changes in species assemblages under ocean warming (Gascuel *et al.* 2008; du Pontavice *et al.* 2019), other climate-induced biological responses at individual and population levels that may amplify the overall climate change impacts on kinetic and trophic transfer efficiency, are not represented. We also do not consider neither the effects of extreme events such as marine heatwaves, nor the impact of the projected increase in the acidification and reduction in dissolved oxygen in European seas (Peck *et al.* 2020). These combined effects may amplify the effect of climate change on marine organisms with large variability in species' responses (Kroeker *et al.* 2013; Pörtner *et al.* 2017; Bindoff *et al.* 2019). Warming and decrease in oxygen content are, notably, projected to impact growth of fishes, leading to reductions in individual- and assemblage-level body size (Cheung *et al.* 2013a) which may, in turn, affect trophic interactions and biomass transfers.

Finally, in EcoTroph, the intensity of top-down controls is integrated in order to account for the effects of the fishing-induced release of predation relatively to a theoretical unexploited ecosystem. The sensitivity analyses showed that assuming larger top down controls conducts to stronger projected impacts of climate change on the biomass at the low TLs (Appendix C - Supplementary material C.2). This sensitivity analysis highlights the importance of trophic controls to understand the responses of marine ecosystems to climate change.

4.4.3. Contribution of EcoTroph modelling to explore the future of European fisheries

European seas had been intensively exploited by fisheries throughout the second half of the 20th century with a peak at 7.2 million tons of catch in the '70s which catches were halved by the early 21st century due to overfishing and fishing regulation (Gascuel *et al.* 2016; Pauly & Zeller 2016). A decrease in fishing pressure was observed over the last fifteen years and the mean fishing mortality rate of assessed stocks was reduced in all the ecosystems in Europeans seas of Northeast Atlantic (Hervann & Gascuel 2020; STECF 2020). Over-exploited fish stocks have started to recover slowly and abundance of fish stock increased significantly in recent years (Hervann & Gascuel 2020; STECF 2020). However, this study highlights that climate change will challenge the future recovery of these fish stocks, with projected decrease in overall biomass in the 21st century.

While the differences in the projected biomass are small between two fishing scenarios considered here, the decline of fisheries catch is expected to be lower if the fishing loss rate remains constant. This is due to a compensation effect induced by faster trophic transfer under ocean warming. If the fishing impact on production and biomass flow (i.e., a constant fishing loss rate)

remains unchanged, the fishing mortality increase due to increase in the flow kinetic and result in the attenuation of the decrease in catch, compared to the decrease in biomass. Following Odum's theory (Odum 1985) that predicts that community respiration (with an increase in P/B ratio) increases in perturbed ecosystems, the perturbations of Europeans ecosystems results in an increase in the flow kinetic which conduct, in turn, to an attenuated effect on catch. This effect may mitigate the projected climate-induced decline of the catch and the mitigation is projected to be higher in the areas where the warming and thus the global impact on marine biomass are strong (e.g., in southern North Sea).

Biomass is expected to decrease, resulting in substantial loss of catch regardless of the fishing scenarios, especially in the upper TLs. Changes in ocean conditions of European waters are projected to vary between ecosystems, with some areas being more impacted such as the Celtic Sea, the middle of the North Sea and the South of the Bay of Biscay. In parallel, at species level, the observed shifts in species distribution in Europeans waters (ter Hofstede *et al.* 2010; Simpson *et al.* 2011; Montero-Serra *et al.* 2015; Baudron *et al.* 2020) are expected to accelerate with the future changes in ocean conditions. Hence, European Fisheries may face to two major issues with declines of total catch as well as changes in species composition of the catch that will result in both economic and political repercussions. As suggested by Baudron *et al.* (2020) a revision of the principle of "relative stability" in catch quota allocation (fixed allocation key based on historical catch for each country) would be necessary to address some economic and political issues related to the changes in species assemblages. However, European fisheries should also anticipate the expected losses in catch which may counterbalance the slow recover in stock abundance observed over the last decade, as a result of a more precautionary fisheries management.

4.4.4. Conclusion

Based on the projected changes in biomass of pelagic and benthic secondary producers and the current reported fisheries catch, we projected that the total biomass and catch would decrease by 2090-2099 relative to 2013-2017 under RCP8.5 scenario and a constant fishing mortality scenario. Some areas of the European waters, such as the Celtic sea and the Bay of Biscay, would be more affected than others because of the large variations in temperature and secondary production. Moreover, we simulated an alternative fishing strategy in which fisheries maintain constant their impact on ecosystem production (instead on biomass in a constant fishing mortality scenario). Such a fishing strategy may limit the projected decline in catches compared to a constant fishing mortality strategy. Our study shows that climate change will impact the European fisheries with ecological consequences and potential economic and political repercussions. While managing fisheries is

required to adapt, the projected impacts will not be fully avoided without mitigation of greenhouse gases emissions.

CHAPTER 5

General discussion and perspectives

CHAPTER 5: General discussion and perspectives

5.1. A contribution to the understanding of biomass flows in marine ecosystems

The changing in ocean conditions affects profoundly marine ecosystem structure and functioning. The observed and projected changes tend to alter the flow of energy in marine ecosystems. While there is considerable agreement that climate change will affect the biomass transfer in marine ecosystems, large uncertainties persist relative to the intensity, the direction and the underlying processes. This thesis aims to contribute to fill this gap through a trophic level-based approach.

As the first step, to explore the variability of the biomass flow within marine ecosystems, we identified and calculated two trophodynamics properties characterizing the biomass transfer at the ecosystem scale, and which determine its intensity at every trophic level. On the one hand, trophic transfer efficiency (TTE) is an emergent ecosystem property and a well-known parameter in several marine ecosystem models (Lindeman 1942; Jennings et al. 2008; Niquil et al. 2014; Carozza et al. 2016; Petrik et al. 2019; Eddy et al., Under Review). Slight variations of the TTE can induce large repercussions on marine ecosystems and fisheries (Ryther 1969; Baumann 1995; Rosenberg 2014; Stock et al. 2017). On the other hand, flow kinetic and its associated biomass residence (BRT) time are also critical emergent food properties whose variations may affect directly the functioning of marine food web (Gascuel et al. 2008; Schramski et al. 2015). Based on Maureaud et al. (2017), we calculated the TTE and the BRT in all the coastal ecosystems and highlighted the biomass transfers are characterized by two continua: a “fast-slow continuum” of flow kinetic and an “inefficient-efficient continuum” of TTE, both along a temperature gradient. Biomass flows tend to be slow and efficient in cold waters and faster but less efficient in warmer waters. This pattern is expected to be driven by temperature-induced composition of marine communities which are dominated by slow-growing, long-living and late-maturing species in cold waters and fast-growing short-living, early-maturing species in warmer waters (Juan-Jordá et al. 2013; Beukhof et al. 2019). Interestingly, we identified that TTE in upwelling ecosystems stands out as an exception with low TTE but a strong sensitivity to

the changes in temperature. Our results also suggest that this short-living species inhabiting warmer waters are, on average, and at every trophic level less efficient in transferring biomass toward higher levels, i.e., less efficient in converting their own consumption into new tissues, through growth processes.

By modelling the statistical relationship between temperature and biomass flow, we were able to investigate the future warming-driven spatiotemporal changes in biomass flow. We projected a decline in the TTE and BRT in the food web throughout the 21st century with larger decrease in TTE in polar ecosystems. As we highlight in Eddy et al. (Under Review – Appendix D, Article 3), key questions remain about how transfer efficiency changes with temporal and spatial scales, ecosystems, fishing pressure, and climate change. In this context, our findings show that transfer efficiency is more variable than initially thought. Moreover, we provide, for the first time, quantitative estimates of the warming-induced changes in transfer efficiency between secondary consumers and top predators in marine ecosystems.

Then, we analyzed the consequences of the changes in biomass flow on the trophic structure of food webs by 2100 (Chapter 3). We showed that the projected alterations of biomass transfers in marine ecosystems may lead to a global decline of consumer biomass by 2100 under a “no mitigation policy” scenario. We identified that tropical ecosystems would be the most affected biomes due to the combined declines in net primary production (NPP), flow kinetic and TTE. In polar ecosystems, we found that TTE and flow kinetic would be strongly affected by warming but the projected decline in biomass and production in Arctic and Antarctic ecosystems is moderate. This is due to the projected increase in NPP (and TTE of lower trophic levels) that compensates the losses induced by the decline of the TTE and the acceleration of the biomass flow. In other words, in polar ecosystems, there would be a faster and less efficient biomass flow but an increase in biomass entering the food web by 2100. Also, our projections revealed a trophic amplification of the changes in biomass, with a more pronounced decrease in high TLs. The enhancement of the changes is driven by the cumulative effects of the warming-induced decline in TTE.

Fishing was the main driver of the alteration of marine ecosystems during the 20th century and continues to affect marine ecosystems substantially (IPBES 2019). Fisheries also provide a major source of protein and socio-economic opportunities for coastal communities. Hence, it was essential to integrate fishing in our projections to better understand its effects on marine ecosystems and provide insights about the future changes in fisheries catch. For that purpose, we focused on the European continent shelf ecosystems which are historically highly exploited areas already affected by climate-induced changes in ocean conditions and wherein a high resolution and high resolution and

quality climate model was developed (POLCOMS-ERSEM). The study revealed that biomass and catch are expected to decrease with climate change if fishing mortality remains constant to its current level (in 2013–2017). The strength of the decline is driven by the intensity of the ocean warming and the changes in secondary producers. The temperature-induced decline in TTE is expected to lead to higher impacts on the high trophic levels. Finally, we showed that an alternative fishing strategy in which fisheries maintain constant their impact on ecosystem production (instead of ecosystem biomass) may limit the projected decline in catches compared to a constant fishing mortality strategy. This study reveals that climate change will impact European fisheries with ecological consequences and potential economic and political repercussions.

5.2. Caveats and limitations

This section points out several general limitations of the research presented in this thesis as well as perspectives to address some of these limitations.

The simple structure of EcoTroph which is an advantage in light of multiple aspects (as detailed in the following section; Section 3.3) can also be considered as a limitation. The model provides a generalized diagnosis of climate impacts for all trophic levels and the entire biomass and production of the ecosystem but is not able to provide specific quantitative estimates at species, functional or population levels. From this perspective, EcoTroph cannot be considered as a tool to provide realistic scenarios to manage specific fish stocks. Instead, the model can produce credible quantitative estimates on the long-term changes in ecosystem biomass (see below, Section 5.2.3) and explore the effects of stressors on the food web structure. In chapter 4, we showed that, for instance, the catches of high TLs species which are dominated by large benthic-demersal fish in the major part of the European waters would be more affected by climate than low TLs species dominated by small pelagic species.

The trophic level, which identifies the trophic position of organisms with the food web, may be considered an emergent property of the ecosystem dynamics, providing an *a posteriori* metric of the trophic processes involved. TLs are complicated to estimate in the field since they can vary from and one individual to another (Caddy 1998) and change seasonally or spatially depending on biotic and abiotic factors (Jennings et al. 2002; Chassot et al. 2008; Vinagre et al. 2012; Reed et al. 2017). In this thesis, TL estimates were widely used to calculate the TTE and the BRT (Chapter 2) and to build the catch trophic spectra of European fisheries (Chapter 4). The allocation of a single TL to each taxon may induce large uncertainties although we attempted to take into account the within-taxon variability by distributing catch of every taxon over a range of trophic classes.

In our modelling approach, the EcoTroph model was applied on two spatial scales, the $1^{\circ} \times 1^{\circ}$ grid cells (Chapter 3) and the ICES divisions (Chapter 4). In each of these areas, we modelled the ecosystem by assuming it is independent without exchange between grid cells or divisions. Marine consumers are assumed to feed on their preys within the area and marine species do not migrate beyond the boundary of the areas. Yet, several studies highlighted that some commercially important pelagic fish species, such as tuna-like species, undertake extensive seasonal migrations (Block *et al.* 2011; Trenkel *et al.* 2014). It is likely one of the reasons why the incorporation of fisheries catch has been challenging. We will come back to this point in the section 5.4.2 where the integration of the global fisheries catch is discussed.

In the global EcoTroph model (Chapter 3), we did not take into account the detrital pathway which can represent a substantial source of food for benthic fauna in the shallow shelf seas (Carstensen *et al.* 2003; Duffill Telsnig *et al.* 2018). With the COBALT model in Chapter 3, the spatial variability of biomass transfers is integrated only between pelagic primary production and zooplankton. As a consequence, the biomass transferred to higher TLs via the detrital pathway was likely underestimated in coastal areas. We identified two ways to address this issue that we will detail in the section 5.4.2.

Finally, the implementation of the EcoTroph model developed in the thesis integrates multiple mechanisms from species to community scales to build the biomass flows representation. However, the projections in TTE and flow kinetic are affected only by the warming-induced changes in species assemblages. Our approach can be considered conservative since climate change can affect marine life at species and population levels (Bindoff *et al.* 2019). Also, biomass transfer can be impacted by several other stressors such as deoxygenation and acidification which may exacerbate the warming-induced changes in biomass transfer (Kroeker *et al.* 2013; Cripps *et al.* 2016; Bindoff *et al.* 2019). Acidification is notably expected to deeply affect the lower tropic levels, directly through changes in metabolism (Cripps *et al.* 2016) and indirectly through changes in production and trophic interactions (Nagelkerken & Connell 2015; Cripps *et al.* 2016; Ullah *et al.* 2018). A meta-analysis published in 2015 revealed, for instance, that primary production by temperate non-calcifying plankton is likely to increase with elevated temperature and $p\text{CO}_2$, while tropical plankton may decrease productivity because of acidification (Nagelkerken & Connell 2015). In parallel, the combined effects of warming and oxygen loss this century would lead to changes at individuals scale linked to changes in metabolic rates and ultimately to growth of marine species (Cheung *et al.* 2013a) as well as contraction of viable habitats and species ranges (Stramma *et al.* 2012; Cheung *et al.* 2013a; Deutsch *et al.* 2015).

5.3. A simple and efficient modelling approach to explore the effects of climate change

5.3.1. Three processes at play to model the future of marine ecosystems

Generally, to apply the EcoTroph modelling approach to a specific ecosystem, the outputs from an Ecopath model are required to build the trophic spectra of biomass and catch and to represent fishing effects across the trophic levels. In 2011, Tremblay-Boyer et al. adapted the EcoTroph model to explore the past fishing effects using basic ecological assumptions and environmental forcings. The general approach was promising and opened the way for new implementations of EcoTroph. In this thesis, our modelling approach is the first application of EcoTroph linking the trophic ecology and the projected changes in ocean conditions.

Despite its apparent simplicity and the low number of parameters, EcoTroph falls into the “whole ecosystem models and dynamic system models” category (Plagányi 2007). Indeed, all trophic levels are considered from primary producers to top predators. Within the trophic level-based models (e.g., Ecopath with Ecosim), EcoTroph may be viewed as the ultimate stage in the use of the TL concept for ecosystem modelling. In this approach, individual “species” disappear and are instead combined into classes based only on their trophic levels and the entire ecosystem is represented by the continuous distribution of biomass (biomass trophic spectrum) along from primary producers to top predators. Therefore, EcoTroph does not explicitly resolve the climate-induced impacts on individual species and population. Instead, the model assumes that the shifts in environmental conditions will lead to the emergence of new biomass transfer features in theoretical steady state ecosystems.

One of the strengths of EcoTroph lies in the simplicity of the model formulation based on three clear visible processes which determine biomass or catch (or production, fishing mortalities, etc.) trophic spectra and can integrate a large variety of mechanisms from species to ecosystem scales: the biomass entering the food web (e.g., NPP), the TTE and the flow kinetic at each TL. Hence, the structure allows disentangling easily the effects associated with each process while having the possibility to consider multiple mechanisms at different ecological scales acting on each process. The focus on the TTE (chapter 1) illustrates the potentiality to consider and include the large-scale variations in biomass transfers in EcoTroph (chapter 2). We estimated the spatial patterns and the projected warming-induced in TTE. These estimates were calculated from taxon-specific data (i.e., growth parameters) cumulated at community scale taking into account explicitly the structure of the food web (i.e., species assemblages) (chapter 2). In parallel, we considered trophodynamics

specificity of the planktonic food web by calculating TTE for the lower TLs based on the coupled physical–biological model COBALT (Stock et al. 2014a, b).

Furthermore, our modelling approach can integrate different data sources to consider the changes in ocean conditions. For instance, the biomass entering the food web, which is a pivotal process in EcoTroph, can be estimated from ocean-colour satellite observations and climate model outputs. Also, in the modelling approach developed during the thesis, NPP derived from different Earth system models (ESM) was used to estimate the biomass fuelling the ecosystems at global scale (chapter 3) while, in the European seas, we used the biomass of secondary producers derived from the coupled physical–biogeochemical POLCOMS-ERSEM (Chapter 4). The latter allowed integrating directly the benthic and pelagic secondary production which represents the bulk of the resources available to higher trophic levels. Furthermore, doing so we bypassed the uncertainties related to the trophic transfer between the primary producer and primary consumers using a high quality and resolution model.

Another advantage of our approach is the modularity. Although EcoTroph is a simple model in essence, its structure itself can be adapted to take into account ecological specificities of ecosystems. In chapter 4, for example, in order to consider the trophic dynamics of European continental shelf ecosystems and the benthic–pelagic coupling (Kopp et al. 2015; Giraldo et al. 2017; Cresson et al. 2020), we divided the biomass flow into two coupled trophic pathways, pelagic and benthic–demersal. A trade-off is, however, required to keep the simple nature of EcoTroph and, at the same time, consider the part of the complexity of the ecosystems structure which is susceptible to affect its functioning.

The simple structure and equation of EcoTroph also ease the computational implementation and reduces drastically the computation time. For example, for the global simulations with the parameterizations use in chapter 3 or for Fish-MIP (see Chapter 5, Section 5.2.1), running independently 6,000,000 of EcoTroph models (about 40,000 grid cells x 150 years) takes between 4 and 7 hours after optimizing the computational process. In comparison, for a complex ecosystem model like Atlantis (Fulton et al. 2011) running scenarios takes several days. However, such a modelling approach attempts to integrate all processes from physics to socioeconomics, and can provide stakeholders all the information they need and draw realistic management scenarios. Thanks to the light computational implementation, testing and analyzing assumptions or scenarios are easy and fast.

5.3.2. Effect of Iron limitation in a Pacific food web – A complementary study

Finally, the consistency of the quantitative estimates (see section 5.2.3) and the computational efficiency of EcoTroph allowed us to develop, in the margin of the PhD, a collaboration with the University of Liverpool to study the repercussions of the changes of primary production induced by iron cycle uncertainties on higher TLs (Tagliabue et al., Under Review – Appendix D, Article 2). In this study, we presented evidence that climate change trends in NPP in the eastern tropical Pacific are strongly affected by assumptions associated with phytoplankton iron removal. We found a plausible range of -12.3% to +2.4% in the effect of climate change on NPP, driven by changes in the resilience of the regional iron limitation. These results translate into reductions in projected biomass of upper trophic levels between 57% according to EcoTroph and 82% according to APECOSM (Figure 5.1). The uncertainties in the biological iron cycle are found to clearly contribute additional ambiguity regarding the future of regional ecosystems.

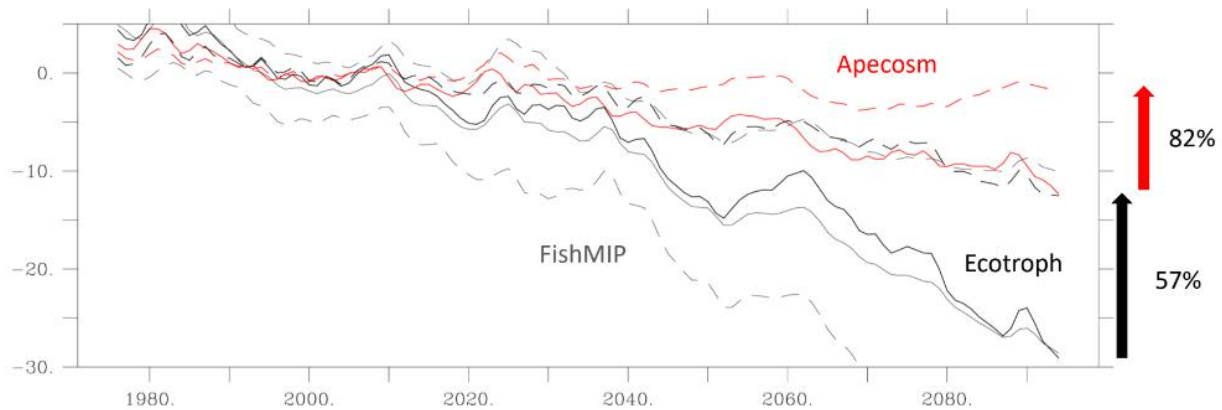


Figure 5.1: The percent change in total consumer biomass within the Pacific Equatorial Divergence province for the control (solid line) and the lowered phytoplankton iron uptake experiment (dashed line) within the EcoTroph (black) and APECOSM (red). The multi-model mean \pm the standard deviation from the Fish-MIP exercise for the same region forced by IPSL-CM5a output is shown in a thin black solid and dashed line. All changes are relative to 1986–2005. The effect of lowered phytoplankton iron uptake for each model is shown with a red (APECOSM) or black (EcoTroph) arrow.

5.3.3. EcoTroph in Fish-MIP

Many global marine ecosystem models were developed in the past decades to analyze the future global changes in structure and functioning of marine ecosystems. The project Fish-MIP gathered all these modelling approaches to provide credible and coherent projections of the future of marine ecosystems (Tittensor et al. 2018). In a first step, the projected climate-induced impact on the total consumer biomass was calculated based on six ecosystem models forced by two ESMs under four RCPs (Lotze et al. 2019). The multimodel intercomparison analysis revealed a consistent global decline in total consumer biomass driven by increasing temperature and decreasing primary production. Also, it highlighted that the climate-induced changes in primary production would be amplified at higher trophic level.

In 2018, EcoTroph joined the Fish-MIP network. Our modelling approach adds a new perspective by summarizing the ecosystem functioning into a biomass flow based on emergent food web properties. Moreover, the EcoTroph structure and computation make it easy and time efficient to test hypotheses on processes and drivers. Our projections in total consumer biomass are fully consistent with the spatial and temporal changes described in Fish-MIP. Specifically, based on the IPSL (the ESM developed by the Institut Pierre Simon Laplace; Dufresne et al., 2013), we found that the 17% decline in consumer biomass is consistent with the range of changes estimated from the Fish-MIP models, EcoTroph projections follow the same trend than the 2 other models (Macroecological model and Bioeconomic mArine Trophic Size-spectrum model; see Chapter 3) with a slowing down of the decline in the late 2080s (Figure 5.2). Furthermore, EcoTroph model revealed an amplification of the changes in NPP when moving up the food web due to the warming-induced decline of TTE. In further analysis based on the global ecosystem models of Fish-MIP, we showed a consistent trophic amplification between NPP and total consumer biomass as well as a large spatial variability depending notably on the projected changes in temperature and NPP (Guibourd et al., In Prep, Master supervision).

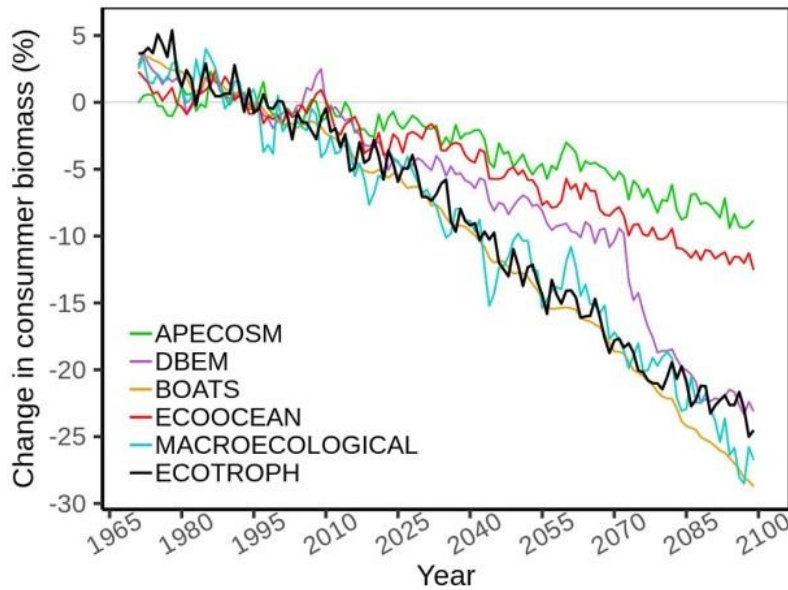


Figure 5.2: Comparison of the EcoTroph projections with the Fish-MIP projections. Changes in total consumer biomass between 1970 and 2100 relative to the reference period 1986–2005 for 5 ecosystem models and for EcoTroph, for RCP8.5 and with the earth system model IPSL.

The previous Fish-MIP study was a crucial step toward the understanding of climate impacts on the global ocean ecosystem (Lotze *et al.* 2019). The projected total consumer biomass is a blend of positive and negative responses in total consumer biomass that mirror the projection changes in NPP and to lesser extent temperature. Moreover, the changes projected by a subset of ecosystem models are also driven by oxygen, salinity and ocean advection (Cheung *et al.* 2011; Blanchard *et al.* 2012; Fernandes *et al.* 2013; Carozza *et al.* 2016). Hence, it is challenging to distangle the different effects in the different ecosystems models ranging from size-based structure to species distribution. That is the reason why we are currently working on a new step of Fish MIP in which we isolate the responses to the two primary climate drivers (NPP and temperature) for each marine ecosystem model, in order to better understand why they respond differently. We are currently analyzing the differences in the climate responses among MEMs. The preliminary results reveal that the projected spatial changes in NPP drive the spatial pattern of the changes in total system biomass with an intensification of the changes induced by global warming. Interestingly, large spatial differences in response to changes in temperature and NPP are observed across the different ecosystems models for the higher trophic level biomass (Heneghan *et al.*, In Prep.).

A recent study of Boyce *et al.* (2020) complemented the previous work of Fish-MIP by combining the total consumer biomass projections and socioeconomic indicators (e.g., gross domestic

product, human development index) at national and global scales. It revealed that maritime nations with poor socioeconomic would experience the greatest projected decline in consumer biomass under RCP8.5. Besides illustrate how the projections of Fish-MIP can provide insights on the socioeconomic consequences of climate change, the study raises the question of the multi-model ensemble averages. In such approach, the projections of the different models are considered equally plausible and the mean future trends are calculated and analyzed despite the great variability among individual projections (e.g., Bryndum-Buchholz et al. 2019; Lotze et al. 2019). On the one hand, the non-independence of models and the potential for extreme projections to influence an ensemble average may bias the multi-model ensemble average projections. On the other hand, the non-independence in itself is not an issue but the source of the non-independence. The non-independence between two models can result from the same ecological process which is modelled differently and, in that case, the non-independence cannot be considered as a bias. Moreover, there is no apparent reason to give less weight to a model because of its extreme projections.

Furthermore, the model intercomparison approaches may benefit by adopting statistical analyses increasing statistical rigour through the evaluation of the projection variability and uncertainty (Boyce et al. 2020). One of the statistical methods to analyze the future changes in biomass (or other ecological variable) could be based on mixed-effects modelling approach (Bolker et al. 2009). It allows testing the significance of the changes and the effects of human impacts scenarios (e.g., scenario) by considering the inter-individual variability (e.g., inter-model variability among ecosystem models and ESMs).

Next steps in Fish-MIP will include scenario of human activities and management approaches (e.g., dynamic scenario of fishing) since a large component of future changes will also depend on the trajectories of human impacts (fisheries, aquaculture, pollution...). The goal will be to analyze the combined (and likely synergistic) responses of marine ecosystems to climate and other anthropogenic stressors and identify the potential leverage for mitigating impacts on the global ocean.

5.3.4. EcoTroph, a tool to assess the impact of marine heat waves

New developments regarding climate change modelling suggest that projecting the ecological impacts of the increase in yearly mean temperature, as we did in this PhD is insufficient, as major expected impacts might be linked to extreme events. In that perspective, a new PhD project should start next fall in line with the current one, dedicated to the assessment of the effects of marine heat waves on the trophic functioning of ecosystems (and under the same joined supervision of Agrocampus Ouest and UBC).

Climate change had led to widespread increase in marine heat waves frequency, intensity and duration (Oliver et al. 2018) and is projected to increase further (Frölicher et al. 2018). Marine heat waves which are characterized by persistent extremely warm ocean temperature are already affecting distribution of marine fishes and invertebrates (Pershing et al. 2018; Li et al. 2019) and altering marine habitats such as coral reefs (Smale et al. 2017) and kelp forests (Reed et al. 2016). Furthermore, marine heat waves are expected to exacerbate the rate and the magnitude of the shift in species distributions over the 21st century (Cheung & Frölicher 2020) which, in turn, may modify the structure and functioning of marine food webs. Marine heat waves occurring over short periods are likely to propagate in food webs over longer periods. Ecosystem impacts will result from the aggregation processes occurring at different time scales. There is thus a challenge to represent these intertwined processes and develop ecosystem modelling approaches, capable of anticipating those effects of short-term climate events over the medium or long term.

The EcoTroph model appears as a suitable tool since it is structurally based on trophic kinetics parameters which is highly sensitive to warming and can account for the propagation of disturbances within the food web. So far, in our implementation of EcoTroph, the model accounts for steady states. One of the challenges of the coming thesis will be to develop a new generation of the model, integrating time dynamic processes in order to analyze the propagation of impacts and their aggregation on a larger scale. Such a dynamic EcoTroph model, applied at different time and space scales, may allow exploring the expected effects of widespread increases in marine heat waves frequency and intensity, and, thus, more robust projections of the impacts of climate change on the productivity and stability of marine ecosystems.

5.4. Climate change and fishing in EcoTroph

5.4.1. The fishing impacts in EcoTroph

In a changing ocean, understanding the future of fisheries, its impact on ecosystems and its sensitivity to climate, is critical to address food security challenges, socioeconomic inequity and political conflicts over the coming century. Several ecosystem models including those in Fish-MIP can incorporate fishing but vary in their representation of fishing activities either through fishing effort (e.g., BOATS, Bioeconomic mArine Trophic Size-spectrum; Carozza *et al.* 2017) or fishing mortality (e.g., DPBM, Dynamic Pelagic Benthic Model; Blanchard et al., 2012). For example, BOATS uses a bioeconomic model to determine spatial and temporal changes in fishing effort which assumes that the resource is either in open access or managed at the maximum sustainable yield (Carozza *et al.*

2016; Galbraith *et al.* 2017). Both scenarios are not representative of the fisheries reality; instead they represent extreme ranges of possible future of fisheries.

EcoTroph model has been previously used to draw diagnosis of the fishing effects on the trophic structure in different case studies (e.g., Gasche *et al.* 2012; Halouani *et al.* 2015; Moullec *et al.* 2017; Valls *et al.*, 2012). Fishing can be integrated either directly using catch trophic spectra i.e., catch distribution across trophic levels or indirectly using fishing mortality or loss rate. In our study on the effect of climate change on European continental shelf ecosystems (Chapter 4), we combined these two approaches to integrate fishing pressure. We used catch trophic spectra based on the current catch (over the 2013–2017) to define the reference state of the ecosystems, and, then, we determined the current fraction of the biomass and the production, respectively, which is caught at each trophic level. The two latter made possible to simulate realistic fishing strategies based on the current fishing impact.

However, the use of the catch trophic spectra induces some difficulties to obtain realistic fishing impact levels. In chapter 4, the current fishing mortality was low compared to the stock assessments in the European waters or modelling approaches (e.g., Moullec *et al.*, 2017). The biomass is likely too large compared to the catches, which suggests that our model overestimated the current biomass (by assuming that the catches are accurately reported). Further investigations on the transfer efficiency and the production fuelling the food web may contribute to reducing the overestimation. The accessibility of the benthic secondary production can also constitute a lever to obtain more realistic biomass estimates and, thus, fishing mortality. In our study, we assumed that the benthic secondary production is fully available for higher trophic levels whereas predators can access only a portion of benthic preys (Tableau *et al.* 2015; Saulnier *et al.* 2020). The proportion of accessible benthic secondary producers is probably relatively low (between 10 and 12.5% according to (van der Veer *et al.* 2011; Tableau *et al.* 2015). Adjusting the accessibility of benthic producers to more realistic levels is likely to constraints the biomass estimates.

To sum up, EcoTroph can integrate predefined and imposed fishing scenarios (e.g., fishing mortality) and, unlike the majority of others marine ecosystem models, the model can also integrate directly the past or current fisheries catches. Hence, our modelling approach, although improvable, can be considered as an efficient tool for exploring the future of fisheries in the changing ocean.

5.4.2. From the European case study to the introduction of global fisheries catch in EcoTroph

In order to improve our understanding of the future of marine ecosystems and provide quantitative assessment of the worldwide impacts of climate change on marine living resources, it is crucial to integrate fishing scenarios in the global ecosystem models. In 2018, two ecosystem models provided projections of the global impacts of climate on fisheries (Cheung et al. 2018). They projected a decrease in total maximum catch potential from 7 to 12% in the world's exclusive economic zones by 2050. The two models are based on different approach (species distribution model vs. size-based models) and they incorporate fisheries based on the maximum sustainable yield concept (Cheung et al. 2010) and on fixed fishing mortality applied to the whole food web and everywhere worldwide (Blanchard et al. 2012).

Following the EcoTroph approach applied to European waters (Chapter 4), we can potentially provide global projections of future catch based on the current fishing impact. The past and current spatialized catch data reconstructed by Sea Around Us (Pauly & Zeller 2016) would allow building catch trophic spectrum in each $1^{\circ} \times 1^{\circ}$ grid cell of the global ocean. Then, the EcoTroph model developed at global scale (Chapter 3) can be adapted to integrate the catch trophic spectrum which would affect both biomass flow and the flow kinetic (see in Chapter 4 how fisheries catch are introduced in EcoTroph). Hence, based on the current catch and the projected changes in NPP and temperature provided by the Earth System models, we are potentially able to model the marine ecosystems and the fishing impact using EcoTroph. However, preliminary analysis failed at modelling the ecosystems in the coastal areas due to an inconsistency between the ecosystem production and the quantity of marine species catch. In other words, from model outputs it comes that coastal ecosystems do not produce enough biomass to support catch. I identified several issues and some potential leverages to reconcile ecosystem production and catch:

- (i) One of the potential issues may be induced by the trophic transfer efficiency (TTE) estimates. In 2017, Stock et al. showed that TTE is key parameters to explain the inconsistency between the regional differences in fish catch and the differences in net primary production (NPP). In this study, the authors identified 3 major energy-related factors that may explain the aforementioned inconsistency: the interregional differences in pelagic and benthic energy pathways, the low TTE in the tropics and the elevated TTE in the benthic-predominant systems. In this thesis, we estimated TTE and assessed its spatial variability along a temperature gradient with low TTEs in the tropics (chapter 2). However, the overall underestimation of TTE (see previous section) could

partly explain the insufficient production. Further investigations could explore the hypothesis by estimating, all being equal, the required TTE to support catch.

(ii) The global EcoTroph model without fishing provides interesting insights regarding the low trophic levels dynamics (Chapter 3). The energy transfer in planktonic food web was integrated by estimated TTE between NPP and mesozooplankton using the COBALT (Carbon, Ocean Biogeochemistry and Lower Trophics) model. It is a first step to integrate the patterns in TTE of lower trophic levels but we considered only the pelagic pathway. In open ocean, the bulk of the transfer of energy occurred between phytoplankton and zooplankton but, in continental shelf ecosystems, NPP also fuelled benthic pathway through downward coupling (Woodland & Secor 2013; Duffill Telsnig et al. 2018; Cresson et al. 2020). Hence, by considering only the pelagic energy transfer in plankton food web, we have ignored the fraction of energy which is transferred from pelagic to benthic pathways. The focus on the European waters (Chapter 4) also showed the importance of the coupling. The POLCOMS-ERSEM model, coupled with EcoTroph, includes the demersal and benthic secondary producers which are fuelled by phytoplankton (through vertical migrations or sinking), bacteria and particulate organic matter. This benthic compartment constitutes by 80% of the secondary producers potentially available for the higher trophic levels and the secondary producers (benthos + zooplankton) allow producing a sufficient amount of biomass to support the European catches, and likely all fisheries occurring in coastal waters. Further investigation would be required to consider the benthic-pelagic coupling especially in the coastal areas.

(iii) The challenge, here, is to assess the fraction of NPP which is transferred to the benthic pathway on a global scale. The downward flux of organic matter is driven by multiple factors. One of the main drivers is the bathymetry, as in deeper ocean NPP is remineralized within the microbial loop before reaching the seabed (Suess 1980; Baustian et al. 2014). The proportion of NPP sinking to the seabed and potentially available to be consumed by zoobenthos also varies with the depth of the photic zone and the productivity (Dunne et al. 2005; Pomeroy et al. 2007; Baustian et al. 2014). Dunne et al. (2005) estimated the fraction of the NPP that sink out the photic depth (pe-ratio) using an empirical equation based on SST, NPP and the photic zone depth. The pe-ratio is already used in two modelling works to link ocean productivity and fisheries catch (van Denderen et al. 2018; Petrik et al. 2019). In coastal areas, a large proportion of NPP reaches the seabed with the greatest value at mid and high latitude (Figure 5.3). Hence, the introduction of those estimates would substantially increase the production fuelling higher the biomass flow and the overall ecosystem productivity.

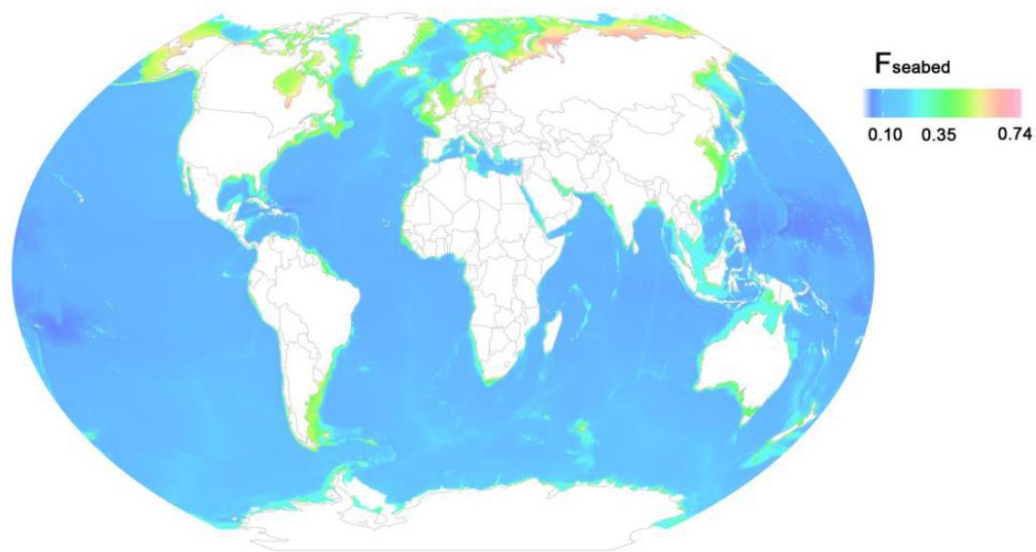


Figure 5.3: Map of the predicted fraction of NPP that reaches the seabed (Derived from van Denderen et al. 2018; Supplementary materials).

Overall, the three points presented above would contribute to reconciling the ecosystem production and the fisheries catch in EcoTroph. However, other ways could be explored to improve integration of fisheries catch in the global EcoTroph model. The spatial scale of our analysis ($1^\circ \times 1^\circ$ grid cells) could be too small given the ontogenetic and seasonal migrations of several pelagic species (Block et al. 2011; Trenkel et al. 2014). Therefore, EcoTroph could be applied in larger areas, such as national EEZ or Large marine ecosystems in coastal zones. At the scale of the global ocean, it should probably consider functional units, such as the 56 biogeochemical provinces which characterized by unique and distinguishable environmental conditions (Longhurst 2007; Reygondeau et al. 2013).

5.5. Concluding remarks

In this thesis, we developed a new method to model the biomass flows in marine food webs through which we examined the effect of climate change on marine ecosystems. Our analyses of the global ocean and the European seas have generated new insights into the future of marine ecosystems under global change. Also, the projections of changes in ecosystem biomass and catches contributed to ongoing global ocean modelling initiatives such as the Fisheries and Marine Ecosystems Impact Models Intercomparison Project (Fish-MIP), through which the results inform assessments by the Intergovernmental Panel for Climate Change (IPCC). Ultimately, the knowledge generated from this thesis relates directly and indirectly to the science that is needed to meet important societal

Chapter 5 - General discussion and perspectives

challenges such as the United Nations Sustainable Development Goals (SDGs), specifically the goal of sustaining life below water (SDG14), food security (SDG2) and livelihoods (SDG1). This study provides further support to the need for drastic reduction of greenhouse gases emissions while, at the same time, managing fisheries to adapt and reduce the climate change-related impacts on marine ecosystems and fisheries.

Bibliography

- Adams, S.M., Kimmel, B.L. & Ploskey, G.R. (1983). Sources of Organic Matter for Reservoir Fish Production: A Trophic-Dynamics Analysis. *Canadian Journal of Fisheries and Aquatic Sciences*, 40, 1480–1495.
- Agawin, N.S.R., Duarte, C.M. & Agustí, S. (2000). Nutrient and temperature control of the contribution of picoplankton to phytoplankton biomass and production. *Limnology and Oceanography*, 45, 591–600.
- Andersen, K.H., Beyer, J.E. & Lundberg, P. (2009). Trophic and individual efficiencies of size-structured communities. *Proceedings of the Royal Society B: Biological Sciences*, 276, 109–114.
- Andersen, K.H., Jacobsen, N.S. & Farnsworth, K.D. (2016). The theoretical foundations for size spectrum models of fish communities. *Canadian Journal of Fisheries and Aquatic Sciences*, 73, 575–588.
- Anderson, C.N.K., Hsieh, C., Sandin, S.A., Hewitt, R., Hollowed, A., Beddington, J., *et al.* (2008). Why fishing magnifies fluctuations in fish abundance. *Nature*, 452, 835–839.
- Anticamara, J.A., Watson, R., Gelchu, A. & Pauly, D. (2011). Global fishing effort (1950–2010): Trends, gaps, and implications. *Fisheries Research*, 107, 131–136.
- Armengol, L., Calbet, A., Franchy, G., Rodríguez-Santos, A. & Hernández-León, S. (2019). Planktonic food web structure and trophic transfer efficiency along a productivity gradient in the tropical and subtropical Atlantic Ocean. *Sci Rep*, 9, 2044.
- Asch, R.G. (2015). Climate change and decadal shifts in the phenology of larval fishes in the California Current ecosystem. *Proceedings of the National Academy of Sciences*, 112, E4065–E4074.
- Asch, R.G., Pilcher, D.J., Rivero-Calle, S. & M. Holding, J. (2016). Demystifying Models: Answers to Ten Common Questions That Ecologists Have About Earth System Models. *Limnology and Oceanography Bulletin*, 25, 65–70.
- Asch, R.G., Stock, C.A. & Sarmiento, J.L. (2019). Climate change impacts on mismatches between phytoplankton blooms and fish spawning phenology. *Glob Change Biol*, gcb.14650.
- Atkinson, A., Siegel, V., Pakhomov, E. & Rothery, P. (2004). Long-term decline in krill stock and increase in salps within the Southern Ocean. *Nature*, 432, 100–103.
- Barange, M., Merino, G., Blanchard, J.L., Scholtens, J., Harle, J., Allison, E.H., *et al.* (2014). Impacts of climate change on marine ecosystem production in societies dependent on fisheries. *Nature Climate Change*, 4, 211–216.
- Barneche, D.R. & Allen, A.P. (2018). The energetics of fish growth and how it constrains food-web trophic structure. *Ecology Letters*, 21, 836–844.
- Barton, A.D., Irwin, A.J., Finkel, Z.V. & Stock, C.A. (2016). Anthropogenic climate change drives shift and shuffle in North Atlantic phytoplankton communities. *Proceedings of the National Academy of Sciences*, 113, 2964–2969.

Bibliography

- Bates, A.E., Pecl, G.T., Frusher, S., Hobday, A.J., Wernberg, T., Smale, D.A., *et al.* (2014). Defining and observing stages of climate-mediated range shifts in marine systems. *Global Environmental Change*, 26, 27–38.
- Baudron, A.R., Brunel, T., Blanchet, M., Hidalgo, M., Chust, G., Brown, E.J., *et al.* (2020). Changing fish distributions challenge the effective management of European fisheries. *Ecography*, 43, 494–505.
- Baum, J.K. & Worm, B. (2009). Cascading top-down effects of changing oceanic predator abundances. *Journal of Animal Ecology*, 78, 699–714.
- Baumann, M. (1995). A comment on transfer efficiencies. *Fisheries Oceanography*, 4, 264–266.
- Baustian, M.M., Hansen, G.J.A., de Kluijver, A., Robinson, K., Henry, E.N., Knoll, L.B., *et al.* (2014). Linking the bottom to the top in aquatic ecosystems: mechanisms and stressors of benthic-pelagic coupling. *Eco-DAS X*, 38–60.
- Beaugrand, G., Conversi, A., Atkinson, A., Cloern, J., Chiba, S., Fonda-Umani, S., *et al.* (2019). Prediction of unprecedented biological shifts in the global ocean. *Nat. Clim. Chang.*, 9, 237–243.
- Beaugrand, G., Conversi, A., Chiba, S., Edwards, M., Fonda-Umani, S., Greene, C., *et al.* (2014). Synchronous marine pelagic regime shifts in the Northern Hemisphere. *Philosophical Transactions of the Royal Society B: Biological Sciences*, 370, 20130272–20130272.
- Beaugrand, G., Edwards, M. & Legendre, L. (2010). Marine biodiversity, ecosystem functioning, and carbon cycles. *Proceedings of the National Academy of Sciences*, 107, 10120–10124.
- Beaugrand, G., Edwards, M., Raybaud, V., Goberville, E. & Kirby, R.R. (2015). Future vulnerability of marine biodiversity compared with contemporary and past changes. *Nature Climate Change*, 5, 695–701.
- Benoît, E. & Rochet, M.-J. (2004). A continuous model of biomass size spectra governed by predation and the effects of fishing on them. *Journal of Theoretical Biology*, 226, 9–21.
- Beukhof, E., Frelat, R., Pecuchet, L., Maureaud, A., Dencker, T.S., Sólmundsson, J., *et al.* (2019). Marine fish traits follow fast-slow continuum across oceans. *Sci Rep*, 9, 17878.
- Bianchi, G. (2000). Impact of fishing on size composition and diversity of demersal fish communities. *ICES Journal of Marine Science*, 57, 558–571.
- Bindoff, N.L., Cheung, W.W.L., Kairo, J.G., Guinder, V.A., Hallberg, R., Hilmi, N., *et al.* (2019). Changing Ocean, Marine Ecosystems, and Dependent Communities. In: *IPCC Special Report on the Ocean and Cryosphere in a Changing Climate*.
- Blanchard, J.L., Andersen, K.H., Scott, F., Hintzen, N.T., Piet, G. & Jennings, S. (2014). Evaluating targets and trade-offs among fisheries and conservation objectives using a multispecies size spectrum model. *Journal of Applied Ecology*, 51, 612–622.
- Blanchard, J.L., Heneghan, R.F., Everett, J.D., Trebilco, R. & Richardson, A.J. (2017). From Bacteria to Whales: Using Functional Size Spectra to Model Marine Ecosystems. *Trends in Ecology & Evolution*, 32, 174–186.
- Blanchard, J.L., Jennings, S., Holmes, R., Harle, J., Merino, G., Allen, J.I., *et al.* (2012). Potential consequences of climate change for primary production and fish production in large marine ecosystems. *Philosophical Transactions of the Royal Society B: Biological Sciences*, 367, 2979–2989.
- Blanchard, J.L., Law, R., Castle, M.D. & Jennings, S. (2011). Coupled energy pathways and the resilience of size-structured food webs. *Theor Ecol*, 4, 289–300.

Bibliography

- Block, B.A., Jonsen, I.D., Jorgensen, S.J., Winship, A.J., Shaffer, S.A., Bograd, S.J., *et al.* (2011). Tracking apex marine predator movements in a dynamic ocean. *Nature*, 475, 86–90.
- Bolker, B.M., Brooks, M.E., Clark, C.J., Geange, S.W., Poulsen, J.R., Stevens, M.H.H., *et al.* (2009). Generalized linear mixed models: a practical guide for ecology and evolution. *Trends in Ecology & Evolution*, 24, 127–135.
- Bopp, L., Resplandy, L., Orr, J.C., Doney, S.C., Dunne, J.P., Gehlen, M., *et al.* (2013). Multiple stressors of ocean ecosystems in the 21st century: projections with CMIP5 models, 21.
- Boyce, D.G., Dowd, M., Lewis, M.R. & Worm, B. (2014). Estimating global chlorophyll changes over the past century. *Progress in Oceanography*, 122, 163–173.
- Boyce, D.G., Frank, K.T., Worm, B. & Leggett, W.C. (2015). Spatial patterns and predictors of trophic control in marine ecosystems. *Ecology Letters*, 18, 1001–1011.
- Boyce, D.G., Lotze, H.K., Tittensor, D.P., Carozza, D.A. & Worm, B. (2020). Future ocean biomass losses may widen socioeconomic equity gaps. *Nat Commun*, 11, 2235.
- Branch, T.A., Jensen, O.P., Ricard, D., Ye, Y. & Hilborn, R. (2011). Contrasting Global Trends in Marine Fishery Status Obtained from Catches and from Stock Assessments: Global Trends in Marine Fishery Status. *Conservation Biology*, 25, 777–786.
- Branch, T.A., Watson, R., Fulton, E.A., Jennings, S., McGilliard, C.R., Pablico, G.T., *et al.* (2010). The trophic fingerprint of marine fisheries. *Nature*, 468, 431–435.
- Britten, G.L., Dowd, M., Minto, C., Ferretti, F., Boero, F. & Lotze, H.K. (2014). Predator decline leads to decreased stability in a coastal fish community. *Ecology Letters*, 17, 1518–1525.
- Brown, J.H., Gillooly, J.F., Allen, A.P., Savage, V.M. & West, G.B. (2004). Toward a metabolic theory of ecology. *Ecology*, 85, 1771–1789.
- Bruno, J.F., Carr, L.A. & O'Connor, M.I. (2015). Exploring the role of temperature in the ocean through metabolic scaling. *Ecology*, 96, 3126–3140.
- Bryndum-Buchholz, A., Tittensor, D.P., Blanchard, J.L., Cheung, W.W.L., Coll, M., Galbraith, E.D., *et al.* (2019). Twenty-first-century climate change impacts on marine animal biomass and ecosystem structure across ocean basins. *Global Change Biology*, 25, 459–472.
- Burrows, M.T., Schoeman, D.S., Buckley, L.B., Moore, P., Poloczanska, E.S., Brander, K.M., *et al.* (2011). The Pace of Shifting Climate in Marine and Terrestrial Ecosystems. *Science*, 334, 652–655.
- Burrows, M.T., Schoeman, D.S., Richardson, A.J., Molinos, J.G., Hoffmann, A., Buckley, L.B., *et al.* (2014). Geographical limits to species-range shifts are suggested by climate velocity. *Nature*, 507, 492–495.
- Butenschön, M., Clark, J., Aldridge, J.N., Allen, J.I., Artioli, Y., Blackford, J., *et al.* (2016). ERSEM 15.06: a generic model for marine biogeochemistry and the ecosystem dynamics of the lower trophic levels. *Geoscientific Model Development*, 9, 1293–1339.

- Cabré, A., Marinov, I. & Leung, S. (2015). Consistent global responses of marine ecosystems to future climate change across the IPCC AR5 earth system models. *Climate Dynamics*, 45, 1253–1280.
- Caddy, J.F. (1998). How Pervasive is “Fishing Down Marine Food Webs”? *Science*, 282, 1383a–11383.
- Calbet, A., Sazhin, A.F., Nejstgaard, J.C., Berger, S.A., Tait, Z.S., Olmos, L., *et al.* (2014). Future Climate Scenarios for a Coastal Productive Planktonic Food Web Resulting in Microplankton Phenology Changes and Decreased Trophic Transfer Efficiency. *PLoS ONE*, 9, e94388.

Bibliography

- Carozza, D.A., Bianchi, D. & Galbraith, E.D. (2016). The ecological module of BOATS-1.0: a bioenergetically constrained model of marine upper trophic levels suitable for studies of fisheries and ocean biogeochemistry. *Geoscientific Model Development*, 9, 1545–1565.
- Carozza, D.A., Bianchi, D. & Galbraith, E.D. (2017). Formulation, General Features and Global Calibration of a Bioenergetically-Constrained Fishery Model. *PLoS One*, 12, e0169763.
- Carstensen, J., Conley, D. & Müller-Karulis, B. (2003). Spatial and temporal resolution of carbon fluxes in a shallow coastal ecosystem, the Kattegat. *Mar. Ecol. Prog. Ser.*, 252, 35–50.
- CBD. (2010). *Biodiversity, development and poverty alleviation: recognizing the role of biodiversity for human well-being ; International Day for Biological Diversity, 22 May 2010*. Secretariat of the Convention on Biological Diversity, Montreal.
- Chassot, E., Bonhommeau, S., Dulvy, N.K., Mélin, F., Watson, R., Gascuel, D., *et al.* (2010). Global marine primary production constrains fisheries catches. *Ecology Letters*, 13, 495–505.
- Chassot, E., Rouyer, T., Trenkel, V.M. & Gascuel, D. (2008). Investigating trophic-level variability in Celtic Sea fish predators. *Journal of Fish Biology*, 73, 763–781.
- Cheung, W.W.L. (2018). The future of fishes and fisheries in the changing oceans. *Journal of Fish Biology*, 92, 790–803.
- Cheung, W.W.L., Bruggeman, J. & Butenschon, M. (2018). Projected changes in global and national potential marine fisheries catch under climate change scenarios in the twenty-first century. In: *Impacts of climate change on fisheries and aquaculture: synthesis of current knowledge, adaptation and mitigation options* (eds. Barange, M., Bahri, T., Beveridge, M.C.M., Cochrane, K., Funge-Smith, S. & Poulain, F.).
- Cheung, W.W.L., Dunne, J., Sarmiento, J.L. & Pauly, D. (2011). Integrating ecophysiology and plankton dynamics into projected maximum fisheries catch potential under climate change in the Northeast Atlantic. *ICES Journal of Marine Science*, 68, 1008–1018.
- Cheung, W.W.L. & Frölicher, T.L. (2020). Marine heatwaves exacerbate climate change impacts for fisheries in the northeast Pacific. *Sci Rep*, 10, 6678.
- Cheung, W.W.L., Frölicher, T.L., Asch, R.G., Jones, M.C., Pinsky, M.L., Reygondeau, G., *et al.* (2016). Building confidence in projections of the responses of living marine resources to climate change. *ICES Journal of Marine Science*, 73, 1283–1296.
- Cheung, W.W.L., Lam, V.W.Y., Sarmiento, J.L., Kearney, K., Watson, R. & Pauly, D. (2009). Projecting global marine biodiversity impacts under climate change scenarios. *Fish and Fisheries*, 10, 235–251.
- Cheung, W.W.L., Lam, V.W.Y., Sarmiento, J.L., Kearney, K., Watson, R., Zeller, D., *et al.* (2010). Large-scale redistribution of maximum fisheries catch potential in the global ocean under climate change: CLIMATE CHANGE IMPACTS ON CATCH POTENTIAL. *Global Change Biology*, 16, 24–35.
- Cheung, W.W.L., Sarmiento, J.L., Dunne, J., Frölicher, T.L., Lam, V.W.Y., Deng Palomares, M.L., *et al.* (2012). Shrinking of fishes exacerbates impacts of global ocean changes on marine ecosystems. *Nature Climate Change*, 3, 254–258.
- Cheung, W.W.L., Sarmiento, J.L., Frölicher, T.L., Lam, V.W.Y., Deng Palomares, M.L., Watson, R., *et al.* (2013a). Shrinking of fishes exacerbates impacts of global ocean changes on marine ecosystems. *Nature Climate Change*, 3, 254–258.
- Cheung, W.W.L., Watson, R., Morato, T., Pitcher, T. & Pauly, D. (2007). Intrinsic vulnerability in the global fish catch. *Marine Ecology Progress Series*, 333, 1–12.

Bibliography

- Cheung, W.W.L., Watson, R. & Pauly, D. (2013b). Signature of ocean warming in global fisheries catch. *Nature*, 497, 365–368.
- Christensen, V., Coll, M., Piroddi, C., Steenbeek, J., Buszowski, J. & Pauly, D. (2014). A century of fish biomass decline in the ocean. *Marine Ecology Progress Series*, 512, 155–166.
- Christensen, V. & Pauly, D. (1992). ECOPATH II — a software for balancing steady-state ecosystem models and calculating network characteristics. *Ecological Modelling*, 61, 169–185.
- Christensen, V. & Pauly, D. (1993). *Trophic models of aquatic ecosystems*. ICLARM conference proceedings. International Center for Living Aquatic Resources Management ; International Council for the Exploration of the Sea : Danish International Development Agency, Makati, Metro Manila, Philippines : Copenhagen K., Denmark.
- Chust, G., Allen, J.I., Bopp, L., Schrum, C., Holt, J., Tsiaras, K., *et al.* (2014). Biomass changes and trophic amplification of plankton in a warmer ocean. *Global Change Biology*, 20, 2124–2139.
- Coll, M., Libralato, S., Tudela, S., Palomera, I. & Pranovi, F. (2008). Ecosystem Overfishing in the Ocean. *PLoS ONE*, 3, e3881.
- Colléter, M., Gascuel, D., Ecoutin, J.-M. & Tito de Morais, L. (2012). Modelling trophic flows in ecosystems to assess the efficiency of marine protected area (MPA), a case study on the coast of Sénégal. *Ecological Modelling*, 232, 1–13.
- Colléter, M., Valls, A., Guitton, J., Lyne, M., Sánchez, F.A.-, Christensen, V., *et al.* (2013). EcoBase: a repository solution to gather and communicate information from EwE models, 69.
- Conover, D.O. & Munch, S.B. (2002). Sustaining Fisheries Yields Over Evolutionary Time Scales. *Science*, 297, 94–96.
- Copernicus Climate Change Service. (2020). Marine biogeochemistry data for the Northwestern European shelf and Mediterranean sea from 2006 up to 2100 derived from climate projections.
- Cortes, E. (1999). Standardized diet compositions and trophic levels of sharks. *ICES Journal of Marine Science*, 56, 707–717.
- Costello, C., Ovando, D., Clavelle, T., Strauss, C.K., Hilborn, R., Melnychuk, M.C., *et al.* (2016). Global fishery prospects under contrasting management regimes. *Proceedings of the National Academy of Sciences*, 113, 5125–5129.
- Cresson, P., Chouvelon, T., Bustamante, P., Bănar, D., Baudrier, J., Le Loc'h, F., *et al.* (2020). Primary production and depth drive different trophic structure and functioning of fish assemblages in French marine ecosystems. *Progress in Oceanography*, 102343.
- Cripps, G., Flynn, K.J. & Lindeque, P.K. (2016). Ocean Acidification Affects the Phyto-Zoo Plankton Trophic Transfer Efficiency. *PLoS One*, 11, e0151739.
- Cury, P.M., Boyd, I.L., Bonhommeau, S., Anker-Nilssen, T., Crawford, R.J.M., Furness, R.W., *et al.* (2011). Global Seabird Response to Forage Fish Depletion--One-Third for the Birds. *Science*, 334, 1703–1706.
- Cushing, D.H. (1969). The Regularity of the Spawning Season of Some Fishes. *ICES Journal of Marine Science*, 33, 81–92.
- Cushing, D.H. (1990). Plankton Production and Year-class Strength in Fish Populations: an Update of the Match/Mismatch Hypothesis. In: *Advances in Marine Biology* (eds. Blaxter, J.H.S. & Southward, A.J.). Academic Press, pp. 249–293.

- Day, L., Kopp, D., Robert, M. & Le Bris, H. (2019). Trophic ecology of large gadiforms in the food web of a continental shelf ecosystem. *Progress in Oceanography*, 175, 105–114.
- van Denderen, P.D., Lindegren, M., MacKenzie, B.R., Watson, R.A. & Andersen, K.H. (2018). Global patterns in marine predatory fish. *Nature Ecology & Evolution*, 2, 65–70.
- Deutsch, C., Ferrel, A., Seibel, B., Pörtner, H.O. & Huey, R.B. (2015). Climate change tightens a metabolic constraint on marine habitats. *Science*, 348, 1132–1135.
- Devine, J.A., Baker, K.D. & Haedrich, R.L. (2006). Deep-sea fishes qualify as endangered: Fisheries. *Nature*, 439, 29–29.
- Duffill Telsnig, J.I., Jennings, S., Mill, A.C., Walker, N.D., Parnell, A.C. & Polunin, N.V.C. (2018). Estimating contributions of pelagic and benthic pathways to consumer production in coupled marine food webs. *J Anim Ecol*, 1365-2656.12929.
- Dufour, F., Arrizabalaga, H., Irigoien, X. & Santiago, J. (2010). Climate impacts on albacore and bluefin tunas migrations phenology and spatial distribution. *Progress in Oceanography*, 86, 283–290.
- Dufresne, J.-L., Foujols, M.-A., Denvil, S., Caubel, A., Marti, O., Aumont, O., *et al.* (2013). Climate change projections using the IPSL-CM5 Earth System Model: from CMIP3 to CMIP5. *Climate Dynamics*, 40, 2123–2165.
- Dulvy, N.K., Rogers, S.I., Jennings, S., Stelzenmiller, V., Dye, S.R. & Skjoldal, H.R. (2008). Climate change and deepening of the North Sea fish assemblage: a biotic indicator of warming seas. *Journal of Applied Ecology*, 45, 1029–1039.
- Dunne, J.P., Armstrong, R.A., Gnanadesikan, A. & Sarmiento, J.L. (2005). Empirical and mechanistic models for the particle export ratio: MODELING THE PARTICLE EXPORT RATIO. *Global Biogeochem. Cycles*, 19, n/a-n/a.
- Dunne, J.P., John, J.G., Adcroft, A.J., Griffies, S.M., Hallberg, R.W., Shevliakova, E., *et al.* (2012). GFDL's ESM2 Global Coupled Climate–Carbon Earth System Models. Part I: Physical Formulation and Baseline Simulation Characteristics. *Journal of Climate*, 25, 6646–6665.
- Eddy, T.D., Bernhardt, J.R., Blanchard, J.L., Cheung, W.W.L., Colléter, M., du Pontavice, H., *et al.* (2021). Energy Flow Through Marine Ecosystems: Confronting Transfer Efficiency. *Trends in Ecology & Evolution*, 36, 76–86.
- Edeline, E., Carlson, S.M., Stige, L.C., Winfield, I.J., Fletcher, J.M., James, J.B., *et al.* (2007). Trait changes in a harvested population are driven by a dynamic tug-of-war between natural and harvest selection. *Proceedings of the National Academy of Sciences*, 104, 15799–15804.
- Edwards, M. & Richardson, A.J. (2004). Impact of climate change on marine pelagic phenology and trophic mismatch. *Nature*, 430, 881–884.
- Elton, C.S. (1927). *Animal ecology, by Charles Elton; with an introduction by Julian S. Huxley*. Macmillan Co., New York,.
- Enberg, K., Jørgensen, C., Dunlop, E.S., Varpe, Ø., Boukal, D.S., Baulier, L., *et al.* (2012). Fishing-induced evolution of growth: concepts, mechanisms and the empirical evidence: Fishing-induced evolution of growth. *Marine Ecology*, 33, 1–25.

Bibliography

- Engelhard, G.H., Peck, M.A., Rindorf, A., C. Smout, S., van Deurs, M., Raab, K., *et al.* (2014a). Forage fish, their fisheries, and their predators: who drives whom? *ICES Journal of Marine Science*, 71, 90–104.
- Engelhard, G.H., Righton, D.A. & Pinnegar, J.K. (2014b). Climate change and fishing: a century of shifting distribution in North Sea cod. *Glob Change Biol*, 20, 2473–2483.
- Essington, T.E., Beaudreau, A.H. & Wiedenmann, J. (2006). Fishing through marine food webs. *Proceedings of the National Academy of Sciences*, 103, 3171–3175.
- Estes, J.A., Heithaus, M., McCauley, D.J., Rasher, D.B. & Worm, B. (2016). Megafaunal Impacts on Structure and Function of Ocean Ecosystems. *Annual Review of Environment and Resources*, 41, 83–116.
- Estes, J.A., Terborgh, J., Brashares, J.S., Power, M.E., Berger, J., Bond, W.J., *et al.* (2011). Trophic Downgrading of Planet Earth. *Science*, 333, 301–306.
- FAO (Ed.). (2018). *Meeting the sustainable development goals*. The state of world fisheries and aquaculture. Rome.
- Fernandes, J.A., Cheung, W.W.L., Jennings, S., Butenschön, M., de Mora, L., Frölicher, T.L., *et al.* (2013). Modelling the effects of climate change on the distribution and production of marine fishes: accounting for trophic interactions in a dynamic bioclimate envelope model. *Glob Change Biol*, 19, 2596–2607.
- Ferreira, A., Stige, L., Neuheimer, A., Bogstad, B., Yaragina, N., Prokopchuk, I., *et al.* (2020). Match-mismatch dynamics in the Norwegian-Barents Sea system. *Mar. Ecol. Prog. Ser.*, LFC, 1–14.
- Ferretti, F., Worm, B., Britten, G.L., Heithaus, M.R. & Lotze, H.K. (2010). Patterns and ecosystem consequences of shark declines in the ocean: Ecosystem consequences of shark declines. *Ecology Letters*, no-no.
- Fossheim, M., Primicerio, R., Johannesen, E., Ingvaldsen, R.B., Aschan, M.M. & Dolgov, A.V. (2015). Recent warming leads to a rapid borealization of fish communities in the Arctic. *Nature Climate Change*, 5, 673–677.
- Frainer, A., Primicerio, R., Kortsch, S., Aune, M., Dolgov, A.V., Fossheim, M., *et al.* (2017). Climate-driven changes in functional biogeography of Arctic marine fish communities. *Proc Natl Acad Sci USA*, 114, 12202–12207.
- Frank, K.T. (2005). Trophic Cascades in a Formerly Cod-Dominated Ecosystem. *Science*, 308, 1621–1623.
- Friedland, K.D., Stock, C.A., Drinkwater, K.F., Link, J.S., Leaf, R.T., Shank, B.V., *et al.* (2012). Pathways between Primary Production and Fisheries Yields of Large Marine Ecosystems. *PLoS ONE*, 7, e28945.
- Froese, R. & Pauly, D. (Eds.). (2000). *FishBase 2000: concepts, design and data sources*. ICLARM Contribution. ICLARM, Makati City, Philippines.
- Froese, R. & Pauly, D. (2020). FishBase - World Wide Web electronic publication - www.fishbase.org (03/2020).
- Frölicher, T.L., Fischer, E.M. & Gruber, N. (2018). Marine heatwaves under global warming. *Nature*, 560, 360–364.

Bibliography

- Frölicher, T.L., Rodgers, K.B., Stock, C.A. & Cheung, W.W.L. (2016). Sources of uncertainties in 21st century projections of potential ocean ecosystem stressors: UNCERTAINTIES IN STRESSOR PROJECTIONS. *Global Biogeochemical Cycles*, 30, 1224–1243.
- Fulton, E.A., Fuller, M., Smith, A.D.M. & Punt, A. (2004). Ecological indicators of the ecosystem effects of fishing: final report.
- Fulton, E.A., Link, J.S., Kaplan, I.C., Savina-Rolland, M., Johnson, P., Ainsworth, C., *et al.* (2011). Lessons in modelling and management of marine ecosystems: the Atlantis experience: Lessons learnt with Atlantis. *Fish and Fisheries*, 12, 171–188.

- Galbraith, E.D., Carozza, D.A. & Bianchi, D. (2017). A coupled human-Earth model perspective on long-term trends in the global marine fishery. *Nat Commun*, 8, 14884.
- García Molinos, J., Halpern, B.S., Schoeman, D.S., Brown, C.J., Kiessling, W., Moore, P.J., *et al.* (2016). Climate velocity and the future global redistribution of marine biodiversity. *Nature Climate Change*, 6, 83–88.
- Gasche, L. & Gascuel, D. (2013). EcoTroph: a simple model to assess fishery interactions and their impacts on ecosystems. *ICES Journal of Marine Science*, 70, 498–510.
- Gasche, L., Gascuel, D., Shannon, L. & Shin, Y.-J. (2012). Global assessment of the fishing impacts on the Southern Benguela ecosystem using an EcoTroph modelling approach. *Journal of Marine Systems*, 90, 1–12.
- Gascuel, D. (2005). The trophic-level based model: A theoretical approach of fishing effects on marine ecosystems. *Ecological Modelling*, 189, 315–332.
- Gascuel, D., Bozec, Y., Chassot, E., Colomb, A. & Laurans, M. (2005). The trophic spectrum: theory and application as an ecosystem indicator. *ICES Journal of Marine Science*, 62, 443–452.
- Gascuel, D., Coll, M., Fox, C., Guénette, S., Guitton, J., Kenny, A., *et al.* (2016). Fishing impact and environmental status in European seas: a diagnosis from stock assessments and ecosystem indicators. *Fish and Fisheries*, 17, 31–55.
- Gascuel, D., Guenette, S. & Pauly, D. (2011). The trophic-level-based ecosystem modelling approach: theoretical overview and practical uses. *ICES Journal of Marine Science*, 68, 1403–1416.
- Gascuel, D., Morissette, L., Palomares, M.L.D. & Christensen, V. (2008). Trophic flow kinetics in marine ecosystems: Toward a theoretical approach to ecosystem functioning. *Ecological Modelling*, 217, 33–47.
- Gascuel, D. & Pauly, D. (2009). EcoTroph: Modelling marine ecosystem functioning and impact of fishing. *Ecological Modelling*, 220, 2885–2898.
- Gattuso, J.-P., Magnan, A., Bille, R., Cheung, W.W.L., Howes, E.L., Joos, F., *et al.* (2015). Contrasting futures for ocean and society from different anthropogenic CO₂ emissions scenarios. *Science*, 349, aac4722–aac4722.
- Genner, M.J., Sims, D.W., Southward, A.J., Budd, G.C., Masterson, P., Mchugh, M., *et al.* (2010). Body size-dependent responses of a marine fish assemblage to climate change and fishing over a century-long scale. *Global Change Biology*, 16, 517–527.
- Gillooly, J.F., Brown, J.H., West, G.B., Savage, V.M. & Charnov, E.L. (2001). Effects of Size and Temperature on Metabolic Rate. *Science*, 293, 2248–2251.
- Giorgetta, M.A., Jungclaus, J., Reick, C.H., Legutke, S., Bader, J., Böttinger, M., *et al.* (2013). Climate and carbon cycle changes from 1850 to 2100 in MPI-ESM simulations for the Coupled Model

Bibliography

- Intercomparison Project phase 5: Climate Changes in MPI-ESM. *Journal of Advances in Modeling Earth Systems*, 5, 572–597.
- Giraldo, C., Ernande, B., Cresson, P., Kopp, D., Cachera, M., Travers-Trolet, M., *et al.* (2017). Depth gradient in the resource use of a fish community from a semi-enclosed sea: Benthic-pelagic coupling in fish diet. *Limnol. Oceanogr.*, 62, 2213–2226.
- Golden, C.D., Allison, E.H., Cheung, W.W.L., Dey, M.M., Halpern, B.S., McCauley, D.J., *et al.* (2016). Nutrition: Fall in fish catch threatens human health. *Nature*, 534, 317–320.
- Gregg, W.W. & Rousseaux, C.S. (2014). Decadal trends in global pelagic ocean chlorophyll: A new assessment integrating multiple satellites, in situ data, and models. *Journal of Geophysical Research: Oceans*, 119, 5921–5933.
- Halouani, G., Gascuel, D., Hattab, T., Lasram, F.B.R., Coll, M., Tsagarakis, K., *et al.* (2015). Fishing impact in Mediterranean ecosystems: an EcoTroph modeling approach. *Journal of Marine Systems*, 150, 22–33.
- Halpern, B.S., Frazier, M., Potapenko, J., Casey, K.S., Koenig, K., Longo, C., *et al.* (2015). Spatial and temporal changes in cumulative human impacts on the world's ocean. *Nature Communications*, 6.
- Hátún, H., Payne, M.R. & Jacobsen, J.A. (2009). The North Atlantic subpolar gyre regulates the spawning distribution of blue whiting (*Micromesistius poutassou*). *Can. J. Fish. Aquat. Sci.*, 66, 759–770.
- Heilmayer, O., Brey, T. & Pörtner, H.O. (2004). Growth efficiency and temperature in scallops: a comparative analysis of species adapted to different temperatures. *Functional Ecology*, 18, 641–647.
- Heithaus, M.R., Frid, A., Wirsing, A.J. & Worm, B. (2008). Predicting ecological consequences of marine top predator declines. *Trends in Ecology & Evolution*, 23, 202–210.
- Heneghan, R.F., Everett, J.D., Blanchard, J.L. & Richardson, A.J. (2016). Zooplankton Are Not Fish: Improving Zooplankton Realism in Size-Spectrum Models Mediates Energy Transfer in Food Webs. *Frontiers in Marine Science*, 3.
- Hervann, P.-Y. & Gascuel, D. (2020). Exploring the impacts of fishing and environment on the Celtic Sea ecosystem since 1950. *Fisheries Research*, 225, 105472.
- Hidalgo, M., Rouyer, T., Molinero, J., Massutí, E., Moranta, J., Guijarro, B., *et al.* (2011). Synergistic effects of fishing-induced demographic changes and climate variation on fish population dynamics. *Marine Ecology Progress Series*, 426, 1–12.
- Hilborn, R., Amoroso, R.O., Anderson, C.M., Baum, J.K., Branch, T.A., Costello, C., *et al.* (2020). Effective fisheries management instrumental in improving fish stock status. *Proc Natl Acad Sci USA*, 117, 2218–2224.
- Hilborn, R., Amoroso, R.O., Bogazzi, E., Jensen, O.P., Parma, A.M., Szuwalski, C., *et al.* (2017). When does fishing forage species affect their predators? *Fisheries Research*, 191, 211–221.
- Hoegh-Guldberg, O., Jacob, D., Taylor, M., Bindi, M., Brown, S., Camilloni, I., *et al.* (2018). Impacts of 1.5°C of Global Warming on Natural and Human Systems, 138.
- ter Hofstede, R., Hiddink, J. & Rijnsdorp, A. (2010). Regional warming changes fish species richness in the eastern North Atlantic Ocean. *Mar. Ecol. Prog. Ser.*, 414, 1–9.

Bibliography

- Horta e Costa, B., Assis, J., Franco, G., Erzini, K., Henriques, M., Gonçalves, E., *et al.* (2014). Tropicalization of fish assemblages in temperate biogeographic transition zones. *Mar. Ecol. Prog. Ser.*, 504, 241–252.
- Hughes, K.M., Dransfeld, L. & Johnson, M.P. (2014). Changes in the spatial distribution of spawning activity by north-east Atlantic mackerel in warming seas: 1977–2010. *Marine Biology*, 161, 2563–2576.
- Hutchings, J.A. (2005). Life history consequences of overexploitation to population recovery in Northwest Atlantic cod (*Gadus morhua*). *Canadian Journal of Fisheries and Aquatic Sciences*, 62, 824–832.
- ICES. (2020). Official Nominal Catches 2006-2017. Version 01-08-2020. Accessed 01-08-2020 via <http://ices.dk/marine-data/dataset-collections/Pages/Fish-catch-and-stock-assessment.aspx>.
- IPBES. (2019). *Summary for policymakers of the global assessment report on biodiversity and ecosystem services*. Zenodo.
- IPCC. (2014). *Climate Change 2014: Synthesis Report. Contribution of Working Groups I, II and III to the Fifth Assessment Report of the Intergovernmental Panel on Climate Change*. IPCC, Geneva, Switzerland.
- IPCC. (2019a). *IPCC Special Report on the Ocean and Cryosphere in a Changing Climate*. In press.
- IPCC. (2019b). Summary for Policymakers. In: *IPCC Special Report on the Ocean and Cryosphere in a Changing Climate* (eds. Pörtner, H.-O., Robert, D.C., Masson-Delmotte, V., Zhai, P., Poloczanska, E., Mintenbeck, K., *et al.*).
- Irigoiien, X., Klevjer, T.A., Røstad, A., Martinez, U., Boyra, G., Acuña, J.L., *et al.* (2014). Large mesopelagic fishes biomass and trophic efficiency in the open ocean. *Nature Communications*, 5.
- Irwin, A.J., Finkel, Z.V., Schofield, O.M.E. & Falkowski, P.G. (2006). Scaling-up from nutrient physiology to the size-structure of phytoplankton communities. *Journal of Plankton Research*, 28, 459–471.
- Jennings, S. & Collingridge, K. (2015). Predicting Consumer Biomass, Size-Structure, Production, Catch Potential, Responses to Fishing and Associated Uncertainties in the World's Marine Ecosystems. *PLOS ONE*, 10, e0133794.
- Jennings, S., Greenstreet, Simon.P.R. & Reynolds, John.D. (1999). Structural change in an exploited fish community: a consequence of differential fishing effects on species with contrasting life histories. *Journal of Animal Ecology*, 68, 617–627.
- Jennings, S., Melin, F., Blanchard, J.L., Forster, R.M., Dulvy, N.K. & Wilson, R.W. (2008). Global-scale predictions of community and ecosystem properties from simple ecological theory. *Proceedings of the Royal Society B: Biological Sciences*, 275, 1375–1383.
- Jennings, S., Warr, K.J. & Mackinson, S. (2002). Use of size-based production and stable isotope analyses to predict trophic transfer efficiencies and predator-prey body mass ratios in food webs. *Marine Ecology Progress Series*, 240, 11–20.
- Jones, M.C. & Cheung, W.W.L. (2015). Multi-model ensemble projections of climate change effects on global marine biodiversity. *ICES Journal of Marine Science*, 72, 741–752.

Bibliography

Jørgensen, C., Ernande, B. & Fiksen, Ø. (2009). ORIGINAL ARTICLE: Size-selective fishing gear and life history evolution in the Northeast Arctic cod: Size-selective fishing and life history evolution. *Evolutionary Applications*, 2, 356–370.

Juan-Jordá, M.J., Mosqueira, I., Freire, J. & Dulvy, N.K. (2013). Life in 3-D: life history strategies in tunas, mackerels and bonitos. *Rev Fish Biol Fisheries*, 23, 135–155.

Kaplan, I.C., Brown, C.J., Fulton, E.A., Gray, I.A., Field, J.C. & Smith, A.D.M. (2013). Impacts of depleting forage species in the California Current. *Environmental Conservation*, 40, 380–393.

Kirby, R.R. & Beaugrand, G. (2009). Trophic amplification of climate warming. *Proceedings of the Royal Society B: Biological Sciences*, 276, 4095–4103.

Kirby, R.R., Beaugrand, G. & Lindley, J.A. (2009). Synergistic Effects of Climate and Fishing in a Marine Ecosystem. *Ecosystems*, 12, 548–561.

Kopp, D., Lefebvre, S., Cachera, M., Villanueva, M.C. & Ernande, B. (2015). Reorganization of a marine trophic network along an inshore–offshore gradient due to stronger pelagic–benthic coupling in coastal areas. *Progress in Oceanography*, 130, 157–171.

Kortsch, S., Primicerio, R., Aschan, M., Lind, S., Dolgov, A.V. & Planque, B. (2018). Food-web structure varies along environmental gradients in a high-latitude marine ecosystem. *Ecography*.

Kortsch, S., Primicerio, R., Fossheim, M., Dolgov, A.V. & Aschan, M. (2015). Climate change alters the structure of arctic marine food webs due to poleward shifts of boreal generalists. *Proceedings of the Royal Society B: Biological Sciences*, 282, 20151546.

Kroeker, K.J., Kordas, R.L., Crim, R., Hendriks, I.E., Ramajo, L., Singh, G.S., *et al.* (2013). Impacts of ocean acidification on marine organisms: quantifying sensitivities and interaction with warming. *Global Change Biology*, 19, 1884–1896.

Kwiatkowski, L., Aumont, O. & Bopp, L. (2019). Consistent trophic amplification of marine biomass declines under climate change. *Global Change Biology*, 25, 218–229.

Kwiatkowski, L., Bopp, L., Aumont, O., Ciais, P., Cox, P.M., Laufkötter, C., *et al.* (2017). Emergent constraints on projections of declining primary production in the tropical oceans. *Nature Climate Change*, 7, 355–358.

Laufkötter, C., Vogt, M., Gruber, N., Aita-Noguchi, M., Aumont, O., Bopp, L., *et al.* (2015). Drivers and uncertainties of future global marine primary production in marine ecosystem models. *Biogeosciences*, 12, 6955–6984.

Laurent, A.G. (1963). The Lognormal Distribution and the Translation Method: Description and Estimation Problems. *Journal of the American Statistical Association*, 58, 231–235.

Law, R. (2000). Fishing, selection, and phenotypic evolution. *ICES Journal of Marine Science*, 57, 659–668.

Li, L., Hollowed, A.B., Cokelet, E.D., Barbeaux, S.J., Bond, N.A., Keller, A.A., *et al.* (2019). Subregional differences in groundfish distributional responses to anomalous ocean bottom temperatures in the northeast Pacific. *Glob Change Biol*, 25, 2560–2575.

Libralato, S., Coll, M., Tudela, S., Palomera, I. & Pranovi, F. (2008). Novel index for quantification of ecosystem effects of fishing as removal of secondary production. *Marine Ecology Progress Series*, 355, 107–129.

Bibliography

- Lindeman, R.L. (1942). The Trophic-Dynamic Aspect of Ecology. *Ecology*, 23, 399–417.
- Lindley, J.A., Beaugrand, G., Luczak, C., Dewarumez, J.-M. & Kirby, R.R. (2010). Warm-water decapods and the trophic amplification of climate in the North Sea. *Biol. Lett.*, 6, 773–776.
- Link, J.S. & Watson, R.A. (2019). Global ecosystem overfishing: Clear delineation within real limits to production. *Sci. Adv.*, 5, eaav0474.
- Longhurst, A.R. (2007). *Ecological geography of the sea*. 2nd ed. Academic Press, Amsterdam ; Boston, MA.
- Lotze, H.K., Tittensor, D.P., Bryndum-Buchholz, A., Eddy, T.D., Cheung, W.W.L., Galbraith, E.D., *et al.* (2019). Global ensemble projections reveal trophic amplification of ocean biomass declines with climate change. *Proceedings of the National Academy of Sciences*, 116, 12907–12912.

- M**acer, C.T. (1977). Some aspects of the biology of the horse mackerel [*Trachurus trachurus* (L.)] in waters around Britain. *J Fish Biology*, 10, 51–62.
- Maureaud, A., Gascuel, D., Colléter, M., Palomares, M.L.D., Du Pontavice, H., Pauly, D., *et al.* (2017). Global change in the trophic functioning of marine food webs. *PLOS ONE*, 12, e0182826.
- Maury, O. (2010). An overview of APECOSM, a spatialized mass balanced “Apex Predators ECOSystem Model” to study physiologically structured tuna population dynamics in their ecosystem. *Progress in Oceanography*, 84, 113–117.
- McCauley, D.J., Pinsky, M.L., Palumbi, S.R., Estes, J.A., Joyce, F.H. & Warner, R.R. (2015). Marine defaunation: Animal loss in the global ocean. *Science*, 347, 1255641–1255641.
- Michel, C., Bluhm, B., Gallucci, V., Gaston, A.J., Gordillo, F.J.L., Gradinger, R., *et al.* (2012). Biodiversity of Arctic marine ecosystems and responses to climate change. *Biodiversity*, 13, 200–214.
- Montero-Serra, I., Edwards, M. & Genner, M.J. (2015). Warming shelf seas drive the subtropicalization of European pelagic fish communities. *Global Change Biology*, 21, 144–153.
- Morán, X.A.G., López-Urrutia, Á., Calvo-Díaz, A. & Li, W.K.W. (2010). Increasing importance of small phytoplankton in a warmer ocean. *Global Change Biology*, 16, 1137–1144.
- Moullec, F., Gascuel, D., Bentorcha, K., Guénette, S. & Robert, M. (2017). Trophic models: What do we learn about Celtic Sea and Bay of Biscay ecosystems? *Journal of Marine Systems*, 172, 104–117.
- Murphy, E.J., Cavanagh, R.D., Drinkwater, K.F., Grant, S.M., Heymans, J.J., Hofmann, E.E., *et al.* (2016). Understanding the structure and functioning of polar pelagic ecosystems to predict the impacts of change. *Proceedings of the Royal Society B: Biological Sciences*, 283, 20161646.
- Myers, R.A. & Worm, B. (2003). Rapid worldwide depletion of predatory fish communities. *Nature*, 423, 280–283.

- N**agelkerken, I. & Connell, S.D. (2015). Global alteration of ocean ecosystem functioning due to increasing human CO₂ emissions. *Proceedings of the National Academy of Sciences*, 112, 13272–13277.
- Niquil, N., Baeta, A., Marques, J., Chaalali, A., Lobry, J. & Patrício, J. (2014). Reaction of an estuarine food web to disturbance: Lindeman’s perspective. *Marine Ecology Progress Series*, 512, 141–154.

- O**dum, E.P. (1969). The Strategy of Ecosystem Development. *Science*, 164, 262–270.
- Odum, E.P. (1985). Trends Expected in Stressed Ecosystems. *BioScience*, 35, 419–422.

Bibliography

- Odum, W. & Heald, E. (1975). The detritus-based food web of an estuarine mangrove community. In: *Estuarine research*. Cronin LE, New York, NY, p. 265–286.
- Oliver, E.C.J., Donat, M.G., Burrows, M.T., Moore, P.J., Smale, D.A., Alexander, L.V., *et al.* (2018). Longer and more frequent marine heatwaves over the past century. *Nat Commun*, 9, 1324.
- Olmos, M., Payne, M.R., Nevoux, M., Prévost, E., Chaput, G., Du Pontavice, H., *et al.* (2020). Spatial synchrony in the response of a long range migratory species (*Salmo salar*) to climate change in the North Atlantic Ocean. *Glob Change Biol*, 26, 1319–1337.
- Olsen, E.M., Heino, M., Lilly, G.R., Morgan, M.J., Brattey, J., Ernande, B., *et al.* (2004). Maturation trends indicative of rapid evolution preceded the collapse of northern cod. *Nature*, 428, 932–935.
- P**alomares, M.L.D. & Pauly, D. (1998). Predicting food consumption of fish populations as functions of mortality, food type, morphometrics, temperature and salinity. *Marine and Freshwater Research*, 49, 447.
- Palomares, M.L.D. & Pauly, D. (2020). SeaLifeBase - World Wide Web electronic publication - www.sealifebase.org version (03/2020).
- Pauly, D. (1998a). Fishing Down Marine Food Webs. *Science*, 279, 860–863.
- Pauly, D. (1998b). Fishing Down Marine Food Webs. *Science*, 279, 860–863.
- Pauly, D. & Cheung, W.W.L. (2017). Sound physiological knowledge and principles in modeling shrinking of fishes under climate change. *Global Change Biology*.
- Pauly, D. & Christensen, V. (1995). Primary production required to sustain global fisheries. *Nature*, 374, 255–257.
- Pauly, D., Hilborn, R. & Branch, T.A. (2013). Fisheries: does catch reflect abundance? *Nature*, 494, 303.
- Pauly, D. & Zeller, D. (2016). Catch reconstructions reveal that global marine fisheries catches are higher than reported and declining. *Nature Communications*, 7.
- Peck, L.S. (2016). A Cold Limit to Adaptation in the Sea. *Trends in Ecology & Evolution*, 31, 13–26.
- Peck, L.S., Webb, K.E. & Bailey, D.M. (2004). Extreme sensitivity of biological function to temperature in Antarctic marine species. *Functional Ecology*, 18, 625–630.
- Peck, M.A., Catalán, I.A., Damalas, Elliott, M., Ferreira, J.G., Hamon, K.G., *et al.* (2020). *Climate change and European Fisheries and Aquaculture: “CERES” Project Synthesis Report*. Universität Hamburg.
- Pecl, G.T., Araújo, M.B., Bell, J.D., Blanchard, J., Bonebrake, T.C., Chen, I.-C., *et al.* (2017). Biodiversity redistribution under climate change: Impacts on ecosystems and human well-being. *Science*, 355, eaai9214.
- Pereira, H.M., Leadley, P.W., Proença, V., Alkemade, R., Scharlemann, J.P.W., Fernandez-Manjarrés, J.F., *et al.* (2010). Scenarios for Global Biodiversity in the 21st Century. *Science*, 330, 1496–1501.
- Perry, A.L. (2005). Climate Change and Distribution Shifts in Marine Fishes. *Science*, 308, 1912–1915.
- Perry, R.I., Cury, P., Brander, K., Jennings, S., Möllmann, C. & Planque, B. (2010). Sensitivity of marine systems to climate and fishing: Concepts, issues and management responses. *Journal of Marine Systems*, 79, 427–435.
- Pershing, A., Dayton, A., Franklin, B. & Kennedy, B. (2018). Evidence for Adaptation from the 2016 Marine Heatwave in the Northwest Atlantic Ocean. *Oceanog*, 31.

Bibliography

- Petrik, C.M., Stock, C.A., Andersen, K.H., van Denderen, P.D. & Watson, J.R. (2019). Bottom-up drivers of global patterns of demersal, forage, and pelagic fishes. *Progress in Oceanography*, 176, 102124.
- Petrik, C.M., Stock, C.A., Andersen, K.H., van Denderen, P.D. & Watson, J.R. (2020). Large Pelagic Fish Are Most Sensitive to Climate Change Despite Pelagification of Ocean Food Webs. *Front. Mar. Sci.*, 7, 588482.
- Pikitch, E.K., Rountos, K.J., Essington, T.E., Santora, C., Pauly, D., Watson, R., *et al.* (2014). The global contribution of forage fish to marine fisheries and ecosystems. *Fish and Fisheries*, 15, 43–64.
- Pinsky, M.L., Selden, R.L. & Kitchel, Z.J. (2020). Climate-Driven Shifts in Marine Species Ranges: Scaling from Organisms to Communities. *Annual Review of Marine Science*, 12.
- Pinsky, M.L., Worm, B., Fogarty, M.J., Sarmiento, J.L. & Levin, S.A. (2013). Marine Taxa Track Local Climate Velocities. *Science*, 341, 1239–1242.
- Plagányi, É.E. (2007). *Models for an ecosystem approach to fisheries*. FAO fisheries technical paper. Food and Agriculture Organization of the United Nations, Rome.
- Planque, B., Fromentin, J.-M., Cury, P., Drinkwater, K.F., Jennings, S., Perry, R.I., *et al.* (2010). How does fishing alter marine populations and ecosystems sensitivity to climate? *Journal of Marine Systems*, 79, 403–417.
- Poloczanska, E.S., Brown, C.J., Sydeman, W.J., Kiessling, W., Schoeman, D.S., Moore, P.J., *et al.* (2013). Global imprint of climate change on marine life. *Nature Climate Change*, 3, 919–925.
- Poloczanska, E.S., Burrows, M.T., Brown, C.J., García Molinos, J., Halpern, B.S., Hoegh-Guldberg, O., *et al.* (2016). Responses of Marine Organisms to Climate Change across Oceans. *Frontiers in Marine Science*, 3.
- Pomeroy, L., leB. Williams, P., Azam, F. & Hobbie, J. (2007). The Microbial Loop. *Oceanog.*, 20, 28–33.
- du Pontavice, H. (2019). Changing biomass flows in marine ecosystems: from the past to the future. In: *Predicting Future Oceans*. Elsevier, pp. 121–128.
- du Pontavice, H., Gascuel, D., Reygondeau, G., Maureaud, A. & Cheung, W.W.L. (2019). Climate change undermines the global functioning of marine food webs. *Glob Change Biol*, gcb.14944.
- Pontavice, H., Gascuel, D., Reygondeau, G., Stock, C. & Cheung, W.W.L. (2021). Climate-induced decrease in biomass flow in marine food webs may severely affect predators and ecosystem production. *Glob Change Biol*, gcb.15576.
- Pörtner, H.O., Bock, C. & Mark, F.C. (2017). Oxygen- and capacity-limited thermal tolerance: bridging ecology and physiology. *The Journal of Experimental Biology*, 220, 2685–2696.
- Pörtner, H.O. & Farrell, A.P. (2008). ECOLOGY: Physiology and Climate Change. *Science*, 322, 690–692.
- Pörtner, H.O., Karl, D.M., Boyd, P.W., Cheung, W.W.L., Lluch-Cota, S.E., Nojiri, Y., *et al.* (2014). Ocean Systems. In: *Climate Change 2014: Impacts, Adaptation, and Vulnerability. Part A: Global and Sectoral Aspects. Contribution of Working Group II to the Fifth Assessment Report of the Intergovernmental Panel on Climate Change*. [Field, C.B., V.R. Barros, D.J. Dokken, K.J. Mach, M.D. Mastrandrea, T.E. Bilir, M. Chatterjee, K.L. Ebi, Y.O. Estrada, R.C. Genova, B. Girma, E.S. Kissel, A.N. Levy, S. MacCracken, P.R. Mastrandrea, and L.L. White (eds.)]. Cambridge University Press, Cambridge, United Kingdom and New York, NY, USA, pp. 411–484.
- Pörtner, H.O., Peck, L.S. & Somero, G.N. (2012). Mechanisms Defining Thermal Limits and Adaptation in Marine Ectotherms: An Integrative View. In: *Antarctic Ecosystems* (eds. Rogers, A.D., Johnston, N.M., Murphy, E.J. & Clarke, A.). John Wiley & Sons, Ltd, Chichester, UK, pp. 379–416.

Bibliography

- Pörtner, H.O. & Peck, M.A. (2010). Climate change effects on fishes and fisheries: towards a cause-and-effect understanding. *Journal of Fish Biology*, 77, 1745–1779.
- Pörtner, H.O., Storch, D. & Heilmayer, O. (2005). Constraints and trade-offs in climate-dependent adaptation: energy budgets and growth in a latitudinal cline. *Scientia Marina*, 16.
- Post, D.M. (2002). The long and short of food-chain length. *Trends in Ecology & Evolution*, 17, 269–277.
- Poulard, J. & Blanchard, F. (2005). The impact of climate change on the fish community structure of the eastern continental shelf of the Bay of Biscay. *ICES Journal of Marine Science*, 62, 1436–1443.

- R** Core Team. (2020). R: A language and environment for statistical computing. R Foundation for Statistical Computing, Vienna, Austria.
- Rasher, D.B., Steneck, R.S., Halfar, J., Kroeker, K.J., Ries, J.B., Tinker, M.T., *et al.* (2020). Keystone predators govern the pathway and pace of climate impacts in a subarctic marine ecosystem. *Science*, 369, 1351–1354.
- Reed, D., Washburn, L., Rassweiler, A., Miller, R., Bell, T. & Harrer, S. (2016). Extreme warming challenges sentinel status of kelp forests as indicators of climate change. *Nat Commun*, 7, 13757.
- Reed, J., Shannon, L., Velez, L., Akoglu, E., Bundy, A., Coll, M., *et al.* (2017). Ecosystem indicators—accounting for variability in species’ trophic levels. *ICES Journal of Marine Science*, 74, 158–169.
- Reygondeau, G., Longhurst, A., Martinez, E., Beaugrand, G., Antoine, D. & Maury, O. (2013). Dynamic biogeochemical provinces in the global ocean: DYNAMIC BIOGEOCHEMICAL PROVINCES. *Global Biogeochemical Cycles*, 27, 1046–1058.
- Ricker, W.E. (1981). Changes in the average size and average age of Pacific salmon. *Canadian Journal of Fisheries and Aquatic Sciences*, 38, 1636–1656.
- Ricklefs, R.E. & Miller, G.L. (2000). *Ecology*. 4th ed. W.H. Freeman & Co, New York.
- Rosenberg, A.A. (Ed.). (2014). *Developing new approaches to global stock status assessment and fishery production potential of the seas*. FAO fisheries and aquaculture circular. Food and Agriculture Organization of the United Nations, Rome.
- Rousseau, Y., Watson, R.A., Blanchard, J.L. & Fulton, E.A. (2019). Evolution of global marine fishing fleets and the response of fished resources. *Proc Natl Acad Sci USA*, 116, 12238–12243.
- Rutterford, L.A., Simpson, S.D., Jennings, S., Johnson, M.P., Blanchard, J.L., Schön, P.-J., *et al.* (2015). Future fish distributions constrained by depth in warming seas. *Nature Climate Change*, 5, 569–573.
- Ryther, J.H. (1969). Photosynthesis and Fish Production in the Sea. *Science*, 166, 72–76.

- S**aulnier, E., Le Bris, H., Tableau, A., Dauvin, J.C. & Brind’Amour, A. (2020). Food limitation of juvenile marine fish in a coastal and estuarine nursery. *Estuarine, Coastal and Shelf Science*, 241, 106670.
- Schlüter, M.H., Merico, A., Reginatto, M., Boersma, M., Wiltshire, K.H. & Greve, W. (2010). Phenological shifts of three interacting zooplankton groups in relation to climate change: ZOOPLANKTON PHENOLOGY UNDER CLIMATE CHANGE. *Global Change Biology*, no-no.

Bibliography

- Schramski, J.R., Dell, A.I., Grady, J.M., Sibly, R.M. & Brown, J.H. (2015). Metabolic theory predicts whole-ecosystem properties. *Proceedings of the National Academy of Sciences*, 112, 2617–2622.
- Shephard, S., Fung, T., Houle, J.E., Farnsworth, K.D., Reid, D.G. & Rossberg, A.G. (2012). Size-selective fishing drives species composition in the Celtic Sea. *ICES Journal of Marine Science*, 69, 223–234.
- Shin, Y.-J. & Cury, P. (2001). Exploring fish community dynamics through size-dependent trophic interactions using a spatialized individual-based model. *Aquat. Living Resour.*, 16.
- Shin, Y.-J. & Cury, P. (2004). Using an individual-based model of fish assemblages to study the response of size spectra to changes in fishing. *Canadian Journal of Fisheries and Aquatic Sciences*, 61, 414–431.
- Siddon, E.C., Kristiansen, T., Mueter, F.J., Holsman, K.K., Heintz, R.A. & Farley, E.V. (2013). Spatial Match-Mismatch between Juvenile Fish and Prey Provides a Mechanism for Recruitment Variability across Contrasting Climate Conditions in the Eastern Bering Sea. *PLoS ONE*, 8, e84526.
- Simpson, S.D., Jennings, S., Johnson, M.P., Blanchard, J.L., Schön, P.-J., Sims, D.W., *et al.* (2011). Continental Shelf-Wide Response of a Fish Assemblage to Rapid Warming of the Sea. *Current Biology*, 21, 1565–1570.
- Smale, D., Wernberg, T. & Vanderklift, M. (2017). Regional-scale variability in the response of benthic macroinvertebrate assemblages to a marine heatwave. *Mar. Ecol. Prog. Ser.*, 568, 17–30.
- Small, C. & Cohen, J.E. (2004). Continental Physiography, Climate, and the Global Distribution of Human Population. *Current Anthropology*, 45, 269–277.
- Smetacek, V. & Nicol, S. (2005). Polar ocean ecosystems in a changing world. *Nature*, 437, 362–368.
- Smith, A.D.M., Brown, C.J., Bulman, C.M., Fulton, E.A., Johnson, P., Kaplan, I.C., *et al.* (2011). Impacts of Fishing Low-Trophic Level Species on Marine Ecosystems. *Science*, 333, 1147–1150.
- STECF. (2020). *Scientific, Technical and Economic Committee for Fisheries (STECF): 62nd plenary meeting report (PLEN-19-03)*.
- Steinacher, M., Joos, F., Frolicher, T.L., Bopp, L., Cadule, P., Cocco, V., *et al.* (2010). Projected 21st century decrease in marine productivity: a multi-model analysis, 27.
- Stock, C.A. & Dunne, J. (2010). Controls on the ratio of mesozooplankton production to primary production in marine ecosystems. *Deep Sea Research Part I: Oceanographic Research Papers*, 57, 95–112.
- Stock, C.A., Dunne, J.P. & John, J.G. (2014a). Drivers of trophic amplification of ocean productivity trends in a changing climate. *Biogeosciences*, 11, 7125–7135.
- Stock, C.A., Dunne, J.P. & John, J.G. (2014b). Global-scale carbon and energy flows through the marine planktonic food web: An analysis with a coupled physical–biological model. *Progress in Oceanography*, 120, 1–28.
- Stock, C.A., John, J.G., Rykaczewski, R.R., Asch, R.G., Cheung, W.W.L., Dunne, J.P., *et al.* (2017a). Reconciling fisheries catch and ocean productivity. *Proceedings of the National Academy of Sciences*, 114, E1441–E1449.
- Stock, C.A., John, J.G., Rykaczewski, R.R., Asch, R.G., Cheung, W.W.L., Dunne, J.P., *et al.* (2017b). Reconciling fisheries catch and ocean productivity. *Proc. Natl. Acad. Sci. U. S. A.*, 114, E1441–E1449.

Bibliography

- Stramma, L., Prince, E.D., Schmidtko, S., Luo, J., Hoolihan, J.P., Visbeck, M., *et al.* (2012). Expansion of oxygen minimum zones may reduce available habitat for tropical pelagic fishes. *Nature Climate Change*, 2, 33–37.
- Strayer, D. (1991). Notes on Lindeman's Progressive Efficiency. *Ecology*, 72, 348–350.
- Stuart-Smith, R.D., Edgar, G.J., Barrett, N.S., Kininmonth, S.J. & Bates, A.E. (2015). Thermal biases and vulnerability to warming in the world's marine fauna. *Nature*.
- Suess, E. (1980). Particulate organic carbon flux in the oceans—surface productivity and oxygen utilization. *Nature*, 288, 260–263.
- Sunday, J.M., Bates, A.E. & Dulvy, N.K. (2011). Global analysis of thermal tolerance and latitude in ectotherms. *Proceedings of the Royal Society B: Biological Sciences*, 278, 1823–1830.

- T**ableau, A., Le Bris, H. & Brind'Amour, A. (2015). Available Benthic Energy Coefficient (ABEC): a generic tool to estimate the food profitability in coastal fish nurseries. *Mar. Ecol. Prog. Ser.*, 522, 203–218.
- Thackeray, S.J., Henrys, P.A., Hemming, D., Bell, J.R., Botham, M.S., Burthe, S., *et al.* (2016). Phenological sensitivity to climate across taxa and trophic levels. *Nature*, 535, 241–245.
- Tittensor, D.P., Eddy, T.D., Lotze, H.K., Galbraith, E.D., Cheung, W.W.L., Barange, M., *et al.* (2018). A protocol for the intercomparison of marine fishery and ecosystem models: Fish-MIP v1.0. *Geoscientific Model Development*, 11, 1421–1442.
- Tittensor, D.P., Mora, C., Jetz, W., Lotze, H.K., Ricard, D., Berghe, E.V., *et al.* (2010). Global patterns and predictors of marine biodiversity across taxa. *Nature*, 466, 1098–1101.
- Trebilco, R., Baum, J.K., Salomon, A.K. & Dulvy, N.K. (2013). Ecosystem ecology: size-based constraints on the pyramids of life. *Trends in Ecology & Evolution*, 28, 423–431.
- Tremblay-Boyer, L., Gascuel, D., Watson, R., Christensen, V. & Pauly, D. (2011). Modelling the effects of fishing on the biomass of the world's oceans from 1950 to 2006. *Marine Ecology Progress Series*, 442, 169–185.
- Trenkel, V.M., Huse, G., MacKenzie, B.R., Alvarez, P., Arrizabalaga, H., Castonguay, M., *et al.* (2014). Comparative ecology of widely distributed pelagic fish species in the North Atlantic: Implications for modelling climate and fisheries impacts. *Progress in Oceanography*, 129, 219–243.

- U**llah, H., Nagelkerken, I., Goldenberg, S.U. & Fordham, D.A. (2018). Climate change could drive marine food web collapse through altered trophic flows and cyanobacterial proliferation. *PLOS Biology*, 16, e2003446.
- Uriarte, A., Alvarez, P., Iversen, S., Molloy, J., Villamor, B., Martíns, M.M., *et al.* (2001). Spatial pattern of migration and recruitment of north east atlantic mackerel, 40.

- V**alls, A., Gascuel, D., Guénette, S. & Francour, P. (2012). Modeling trophic interactions to assess the effects of a marine protected area: case study in the NW Mediterranean Sea. *Marine Ecology Progress Series*, 456, 201–214.
- Vancoppenolle, M., Bopp, L., Madec, G., Dunne, J., Ilyina, T., Halloran, P.R., *et al.* (2013). Future Arctic Ocean primary productivity from CMIP5 simulations: Uncertain outcome, but consistent

Bibliography

- mechanisms: FUTURE ARCTIC OCEAN PRIMARY PRODUCTIVITY. *Global Biogeochemical Cycles*, 27, 605–619.
- van der Veer, H., Koot, J., Aarts, G., Dekker, R., Diderich, W., Freitas, V., *et al.* (2011). Long-term trends in juvenile flatfish indicate a dramatic reduction in nursery function of the Balgzand intertidal, Dutch Wadden Sea. *Mar. Ecol. Prog. Ser.*, 434, 143–154.
- Verges, A., Steinberg, P.D., Hay, M.E., Poore, A.G.B., Campbell, A.H., Ballesteros, E., *et al.* (2014). The tropicalization of temperate marine ecosystems: climate-mediated changes in herbivory and community phase shifts. *Proceedings of the Royal Society B: Biological Sciences*, 281, 20140846–20140846.
- Vinagre, C., Salgado, J.P., Mendonça, V., Cabral, H. & Costa, M.J. (2012). Isotopes reveal fluctuation in trophic levels of estuarine organisms, in space and time. *Journal of Sea Research*, 72, 49–54.
- W**ard, P. & Myers, R.A. (2005). Shifts in open-ocean fish communities coinciding with the commencement of commercial fishing. *Ecology*, 86, 835–847.
- Woodland, R.J. & Secor, D.H. (2013). Benthic-pelagic coupling in a temperate inner continental shelf fish assemblage. *Limnol. Oceanogr.*, 58, 966–976.
- Worm, B. & Branch, T.A. (2012). The future of fish. *Trends in Ecology & Evolution*, 27, 594–599.
- Worm, B., Hilborn, R., Baum, J.K., Branch, T.A., Collie, J.S., Costello, C., *et al.* (2009). Rebuilding Global Fisheries. *Science*, 325, 578–585.
- Worm, B. & Lotze, H.K. (2016). Marine Biodiversity and Climate Change. In: *Climate Change*. Elsevier, pp. 195–212.
- Y**e, Y. & Gutierrez, N.L. (2017). Ending fishery overexploitation by expanding from local successes to globalized solutions. *Nature Ecology & Evolution*, 1, 0179.

Appendix A – Chapter 2

Supplementary material A.1: Estimation of biomass flow parameters

In this analysis, three biomass flow parameters were calculated to estimate the trophic transfer efficiency (TTE) and the biomass residence time (BRT): P/B (Production to Biomass), P/Q (Production to Consumption) and Q/B (Consumption to Biomass).

For finfish, we used empirical equation while for the other species P/B and P/Q were extracted from EcoBase. Here, we present the equation that we used for finfish (i) and we detail the method to extract P/B and P/Q for the other species.

(i) Finfish

The production to biomass ratio (P/B) can be interpreted as a measure of the speed of biomass flow and estimated for any species j using their thermal habitat (T_i) in the grid cell i and the species growth coefficient (K_j) from Von Bertalanffy growth models (Gascuel *et al.* 2008):

$$\left(\frac{P}{B}\right)_{i,j} = 1.06 \times e^{0.018T_i} \times K_j^{0.75} \quad \text{Eq. S1}$$

The relative food-consumption was estimated using an empirical equation (Palomares & Pauly 1998):

$$\left(\frac{Q}{B}\right)_{i,j} = 10^{(7.964 - 0.204 \times \log_{10}(W_j) - \frac{1.965 \times 1000}{T_i} + 0.083 \times A_j)} \times d_j \quad \text{Eq. S2}$$

where $(Q/B)_{i,j}$ is the relative food-consumption for taxonomic group j in the grid cell i , W_j is the asymptotic weight of the von Bertalanffy growth curve, A_j is the aspect ratio of the fish caudal fin and d_j is a parameter describing the diet (herbivory, omnivory, carnivory, detrivory, herbivory/detrivory and carnivory/detrivory).

(ii) Other species

For the other species, the empirical equations presented above are not valid. So, we extracted directly P/B and P/Q from EcoBase, the repository of all published Ecopath models (Colleter *et al.* 2013).

These parameters are potentially varying in space and may be model-dependent. That is why we developed a procedure to obtain these two biomass parameters from multiple models taking into account the spatial variation. For each parameter in each grid cell:

Step 1: We tested if the grid cell is included in the spatial coverage of at least 2 Ecopath models

a. If so, we use the mean of the parameters from those two or more models

- b. Otherwise, we moved to step 2

Step 2: We tested if there are at least 2 Ecopath models **included** in the FAO area where the grid cell is:

- a. If so, we use the mean of the parameters from those two or more models
- b. Otherwise, we moved to step 3

Step 3: We tested if there are at least 2 Ecopath models **partially included** in the FAO area where the grid cell is:

- a. If so, we use the mean of the parameters from those two or more models
- b. Otherwise, we moved to step 4

Step 4: We took the world average of the parameter in the grid cell.

Bibliography

- Gascuel, D., Morissette, L., Palomares, M.L.D. & Christensen, V. (2008). Trophic flow kinetics in marine ecosystems: Toward a theoretical approach to ecosystem functioning. *Ecol. Model.*, 217, 33–47.
- Palomares, M.L.D. & Pauly, D. (1998). Predicting food consumption of fish populations as functions of mortality, food type, morphometrics, temperature and salinity. *Mar. Freshw. Res.*, 49, 447.

Supplementary material A.2: Model Ecopath

Table A.2: List of the 72 selected Ecopath models extracted from EcoBase (Colléter *et al.* 2013) used to calculate the correction parameters of the trophic transfer efficiency and to compare the trophic trophic transfer parameters calculated from biomass and catch.

Number in EcoBase	Location	Period	Reference
252	Aleutian Islands	1963-1963	(Guénette <i>et al.</i> 2006)
405	Australia North West Shelf	1986-1991	(Bulman <i>et al.</i> 2006b)
7	Azores archipelago	1997-1997	(Guénette & Morato 2001)
63	Barents Sea	1990-1990	(Blanchard <i>et al.</i> 2002)
633	Bay of Biscay	1970-1971	(Ainsworth <i>et al.</i> 2001)
736	Bay of Biscay	1980	(Moullec <i>et al.</i> 2017)
634	Bay of Biscay	1998-1999	(Ainsworth <i>et al.</i> 2001)
335	Bay of Biscay	1994-2005	(Lassalle <i>et al.</i> 2012)
737	Bay of Biscay	2013	(Moullec <i>et al.</i> 2017)
478	British Columbia coast	1950-2000	(Preikshot 2007)
486	Cape Verde	1981-1985	(Stobberup <i>et al.</i> 2002)
24	Caribbean	1980-1981	(Morissette <i>et al.</i> 2008)
734	Celtic Sea	1980	(Moullec <i>et al.</i> 2017)
735	Celtic Sea	2013	(Moullec <i>et al.</i> 2017)
732	Celtic Sea-Biscay	1980	(Bentorcha <i>et al.</i> 2017)
733	Celtic Sea-Biscay	2012	(Bentorcha <i>et al.</i> 2017)
239	Central Gulf of California	1978-1980	(Arreguín-Sánchez <i>et al.</i> 2002)
406	East Bass Strait	1994	(Bulman <i>et al.</i> 2006a)
40	Eastern Scotian Shelf	1980-1986	(Bundy 2004)
41	Eastern Scotian Shelf	1995-2000	(Bundy 2004)
705	Georges Bank	1996-2000	(Link <i>et al.</i> 2006)
726	Guinea	1998-1999	(Gascuel <i>et al.</i> 2009)
725	Guinea	2004-2004	(Gascuel <i>et al.</i> 2009)
450	Gulf of California	1990-2000	(Lercari & Arreguín-Sánchez 2009)
739	Gulf of Gabes	2000-2005	(Hattab <i>et al.</i> 2013)
444	Gulf of Maine	1977-1987	(Heymans 2001)
704	Gulf of Maine	1996-2000	(Link <i>et al.</i> 2006)
520	Gulf of Mexico	1950-1951	(Walters <i>et al.</i> 2008)
412	Gulf of Thailand	1963-1964	(Christensen 1998)
487	Humboldt Current	1995-1996	(Tam <i>et al.</i> 2008)
448	Irish Sea	1973-1974	(Lees & Mackinson 2007)
307	Jalisco and Colima Coast	1995-1996	(Galván Piña 2005)
64	Low Barents sea	1995-1996	(Blanchard <i>et al.</i> 2002)
689	Mauritania	1991-1991	(Guénette <i>et al.</i> 2014)

707	Mid-Atlantic Bight	1996-2000	(Link <i>et al.</i> 2006)
502	North Benguela	1967-1968	(Watermeyer <i>et al.</i> 2008b)
503	North Benguela	1990-1991	(Watermeyer <i>et al.</i> 2008b)
479	North East Pacific	1950-1950	(Preikshot 2007)
413	North Sea	1974-1975	(Christensen <i>et al.</i> 2002)
680	North Sea	1991-1992	(Lees & Mackinson 2007)
457	North Sea	1981-1982	(Christensen n.d.)
410	North South of China Sea	1970-1971	(Cheung 2007)
115	Northern Benguela	1956-1957	(Heymans & Sumaila 2007)
674	Northern British Columbia	1950-1951	(Ainsworth <i>et al.</i> 2002)
675	Northern British Columbia	2000-2001	(Ainsworth <i>et al.</i> 2002)
519	Northern Californian Current	1960-1969	(Walters <i>et al.</i> 2010)
521	Northern Californian Current	1990-2000	(Field 2004)
462	Northern Gulf of St Lawrence	1990-1991	(Savenkoff <i>et al.</i> 2004a)
488	Northern Humboldt Current	1997-1998	(Tam <i>et al.</i> 2008)
439	Peru	1953-1953	(Guénette <i>et al.</i> 2008)
135	Sierra Leone	1964-1965	(Heymans & Vakily 2004)
137	Sierra Leone	1990-1991	(Heymans & Vakily 2004)
136	Sierra Leone	1978-1979	(Heymans & Vakily 2004)
325	Sur de Sinaloa	1994-1997	(Salcido Guevera 2006)
291	Sonda de Campeche	1988-1994	(Zetina-Rejón & Arreguín-Sánchez 2003)
485	South Benguela	1978-1979	(Shannon <i>et al.</i> 2003)
438	South East Alaska	1963-1963	(Guénette <i>et al.</i> 2006)
506	South of Benguela	1960-1961	(Watermeyer <i>et al.</i> 2008a)
687	South western Gulf of Mexico	1970-1980	(Arreguín-Sánchez <i>et al.</i> 1993)
145	Southern Gulf of St. Lawrence	1980-1981	(Savenkoff <i>et al.</i> 2004b)
706	Southern New England	1996-2000	(Link <i>et al.</i> 2006)
441	Sri Lanka	2000-2001	(Haputhantri <i>et al.</i> 2008)
477	Strait of Georgia	1950-1950	(Preikshot 2007)
328	Strait of Georgia	1950-1950	(Martell <i>et al.</i> 2002)
703	Tasmanian waters	1993-2007	(Watson <i>et al.</i> 2013)
99	USA, Mid Atlantic Bight	1995-1998	(Okey 2001)

305	West coast of Sabah	1972-1973	(Garces <i>et al.</i> 2003)
727	West Florida Shelf Historic Model	1997-1998	(Chagaris <i>et al.</i> 2015)
461	West Scotland	2000-2004	(Morissette & Pitcher 2005)
175	Western Bering Sea	1981-1990	(Aydin <i>et al.</i> 2002)
526	Western Channel	1993-1994	(Araújo <i>et al.</i> 2005)
403	Western Channel	1973-1973	(Araújo <i>et al.</i> 2005)

Bibliography - Ecopath models

- Ainsworth, C., Ferriss, B., Leblond, E. & Guénette, S. (2001). The Bay of Biscay, France; 1998 and 1970 models. *Fish. Cent. Res. Rep.*, Fisheries Impacts on North Atlantic Ecosystems: Models and Analyses, 9.
- Ainsworth, C., Heymans, Johanna J. (Sheila), Pitcher, T. & Vasconcellos, M. (2002). Ecosystem models of Northern British Columbia for the time periods 2000, 1950, 1900 and 1750.
- Araújo, J.N., Mackinson, S., Ellis, J.R. & Hart, P.J.B. (2005). An Ecopath model of the western English Channel ecosystem with an exploration of its dynamic properties. *CEFAS Sci. Ser. Tech. Rep.*
- Arreguín-Sánchez, F., Arcos, E. & Chávez, E.A. (2002). Flows of biomass and structure in an exploited benthic ecosystem in the gulf of California, Mexico. *Ecol. Model.*, 156, 167–183.
- Arreguín-Sánchez, F., Valero-Pacheco, E. & Chávez, E.A. (1993). A trophic box model of the coastal fish communities of the Southwestern Gulf of Mexico. *Trophic Models Aquat. Ecosyst.*
- Aydin, K.Y., Lapko, V.V., Radchenko, V.I. & Livingston, P.A. (2002). A Comparison of the Eastern Bering and Western Bering Sea Shelf and Slope Ecosystems Through the Use of Mass-Balance Food Web Models. *NOAA Tech. Memo.*, 87.
- Bentorcha, A., Gascuel, D. & Guénette, S. (2017). Using trophic models to assess the impact of fishing in the Bay of Biscay and the Celtic Sea. *Aquat. Living Resour.*, 30, 7.
- Blanchard, J.L., Pinnegar, J.K. & Mackinson, S. (2002). Exploring Marine Mammal-Fishery Interactions Using “ecopath With Ecosim”: Modelling the Barents Sea Ecosystem. *Cent. Environ. Fish. Aquac. Sci.*, 52.
- Bulman, C., CSIRO Marine and Atmospheric Research & Fisheries Research & Development Corporation (Australia). (2006a). *Trophic dynamics of the eastern shelf and slope of the South East Fishery: impacts of and on the fishery*. CSIRO Marine and Atmospheric Research, Hobart, Tas.
- Bulman, C., CSIRO Marine and Atmospheric Research, North West Shelf Joint Environmental Management Study & Western Australia. (2006b). *Trophic webs and modelling of Australia’s*

- North West Shelf*. CSIRO Marine and Atmospheric Research ; Government of Western Australia, Hobart, Tas.; Perth, W.A.
- Bundy. (2004). *Mass balance models of the eastern Scotian Shelf before and after the cod collapse and other ecosystem changes* (No. 2520). Canadian Technical Report of Fisheries and Aquatic Sciences.
- Chagaris, D.D., Mahmoudi, B., Walters, C.J. & Allen, M.S. (2015). Simulating the Trophic Impacts of Fishery Policy Options on the West Florida Shelf Using Ecopath with Ecosim. *Mar. Coast. Fish.*, 7, 44–58.
- Cheung, W.W.L. (2007). Vulnerability of marine fishes to fishing : from global overview to the northern South China Sea.
- Christensen, V. (1998). Fishery-induced changes in a marine ecosystem: insight from models of the Gulf of Thailand. *J. Fish Biol.*, 53, 128–142.
- Christensen, V. (n.d.). A model of trophic interactions in the North Sea in 1981, the Year of the Stomach, 28.
- Christensen, V., Reck, G. & Maclean, J.L. (2002). Proceedings of the INCO-DC Conference Placing Fisheries in their Ecosystem Context. *ACP-EU Fish. Res. Rep.*, 79.
- Field, J.C. (2004). Application of ecosystem-based fishery management approaches in the Northern California Current. School of Aquatic and Fishery Sciences, University of Washington, Seattle.
- Galván Piña, V.H. (2005). Impacto de la pesca en la estructura, función y productividad del ecosistema de la Plataforma Continental de las costas de Jal. Instituto Politécnico Nacional, La Paz.
- Garces, L.R., Man, A., Ahmad, A.T., Mohamad-Norizam, M. & Silvestre, G.T. (2003). A Trophic Model of the Coastal Fisheries Ecosystem off the West Coast of Sabah and Sarawak, Malaysia. *WorldFish Cent. Conf. Proc.*, Assessment, management and future directions for coastal fisheries in Asian countries, 1120.
- Gascuel, D., Guénette, S., Diallo, I. & Sidibé, A. (2009). *Impact de la pêche sur l'écosystème marin de Guinée - modélisation EwE 1985/2005* (No. 17–4). Fisheries Centre Research Reports. University of British Columbia.
- Guénette, S., Christensen, V. & Pauly, D. (2008). Trophic modelling of the Peruvian upwelling ecosystem: Towards reconciliation of multiple datasets. *Prog. Oceanogr.*, 79, 326–335.
- Guénette, S., Heymans, S.J., Christensen, V. & Trites, A.W. (2006). Ecosystem models show combined effects of fishing, predation, competition, and ocean productivity on Steller sea lions (*Eumetopias jubatus*) in Alaska. *Can. J. Fish. Aquat. Sci.*, 63, 2495–2517.

- Guénette, S., Meissa, B. & Gascuel, D. (2014). Assessing the Contribution of Marine Protected Areas to the Trophic Functioning of Ecosystems: A Model for the Banc d'Arguin and the Mauritanian Shelf. *PLoS ONE*, 9, e94742.
- Guénette, S. & Morato, T. (2001). The Azores Archipelago 1997. *Fish. Cent. Res. Rep.*, Fisheries Impacts on North Atlantic Ecosystems : Models and Analyses, 9, 241–270.
- Haputhantri, S.S.K., Villanueva, M.C.S. & Moreau, J. (2008). Trophic interactions in the coastal ecosystem of Sri Lanka: An ECOPATH preliminary approach. *Estuar. Coast. Shelf Sci.*, 76, 304–318.
- Hattab, T., Ben Rais Lasram, F., Albouy, C., Romdhane, M.S., Jarboui, O., Halouani, G., *et al.* (2013). An ecosystem model of an exploited southern Mediterranean shelf region (Gulf of Gabes, Tunisia) and a comparison with other Mediterranean ecosystem model properties. *J. Mar. Syst.*, 128, 159–174.
- Heymans, J.J. (2001). The Gulf of Maine, 1977-1986. *Fish. Impacts N. Atl. Ecosyst. Models Anal.*
- Heymans, S.J.J. & Sumaila, U.R. (2007). Updated ecosystem model for the Northern Benguela ecosystem, Namibia. *INCOFISH Ecosyst. Models Transiting Ecopath Ecospace*.
- Heymans, S.J.J. & Vakily, J.M. (2004). Structure and dynamics of the marine ecosystem off Sierra Leone for three time periods: 1964, 1978, 1990. *Fish. Cent. Res. Rep.*, West African marine ecosystems: models and fisheries impacts, 12, 160–169.
- Lassalle, G., Gascuel, D., Le Loc'h, F., Lobry, J., Pierce, G.J., Ridoux, V., *et al.* (2012). An ecosystem approach for the assessment of fisheries impacts on marine top predators: the Bay of Biscay case study. *ICES J. Mar. Sci.*, 69, 925–938.
- Lees, K. & Mackinson, S. (2007). An ecosystem model of the North Sea to support an ecosystem approach to fisheries management: description and parameterisation. *Sci. Ser. Tech. Rep.*, 49.
- Lercari, D. & Arreguín-Sánchez, F. (2009). An ecosystem modelling approach to deriving viable harvest strategies for multispecies management of the Northern Gulf of California. *Aquat. Conserv. Mar. Freshw. Ecosyst.*, 19, 384–397.
- Link, J.S., Griswold, C.A., Methratta, E.T. & Gunnard, J. (2006). Documentation for the Energy Modeling and Analysis eExercise (EMAX). *Northeast Fish. Sci. Cent. Ref. Doc.*, 06, 176.
- Martell, S.J.D., Beattie, A.I., Walters, C.J., Nayar, T. & Briese, R. (2002). Simulating fisheries management strategies in the Strait of Georgia ecosystem using Ecopath and Ecosim. *Fish. Cent. Res. Rep.*, The Use of Ecosystem Models to Investigate Multispecies Management Strategies for Capture Fisheries, 13, 159.

- Morissette, L., Kaschner, K., Melgo, J.L. & Gerber, L.R. (2008). Food Web Models and Data for Studying the Interactions between Marine Mammals and Fisheries. *60 La Réunion. Annu. Comm. Balein. Ecosyst. Model. Subcomm.*, 52.
- Morissette, L. & Pitcher, T. (2005). Model structure and balancing Ecosystem Simulation Models of Scotland's West Coast and Sea Lochs. *Fish. Cent. Res. Rep.*, Ecosystem Simulation Models of Scotland's West Coast and Sea Lochs, 13, 5–24.
- Moullec, F., Gascuel, D., Bentorcha, K., Guénette, S. & Robert, M. (2017). Trophic models: What do we learn about Celtic Sea and Bay of Biscay ecosystems? *J. Mar. Syst.*, 172, 104–117.
- Okey, T.A. (2001). A “straw-man” Ecopath model of the Middle Atlantic Bight continental shelf, United States. *Fish. Cent. Res. Rep.*, Fisheries Impacts on North Atlantic Ecosystems: Models and Analyses, 9, 151–166.
- Preikshot, D.B. (2007). The influence of geographic scale, climate and trophic dynamics upon North Pacific oceanic ecosystem models.
- Salcido Guevera, L.A. (2006). Estructura y flujos de biomasa en un ecosistema bentónico explotado en el sur de sinaloa, México. Instituto Politécnico Nacional, La Paz.
- Savenkoff, C., Bourdages, H., Castonguay, M., Morissette, L., Chabot, D. & Hammill, M.O. (2004a). *Input data and parameter estimates for ecosystem models of the northern Gulf of St. Lawrence (mid-1990s)* (Canadian Technical Report of Fisheries and Aquatic Sciences No. 2531).
- Savenkoff, C., Bourdages, H., Swain, D.P., Despatie, S.-P., Hanson, J.M., Méthot, R., *et al.* (2004b). *Input data and parameter estimates for ecosystem models of the southern Gulf of St. Lawrence (mid-1980s and mid-1990s)* (Canadian Technical Report of Fisheries and Aquatic Sciences No. 2529).
- Shannon, L.J., Moloney, C.L., Jarre, A. & Field, J.G. (2003). Trophic flows in the southern Benguela during the 1980s and 1990s. *J. Mar. Syst.*, 39, 83–116.
- Stobberup, K.A., Ramos, V.M., Coelho, M.L. & Erzini, K. (2002). Changes in the coastal ecosystem of the Cape Verde Archipelago over the last two decades: A simulation study using Ecosim. *Fish. Cent. Res. Rep.*, West African marine ecosystems: models and fisheries impacts, 12, 19.
- Tam, J., Taylor, M.H., Blaskovic, V., Espinoza, P., Michael Ballón, R., Díaz, E., *et al.* (2008). Trophic modeling of the Northern Humboldt Current Ecosystem, Part I: Comparing trophic linkages under La Niña and El Niño conditions. *Prog. Oceanogr.*, 79, 352–365.
- Walters, C., Christensen, V., Walters, W. & Rose, K. (2010). Representation of multistanza life histories in Ecospace models for spatial organization of ecosystem trophic interaction patterns. *Bull. Mar. Sci.*, 86, 21.

- Walters, C., Martell, S.J.D., Christensen, V. & Mahmoudi, B. (2008). An Ecosim Model for Exploring Gulf of Mexico Ecosystem Management Options: Implications of Including Multistanza Life-History Models for Policy Predictions. *Bull. Mar. Sci.*, 83, 21.
- Watermeyer, K., Shannon, L. & Griffiths, C. (2008a). Changes in the trophic structure of the southern Benguela before and after the onset of industrial fishing. *Afr. J. Mar. Sci.*, 30, 351–382.
- Watermeyer, K., Shannon, L., Roux, J.-P. & Griffiths, C. (2008b). Changes in the trophic structure of the northern Benguela before and after the onset of industrial fishing. *Afr. J. Mar. Sci.*, 30, 383–403.
- Watson, R.A., Nowara, G.B., Tracey, S.R., Fulton, E.A., Bulman, C.M., Edgar, G.J., *et al.* (2013). Ecosystem model of Tasmanian waters explores impacts of climate-change induced changes in primary productivity. *Ecol. Model.*, 264, 115–129.
- Zetina-Rejón, M.J. & Arreguín-Sánchez, F. (2003). Flujos de energía y estructura trófica de la Sonda de Campeche, Suroeste del Golfo de México. *Mem. III Foro Camarón Golfo México Mar Caribe*, 92.

Supplementary material A.3: Correction terms based on ecotrophic efficiency and biomass accumulation

In order to convert partial transfer efficiency into trophic transfer efficiency (TTE) (see theoretical graph in Fig. 3 in the manuscript), we introduced correction terms based on the ecotrophic efficiency (EE) and the accumulation rate of biomass within each species or taxon (B_{acc}) and equal to $EE - B_{acc}$ (which measures the fraction of the production of a given taxon not transferred to detritus and not accumulated by the taxon, and thus available for trophic transfers through consumption by predators; see theoretical graph on Fig. S1).

EE and B_{acc} were extracted from a selection of coastal Ecopath models (Supplementary material A.2) included in the EcoBase database. These parameters were calculated for each ecosystem type and for each trophic level (Fig A.3a).

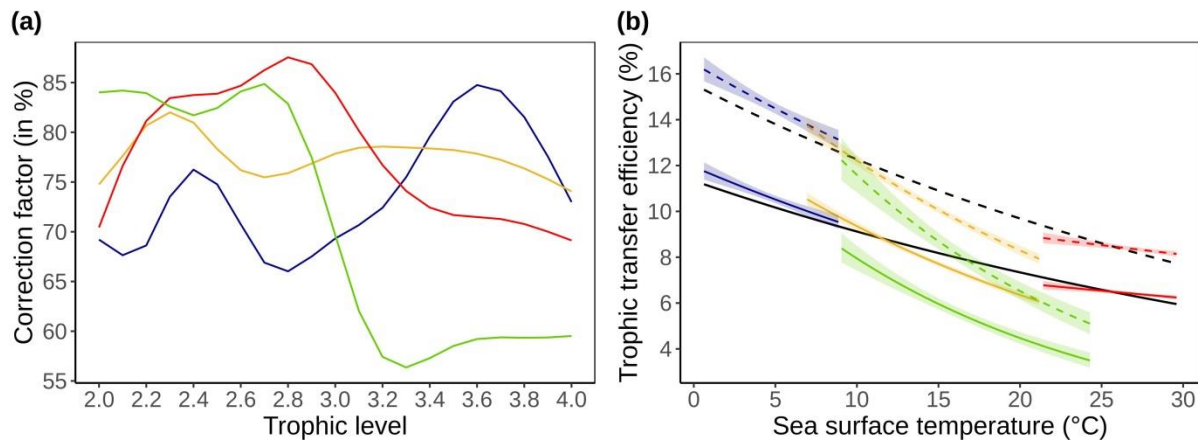


Figure A.3: (a) Correction factor for each trophic level and for each ecosystem type calculated using the Ecopath models from Ecobase. (b) Predicted mean values of TTE including the correction terms in solid line and removing the correction terms in dashed line. The colors refer to the ecosystem types: polar in blue, temperate in orange, tropical in red and in upwelling in green.

Polar, temperate and tropical ecosystems exhibit similar patterns in EE for the low Trophic Levels (TLs) between 0.70 and 0.85. That suggests that at low TLs ($TL < 3$), losses generated by non-predation natural mortalities are low. At high TLs, EE shows large variations depending on the ecosystem types. EE increases in polar ecosystem by TL 3.7 while EE decreases slightly in temperate ecosystems. The losses generated by non-predation mortalities appear higher in upwelling and, to a lesser extent, in tropical ecosystems wherein EE decreases to less than 0.70 and 0.60, respectively.

Then, we evaluated the effect of this correction on the predicted TTE by comparing the predicted TTE (modelled using SST and the ecosystem types) and the predicted TTE by removing the

correction (Fig. A.3b). A consistent effect of the sea water temperature is observed with or without the correction and the differences between the ecosystem types are similar as well.

Supplementary material A.4: Sensitivity analysis: inclusion of fishing indicators in the temperature effect model

We tested two fishing indicators, the amount of catch per surface unit (which measures the fishing intensity) and the mean trophic level of catch (MTL, which is a measure of the fishing strategy at the scale of the ecosystem) as additional variables in the model presented in the main analysis. The aim of this sensitivity analysis is to explore the effects of the amount of catch and the fraction of the food web which is caught on the model developed to explain the temperature effects. In each $1^{\circ}\times 1^{\circ}$ grid cell, we calculated the amount of catch per squared kilometer (catch.km^{-2}) and the MTL of catch. The catch.km^{-2} and the MTL were added as continuous and categorical variables in the two models, for trophic transfer efficiency (TTE) and biomass residence time (BRT). Catch.km^{-2} was divided into 3 categories: low catch level ($<100\text{kg.km}^{-1}\text{.year}^{-1}$), medium catch level between 100kg and $2\text{t.km}^{-1}\text{.year}^{-1}$) and high catch level ($>2\text{t.km}^{-1}\text{.year}^{-1}$), while MTLs were divided into: the lowest MTLs (<3.15), medium MTLs (between 3.15 and 3.4) and high MTLs (>3.4).

Table A.4: Description of the eight tested models including a fishing variable and the associated deviance and p-value.

Model for trophic transfer efficiency			
Variables in the model	Additional fishing variable	P-value of the fishing variable	Deviance explained by the fishing variable
SST and Ecosystem type	Catch.km-2 as a continuous variable	1.048e-07	0.3%
	Catch.km-2 as a categorical variable	6.989e-12	0.5%
	MTL as a continuous variable	$< 2.2\text{e-}16$	0.7%
	MTL as a categorical variable	2.576e-12	0.5%
Model for biomass residence time			
Variables in the model	Additional fishing variable	P-value of the fishing variable	Deviance explained by the fishing variable
SST and Ecosystem type	Catch.km-2 as a continuous variable	$< 2.2\text{e-}16$	1.4%
	Catch.km-2 as a categorical variable	$< 2.2\text{e-}16$	4.6%
	MTL as a continuous variable	1.360e-13	0.4%
	MTL as a categorical variable	3.419e-15	0.6%

The p-values associated to the added fishing variables show that including fishing variables improved the models for both the TTE and the BRT (Table A.4). However, these variables explained a low fraction of the total deviance except for the catch/km² when it is included as a categorical variable in the model for the BRT. Therefore, the amount of catch and the mean trophic level of catch have a

little effect on the TTE estimates while the BRT model is more sensitive to the amount of catch. The BRT estimates are lower in case of large fishing pressures (Figure A.4.1). However, the trends in BRT according to SST remain unchanged with or without the fishing effect and the associated relationships per ecosystem type are also weakly sensitive (Figure A.4.2).

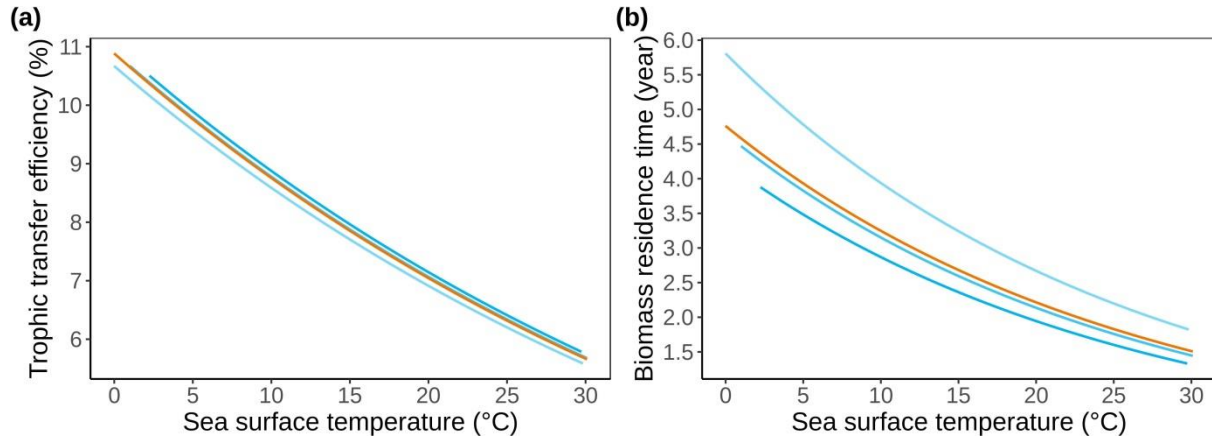


Figure A.4.1: Predicted values of TTE (a) and BRT (b) from the models including only SST. The orange curve represents the model without fishing variables and the blue curves represent the predicted values from the model including the 3 categories of catch volume from low amount of catch (in light color) to high amount of catch (in dark color).

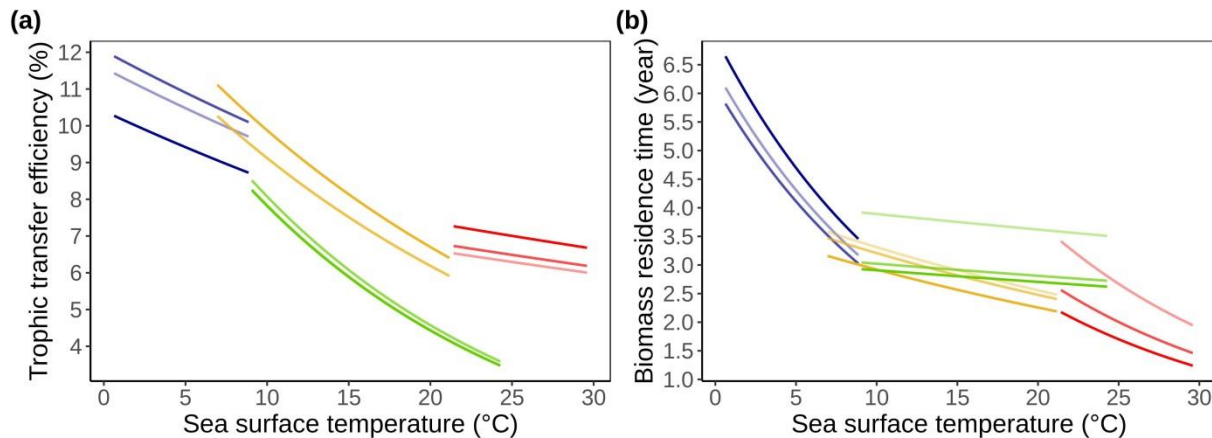


Figure A.4.2: Predicted values of TTE (a) and BRT (b) in polar (in blue), temperate (in orange), tropical (in red) and in upwelling (in green) ecosystems for each categories of catch volume from low amount of catch (in light color) to high amount of catch (in dark color).

Supplementary material A.5: Sensitivity analysis: The use of Ecopath models to compare parameter estimates using biomass and catch data

We used a selection of Ecopath models from EcoBase (Colléter *et al.* 2013) to compare the estimates of the trophic transfer efficiency (TTE) and biomass residence time (BRT) based on the species composition of biomass and catch. Trophic parameters were calculated using a selection of 72 Ecopath models (Supplementary material A.2), using separately biomass and catch data per functional groups in each selected Ecopath model. Taxon-specific trophic parameters (P/B and P/Q) were transformed into trophic spectra thanks to the EcoTroph methodology (see Maureaud *et al.* 2017) and as for the SeaAroundUs catch data, we obtained P/B and P/Q by trophic class, by grid cell and by year weighted by biomass (and catch, respectively). To compare TTE using catch and biomass, we use the partial transfer efficiency (TTE without correction). Indeed, the correction would obviously be the same for TTE based on catch and on biomass, since in this sensitivity analysis we compare two types of input data to calculate the transfer efficiency (catch and biomass) for the same model.

The use of a selection of Ecopath Models demonstrated that the observed patterns in terms of TTE and BRT were similar using biomass data instead of catch: (i) Biomass transfers are slower and more efficient in polar ecosystems than in temperate and in tropical ecosystems in terms of mean and median; (ii) Upwelling systems are characterized by the least efficient transfers and residence times are low but remain higher in tropical ecosystems (Fig A.5a, b).

Besides, results show that TTE and BRT from catch and biomass data are positively correlated ($r=0.68$; $p\text{-value} < 2.2e-16$ and $r=0.65$; $p\text{-value}=2.2e-16$) (Fig S6c, d). However, there is a systematic bias with an overall overestimation of BRT and underestimations of TTE using catch data. TTE is, on average, between 5.7% and 6.9% higher (depending on the ecosystem type) when using biomass data and the BRT is, in average, between 0.7 and 1.9 years higher.

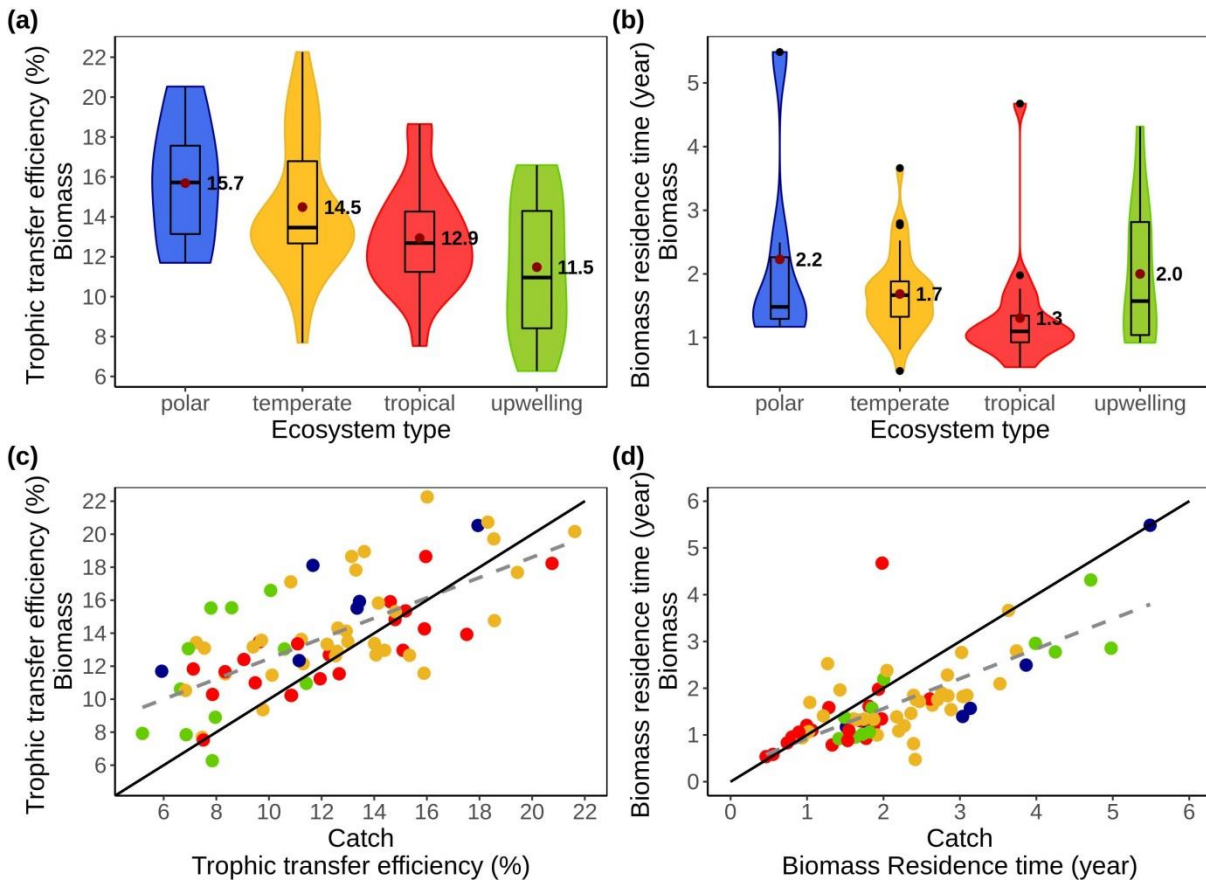


Figure A.5: (a.) Distribution and mean values of TTE in each ecosystem type and (b.) distribution and mean values of BRT in each ecosystem type (b.). The red dots and the associated values are the mean values of TTE and BRT for each ecosystem type. Comparison between TTE (c.) and BRT (d.) calculated from biomass data and from catch data in a selection of 72 Ecopath models. Colors represent the models ecosystem types (tropical in red, temperate in yellow, polar in blue and upwelling in green). The black line is the identity line ($x=y$) and the dashed grey line is the linear relation between indicators calculated from biomass and catch data.

The overestimation in BRT may be due to the under-representation of non-exploited species at low trophic levels (e.g., zooplankton) which are species with high speed of biomass flow (high P/B) (Gascuel *et al.* 2008, 2011) and consequently a low BRT. Furthermore, landings do not include the non-exploited and non-accessible part of the ecosystem which can play a major role in marine food webs (Maureaud *et al.* 2017). Fisheries data can also skew the perception of the ecosystem structure because of the fishing strategy (e.g. targeting specific species) and fishing regulations. However, it is extremely difficult to identify how fishing strategies or regulations may affect the species composition of the catch.

This comparison of the indicators model by model has some limitations because Ecopath data strongly differ from those used in the paper for worldwide coastal waters. While the latter ones refer to species and 1°x1° rectangle, Ecopath data are aggregated in trophic boxes, depending on the goal of the model, and the spatial extents of models vary from the entire Northeast Atlantic to small areas such as the Strait of Georgia. However, this sensitivity analysis still gives an idea of the differences between biomass and catch and confirms the effects of temperature between the ecosystem types.

Bibliography

- Branch, T.A., Watson, R., Fulton, E.A., Jennings, S., McGilliard, C.R., Pablico, G.T., *et al.* (2010). The trophic fingerprint of marine fisheries. *Nature*, 468, 431–435.
- Colléter, M., Valls, A., Guitton, J., Lyne, M., Sánchez, F.A., Christensen, V., *et al.* (2013). EcoBase: a repository solution to gather and communicate information from EwE models, 69.
- Gascuel, D., Guenette, S. & Pauly, D. (2011). The trophic-level-based ecosystem modelling approach: theoretical overview and practical uses. *ICES J. Mar. Sci.*, 68, 1403–1416.
- Gascuel, D., Morissette, L., Palomares, M.L.D. & Christensen, V. (2008). Trophic flow kinetics in marine ecosystems: Toward a theoretical approach to ecosystem functioning. *Ecol. Model.*, 217, 33–47.
- Maureaud, A., Gascuel, D., Colléter, M., Palomares, M.L., Du Pontavice, H., Pauly, D., *et al.* (2017). Global change in the trophic functioning of marine food webs. *PloS One*, 12, e0182826.
- Pauly, D., Hilborn, R. & ch, T.A. (2013). Fisheries: does catch reflect abundance? *Nature*, 494, 303.

Supplementary material A.6: Sensitivity analysis: fisheries do not catch the lower fraction of the ecosystem

In our analysis, we estimated the food web functioning parameters from trophic level TL=2 to TL=4 based on catch data. However, the major part of the catch are in the upper part of the food web (TL>2.5). Thus, the inclusion of the fraction of the ecosystem between TL=2 and TL=2.5, where catch composition does not reflect the species composition in the ecosystem, may bias our estimates. In this lower part of the food web, a large fraction of the biomass is made of groups such as zooplankton, larvae, benthic fauna... that are not caught by fisheries. Therefore, we calculated our trophic parameters between TL=2.5 and TL=4 to evaluate the potential bias of our estimates.

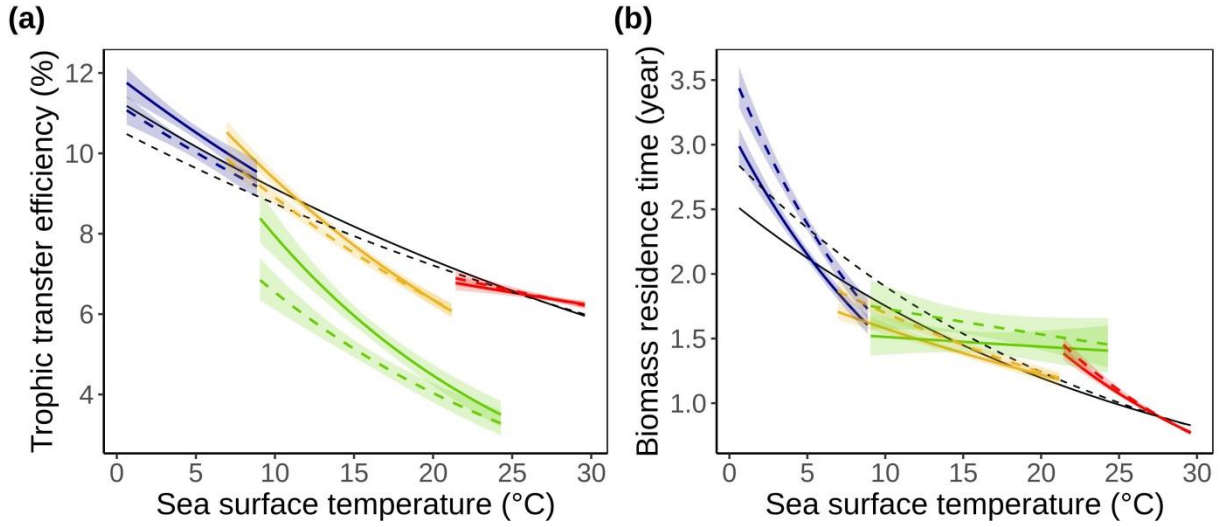


Figure A.6: Predicted values of trophic transfer efficiency and biomass residence time in polar (in blue), temperate (in orange), tropical (in red) and in upwelling (in green) ecosystems between TL=2 and TL=4 (in solid lines) and between TL=2.5 and TL=4 (in dashed lines).

Finally, the models based on the two indicators calculated between TL=2.5 and TL=4 are expressed as follow for trophic transfer efficiency (TTE) and biomass residence time (BRT):

$$TTE = e^{(-2.224 + SST(-0.023 + a) + b)} \times e^{\frac{\alpha^2(TTE)}{2}} \quad BRT = e^{(-1.617 + SST(-0.083 + c) + d)} \times e^{\frac{\alpha^2(BRT)}{2}}$$

where a, b, c and d are specific parameters for each type of ecosystem (Table A.6) and $\alpha^2(TTE)$ and $\alpha^2(BRT)$ are the standard errors associated with the log-normal models to correct the bias due to the log-transformation such as $e^{\frac{\alpha^2(TTE)}{2}} = 1.078641$ and $e^{\frac{\alpha^2(BRT)}{2}} = 1.163384$.

Table A.6: trophic transfer efficiency and biomass residence time estimated by the model in each type of ecosystem.

Ecosystem type	Trophic transfer efficiency		Biomass residence time	
	a	b	c	d
Polar	0	0	0	0
Temperate	-0.011	0.105	0.052	-0.442
Tropical	0.010	-0.218	0.006	0.753
Upwelling	-0.026	-0.057	0.071	-0.615

Supplementary material A.7: Sensitivity analysis: Spatial autocorrelation

We generated randomly 100 grids with 153 non-adjacent grid cells each and far away from at least 1000km (1 example in Figure A.7.1). 1000km was identified as a good trade-off in order to decrease the spatial autocorrelation and a reasonable number of grid cells to model the temperature effect. Indeed, the mean residual semivariograms for the trophic transfer efficiency (TTE) and the biomass residence time (BRT) (based the models built using the subsamples of cells) show that the residuals spatial autocorrelation is very weak (Figure A.7.2).

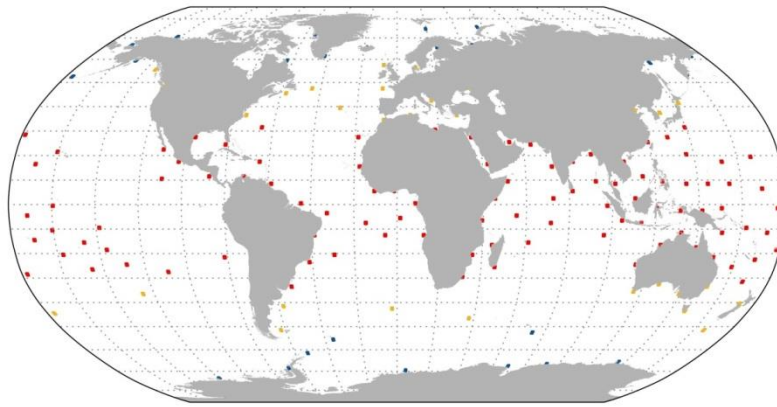


Figure A.7.1: Map of the selection of 153 non-adjacent grid cells far away from at least 1000km.

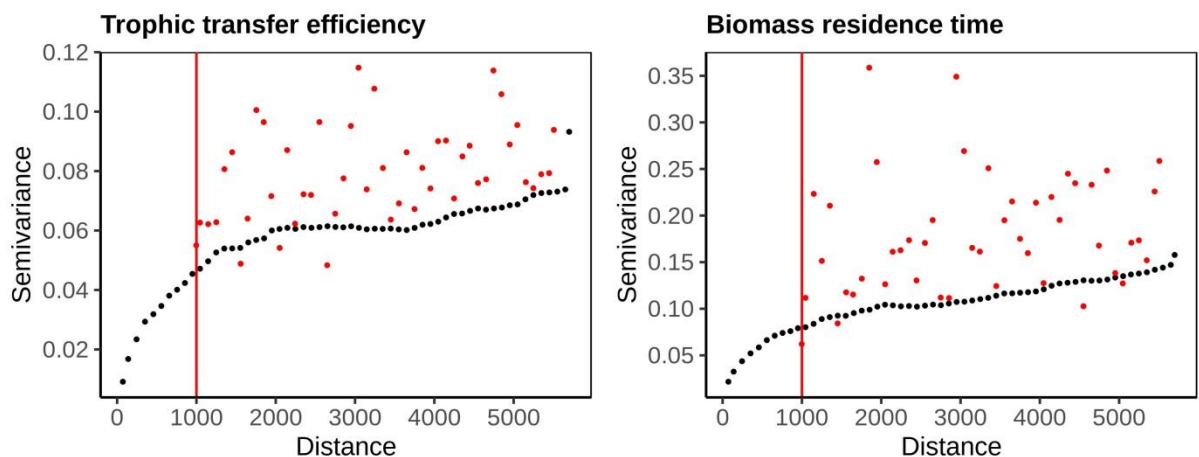


Figure A.7.2: One of the residual variograms for the trophic transfer efficiency and the biomass residence time, respectively, of the full models developed in the study (black dots) and the

model based on the subsample of 153 non-adjacent grid cells (red dots). The red line indicates the minimum distance between the grid cells (1000km).

Then, we modelled the temperature effects using the 100 subsamples and we obtained 100 models for both TTE and BRT. Upwelling cell was removed because of the low number of grid cells for this ecosystem type in the subsamples.

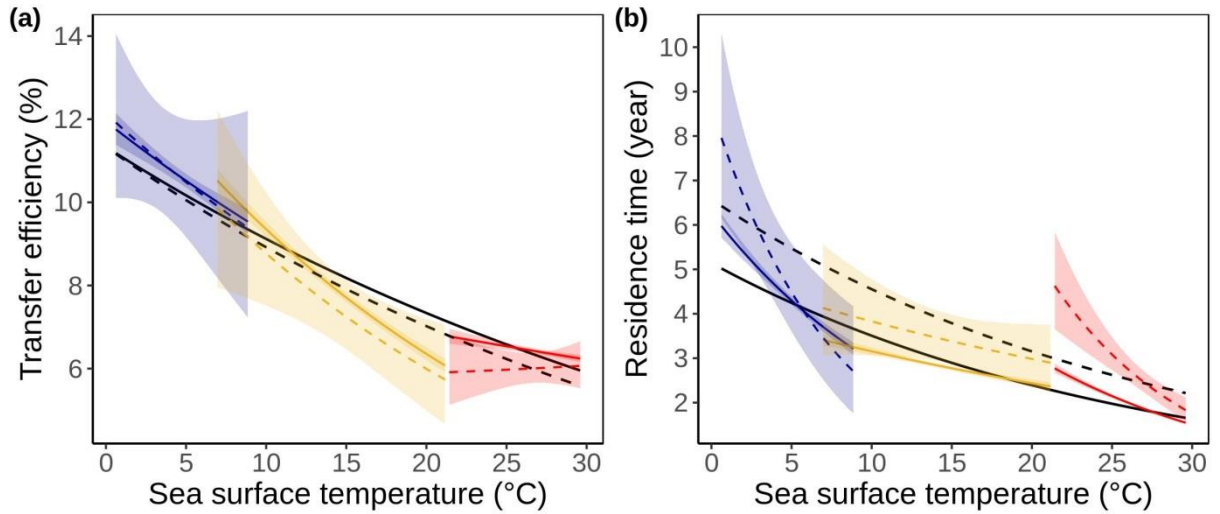


Figure A.7.3: Predicted values of trophic transfer efficiency (a) and biomass residence time (b) in polar (in blue), temperate (in orange), tropical (in red) and in upwelling (in green) ecosystems for the full models developed in the study (solid lines) and for the mean of the 100 models using the 100 subsamples (dashed lines).

The potential biased due to the spatial autocorrelation is low for TTE with a slight effect in tropical ecosystems. Regarding the BRT, the effect is a bit stronger suggesting we underestimated the BRT in temperate and tropical ecosystems (greater values without the spatial autocorrelation) and we underestimated the temperature effects in polar and tropical ecosystems (greater slopes without the spatial autocorrelation)

Supplementary material A.8: Final fitted models of trophic transfer efficiency and biomass residence time

The model is expressed as follow for trophic transfer efficiency (TTE) and biomass residence time (BRT):

$$TTE = e^{(-2.162+SST(-0.025+a)+b)} \times e^{\frac{\alpha^2(TTE)}{2}} \quad BRT = e^{(-1.761+SST(-0.075+c)+d)} \times e^{\frac{\alpha^2(BRT)}{2}}$$

where a, b, c and d are specific parameters for each type of ecosystem (Table A.8.1) and $\alpha^2(TE)$ and $\alpha^2(BT)$ are the standard errors associated with the log-normal models to correct the bias due to the log-transformation such as $e^{\frac{\alpha^2(TTE)}{2}} = 1.038013$ and $e^{\frac{\alpha^2(BRT)}{2}} = 1.076283$ (Laurent, 1963).

Table A.8.1: Parameters to estimate trophic transfer efficiency and biomass residence time in each type of ecosystem.

Ecosystem type	Trophic transfer efficiency		Biomass residence time	
	a	b	c	d
Polar	0	0	0	0
Temperate	-0.013	0.142	0.050	-0.428
Tropical	0.015	-0.352	0.004	0.711
Upwelling	-0.032	0.167	0.070	-0.677

Table A.8.2: total deviance explained by the trophic transfer efficiency and biomass residence time models and deviance explained by each covariate, SST, ecosystem type, SST x ecosystem type.

	SST	Ecosystem type	SST x Ecosystem type	TOTAL
Trophic transfer efficiency	34.7 %	3.9 %	1.5 %	40.1 %
Biomass residence time	46.6 %	0.4 %	1.9 %	48.9 %

The appropriateness of the final fitted models is assessed graphically, based on figures A.8.1 and A.8.2, for TTE and BRT respectively.

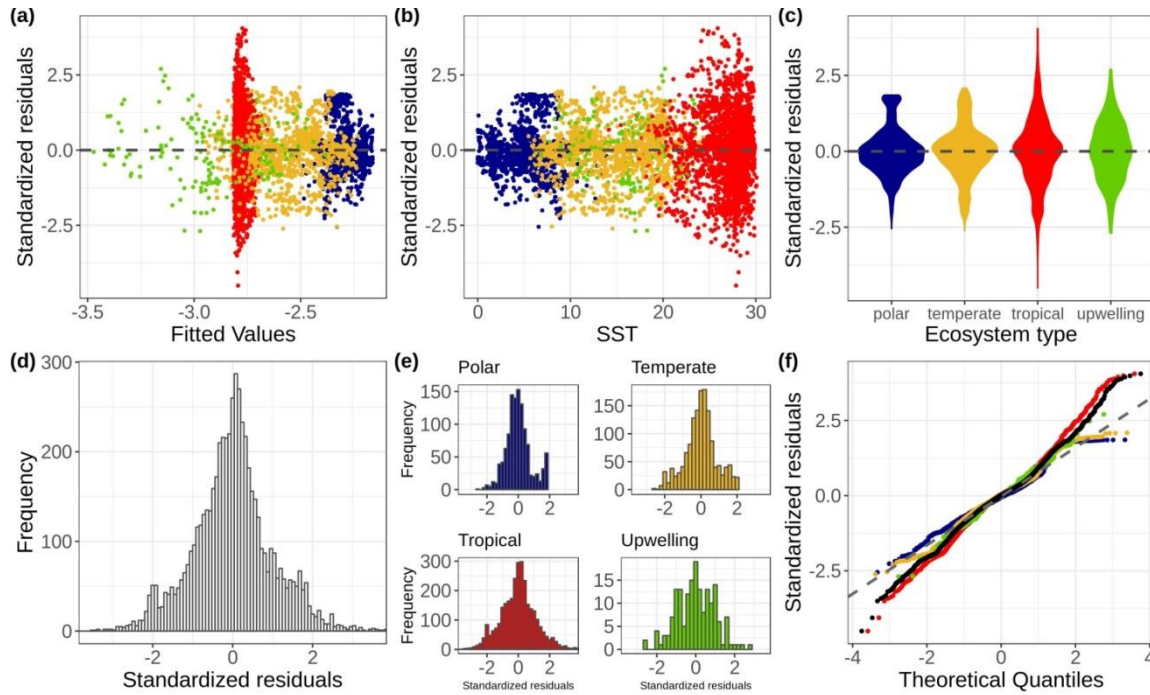


Figure A.8.1: Standardized residuals for the trophic transfer efficiency model. Panel (a) represents the standardized residuals versus the fitted values. Panels (b) and (c) refer to the standardized residuals versus SST and ecosystem type categories, respectively. The global distribution of the standardized residuals is represented on (d) and their distribution for each ecosystem type on (e). Panel (f) is the residuals normal Q–Q plot with the Q–Q line (dashed line). The colors refer to the ecosystem types: polar (in blue), temperate (in orange), tropical (in red) and upwelling (in green).

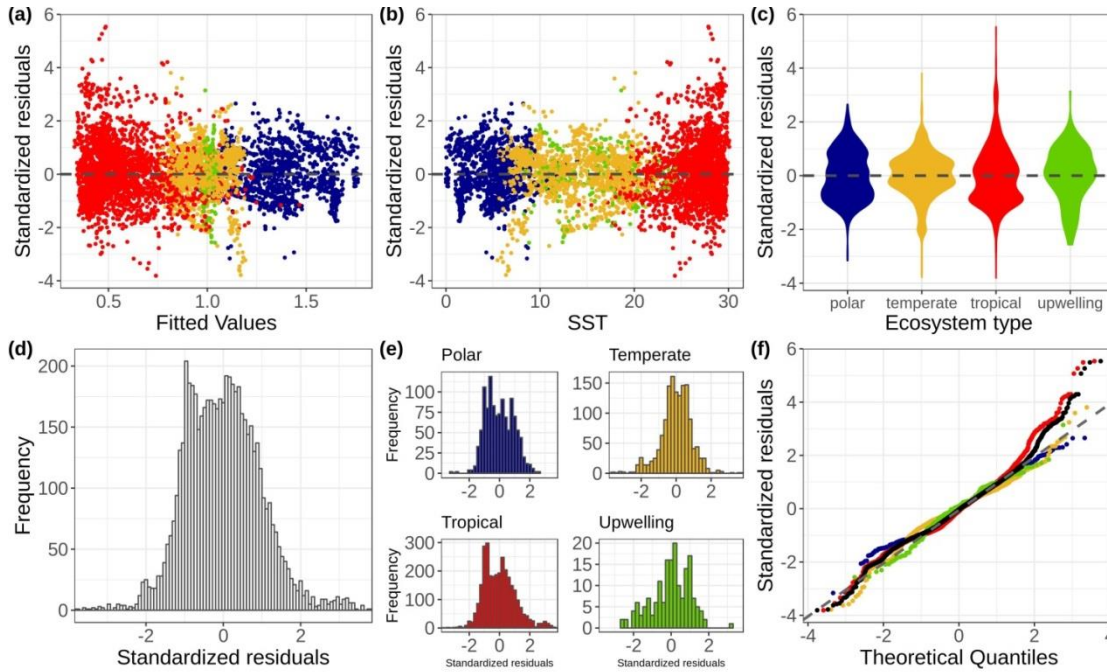


Figure A.8.2: Standardized residuals for the biomass residence time model. Panel (a) represents the standardized residuals versus the fitted values. Panels (b) and (c) refer to the standardized residuals versus SST and ecosystem type categories, respectively. The global distribution of the standardized residuals is represented on (d) and their distribution for each ecosystem type on (e). Panel (f) is the residuals normal Q-Q plot with the Q-Q line (dashed line). The colors refer to the ecosystem types: polar (in blue), temperate (in orange), tropical (in red) and upwelling (in green).

Supplementary material A.9: Past trend in the trophic transfer efficiency and biomass residence time, in each ecosystem type

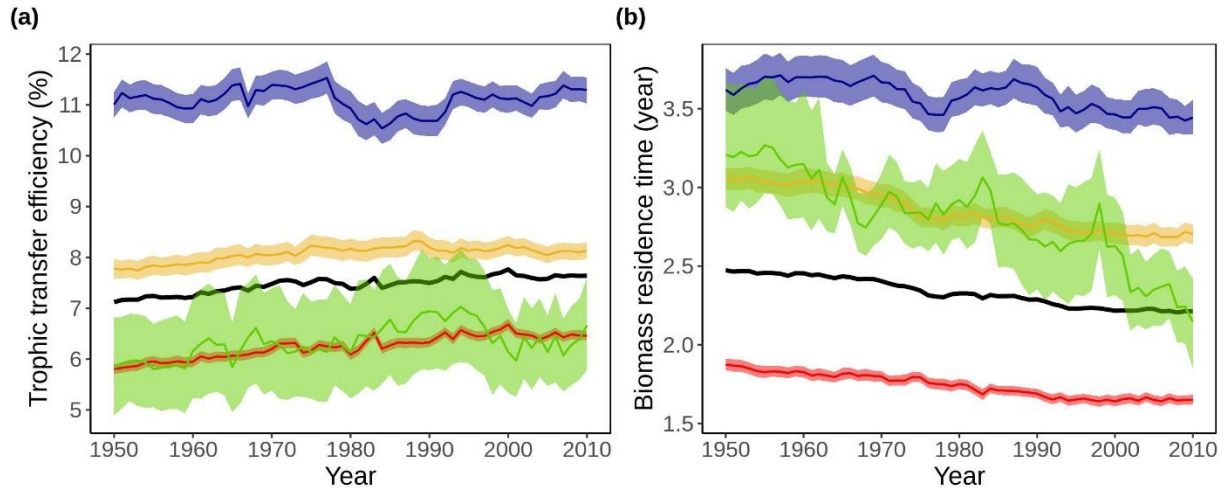


Figure A.9: Mean values of the observed past trend in trophic transfer efficiency and biomass residence time in each ecosystem type. The colors refer to the ecosystem types: polar (in blue), temperate (in orange), tropical (in red) and upwelling (in green). Shaded areas refer to bootstrap confidence intervals at 95%.

The analyses by ecosystem type shows that the trophic transfer efficiency increased in all ecosystem type, except in polar, while biomass transfers became faster everywhere, and especially in upwelling ecosystems.

Appendix B – Chapter 3

Supplementary material B.1: Details regarding the EcoTroph model

In EcoTroph, the trophic functioning of aquatic ecosystems is modelled as a continuous biomass flow surging up the food web, from lower to upper trophic levels (TLs), through predation and ontogenic processes (Gascuel 2005; Gascuel & Pauly 2009; Gascuel *et al.* 2011). Besides, the structure of the ecosystem is represented by the continuous biomass distribution along TLs, called, biomass trophic spectrum (Gascuel *et al.* 2005). In this approach, individual “species” disappear and are instead combined into classes based only on their TLs.

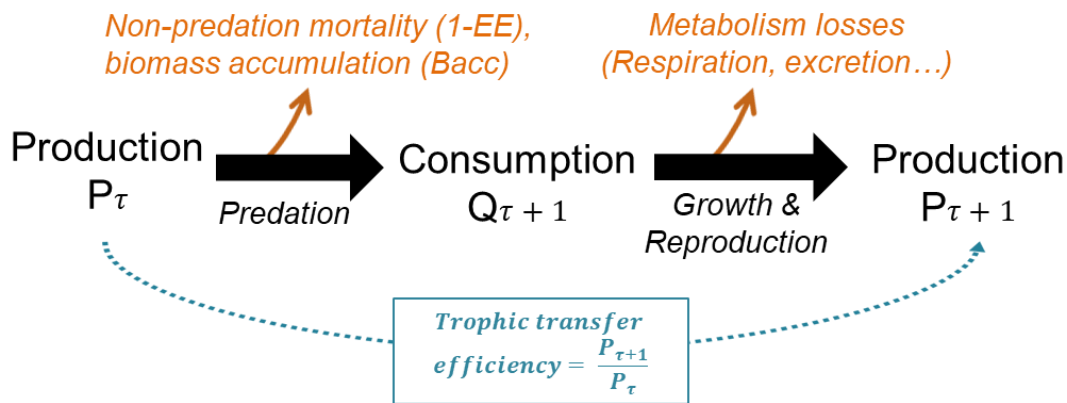


Figure B.1.1: Schematic representation of biomass flow parameters between two trophic levels (TLs). Black arrows represent energy transfers. The prey has a TL τ and the predator has a TL $(\tau + 1)$ (derived from du Pontavice, 2019; Gascuel *et al.*, 2008; Maureaud *et al.*, 2017).

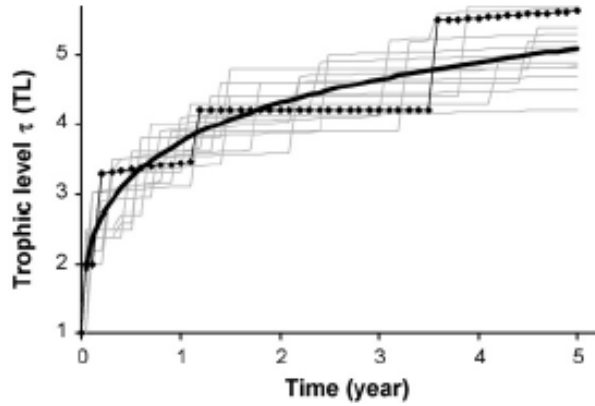


Figure B.1.2: Illustration of the transition from a discrete to continuous representation of biomass flow in an ecosystem. Grey broken lines refer to the trajectories of single particles along trophic levels, while the continuous line refers to the mean trajectory of biomass flow from low to upper trophic levels. (From Gascuel et al. 2008)

TABLE B.1: EcoTroph model: parameters definition and units.

bVariable	Parameter definition	Dimension (units)
$B(\tau)$	Density of biomass at time t and trophic level τ	Ton TL ⁻¹
$B\tau$	Biomass within the trophic class $[\tau, \tau + \Delta\tau[$	Ton
$\Phi(t, \tau)$	Biomass flow at trophic level τ	Ton year ⁻¹
Φ_τ	Mean biomass flow within the trophic class $[\tau, \tau + \Delta\tau[$	Tons year ⁻¹
$K(t, \tau)$	Flow kinetic expressed	TL year ⁻¹
K_τ	Mean flow kinetic within the trophic class $[\tau, \tau + \Delta\tau[$	TL year ⁻¹
μ_τ	Natural loss rate of biomass flow, in the trophic class $[\tau, \tau + \Delta\tau[$	TL ⁻¹
P_τ	production P_τ of the trophic class $[\tau, \tau + \Delta\tau[$	Tons TL year ⁻¹

B.1.1. A non-conservative biomass flow

the biomass flow $\Phi(\tau)$ is not conservative with a loss rate $\psi(\tau)$ at TL = τ , such as:

$$\frac{d\Phi(\tau)}{d\tau} = -\psi(\tau) \Phi(\tau) \quad \text{A.3}$$

Therefore, we calculated the biomass flow equations from Equation (A3):

$$\int_{\tau}^{\tau+\Delta\tau} \frac{1}{\Phi(\tau)} \frac{d\Phi(\tau)}{d\tau} d\tau = \int_{\tau}^{\tau+\Delta\tau} -\psi(\tau) d\tau \quad \text{A.4}$$

$$\ln (\Phi(\tau + \Delta\tau)) - \ln (\Phi(\tau)) = -\psi_{\tau}\Delta\tau \quad \text{A.5}$$

$$\Phi(\tau + \Delta\tau) = \Phi(\tau)e^{-\psi_{\tau}\Delta\tau} \quad \text{A.6}$$

In the present study, the mean loss rate, ψ_{τ} , (expressed in TL^{-1}), within the trophic class $[\tau, \tau + \Delta\tau[$ represents the mean natural losses, μ_{τ} (expressed in TL^{-1}), within the trophic class $[\tau, \tau + \Delta\tau[$ through non-predation mortality, excretion, and respiration. It implies that the biomass flow at a given TL depends on the flow from lower TLs. It also defines the transfer efficiency, TE, within the trophic class $[\tau, \tau + \Delta\tau[$ such as $\text{TE} = \exp(-\mu_{\tau})$. Hence, by replacing;

$$\Phi(\tau + \Delta\tau) = \Phi(\tau)e^{-\mu_{\tau}\Delta\tau} \quad \text{A.7}$$

B.1.2. Discrete approximation of biomass

A discrete approximation of the continuous distribution $B(\tau)$ is used for mathematic al simplification. Hence, the model state variable becomes B_{τ} , the biomass (in tons) under steady-state conditions in the $[\tau, \tau + \Delta\tau[$ trophic class. Equation (A.2) becomes:

$$B_{\tau} = \int_{\tau}^{\tau+\Delta\tau} B(\tau) = \int_{\tau}^{\tau+\Delta\tau} \frac{\Phi(\tau)}{K(\tau)} d\tau = \frac{1}{K_{\tau}} \int_{\tau}^{\tau+\Delta\tau} \Phi(\tau) d\tau = \frac{1}{K_{\tau}} \Phi_{\tau} \Delta\tau \quad \text{A.9}$$

where Φ_{τ} and K_{τ} are the mean biomass flow (in $\text{tons} \cdot \text{year}^{-1}$) and the mean flow kinetic (in $\text{TL} \cdot \text{year}^{-1}$) within the trophic class $[\tau, \tau + \Delta\tau[$, respectively. Equation (A.9) indicates that biomass in the trophic class $[\tau, \tau + \Delta\tau[$, B_{τ} , can be deduced from two parameters: the mean biomass flow Φ_{τ} and mean flow kinetic K_{τ} .

Supplementary material B.2: Study area

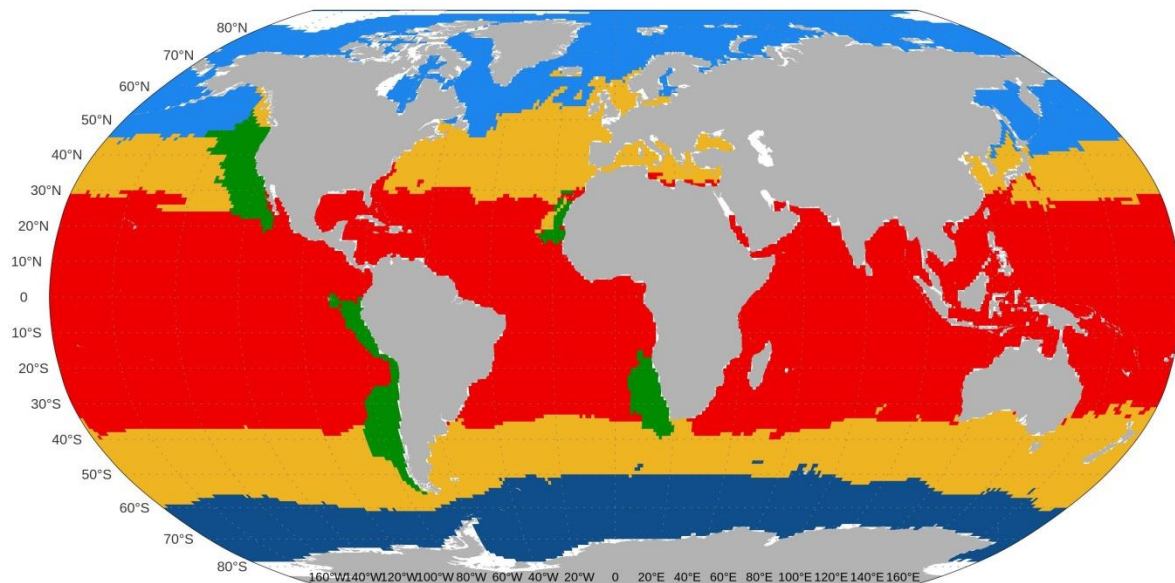


Figure B.2: Map of the areas represented in the dataset and the associated ecosystem types. The colors refer to the ecosystem types: Arctic (in light blue), Antarctic (in dark blue), temperate (in orange), tropical (in red) and upwelling (in green).

Supplementary material B.3: Transfer efficiency of low trophic levels

Method B.3: Approximation of the trophic efficiency for low trophic levels for RCP 2.6. As we did not have the COBALT outputs for RCP2.6, we approximated the amount of biomass which is transfer between NPP and mesozooplankton using the COBALT outputs for RCP8.5. We assumed that the transfer efficiency for low trophic levels for RCP2.6 and RCP8.5 follow the trend than the sea surface temperature (Figure S3.1).

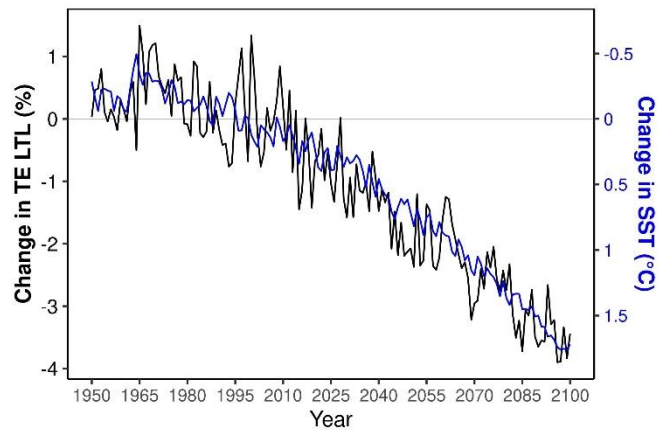


Figure B.3.1: Change in TE LTL (transfer efficiency for low trophic levels; black line and axis) and SST (sea surface temperature; blue line and axis) for GFDL and under RCP8.5 between 1950 and 2100 relative to the reference period 1986-2005.

Thus, we first determined the year from which the global trends in SST for RCP2.6 and RCP8.5 diverge using the differences between two trends (“y” axis on Figure B.3.2). The trends in SST for both scenarios are similar until 2030 (i.e., the difference fluctuates around 0) and then the trends start to diverge between 2030 and 2040 (i.e., the difference increases). Since the difference between the trends seems to be linear, we determined the breaking point by modelling two linear models:

- one model for the first period when the differences fluctuate around 0
- one model for the second period when the difference is positive

We optimized simultaneously the R-squared of the two models and we found a breaking point in 2031.

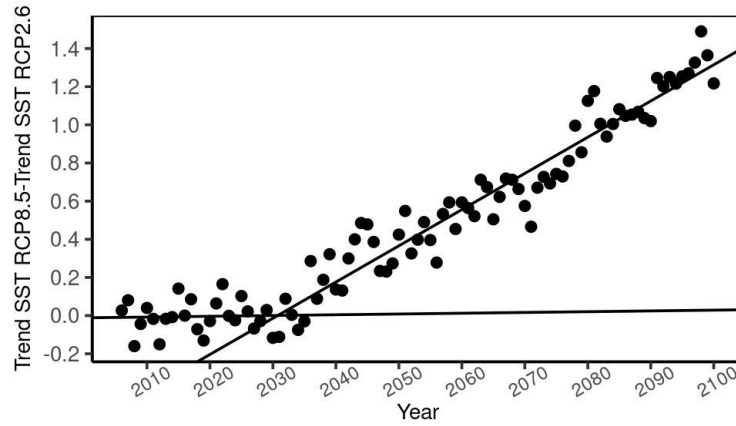


Figure B.3.2: Difference between delta SST (SST in [2090-2099] – SST in [1986-2005]) for RCP8.5 and RCP2.6 (black points). The two lines represent the two linear selected after and before 2031.

Then, we estimated TE LTL for RCP2.6:

- before 2031, using TE LTL estimate s for RCP 8.5 and,
- after 2031, using the average of TE LTL around 2031 (between 2026-2036).

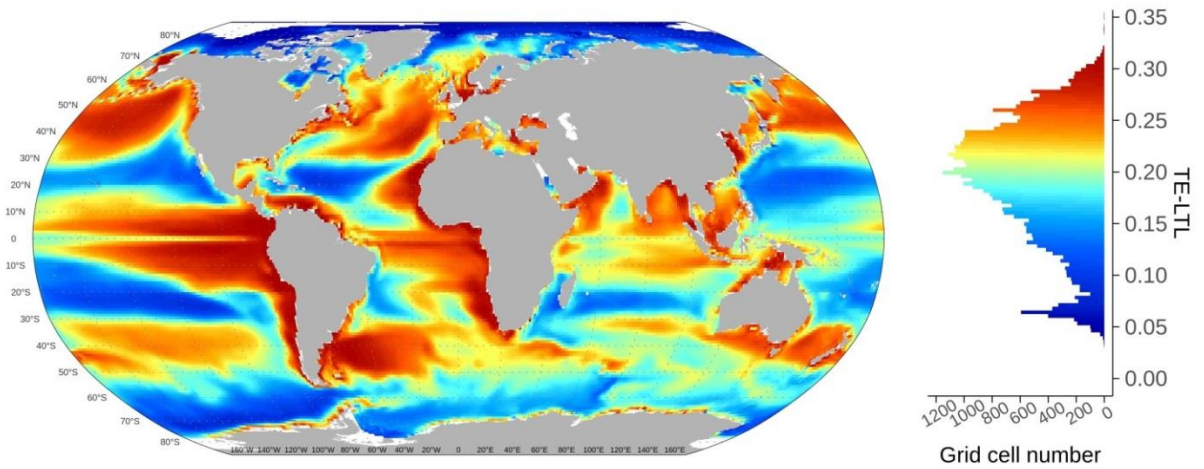


Figure B.3.3: Mean transfer efficiency of the planktonic food web for the period 1986-2005. It is estimated from the planktonic food web COBALT model developed by Stock et al. (2014a, b) (see Methods in the main text).

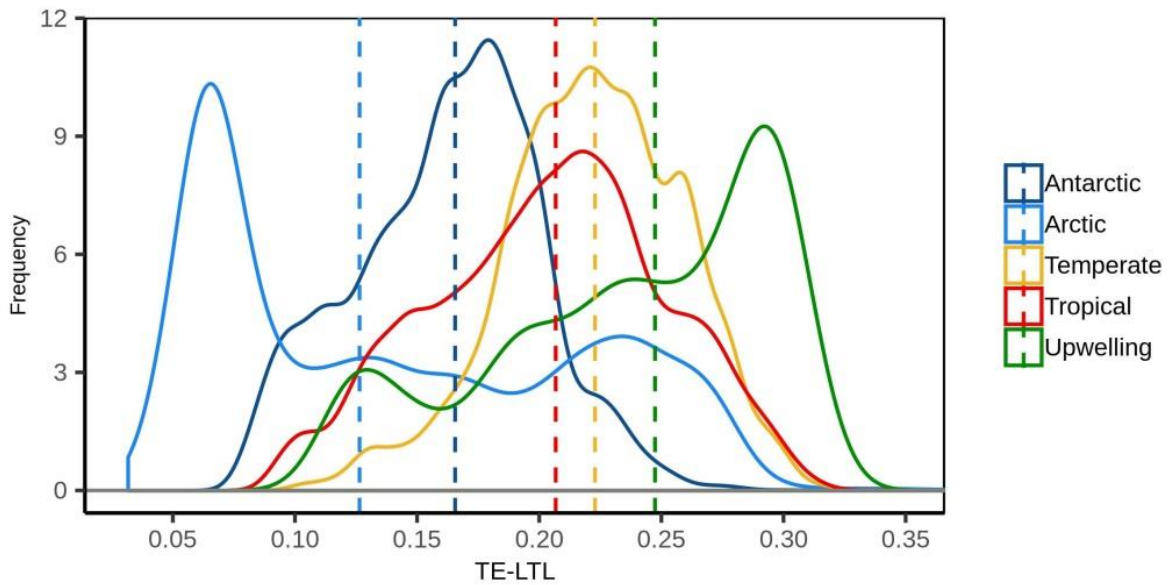


Figure B.3.4: Distribution of TE LTL in each ecosystem type for the period 1986-2005. The vertical lines represent the median TE LTL for each ecosystem type.

Supplementary material B.4: Transfer efficiency of higher trophic levels

Table B.4: Specific parameters to estimate trophic transfer efficiency of higher trophic levels for each type of ecosystem (equation (9), in the Methods section).

Ecosystem type	Trophic transfer efficiency coefficient	
	a	b
Polar	0	0
Temperate	-0.013	0.142
Tropical	0.015	-0.352
Upwelling	-0.032	0.167

Supplementary material B.5: Inter-model variability of the biomass estimates

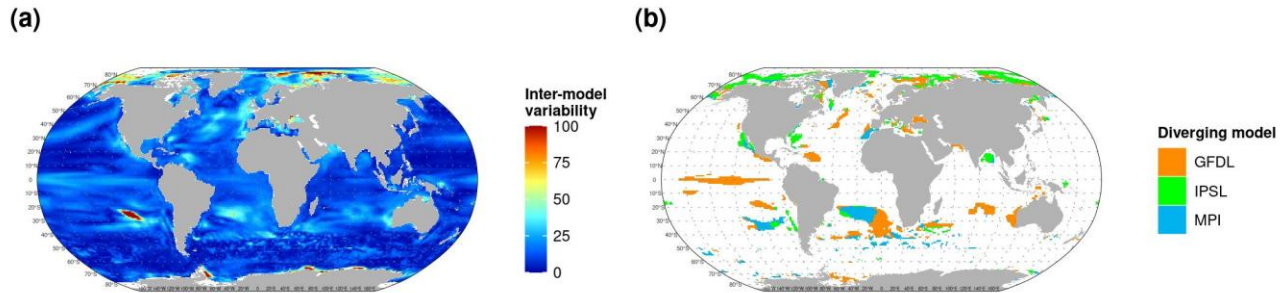


Figure B.5: Inter-model variability of the changes in total consumer biomass under RCP 8.5 in 2090-2099 relative to 1986-2005. Panel (a) represents the variability of the projected changes of biomass among the models (Coefficient of variation in %). Panel (b) shows the grid cells where the three models do not predict the same direction of changes. The color in each grid cell refers to the model that predicts changes in biomass in the opposite direction to those predicted by the two other models.

Supplementary material B.6: Comparison of the EcoTroph projections with the Fish-MIP projections

In a recent compilation of marine ecosystem models developed for the Fisheries and Marine Ecosystem Model Intercomparison Project (Fish-MIP), projections of total consumer biomass was estimated on a global scale by 2100 (Tittensor *et al.* 2018; Lotze *et al.* 2019). In order to test the relevancy of the global changes in total consumer biomass, we compared our results with the total consumer biomass projections coming from five ecosystem models (APECOSM, DBEM, BOATS, EcoOcean and Macroecological model) developed in Fish-MIP (Lotze *et al.* 2019). The comparison of projections was conducted between 1970 and 2100 relative to the reference period 1986–2005 using RCP8.5 with IPSL (Figure B.6).

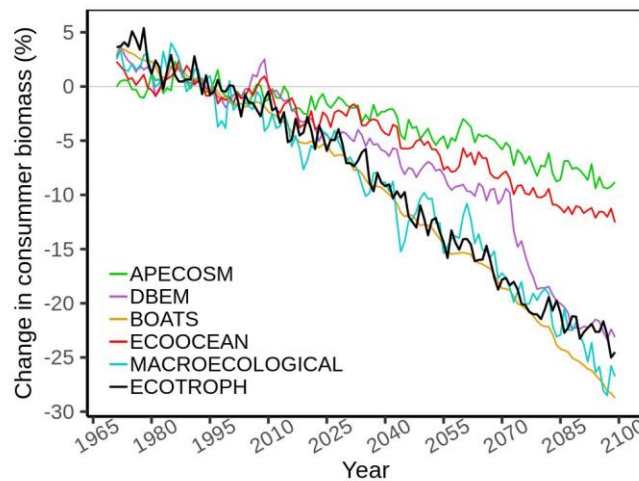


Figure B.6: Comparison of the EcoTroph projections with the Fish-MIP projections. Changes in total consumer biomass between 1970 and 2100 relative to the reference period 1986–2005 for 5 ecosystem models and for EcoTroph, for RCP8.5 and with the earth system model IPSL.

We found that the decline in total consumer biomass projected by EcoTroph is consistent with the range of changes in biomass estimated from the Fish-MIP models, EcoTroph projections follow the same trend than the projected of Macroecological models and BOATS models with a slowing down of the decline in the late 2080s.

Supplementary material B.7: Changes in sea surface temperature

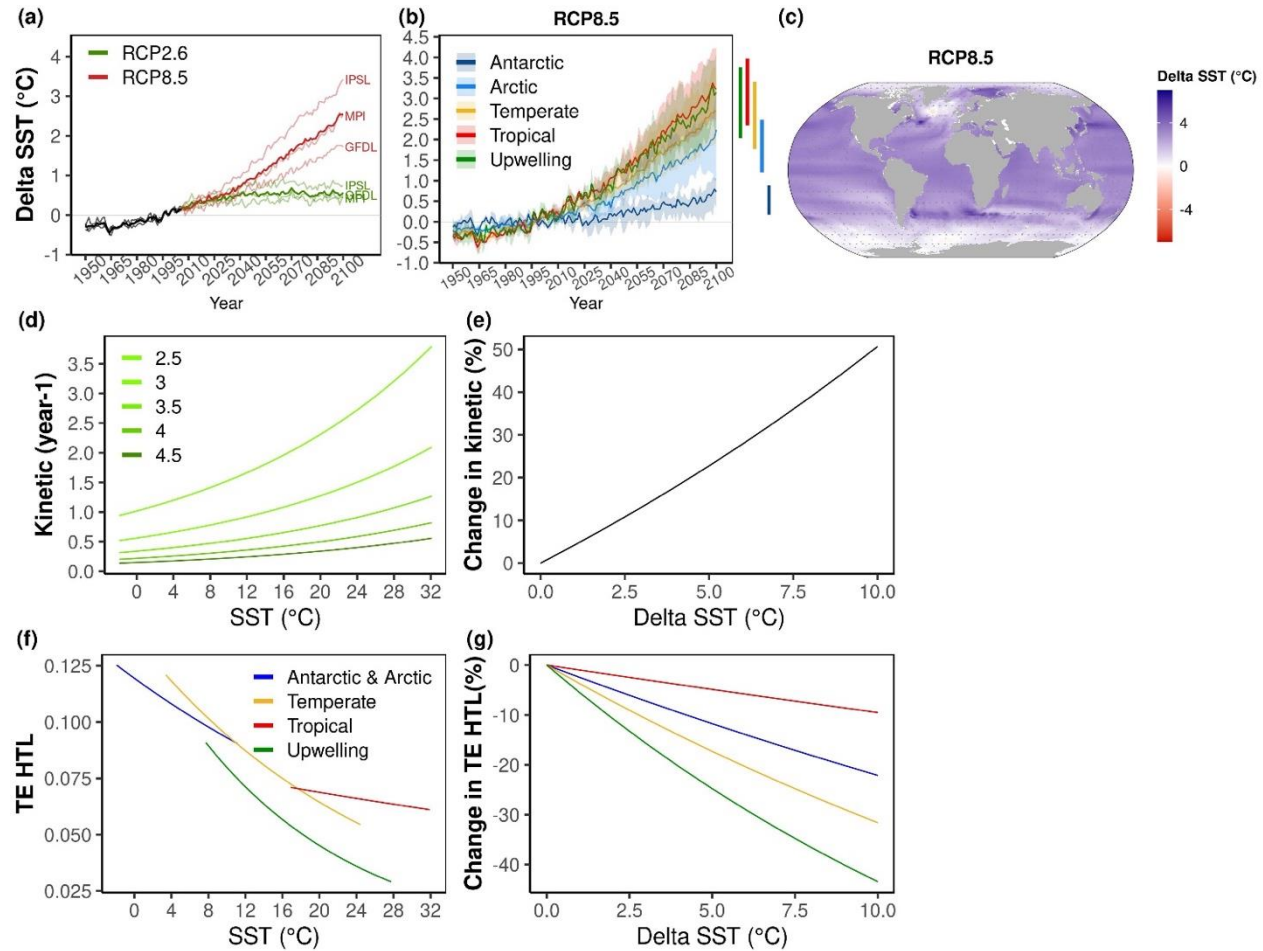


Figure B.7: Projected changes in sea surface temperature (SST) between 1950 and 2100 relative to 1986–2005. Panel (a) represents the changes in SST at global scale for RCP2.6 and RCP8.5. Panel (b) represents the change in each ecosystem type under RCP8.5. The shaded areas around the curves in (b) indicate the inter-model variability and the colour bars outside the box indicate the range of averaged changes of the three Earth system models over 2090–2099. Panel (c) represents the change over the period 2090–2099 in each $1^\circ \times 1^\circ$ grid cell. Panels (d) and (f), show the relationships between SST and, flow kinetic (Gascuel et al., 2008) and TE HTL (transfer efficiency of higher trophic levels; du Pontavice et al., 2020), respectively. Panels (e) and (g), represent the warming effects (from 0 to 10°C increase) on flow kinetic and TE HTL, respectively. In panel (d), the different curves represent the temperature effect on flow kinetic for five trophic levels since flow kinetic depends on temperature and trophic level. Supplementary material B.8: Contribution of each biomass flow parameters to the changes in total biomass consumer for the three Earth system models.

Supplementary material B - References

- du Pontavice, H. (2019). Changing biomass flows in marine ecosystems : From the past to the future. In *Predicting Future Oceans* (p. 121-128). Elsevier. <https://doi.org/10.1016/B978-0-12-817945-1.00012-5>
- Gascuel, D. (2005). The trophic-level based model : A theoretical approach of fishing effects on marine ecosystems. *Ecological Modelling*, 189(3-4), 315-332. <https://doi.org/10.1016/j.ecolmodel.2005.03.019>
- Gascuel, D., Bozec, Y., Chassot, E., Colomb, A., & Laurans, M. (2005). The trophic spectrum : Theory and application as an ecosystem indicator. *ICES Journal of Marine Science*, 62(3), 443-452. <https://doi.org/10.1016/j.icesjms.2004.12.013>
- Gascuel, D., Guenette, S., & Pauly, D. (2011). The trophic-level-based ecosystem modelling approach : Theoretical overview and practical uses. *ICES Journal of Marine Science*, 68(7), 1403-1416. <https://doi.org/10.1093/icesjms/fsr062>
- Gascuel, D., Morissette, L., Palomares, M. L. D., & Christensen, V. (2008). Trophic flow kinetics in marine ecosystems : Toward a theoretical approach to ecosystem functioning. *Ecological Modelling*, 217(1-2), 33-47. <https://doi.org/10.1016/j.ecolmodel.2008.05.012>
- Gascuel, D., & Pauly, D. (2009). EcoTroph : Modelling marine ecosystem functioning and impact of fishing. *Ecological Modelling*, 220(21), 2885-2898. <https://doi.org/10.1016/j.ecolmodel.2009.07.031>
- Lotze, H. K., Tittensor, D. P., Bryndum-Buchholz, A., Eddy, T. D., Cheung, W. W. L., Galbraith, E. D., Barange, M., Barrier, N., Bianchi, D., Blanchard, J. L., Bopp, L., Büchner, M., Bulman, C. M., Carozza, D. A., Christensen, V., Coll, M., Dunne, J. P., Fulton, E. A., Jennings, S., ... Worm, B. (2019). Global ensemble projections reveal trophic amplification of ocean biomass declines with climate change. *Proceedings of the National Academy of Sciences*, 116(26), 12907-12912. <https://doi.org/10.1073/pnas.1900194116>
- Maureaud, A., Gascuel, D., Colléter, M., Palomares, M. L. D., Du Pontavice, H., Pauly, D., & Cheung, W. W. L. (2017). Global change in the trophic functioning of marine food webs. *PLOS ONE*, 12(8), e0182826. <https://doi.org/10.1371/journal.pone.0182826>
- Tittensor, D. P., Eddy, T. D., Lotze, H. K., Galbraith, E. D., Cheung, W. W. L., Barange, M., Blanchard, J. L., Bopp, L., Bryndum-Buchholz, A., Büchner, M., Bulman, C., Carozza, D. A., Christensen, V., Coll, M., Dunne, J. P., Fernandes, J. A., Fulton, E. A., Hobday, A. J., Huber, V., ... Walker, N. D. (2018). A protocol for the intercomparison of marine fishery and ecosystem models : Fish-MIP v1.0.

Geoscientific Model Development, 11(4), 1421-1442. <https://doi.org/10.5194/gmd-11-1421-2018>

Appendix C – Chapter 4

Supplementary material C.1: Sensitivity analysis regarding the top down control

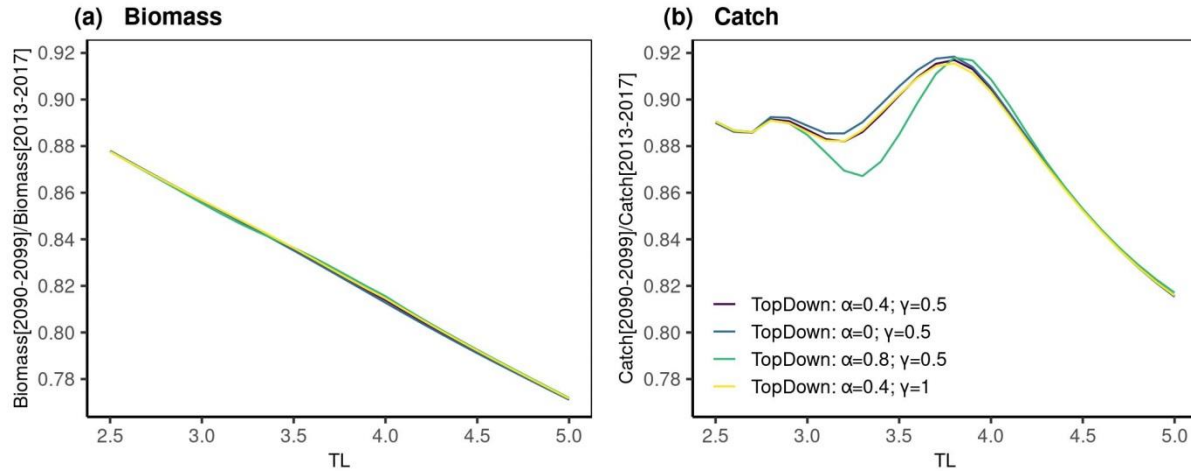


Figure C.1.1: Global projected changes in biomass and catch at each trophic level in 2090-2099 relative to 2013-2017 for four top down configurations ($\alpha=0.4$ and $\gamma=0.5$; $\alpha=0$ and $\gamma=0.5$; $\alpha=0.8$ and $\gamma=0.5$; $\alpha=0.4$ and $\gamma=1$). The change in biomass (a) and catch (b) are presented the simulation where fishing mortality is constant and equal to its value in 2013-2017 for RCP8.5.

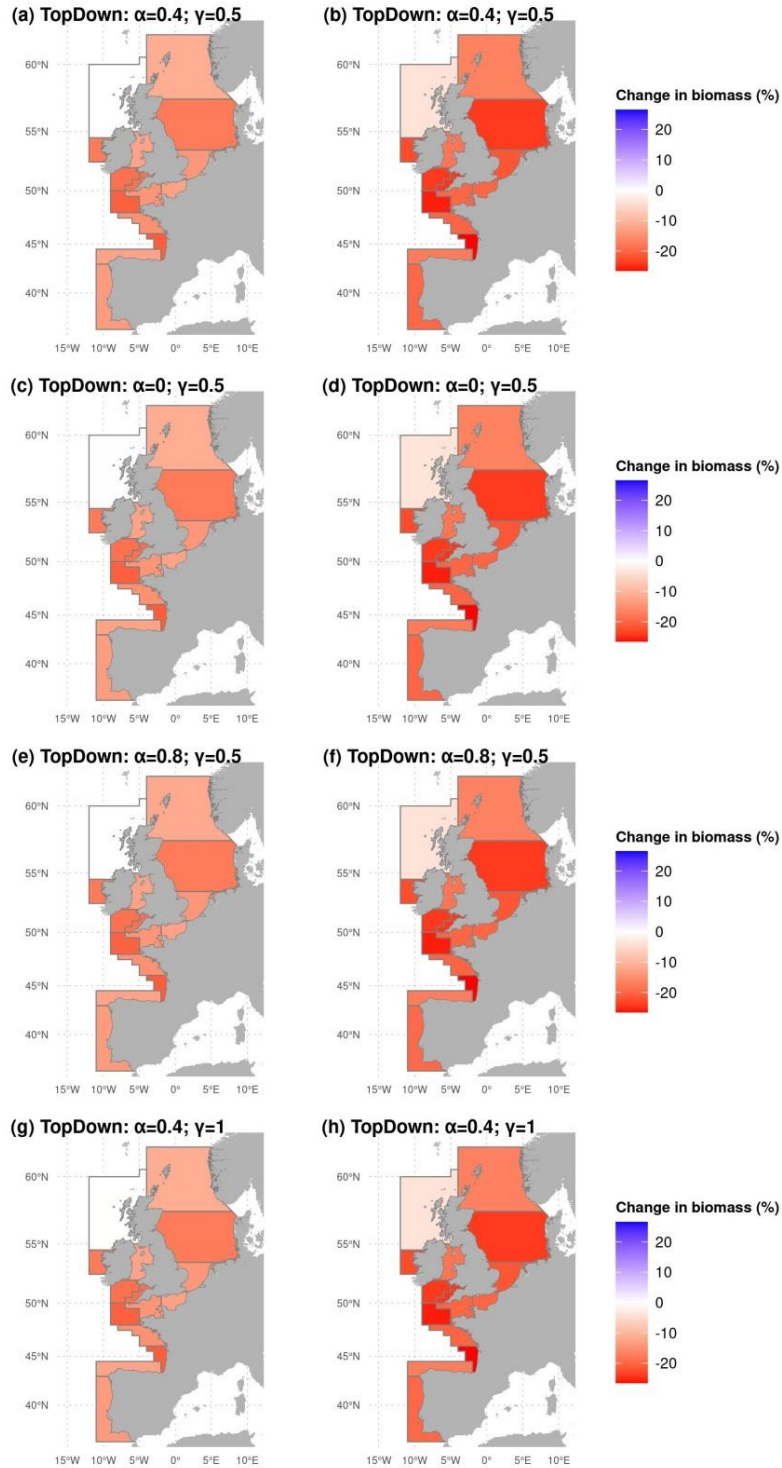


Figure C.1.2: Maps of the changes in biomass in 2090-2099 relative to 2013-2017 for four top down configurations: ($\alpha=0.4$ and $\gamma=0.5$; $\alpha=0$ and $\gamma=0.5$; $\alpha=0.8$ and $\gamma=0.5$; $\alpha=0.4$ and $\gamma=1$). The changes are aggregated between the trophic level 3 and 3.9 (a, c, e, g) and between the trophic level 4 and 5 (b, d, f, h). The changes were calculated with a constant fishing mortality equal to its value in 2013-2017 for RCP8.5. The displayed percentages for biomass (b, d, f, h) represent the percentage of amplification between the changes in biomass at the lower and the upper trophic levels.

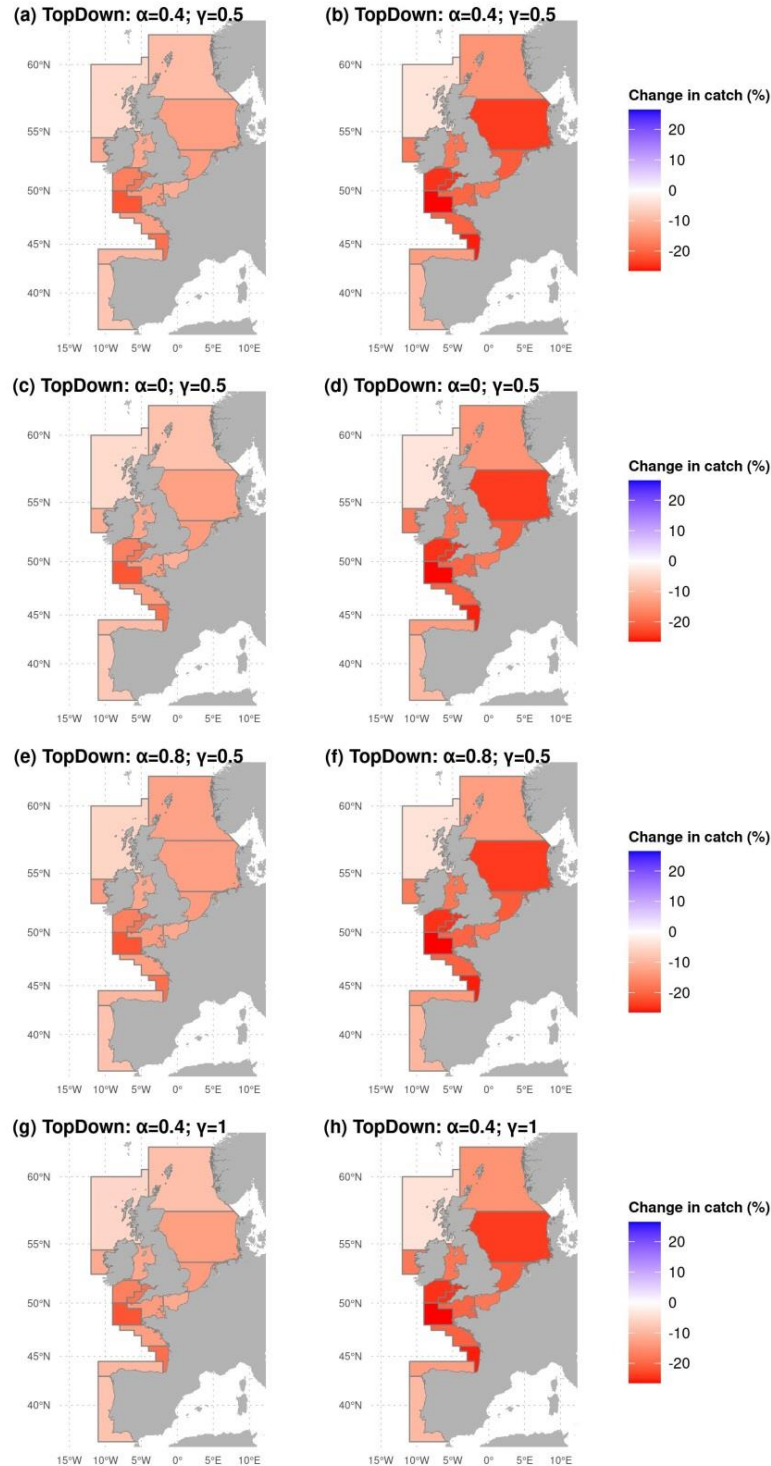


Figure C.1.3: Maps of the changes in catch in 2090-2099 relative to 2013-2017 for four top down configurations: ($\alpha=0.4$ and $\gamma=0.5$; $\alpha=0$ and $\gamma=0.5$; $\alpha=0.8$ and $\gamma=0.5$; $\alpha=0.4$ and $\gamma=1$). The changes are aggregated between the trophic levels 2.5 and 3.5 (a, c, e, g) and between the trophic level 4 and 5 (b, d, f, h). The changes were calculated with a constant fishing mortality equal to its value in 2013-2017 for RCP8.5. The displayed percentages (b, d, f, h) represent the percentage of amplification between the changes in catch at the lower and the upper trophic levels.

Supplementary material C.2: Sensitivity analysis regarding the benthic-pelagic coupling

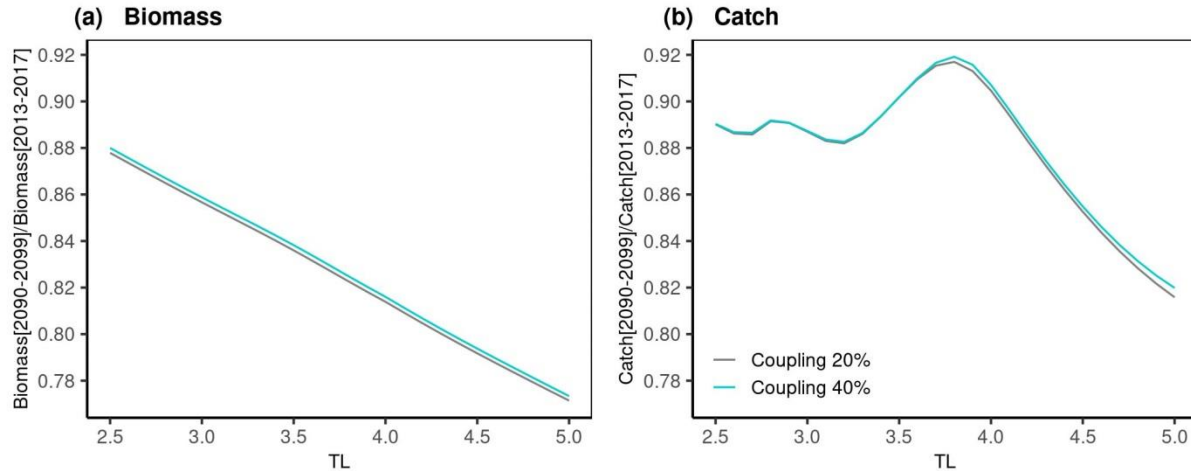


Figure C.2.1: Global projected changes in biomass and catch at each trophic level in 2090-2099 relative to 2013-2017 for a coupling parameter of 20% (coupling parameter of the study) and at 40% (coupling parameter for the sensitivity analysis). The change in biomass (a) and catch (b) are presented the simulation where fishing mortality is constant and equal to its value in 2013-2017 for RCP8.5.

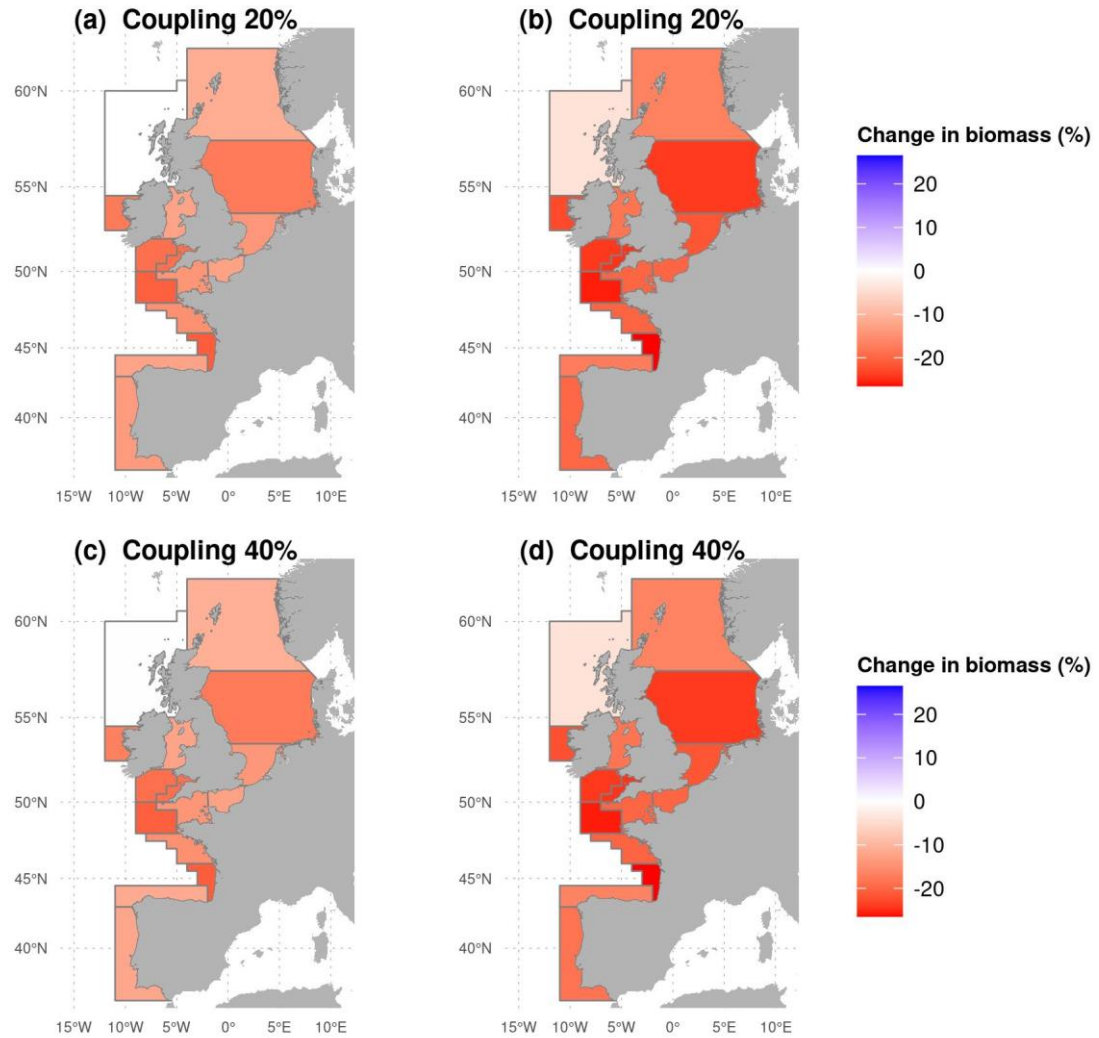


Figure C.2.2: Maps of the changes in biomass in 2090-2099 relative to 2013-2017 for a coupling parameter à 20% (coupling parameter of the study) and at 40% (coupling parameter for the sensitivity analysis). The changes are aggregated between the trophic level 2.5 and 3.5 (a, c) and between the trophic level 4 and 5 (b, d). The changes were calculated with a constant fishing mortality equal to its value in 2013-2017 for RCP8.5. The displayed percentages for biomass (b, d) represent the percentage of amplification between the changes in biomass at the lower and the upper trophic levels.

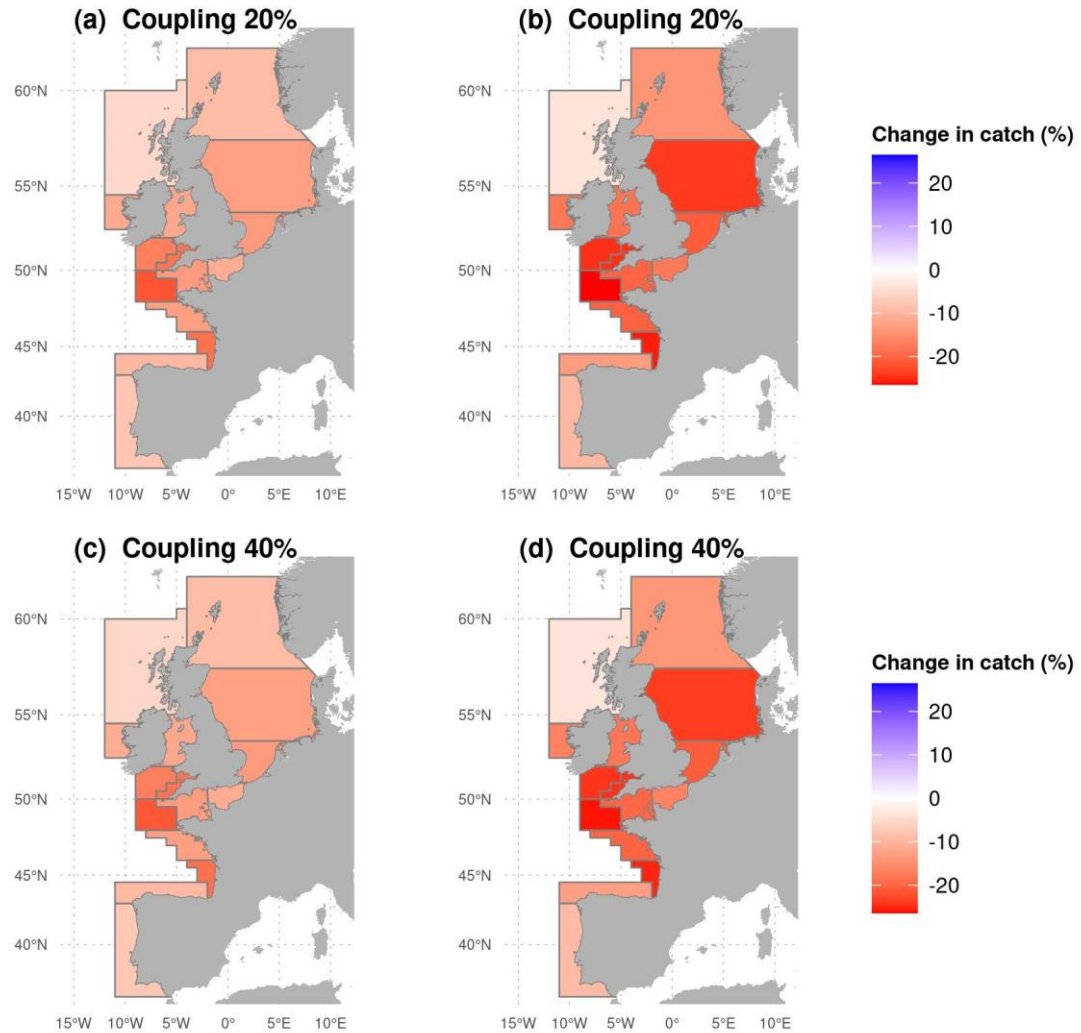


Figure C.2.3: Maps of the changes in catch in 2090-2099 relative to 2013-2017 for a coupling parameter à 20% (coupling parameter of the study) and at 40% (coupling parameter for the sensitivity analysis). The changes are aggregated between the trophic level 2.5 and 3.5 (a, c) and between the trophic level 4 and 5 (b, d). The changes were calculated with a constant fishing mortality equal to its value in 2013-2017 for RCP8.5. The displayed percentages for biomass (b, d) represent the percentage of amplification between the changes in catch at the lower and the upper trophic levels.

Supplementary material C.3: Projected changes in production of secondary producers and sea surface temperature

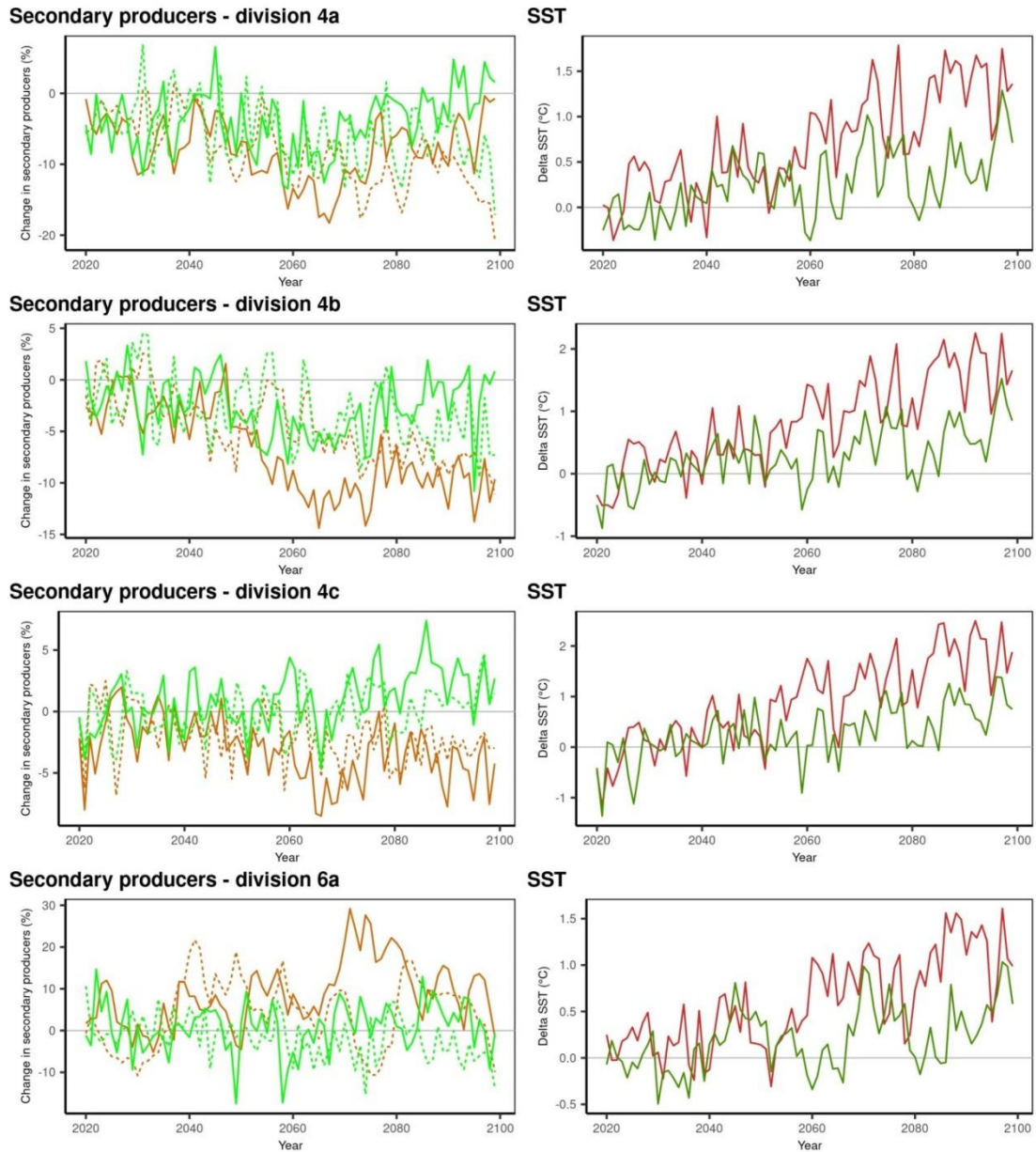


Figure C.3.1: Projected changes in production of secondary producers (left column) and sea surface temperature (SST; right column) between 2020 and 2100 relative to the reference period 2013-2017 for the ICES divisions 4a, 4b, 4c, 6a. The production is divided into the pelagic zooplankton group (in green) and the benthic fauna group (in brown) and the changes are presented for two scenarios RCP4.5 (dotted lines) and RCP8.5 (solid lines). The changes in SST are presented for the two scenarios RCP4.5 (green) and RCP8.5 (red).

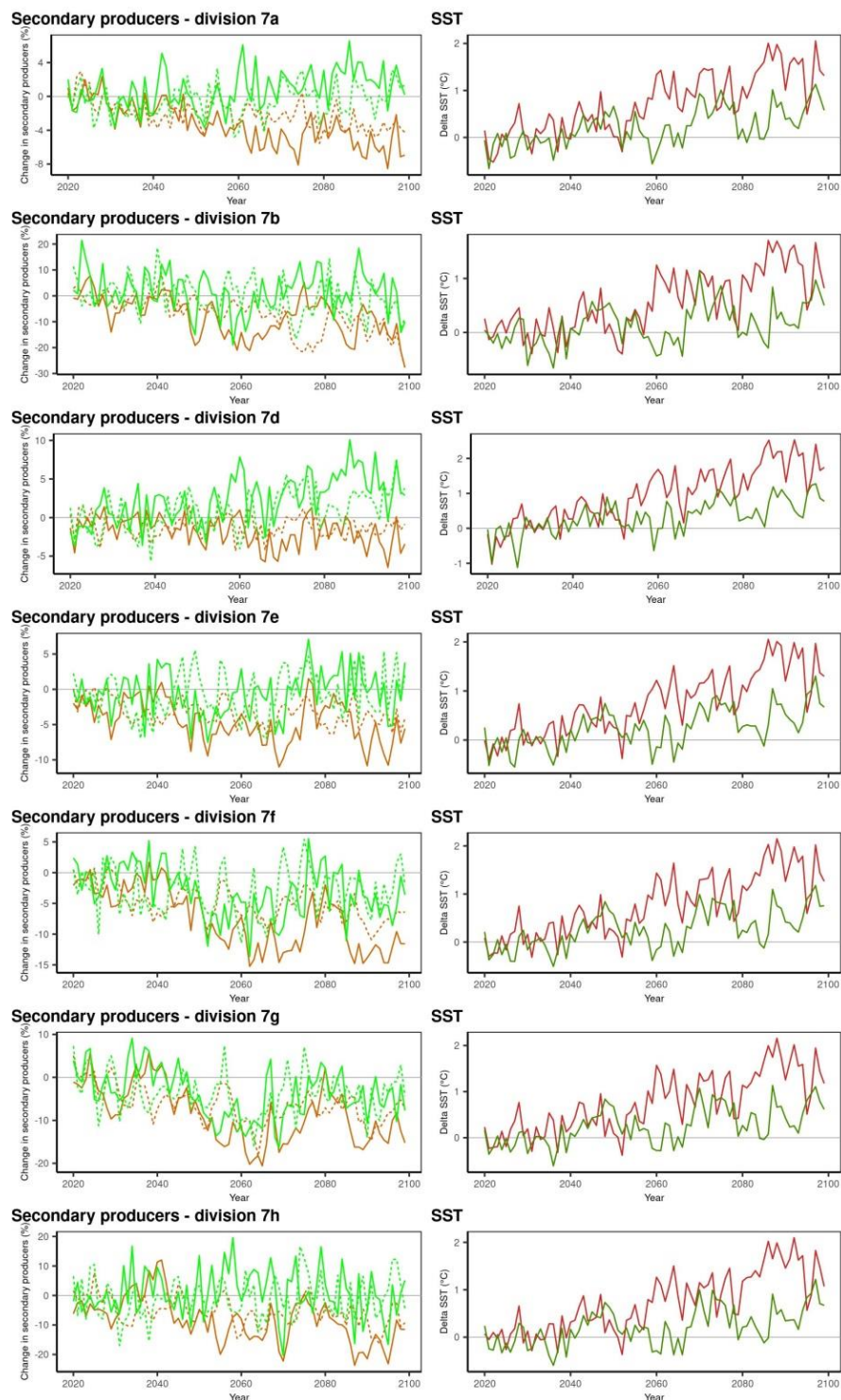
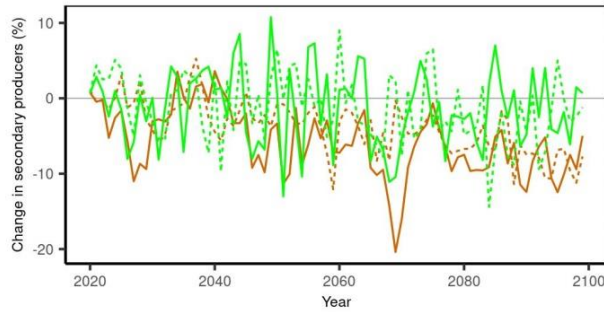
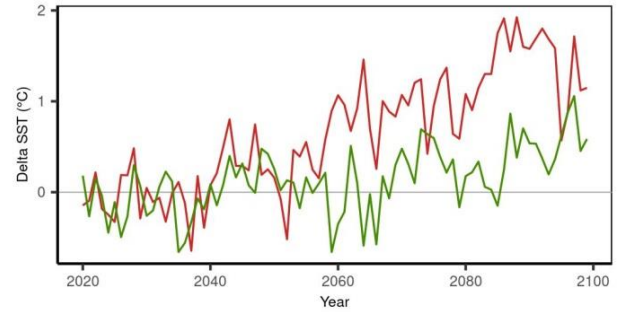


Figure C.3.2: Projected changes in production of secondary producers (left column) and sea surface temperature (SST; right column) between 2020 and 2100 relative to the reference period 2013-2017 for the ICES divisions 7a, 7b, 7d, 7e, 7f, 7g and 7h. The production is divided into the pelagic zooplankton group (in green) and the benthic fauna group (in brown) and the changes are presented for the two scenarios RCP4.5 (dotted lines) and RCP8.5 (solid lines). The changes in SST are presented for the two scenarios RCP4.5 (green) and RCP8.5 (red).

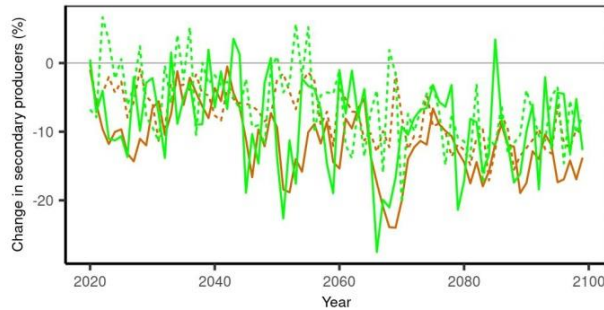
Secondary producers - division 8a



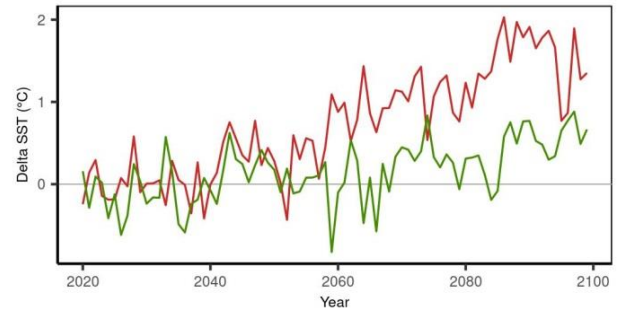
SST



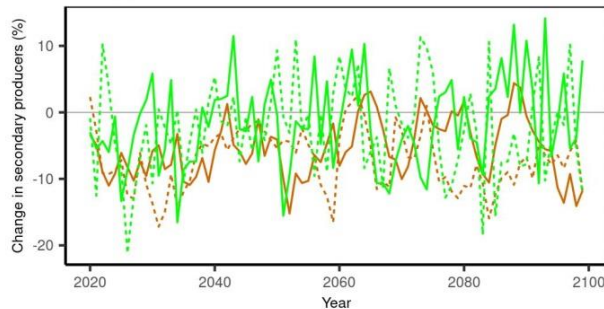
Secondary producers - division 8b



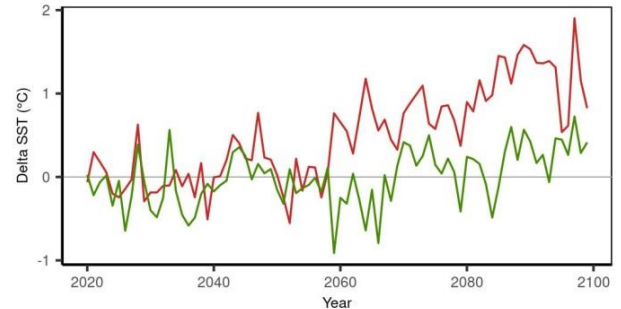
SST



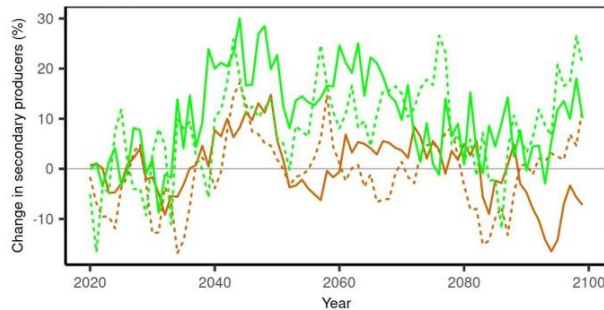
Secondary producers - division 8c



SST



Secondary producers - division 9a



SST

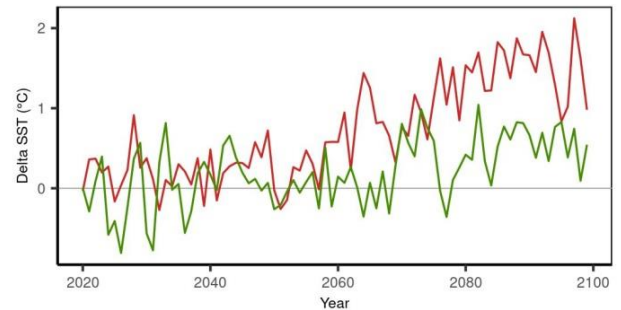


Figure C.3.3: Projected changes in production of secondary producers (left column) and sea surface temperature (SST; right column) between 2020 and 2100 relative to the reference period 2013-2017 for the ICES divisions 8a, 8b, 8c, 9a. The production is divided into the pelagic zooplankton group (in green) and the benthic fauna group (in brown) and the changes are presented for the two scenarios RCP4.5 (dotted lines) and RCP8.5 (solid lines). The changes in SST are presented for the two scenarios RCP4.5 (green) and RCP8.5 (red).

Supplementary material C.4: Reference state of the 15 ICES divisions for the period 2013-2017

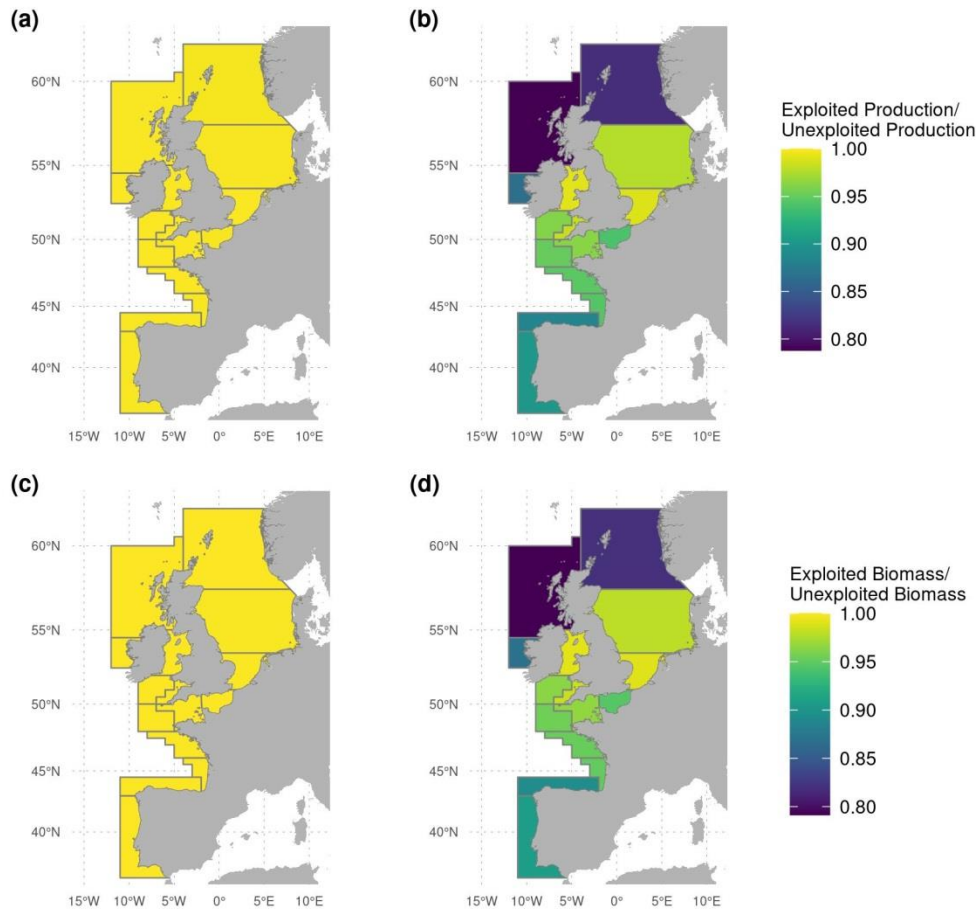


Figure C.4: Map of the ratio between the theoretical unexploited ecosystem and the exploited ecosystem in 2017-2017 for production (a and b) and for biomass (c and d) as well as for lower trophic levels (between TL=2.5 and TL=3.5) (a and c) and for upper trophic levels (between TL=4 and TL=5) (b and d).

The values of the ratio of exploited to unexploited biomass of the upper trophic levels (TLs) (between TL=4 and TL=5) vary between 0.99 and 0.79 (mean value at 0.93) and the ratio of exploited to unexploited production varies between 0.99 and 0.79 (mean value at 0.93). The most impacted areas are the northernmost divisions (4a, 6a and 7b) as well as southern division (8c and 9c). In parallel, the less affected areas are the Irish Seas (7a) and the South of the North Sea (4c). The biomass and production of the lower TLs between TL=2.5 and TL=3.5 appears very little affected by fishing

with a mean ratio exploited/unexploited close to 1. At low TLs, in the majority of the ICES divisions (10 to 15), biomass is even slightly enhanced by fishing due to a release of predation associated to a decrease in predators.

All these values of production and biomass must be analyzed cautiously because the fishing impacts appeared to be low compared to the levels of impact found in the literature (Gascuel *et al.* 2016; Moullec *et al.* 2017; STECF 2020). However, this study does not aim to assess accurately the fishing impacts in 2013-2017. Instead, we defined a reference state in 2013-2017 to explore the effects of climate relative to this state.

Gascuel, D., Coll, M., Fox, C., Guénette, S., Guitton, J., Kenny, A., *et al.* (2016). Fishing impact and environmental status in European seas: a diagnosis from stock assessments and ecosystem indicators. *Fish and Fisheries*, 17, 31–55.

Moullec, F., Gascuel, D., Bentorcha, K., Guénette, S. & Robert, M. (2017). Trophic models: What do we learn about Celtic Sea and Bay of Biscay ecosystems? *Journal of Marine Systems*, 172, 104–117.

STECF. (2020). *Scientific, Technical and Economic Committee for Fisheries (STECF): 62nd plenary meeting report (PLEN-19-03)*.

Supplementary material C.5: The drivers of the changes in biomass in the 15 ICES divisions

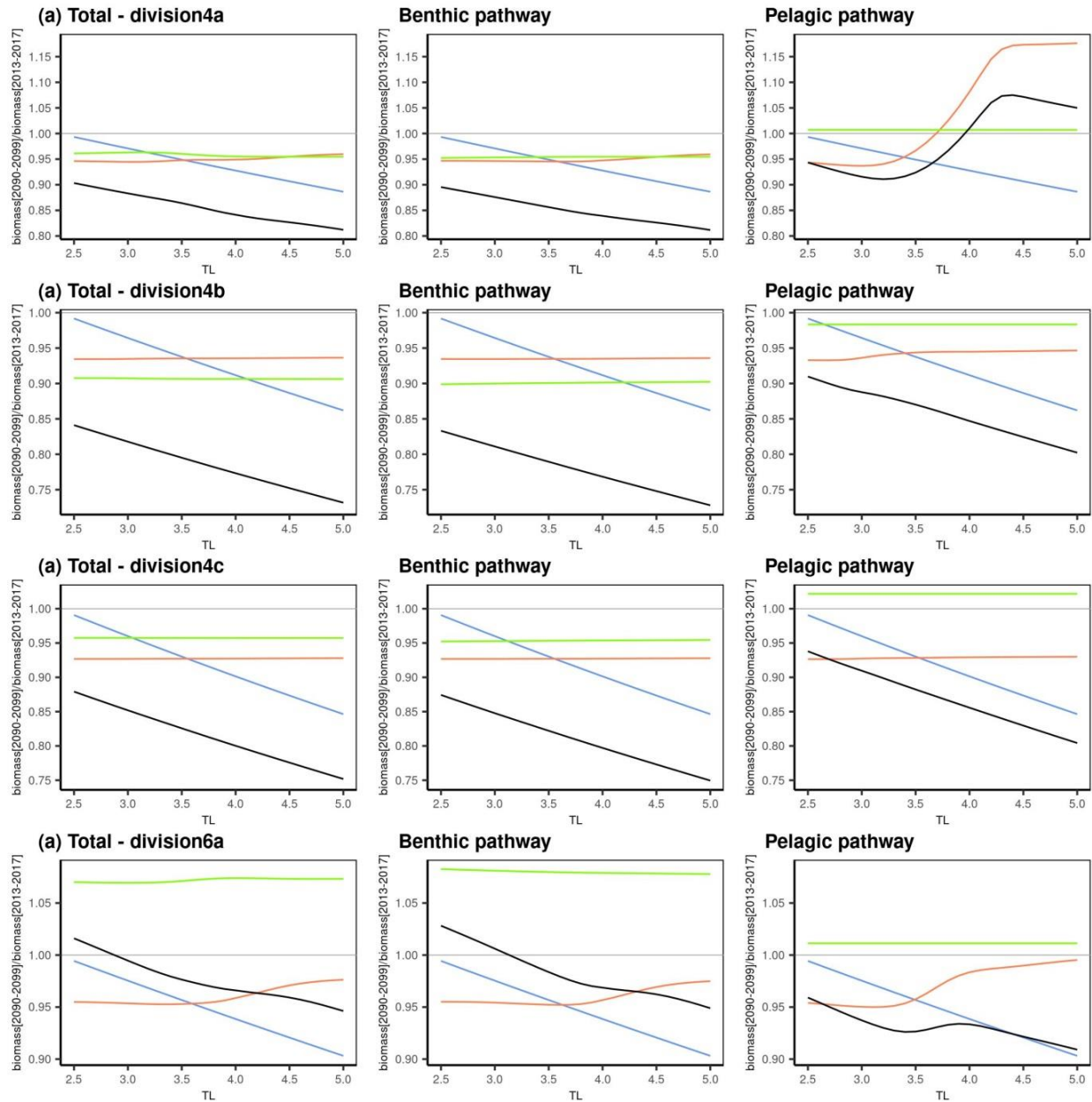


Figure C.5.1: The drivers of the changes in biomass in four ICES divisions (4a, 4b, 4c, 6a) for total biomass, benthic biomass and pelagic biomass. The ratio of biomass trophic spectra in 2090-2099 to the reference period 2013-2017 are derived from the simulations in which each flow parameter is successively isolated (Production of secondary producers, transfer efficiency and Kinetic). The results are presented for RCP8.5 and for the constant fishing mortality simulation.

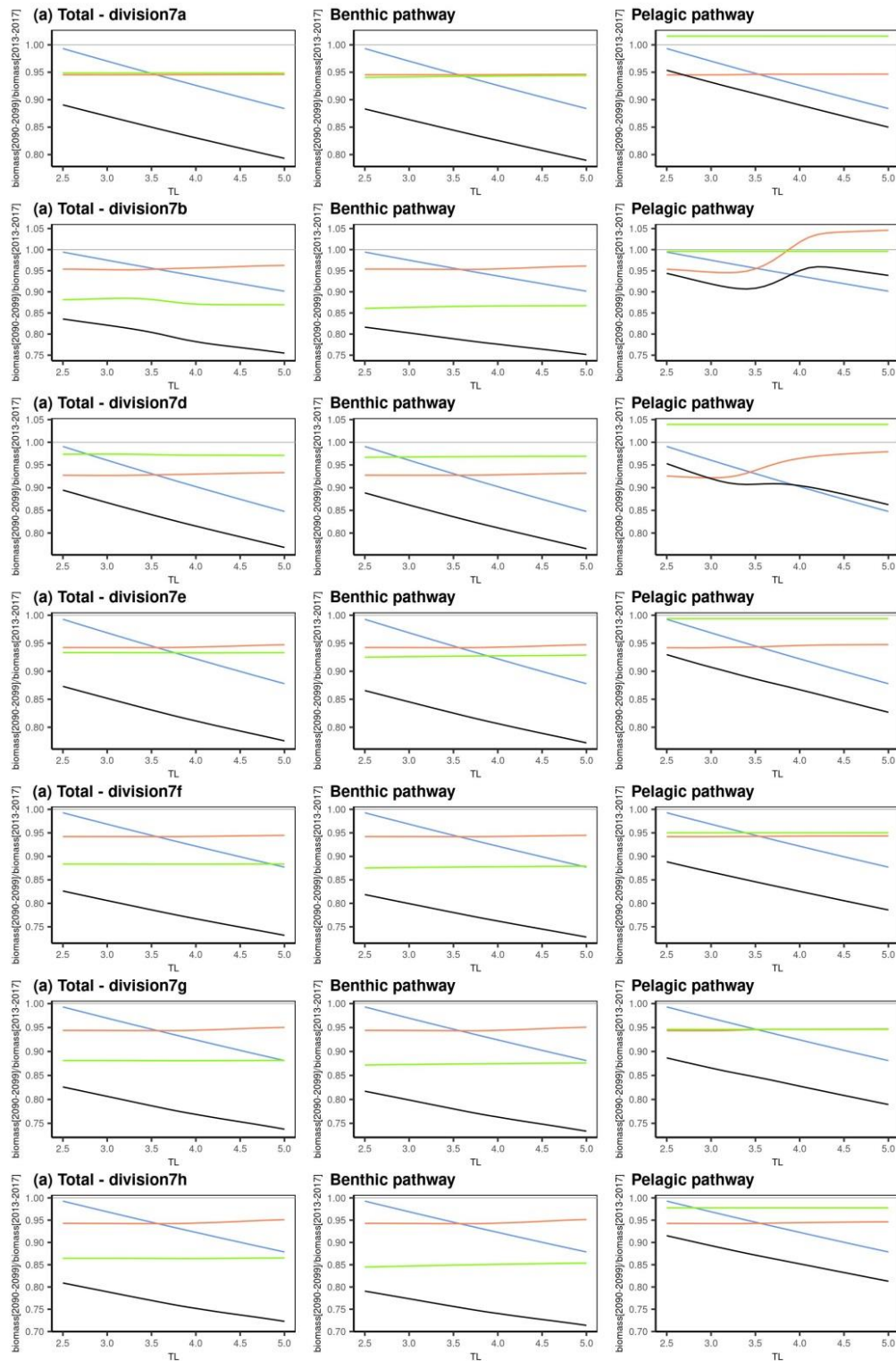


Figure C.5.2: The drivers of the changes in biomass in seven ICES divisions (7a, 7b, 7d, 7e, 7f, 7g, 7h) for total biomass, benthic biomass and pelagic biomass. The ratio of biomass trophic spectra in 2090-2099 to the reference period 2013-2017 are derived from the simulations in which each flow parameter is successively isolated (Production of secondary producers, transfer efficiency and Kinetic). The results are presented for RCP8.5 and for the constant fishing mortality simulation.

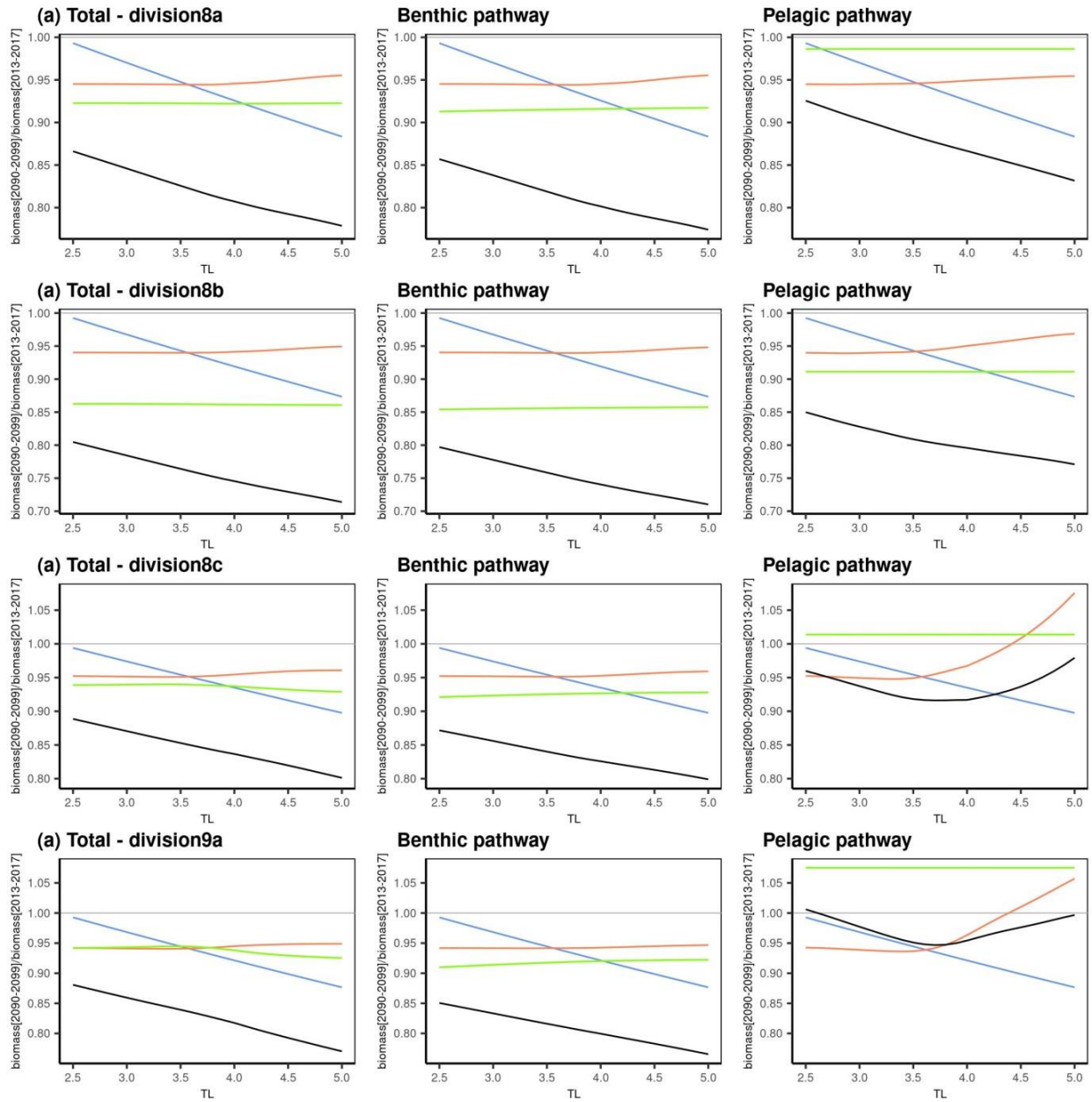


Figure C.5.3: The drivers of the changes in biomass in seven ICES divisions (8a, 8b, 8c, 9a) for total biomass, benthic biomass and pelagic biomass. The ratio of biomass trophic spectra in 2090-2099 to the reference period 2013-2017 are derived from the simulations in which each flow parameter is successively isolated (Production of secondary producers, transfer efficiency and Kinetic). The results are presented for RCP8.5 and for the constant fishing mortality simulation.

Supplementary material C.6: The drivers of the changes in catch in the 15 ICES divisions

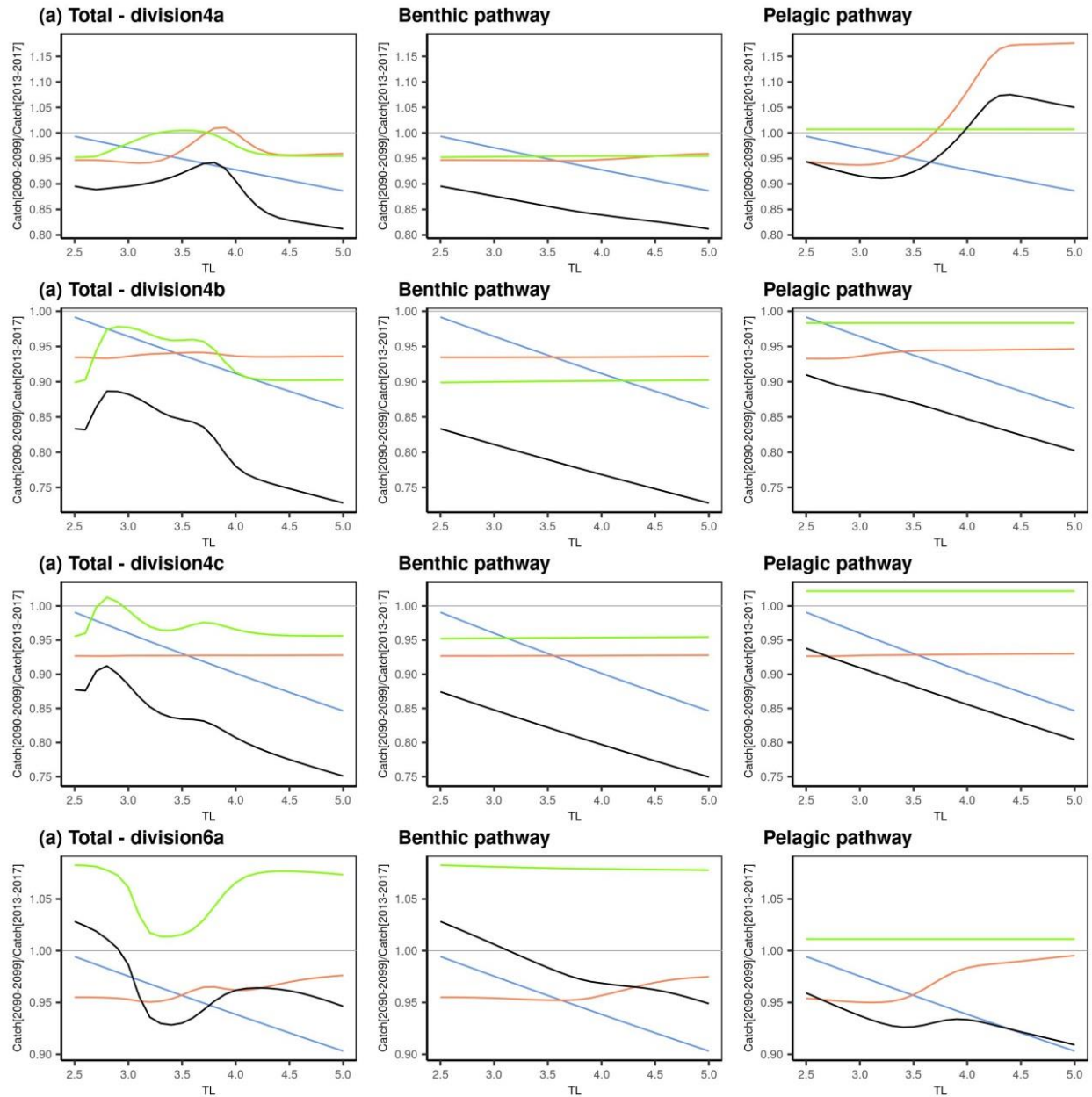


Figure C.6.1: The drivers of the changes in catch in four ICES divisions (4a, 4b, 4c, 6a) for total catch, benthic catch and pelagic catch. The ratio of catch trophic spectra in 2090-2099 to the reference period 2013-2017 are derived from the simulations in which each flow parameter is successively isolated (Production of secondary producers (in green), transfer efficiency (in blue) and Kinetic (in red)). The results are presented for RCP8.5 and for the constant fishing mortality simulation.

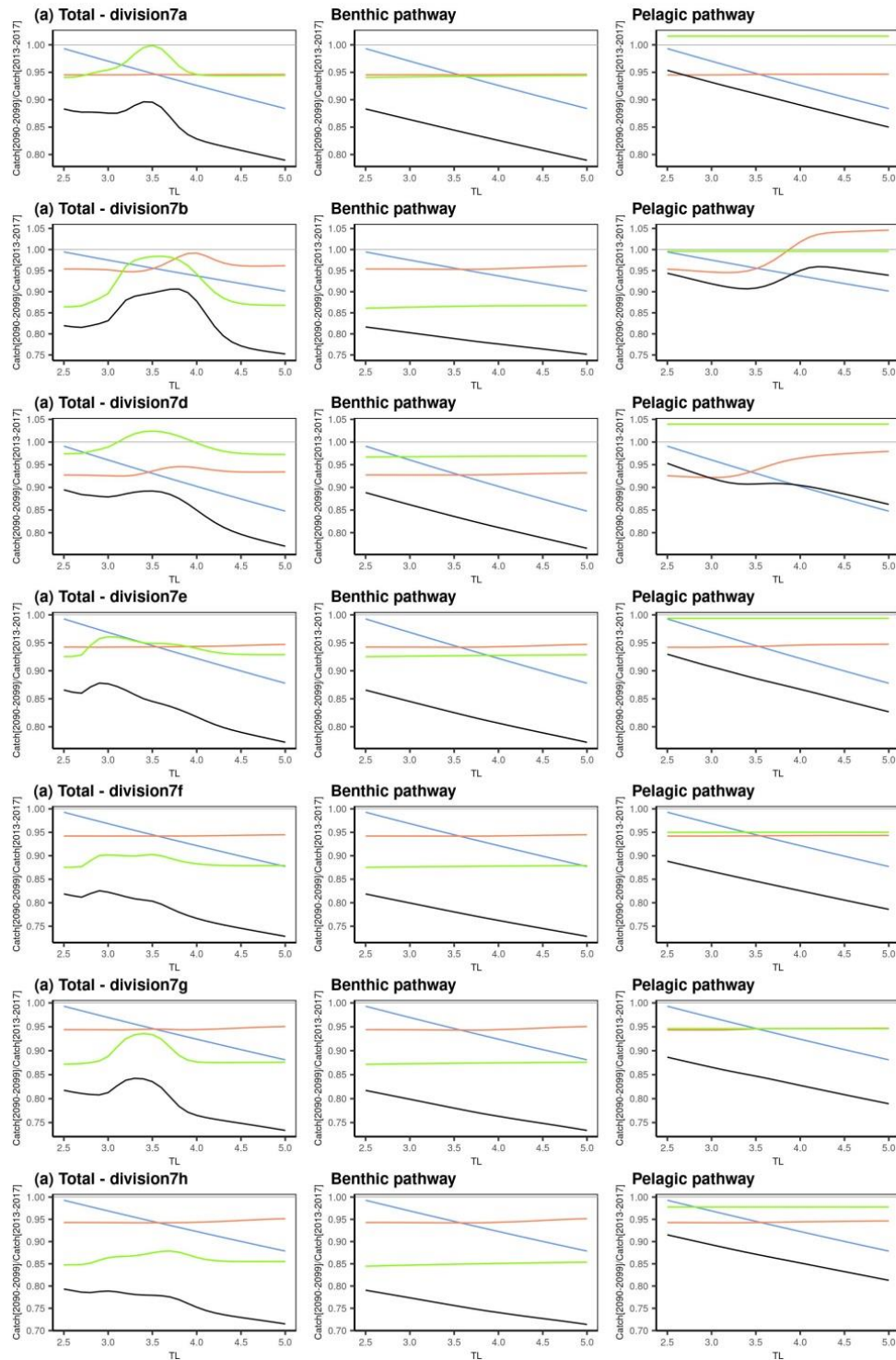


Figure C.6.2: The drivers of the changes in catch in seven ICES divisions (7a, 7b, 7d, 7e, 7f, 7g, 7h) for total catch, benthic catch and pelagic catch. The ratio of catch trophic spectra in 2090-2099 to the reference period 2013-2017 are derived from the simulations in which each flow parameter is successively isolated (Production of secondary producers (in green), transfer efficiency (in blue) and Kinetic (in red)). The results are presented for RCP8.5 and for the constant fishing mortality simulation.

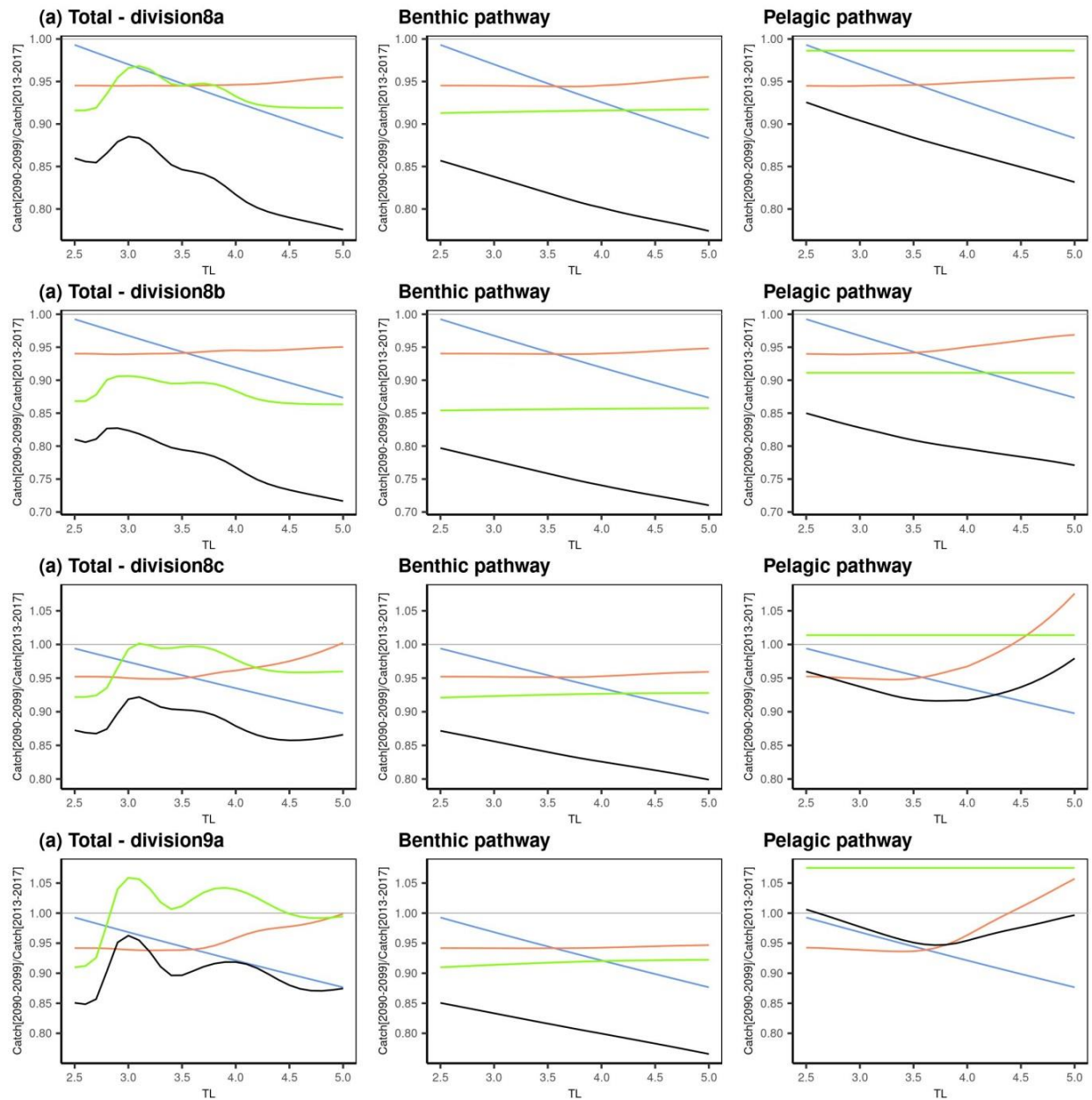


Figure C.6.3: The drivers of the changes in catch in seven ICES divisions (8a, 8b, 8c, 9a) for total catch, benthic catch and pelagic catch. The ratio of catch trophic spectra in 2090-2099 to the reference period 2013-2017 are derived from the simulations in which each flow parameter is successively isolated (Production of secondary producers (in green), transfer efficiency (in blue) and Kinetic (in red)). The results are presented for RCP8.5 and for the constant fishing mortality simulation.

Supplementary material C.7: The changes in biomass of secondary producers against the changes in sea surface temperature

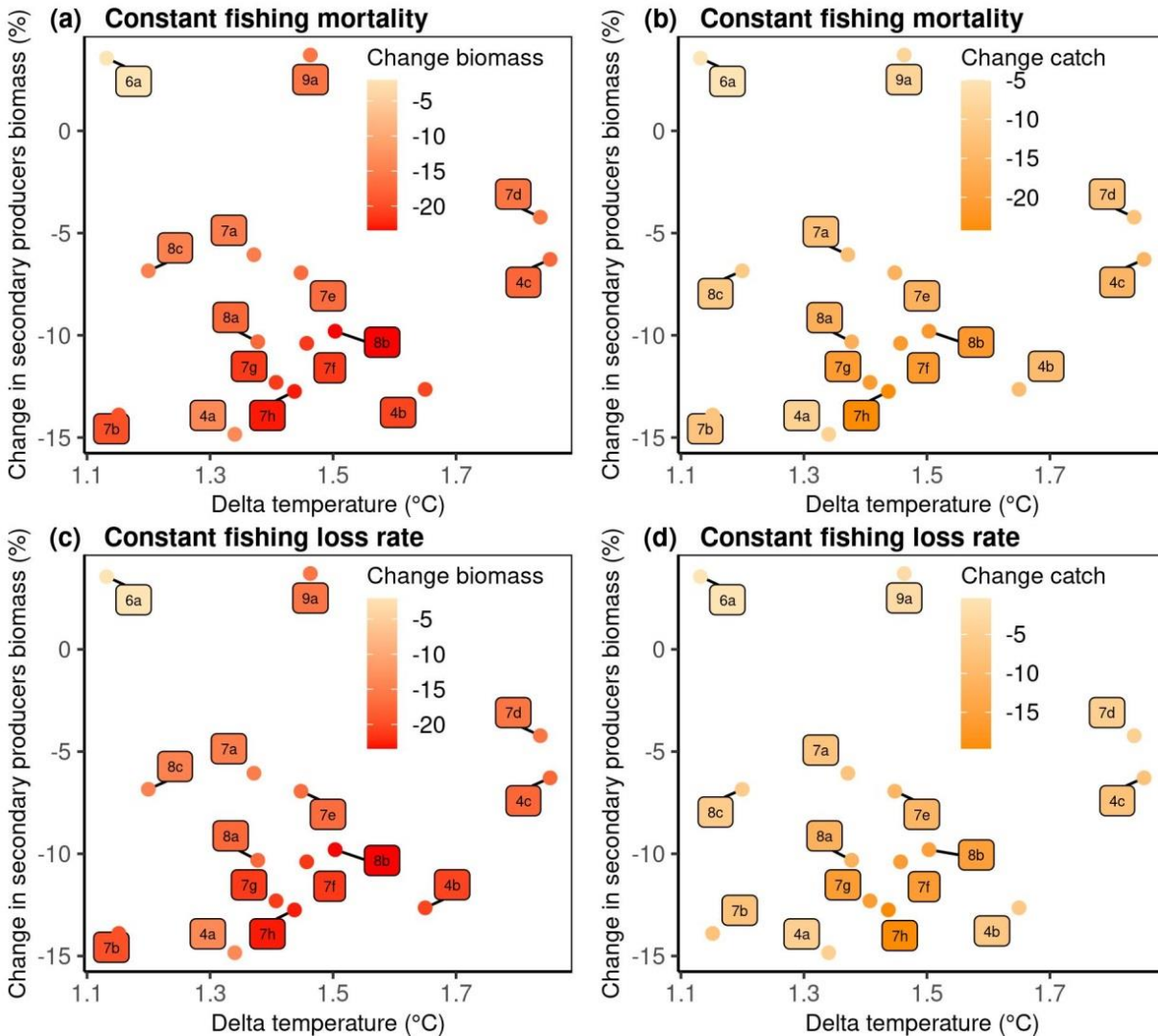


Figure C.7: The changes in biomass of secondary producers against the changes in sea surface temperature in each division for the constant fishing mortality (a and b) and for the constant fishing loss rate (c and d) simulations. The changes in total biomass and catch are presented as colour gradients red and orange, respectively.

Appendix D – Additional contributions

Article 1

Global change in the trophic functioning of marine food webs

PLOS One, 2017

Maureaud, A., Gascuel, D., Colléter, M., Palomares, M. L. D., **du Pontavice, H.**, Pauly, D., & Cheung, W. W. L.

Abstract

The development of fisheries in the oceans, and other human drivers such as climate warming, have led to changes in species abundance, assemblages, trophic interactions, and ultimately in the functioning of marine food webs. Here, using a trophodynamic approach and global databases of catches and life history traits of marine species, we tested the hypothesis that anthropogenic ecological impacts may have led to changes in the global parameters defining the transfers of biomass within the food web. First, we developed two indicators to assess such changes: the Time Cumulated Indicator (TCI) measuring the residence time of biomass within the food web, and the Efficiency Cumulated Indicator (ECI) quantifying the fraction of secondary production reaching the top of the trophic chain. Then, we assessed, at the large marine ecosystem scale, the worldwide change of these two indicators over the 1950±2010 time-periods. Global trends were identified and cluster analyses were used to characterize the variability of trends between ecosystems. Results showed that the most common pattern over the study period is a global decrease in TCI, while the ECI indicator tends to increase. Thus, changes in species assemblages would induce faster and apparently more efficient biomass transfers in marine food webs. Results also suggested that the main driver of change over that period had been the large increase in fishing pressure. The largest changes occurred in ecosystems where “fishing down the marine food web” are most intensive.

Article 2

An iron cycle cascade governs the response of tropical Pacific ecosystems to climate change

Global Change Biology, Under review

Tagliabue A., Barrier N., **du Pontavice H.**, Kwiatkowski L., Aumont O., Bopp L., Cheung W.W.L., Gascuel D., Maury O.

Abstract

Earth system models project that a negative impact of climate change on ocean net primary production (NPP) and upper trophic levels in the eastern tropical Pacific especially. Here, we present evidence that climate change trends in NPP in this region are strongly affected by assumptions associated with phytoplankton iron removal. Across experiments, constrained by their ability to reproduce past variations in tropical ocean NPP, we find a plausible range of -12.3% to +2.4% in the effect of climate change on NPP, driven by changes in the resilience of regional iron limitation. These results translate into reductions in projected end of century modifications to the biomass of upper trophic levels of 50-80%. As uncertainties in the biological iron cycle are found to clearly contribute additional ambiguity regarding the future of regional ecosystems, they highlight the need for better understanding of the iron cycle cascade from plankton to fish.

Article 3

Energy flow through marine ecosystems: confronting transfer efficiency

Trend in Ecology and Evolution, Under review

Eddy T. D., Bernhardt J. R., Blanchard J. L., Colléter M., Cheung W. L. L., **du Pontavice H.**, Fulton E. A., Gascuel D., Kearney K. A., Petrik C. M., Roy T., Rykaczewski R. R., Selden R., Stock C. A., Wabnitz C. C.C., Watson R.

Abstract

Transfer efficiency is the proportion of energy passed between nodes in food webs. It is an emergent, unitless ecosystem property that is difficult to measure and responds dynamically to environmental and ecosystem changes. Because the consequences of changes in transfer efficiency compound through ecosystems, slight variations can have large implications for top predators and fisheries. We review processes controlling transfer efficiency, approaches to estimate it, and known variations across ocean biomes. Both process-level analysis and observed macroscale variations suggest that transfer efficiency is highly variable, impacted by fishing, and will decline with climate change. It is important that we reduce transfer efficiency uncertainty and more fully resolve the processes controlling it in models to effectively anticipate changes in marine resources.

Book chapter

Changing biomass flows in marine ecosystems: from the past to the future

In Predicting Future Oceans, 2019

du Pontavice H.

Abstract

Anthropogenic modifications of the biosphere have led to drastic global changes in the structure and functioning of the marine food webs, and ultimately in the productivity, stability, and resilience of marine ecosystems. This chapter summarizes the temperature effects on biomass transfers in marine food webs. We studied the temperature effects using two characteristics of biomass transfer: the efficiency of the biomass flow and the residence time of the biomass. Our aim was to better understand the functioning of biomass transfer in marine ecosystems since 1950 to be able to produce insights into the future changes due to global climate change. We identified a clear temperature effect on the functioning of the marine ecosystem, suggesting that warmer oceans are likely to result in faster and less efficient biomass flows. The expected changes are obviously a major issue for the future of fisheries and for many other services provided by marine ecosystems to humans.